

**Characterisation of flow regimes of the East Yorkshire Chalk  
Aquifer**

Prodeo Yao Agbotui

Submitted in accordance with the requirements for the degree of  
Doctor of Philosophy

The University of Leeds

School of Earth and Environment

September 2019

The candidate confirms that the work submitted is his/her own and that appropriate credit has been given where reference has been made to the work of others.

This copy has been supplied on the understanding that it is copyright material and that no quotation from the thesis may be published without proper acknowledgement.

The right of Prodeo Yao Agbotui to be identified as Author of this work has been asserted by him in accordance with the Copyright, Designs and Patents Act 1988.

## Acknowledgements

My study has been synonymous with a Floyd Mayweather bout, where I had hoped to win this bout by winning round by round resulting in a slugfest. The hope for winning the slugfest has been kept alive to date because of the support and coaches I have got in my corner. For these people I express my gratitude.

I am most grateful to the UK Commonwealth Scholarship Secretariat and University of Leeds for jointly funding my PhD studies in the UK. Without these two institutions I would not have been able to come back here to up my hydrogeological game. I am thankful to the government of Ghana and the Accra Technical University for granting me my study leave without qualms. I also thank the Ghana Scholarship Secretariat and Prince for facilitating the scholarship process. I also thank the EA and London Petrophysical Society for supporting my fieldwork and conference respectively. My references for this scholarship: Dr Odling, Professors Anornu and Nyarko, and Rev. Woode, thanks for speaking well of me and my suitability for this great opportunity.

Without my Supervisors, I would not have even started and gotten this far. Dr Jared West and Prof Simon Bottrell, I am thankful. Your advice, guidance, encouragement and mentorship are greatly appreciated. I have learned a lot from you and I am very grateful. I owe my hydrogeological thought and ideas to you.

Drs Louise Maurice and Andrew Farrant of the BGS, I thank you for taking me out on my first major fieldwork to the Chalk and answering all my questions on the Chalk. You two gave me a pleasant introduction to the study area. I am grateful. Lou, but for your point injector and guide on how to use it, a major component of my work would have been pointless. Sharon Thomas, Edward Wrathmell, Hannah Threadgould, Andrea Lancaster, Ruth Buckley and James Senior of the EA, thank you for hosting me for my internship. All the scans and archived data I got from you were of enormous help. Thanks for your patience and goodwill. Paul Speight and Mark Morton of YW, thanks for all the data and clarifications. Mark Beswick of the UK MET Office, you have been fantastic. Thank you.

School of Earth and Environment gave me a home I will never forget. I thank Dr Rob Newton, for asking for clarification for the why and what of my work during my Transfer. You woke me up to see my study area as a scientific laboratory. It paid off. Oh Kirk Handley, without you how could I have gotten all this data. My fieldwork was hard and laborious, but you were there to help me remove all the bolts and knots off well lids so I could inject my salt. I am grateful. Josie, I am thankful for your company and thoughts on the nitrates. You gave a soft touch to our fieldtrips. Jane Stocks, thank you for your time and your readiness to help always. Rachel Gasior, Stephen Reid, Fiona Keay and Andy Connelly of the labs, thank you very much. Teresa Honore and Cara Healy, without you two, I would not have had the opportunity to discuss the way forward with my supervisors. Thank you two for planning my meetings. You two have been wonderful.

Now to my family and friends, you have been great and supportive. Oh Efo Justice, Nanayaw and Elton, you know without you guys I wouldn't have gotten the clarity to pull this one off. Most grateful. To my sweet wife, Theodora, I say thank you. Your encouragement, understanding and compromise has made this bout pleasant. You were there to see all the highs and lows. To my little angels, Anna and Mercedes, I am grateful. In times when I felt like giving up, your faces gave me hope and strength to soldier on. I know you were ignored at times, but I will make up when am done. Deo-Gratias, you have been like a watchman on my progress from day one. Even when you were down on your sick bed, your incessant checks on me made me realise that loads of people look to me. I am thankful. Selorm and the Tagbor Family, thanks for your encouragement, love and concern. I greatly indebted to my parents, Efo Chale and Ebea. Thank you two for passing life to me and giving me the coding for a "book" mind. I am thankful for your prayers and encouragement. To all the boys, thanks for your checks on me.

I finally thank Yahweh for granting me fortitude, the gift of study and this great opportunity once more. Those who hold on to you never lack.

## **Abstract**

The Cretaceous Chalk is a fractured aquifer with high permeability and low storage, that supplies about 60% of potable groundwater in the UK. Since the 1970s, groundwater quality in the Chalk aquifer in East Yorkshire focusing on the Kilham catchment area has been threatened by nitrate and pesticide contamination. This project sets out to better characterize the groundwater flow velocities, patterns, and regimes in the East Yorkshire Chalk aquifer to facilitate catchment and source protection zone delineation for aquifer protection. The aims were pursued via: conducting of single open well ambient flow dilution testing and reinterpretation of previous data including geophysical logs, well-to-well tracer tests; well hydraulic head and stream discharge hydrographs; conducting of time-series monitoring of springs and wells for temperature, SEC and major ion composition; re-analyses of archived pumping test data to investigate the hydraulic properties of faults and consequent development of conceptual model of aquifer recharge, throughput and outflow.

Discrete flow horizons were detected at all depths of investigation (up to 70 mgb), but with the majority of flow features at shallow depth in proximity to the water table. Ambient flow pattern in wells is location specific, with strong upwards flows of up to 4 m/min in valley boreholes while boreholes at high elevation typically show downflow, and those at intermediate elevation show crossflows. Previous well-to-well and well-to-spring tracer tests are interpreted as indicating karstic flow via solutionally enlarged bedding features connected by vertical fractures, with groundwater velocities ranging between 40 – 480 m/d, connecting wells and springs 4.2 km apart. Novel approaches for estimating local groundwater velocities from single open-well dilution tests were further developed in this work and applied to the single-well data; these gave velocities in broad agreement with those from well-to-well tracer tests, validating the single well method.

Monitoring data showed that wells and spring temperatures fell in a narrow range (9.2 – 10.1 °C) reflective of average annual (10.3 °C) temperature suggesting sufficient residence time to enable groundwater temperature to equilibrate with that of the aquifer. Groundwater and spring waters are

dominated by  $\text{Ca}^{2+}$  and  $\text{HCO}_3^-$ , with evidence of nitrate contamination (51 – 74 mg/L  $\text{NO}_3^-$ ). Well water SEC is non-varying, whereas that for springs showed variation reflective of both degree of access of soil-derived  $\text{CO}_2$  and seasonal variations in soil biological activity and hence soil  $\text{pCO}_2$ .  $\text{Ca}^{2+}$  and  $\text{HCO}_3^-$  concentration variation in the springs may also indicate seasonal switching between open and closed carbonate systems. Well hydraulic head and groundwater fed stream discharge hydrographs showed seasonal fluctuation, with well hydraulic head variations increasing towards recharge areas. The effects of faults on aquifer transmissivity could not be ascertained via re-analyses of archived pumping tests.

The findings from this work were used to develop both physical and chemical hydrogeological conceptual models for the catchment. The aquifer functions as a hydrogeologic continuum, limiting the utility of the individual source protection zones currently in use by the Environment Agency of England and Wales (EA), but supports the EA's decision to demarcate the entire Chalk outcrop as nitrate vulnerable. Knowledge of ambient well flow velocities, and flow patterns are required for effective planning of future geochemical sampling, contaminant tracking, remediation activity and pumping tests campaigns. Such knowledge allows both depth specific sampling and vertical hydraulic characterisation of depth intervals in wells, which are vital to develop more accurate simulations of contaminant transport. Further hydraulic characterisation of fault zones is also recommended.

## Table of Contents

<b>Acknowledgements.....</b>	<b>iii</b>
<b>Abstract.....</b>	<b>v</b>
<b>List of Tables .....</b>	<b>xi</b>
<b>List of Figures .....</b>	<b>xii</b>
<b>Abbreviations .....</b>	<b>xix</b>
<b>List of symbols .....</b>	<b>1</b>
<b>Chapter 1 Introduction : Project Background and Setting .....</b>	<b>1</b>
1.1 Importance of the Chalk Aquifer and its vulnerability to contamination .....	1
1.2 Nitrate contamination history, its impacts and management practices .....	3
1.3 The importance and relevance of this work .....	8
1.4 Project aim and objectives .....	11
1.5 Thesis layout.....	13
<b>Chapter 2 Literature Review of Study Area.....</b>	<b>15</b>
2.1 Study area .....	15
2.1.1 Physiography, catchment economic activity and surface water hydrology .....	15
2.1.2 Chalk formation and lithology .....	20
2.1.3 Stratigraphy of the Solid Geology.....	22
2.1.4 Paleogene and Quaternary influences .....	25
2.1.5 Tectonics and Chalk structure .....	27
2.2 The effects of geology on the hydrogeology of the Chalk.....	33
2.2.1 Unsaturated zone flow processes and recharge .....	33
2.2.2 Porosity and effective storage .....	37
2.2.3 Hydraulic conductivity variation with depth and flow layering.....	38
2.2.4 Heterogeneity and spatial transmissivity variation of the Chalk Aquifer.....	40
2.2.5 Flow patterns in the Chalk.....	43
2.2.6 Geochemistry of the Northern Chalk Aquifer .....	45
2.3 Summary of the geology and hydrogeology of the Chalk .....	47
<b>Chapter 3 Kilham Catchment and Previous Relevant Work.....</b>	<b>49</b>
3.1 Justification of the catchment of study .....	49
3.2 Previous hydrogeological investigations in the study area.....	51
3.3 Data obtained for the current studies.....	58

3.3.1	EA/BGS .....	58
3.3.2	UK MET Office Data and UK Air Information Resource (UK AIR) rainfall chemistry data. ....	64
3.4	Chapter summary .....	65
<b>Chapter 4 Open-well dilution testing and the characterisation of flow variation with depth .....</b>		<b>67</b>
4.1	Hydraulic conductivity and flow variation with depth in the Chalk	67
4.2	Theory of regional scale groundwater flow .....	69
4.3	Theory of open-well dilution tests and field methodology used	71
4.3.1	Strengths and drawbacks of the technique.....	71
4.3.2	Method and set-up.....	71
4.3.3	Open-well dilution testing principles and analytical techniques .....	73
4.3.4	Analytical and field procedures used in this chapter.....	75
4.4	Field Methodology used in this chapter for ambient open-well dilution testing.....	82
4.5	Ambient open-well dilution tests results and discussion .....	91
4.5.1	Results and discussion of uniform and point emplacement open-well dilution testing .....	91
4.6	Summary of findings .....	124
<b>Chapter 5 Spring and well monitoring and results.....</b>		<b>126</b>
5.1	Springs and their importance in fractured carbonate aquifer studies .....	126
5.2	Classification of carbonate aquifers: conduit or diffuse flow or a combination of both? .....	129
5.3	Specific electrical conductivity and its theory .....	131
5.3.1	Importance of SEC and its measurement.....	131
5.3.2	SEC theory and transport number .....	132
5.3.3	Carbon dioxide and its effect on SEC in carbonate aquifers	135
5.4	Water temperature as a groundwater tracer .....	137
5.5	Groundwater level measurement.....	140
5.5.1	Groundwater level measurements and importance .....	140
5.5.2	Groundwater level monitoring and measurement equipment	142
5.5.3	Relationship between transducer water column and depth to water level in monitoring wells .....	145
5.6	Spring sampling and well monitoring .....	147

5.6.1	Spring SEC and temperature monitoring: site and equipment considerations, installation and data retrieval.....	147
5.6.2	Spring sampling and laboratory analyses.....	152
5.6.3	Water level, SEC and temperature monitoring .....	153
5.7	Spring and well monitoring results and discussions.....	154
5.7.1	Results and discussions of well monitoring .....	154
5.7.2	Results and discussions of spring SEC and temperature monitoring.....	159
5.7.3	Results of spring sampling .....	163
5.7.4	Results of measured and calculated SECs, and transport numbers .....	174
5.7.5	Spring sampling and monitoring discussion .....	179
5.8	Chapter summary .....	182
<b>Chapter 6 Saturated zone flow pattern characterisation using evidence from flow zone characterisation and previous tracer tests .....</b>		<b>184</b>
6.1	Geophysical logs, open-well dilution and tracer tests for determining flow connection of wells and springs.....	184
6.1.1	Flow in the Langtoft Valley .....	185
6.1.2	Flow in the Broachdale Valley .....	196
6.1.3	Flow connection between West End Farm borehole to Kilham Abstraction, Kilham Sewage Works, Bellguy and Bracey Bridge Springs.....	203
6.2	Comparison of velocities of open well-dilution results at Little Kilham Farm well with tracer test velocities .....	210
6.2.1	Results from the implementation of the workflow .....	212
6.3	Pumping tests and transmissivity distribution of the Kilham Catchment .....	215
6.4	Chapter Summary.....	216
<b>Chapter 7 Conceptual model of flow in the Chalk and Kilham catchment.....</b>		<b>218</b>
7.1	Catchment Conceptual model development.....	218
7.1.1	Development of a conceptual model of the study area and the Kilham Catchment .....	219
7.2	Conceptual model summary description.....	236
7.3	Conceptual model uncertainties.....	237
7.4	Implications of this project for groundwater management and resource protection .....	238
7.5	Chapter Summary.....	240

<b>Chapter 8 Conclusions and recommendations .....</b>	<b>241</b>
8.1 Aims and objectives .....	241
8.1.1 Characterisation of flow geometry and topology between wells in the saturated zone, and to the aquifer output (springs). .....	241
8.1.2 Characterisation of the response of boreholes (throughput) and springs (output) to recharge and rainfall events (input) outcomes.....	243
8.1.3 Characterisation of the effects of faults on groundwater flow in the study area outcomes. ....	244
8.1.4 Development of a hydrogeological conceptual model to improve catchment process understanding for effective catchment management outcomes.....	245
8.2 Further work and recommendations .....	246
<b>List of References .....</b>	<b>248</b>

## List of Tables

Table 2.1. Chalk stratigraphic summary .....	25
Table 3.1. Pumping test characteristics and Transmissivity estimations in the Kilham Catchment.....	61
Table 4.1. Borehole details and injection parameters of the 8 tested wells .	86
Table 4.2. Kilham Sewage Works borehole horizontal flow model test parameters.....	93
Table 4.3. Little Kilham Farm horizontal flow model test parameters. 5 – 40 and 60 – 275 minutes profiles used to determine the parameters for depths 18 – 35 mbgl and 35.5 – 48 mbgl respectively. ....	102
Table 4.4. Details of point injection of tracer at depth 45 mbgl and profile properties in Tancred Pit borehole .....	112
Table 4.5. Details of point injection of tracer at depth 39.5 mbgl and profile properties in Weaverthorpe borehole.....	117
Table 4.6. Details of point injection of tracer at depth 33.5 mbgl and profile properties in Weaverthorpe borehole.....	121
Table 5.1: Parameters of major ions used in equations (5.2) to (5.5).....	135
Table 5.2 Location data and details for spring and borehole monitoring sites.....	149
Table 5.3. Field measurements and major ion chemistry of monitored springs for this studies .....	165
Table 5.4. Archived geochemical characteristics from EA monitored boreholes and springs in the study area .....	172
Table 6.1. Results of fracture aperture and well flowing porosity .....	212
Table 6.2. Data of hydraulic gradient in the Little Kilham Farm well using the depth intervals in Figure 6.16.....	214
Table 7.1. Characterisation of the Physical Conceptual Model of the Kilham catchment .....	220
Table 7.2. Characterisation of the Chemical Conceptual Model of the Kilham catchment.....	230

## List of Figures

Figure 1.1: Chalk outcrop in the UK with the study area marked in red. See Figure 1.2 for the location map of the study area. ....	2
Figure 1.2: Location map of study area on geology, with Kilham Catchment, based on topographic highs, marked in red. ....	4
Figure 1.3: Fertilizer nitrogen application rate between the years 1941 – 1972 for the East Yorkshire Region. From Foster and Crease (1974), page 191. ....	5
Figure 1.4: Trend of increasing nitrate concentration in some selected wells and springs in East Yorkshire. Foster and Crease (1974), page 181....	5
Figure 1.5. Recent nitrate trends in wells in the study area, from EA archived geochemical dataset. ....	6
Figure 2.1: Bedrock and superficial geology map of the Chalk Aquifer of East Yorkshire showing the current study area (red square). ....	16
Figure 2.2: Bedrock and superficial geology of the study area. Section ABCDE cut through profile (Figure 2.4) where borehole information on BGS GeoIndex is available. ....	17
Figure 2.3: Digital terrain elevation model of study area showing elevation highs (deep blue) to topographical lows (brown) with the main surface water and drainage features. ....	19
Figure 2.4. Geologic cross-section through the study area, from Place Newton Springs (at Wintringham) (A), through Weaverthorpe (B), Langtoft (C), Kilham (D), to Foston on the Wolds (E) showing the steep scarp and gentle dip slopes. The Chalk group lies unconformably on Amphill Clay and Kimmeridge Clay formations. Refer to section 3.3.1. on the methodology for the development of cross-section. ....	26
Figure 2.5: Structure contours on the base of the Chalk Group showing the main synclinal axis through Kilham. Redrawn from Gale and Rutter (2006) and superimposed on Edina digimap data. ....	28
Figure 2.6: The Howardian Hills-Flamborough Head Fault zone (at Top Corallian level) as determined from seismic data from Chadwick and Evans (2005). The approximate study area is outlined in red. Figs 126-129 relate to Chadwick and Evans (2005). ....	29
Figure 2.7: Fracture types in the Northern Chalk, mapped at Flamborough Head. Adapted from Hartmann et al. (2007). ....	30
Figure 2.8: Map of main faults in the study and Kilham area. Fault line shapefiles were obtained from Farrant et al. (2016). Faults labelled in red were confirmed on the field, those labelled in blue were found from desk study. ....	32
Figure 2.9: Seasonal variation of water flux through the unsaturated zone to the water table (Wellings and Bell, 1980). ....	34

- Figure 2.10 Distribution of transmissivity values measured in the Chalk aquifer, study area (red square) from Gale and Rutter (2006), page 19. Large transmissivities in and around Kilham (purple square and arrow)..... 41
- Figure 2.11. Geological cross-section of study area showing maximum and minimum groundwater levels, thick unsaturated zone of recharge area and groundwater flow direction on scarp and dip slopes. Groundwater levels data obtained from archived EA monitoring wells marked as red rectangles. .... 44
- Figure 3.1. The general study area (grid boundaries), with the Kilham catchment marked in red on topographic highs and the springs and borehole sites used for this study marked out. Further details on location are presented in chapters 4 and 5. .... 50
- Figure 3.2. Drawdown of 3 months duration large scale pumping test superimposed on faults mapped by Farrant et al (2016). Large transmissivities exist in the Broachdale and Langtoft valleys and south of Kilham whilst probable boundary effects are indicated by closeness of the groundwater contours in north-eastern and northern part of area of influence..... 54
- Figure 3.3. Transmissivity, fault and contour map superimposed on geology of the Kilham area. Red transmissivity values are from recovery analysis, whereas black text are from C&J, Theis and Neuman analyses. Purple dashed lines are faults from Farrant et al (2016). .... 59
- Figure 4.1 Tracer profile evolution with time for simple horizontal flow case: (a) uniform diffuse horizontal flow; (b) diffuse uniform flow but with a discrete flowing fracture with a comparatively higher flow; (c) different diffuse flow zones. Adopted and amended from Maurice et al. (2010) 76
- Figure 4.2. Plan view of ambient open-well dilution experiment showing flow line distortion and convergence from the formation width  $D_f$ , into the test well of diameter  $D_w$ , resulting in an artificial increase of flow through the well by a factor of  $\alpha, \approx 2$ , dilutes and washes away tracer from the test interval of the well in the direction of groundwater. Adopted and redrawn from Freeze and Cherry (1979) and Maldaner et al. (2018). .... 78
- Figure 4.3. Tracer concentration decay plot versus time graph for a uniform open well dilution test for a specific sampling depth, at which tracer decay occurs by horizontal flows. The slope of the line is directly related to the darcy flux through the well, and the y-intercept is the natural log of the initial concentration..... 79
- Figure 4.4 Schematic of injected tracer evolution for a well with vertical flow: (a) uniform injection with an upward moving fresh water front; (b) point injection ; (c) flow model, d and e are inflow points, f is outflow. 81
- Figure 4.5. Map of wells in the Kilham catchment and surrounding areas initially targeted for open-well dilution testing. Black squares for tested wells and red triangles for untested wells..... 84

Figure 4.6. Open-well dilution tested wells location superimposed on geology and elevation contours of the Kilham catchment. ....	85
Figure 4.7. Uniform open-well dilution test set-up .....	88
Figure 4.8 Solinst TLC logger response versus salt concentration calibration chart.....	89
Figure 4.9 Point injection set-up.....	90
Figure 4.10. Kilham Sewage Works results: (a) uniform injection profiles; (b) specific discharge with depth plot; (c) borehole crossflow model (ambient).....	92
Figure 4.11. Kilham Sewage Works borehole sample plot of linear regression for the determination of specific discharge for depth 11.5 m bgl. ....	93
Figure 4.12. Kilham Sewage Works borehole point injection at depth 15.5 m. ....	95
Figure 4.13. Kilham Pumping Station borehole results: (a) uniform injection profiles; (b) point injection at depth depth 13.6 m bgl arrowed in red. .	96
Figure 4.14. EA Kilham Pumping Station Observation profile centroid position (black squares) and mass recovery (red circles) with time plot for point injection of 75 g NaCl at 13.6 mbgl .....	97
Figure 4.15. Borehole geophysics (BH 1) results European Geophysical Services (2018). (a) Borehole caliper with diameter enlargements within watertable fluctuation zone and at depth; (b) Ambient flow results with substantial flows occurring between depth 23 – 54 mbgl with no substantial flows occurring above depth 23 mbgl; (c) Flow model (ambient) in observation borehole. ....	98
Figure 4.16 Little Kilham Farm results: (a) caliper log;(b) uniform injection profiles with time;(c) specific discharge with depth plot;point injection (red arrows) profiles for depths (d) 19.5 and (e) 30 mbgl. ....	100
Figure 4.17. Little Kilham Pitrak et al (2007) horizontal flow model regression plot for depth 23.5 mbgl.....	101
Figure 4.18 Little Kilham Farm centroid position (black squares) and mass recovery (red circles) with time plot for point injection of 75 g NaCl at 19.5 mbgl .....	104
Figure 4.19. Little Kilham Farm borehole: (a) caliper log; (b) ambient flow model based on the work presented here with dominant crossflows(thick horizontal arrows) with weak vertical flows (thin arrows);(c) Southern Science (1994) CCTV flow model.....	105
Figure 4.20. Field House, Kilham borehole results: (a) caliper log; (b) uniform injection profiles. ....	107
Figure 4.21. Old Plantation results: (a) caliper log; (b) uniform injection profiles. ....	107
Figure 4.22 Henpit Hole borehole results: (a) caliper log; (b) uniform injection profile; (c) Southern Science (1994) CCTV flow model.....	109

Figure 4.23. Tancred Pit borehole results: (a) caliper log; (b) uniform injection profiles; (c) profiles for point injection (red arrowed) at depth 45 mbgl; (d) centroid position (black squares) and mass recovery (red circles) with time plot for upwards moving profile of point injection of 75 g NaCl at 45 mbgl ..... 111

Figure 4.24. Tancred Pit borehole results: (a) caliper log; upwards (b) velocity profile for depth intervals marked by profile centroid positions (c) current work flow model (ambient) ; (d) Southern Science (1994) CCTV flow model. .... 113

Figure 4.25. Weaverthorpe borehole results: (a) borehole image log with fracture traces; (b) caliper log; (c) uniform injection profiles..... 116

Figure 4.26. Weaverthorpe borehole point injection (red arrowed) for depths: (a) 39.5 m; (b) 33.5 m and (c) 41.5 mbgl. .... 118

Figure 4.27. Weaverthorpe borehole centroid position (black squares) and mass recovery (red circles) with time plot for upwards moving profiles of point injection of 75 g NaCl at: (a) 39.5 m and (b) 33.5 m bgl. .... 119

Figure 4.28. Weaverthorpe borehole: (a) caliper log; (b) velocity profile for depth intervals marked by profile centroid positions; (c) well flow model (ambient) ..... 123

Figure 4.29. Comparison of the flow models for the Weaverthorpe borehole. (a) Caliper log; (b) Flow model of Parker (2009) upflow and downflow converging to outflow 35 mbgl; (c) current ambient flow model from this work ..... 124

Figure 5.1. Schematic of a carbonate fractured aquifer’s spring response to input events: (a) rapid recharge and flow via conduits; (b) diffuse homogenised recharge ..... 127

Figure 5.2: Relationship between activity coefficient and ionic strength for major ions in groundwater, from Freeze and Cherry (1979)..... 134

Figure 5.3: Schematic for the hydraulic head equation ..... 141

Figure 5.4: Pressure transducer in a monitoring well. u is the upstand above ground level, WL is depth to water level from measurement point, WC is the water column depth above the transducer, h is the depth of sensor below the measurement point ..... 143

Figure 5.5: Difference in working principle of the (a) non-vented and (b) vented pressure transducer. Modified from Sorensen and Butcher (2011)..... 144

Figure 5.6. Onset HOBO Conductivity Logger Model U24-001 used for logging SEC at the Springs and Tancred Pit borehole..... 147

Figure 5.7. Location map for monitored sites. S and B coding are for monitored data for current work, EA coding for Environment Agency data, YW coding for Yorkshire Water data. .... 148

Figure 5.8. In-Situ non-vented pressure transducer (Rugged TROLL 100) for monitoring groundwater level in wells. .... 153

- Figure 5.9. Comparison of well hydrographs and Foston Mill discharge hydrograph. (a) Well hydrographs with high amplitude for Weaverthorpe Slack (EAB4) located in a recharge zone in comparison to lower amplitudes in the Kilham area (discharge zone). (b) Foston Mill daily discharge hydrograph and daily precipitation data. .... 156
- Figure 5.10. Well hydrograph general pattern for the Kilham area (discharge zone). Similarity in B3 and YWB1 hydrograph responses to abstraction in YWB1 highlighted (green ellipse and arrowed). Steady state behaviour of YWB1 hydrograph in due to logger going out of measurement range response to high water levels for the period late March to mid May 2018 also highlighted (orange ellipse)..... 158
- Figure 5.11. Comparison of ambient air, spring and borehole temperature. (a) Large seasonal air temperature variation with annual average of 10.3 °C. (b) Springs (S2 and S3) and borehole (B2) temperatures reflective of average ambient air temperature, with S2,S3 and B2 temperatures showing relatively little variation in temperature. Thermal lags between spring and air temperature maximum and minimum also shown..... 160
- Figure 5.12. SEC time seof Bellguy and Place Newton springs, Tancred Pit borehole (B2) and periodically monitored wells..... 162
- Figure 5.13. Distribution of CBEs for sampled springs ..... 164
- Figure 5.14. Time series of major ion concentration: (a)  $\text{Ca}^{2+}$ ; (b)  $\text{HCO}_3^-$ ; (c)  $\text{NO}_3^-$  ..... 168
- Figure 5.15 Time series of major ion concentrations: (a)  $\text{Cl}^-$ ; (b)  $\text{SO}_4^{2-}$ ; (c)  $\text{Na}^+$  ..... 169
- Figure 5.16 Time series of major ion concentrations: (a)  $\text{Mg}^{2+}$ ; (b)  $\text{K}^+$  ..... 170
- Figure 5.17. Measured SEC and transport numbers of monitored springs. (a) Bracey Bridge; (b) Bellguy; (c) Place Newton ..... 175
- Figure 5.18. Measured SEC and transport numbers of EA dataset. (a) Wintringham springs at Grange Garth; (b) Kilham southview springs; (c) Kilham Pumping Station Observation borehole..... 176
- Figure 5.19. Measured SEC and transport numbers of EA dataset. (a) DFm; (b) MHFm; (c) MFm..... 177
- Figure 5.20. Measured SEC and transport numbers of EA dataset. Weaverthorpe Slack borehole..... 178
- Figure 5.21. Graph of measured SEC versus calculated SEC of the major ions for the 3 monitored springs for this work..... 179
- Figure 5.22. Graph of measured SEC versus calculated SEC of the major ions for the 3 monitored springs for this work (red) and EA dataset (blue and black)..... 180
- Figure 6.1: Boreholes flow tested and tracer tested in Langtoft and Broachdale Valleys and Kilham on geology. Contour 100 m outlined in black to show the two valleys. .... 186

- Figure 6.2: Possible and detected flow horizons and directions arrowed in boreholes in the Langtoft Valley. Flow horizons identified by Buckley and Talbot (1994)-red, Southern Science (1994)-green, Parker (2009)-blue, Ward et al. (1998)-grey and the current study-black. .... 188
- Figure 6.3. Map of borehole and spring connectivity in the Kilham area from Ward and Williams (1995), Ward et al., (1997;1998) tracer tests. Black dash arrowed lines show connectivity between wells determined via tracer tests. Tracer injections at Henpit Hole (200 mm), Middledale (MD), Broachdale (BHD), West End Farm (WEF) boreholes. .... 189
- Figure 6.4. Borehole tracer connectivity topology between 65 m deep and 45 m deep Henpit Hole boreholes. Probable flow routes marked: (entirely along strata: 1,4; travel along intermediate routes: 2,3). .... 190
- Figure 6.5. Cross-section of the results of tracer tests and borehole connectivity in the Langtoft Valley, from Ward and Williams (1995); Ward et al. (1998). Connection between two Henpit Hole boreholes (40 m/day). .... 191
- Figure 6.6 Borehole tracer connectivity topology between Middledale and Little Kilham Farm boreholes. Four depths at which tracer was detected in Little Kilham Farm borehole (Farrant et al.,2016). Flow connectivity between two boreholes may be via two bedding parallel pathways: entirely on strata (1); or combination of parallel strata and vertically communicating features (2,3,4). .... 194
- Figure 6.7. Flow pattern between Henpit Hole, Middledale and Little Kilham Farm boreholes in the Langtoft Valley. .... 195
- Figure 6.8. Possible and detected flow horizons and directions in boreholes in the Broachdale Valley from previous and current studies. Buckley and Talbot (1994)-red, Southern Science (1994)-green, Parker (2009)-blue and the current study respectively-black. .... 197
- Figure 6.9. Borehole tracer connectivity topology between Broachdale and Tancred Pit boreholes. Comparing depths of tracer injection and detection shows downdip flow characterised by flow on bedding features and vertically communicating features (1, 2, 3,4). .... 199
- Figure 6.10: Cross-section of Ward and Williams (1995) and Ward et al. (1997) tracer test in the Broachdale Valley showing a fast rapid flow connection between Broachdale and Tancred Pit boreholes. .... 200
- Figure 6.11. Flow pattern diagram in the Broachdale Valley showing zone of developed permeability below the casing base and at depth. Shallow local recharge (blue dashed horizontal and vertical arrows) 202
- Figure 6.12. Marked flow horizons between West End Farm borehole (on the interfluvial) and Kilham Village, Bellguy and Bracey Bridge springs. Flow horizons identified by European Geophysical Services (2018)-red, Ward et al (1998)-grey and this current study-black respectively. .... 204

- Figure 6.13. Borehole and tracer connectivity topology between West End Farm borehole (WEF) and boreholes and springs showing upwards tracer movement from injection to detection points. a. Plan view of possible fast lateral tracer movement around B3 to B1 (1 and 2), S1 and S2 (3, 4 and 5). b. Section view of possible shallower lateral tracer movement as in a. (1,2,3,4,5), and fast but deeper flowpaths under B3 to B1 (7), S2 (8) and S1 (9). ..... 205
- Figure 6.14. Cross-section of Ward and Williams (1995), Ward et al. (1997;1998) tracer tests between West End Farm borehole Kilham, Bellguy and Bracey Bridge springs. Three faults with potential to concentrate flow horizontally, and to depth and up to discharge points marked. Tracer moved up dip towards solutionally enlarged fissures at discharge areas in Kilham, and Bellguy and Bracey Bridge springs. .... 206
- Figure 6.15. Summary of flow pattern between West End Farm borehole, Kilham Sewage Works borehole, Bellguy and Bracey Bridge springs. Flow occurring along bedding plane features, moving either laterally around (1,2,3,4,5) or deeper (7,8,9) under Kilham Abstraction ..... 209
- Figure 6.16. Little Kilham Farm borehole depth interval (1.5 m) properties: a. porosity; b. average horizontal groundwater velocities. Also marked on b are well-to-well tracer test velocity limits (red dash lines) by Ward and Williams (1995). ..... 213
- Figure 7.1. Physical Conceptual Model of the study area around Kilham showing the key physical processes. Red coloured call out boxes contain hydrogeological descriptions that are contributions from this current work to catchment understanding. Black boxes contain pre-existing literature information. .... 229
- Figure 7.2. Chemical Conceptual Model of the study area and Kilham showing the key chemical processes in the model. Red call out boxes and texts are contributions from this current work to catchment understanding. Black boxes contain pre-existing literature information ..... 235

## Abbreviations

ADE	Advective dispersive equation
bgl	Below ground level
BGS	British Geological Survey
CB	Casing base
CCTV	Closed circuit television
C-J	Cooper-Jacob
DTM	Digital terrain model
EA	Environment Agency
EC	Electrical conductivity
EU	European Union
EU WFD	European Union Water Framework Directive
E-W	East west
mAoD	Metres above ordnance datum
mbgl	Metres below ground level
NGR	National Grid Reference
NNE	North North East
NRFA	National River Flow Archive
NVZ	Nitrate vulnerability zone
Max GWL	Maximum groundwater level
Min GWL	Minimum groundwater level
REV	Representative elementary volume
RWL	Rest water level
SEC	Specific electrical conductivity
SPZ	Source Protection Zone
SSE	South South East
tcmd	Thousand cubic metres daily
TDS	Total dissolved solids
TLC	Temperature, water level and conductivity
UK	United Kingdom
UK AIR	United Kingdom Air Information Resource
UK MET Office	United Kingdom Meteorological Office
UKEAP	United Kingdom Eutrophying and Acidifying Network
UoB	University of Birmingham
UoL	University of Leeds
USZ	Unsaturated zone
VE	Vertical exaggeration
WB	Well bottom
WC	Water column
WHO	World Health Organisation
WRC	Water Research Centre
YW	Yorkshire Water
ZFP	Zero flux plane

## List of symbols

$C$	Tracer concentration
$Q_o$	Horizontal volumetric inflow rate of formation water through a well interval
$r_w$	Well radius
$\alpha_B$	Longitudinal coefficient of dispersivity
$q_w$	Horizontal specific discharge in well in a specific depth interval
$q_f$	Horizontal specific discharge in through the formation in a depth interval
$v_{fh}$	Average linear velocity of groundwater in the formation
$\alpha$	Flow correction convergence factor from formation to the well
$V$	Dilution volume in well interval
$A$	Cross-sectional area of well interval
$m$	Slope of tracer decay line
$D_f$	Formation diameter
$D_w$	Well diameter
$\phi_e$	Flowing or effective porosity
$u_v$	Vertical velocity in well
$Q_v$	Vertical discharge in well
$t_{cf}$	Characteristic fracture diffusion time
$a_f$	Fracture aperture size
$D_e$	Effective diffusion coefficient
$\phi_m$	Matrix porosity
$V_{ij}$	Volume of tracer injected
$h_t$	Testable depth
$d_{inj}$	Diameter of injection tube
$t$	Time
$\alpha_T$	Temperature compensation factor
$c_i$	Concentration, $\text{mgL}^{-1}$
$\gamma_i$	Activity coefficient
$Z_i$	Charge of $i_{th}$ ion in solution
$\Lambda_i$	Equivalent electrical conductivity of the $i_{th}$ ion
$a_i$	Activity of $i_{th}$ ion in solution
$M_i$	Molar mass of $i_{th}$ ion in solution
$m_i$	Molal concentration of $i_{th}$ ion in solution
$r_i$	Hydrated ion size
$I$	Ionic strength
$SEC_i$	The specific electrical conductivity of the $i_{th}$ ion
$t_n$	Transport number
$S_t$	Stanton Number
$h_i$	Mechanical energy per unit weight of water at a point in an aquifer
$Z_i$	Elevation head
$\rho_i$	Density of groundwater

$P_i$	Groundwater gauge pressure at the measurement point
$g$	Acceleration due to gravity
$h_{pi}$	Pressure head
$P_{atm}$	Atmospheric pressure
$P_{abs}$	Absolute pressure
$P_{wc}$	Pressure of column of water above transducer
$\gamma_w$	Unit weight of water
$h$	Depth of transducer sensor below measurement point
$TZ^+$	Total major cations concentration, meq/L
$TZ^-$	Total major anions concentration, meq/L
$T_f$	Fracture transmissivity
$T$	Transmissivity of well with respect to a saturated depth
$N$	Number of probable conductive fractures
$\nu$	Kinematic viscosity
$i_f$	Hydraulic gradient in fracture

## **Chapter 1 Introduction : Project Background and Setting**

### **1.1 Importance of the Chalk Aquifer and its vulnerability to contamination**

The Cretaceous Chalk is a very important aquifer in North-West Europe (Downing et al., 1993). In the United Kingdom (UK), the Chalk which crops out in the eastern and southern part of England (Figure 1.1) is the most important aquifer (Allen et al., 1997; Downing, 1998; Knapp, 2005). Groundwater contributes a third of public water supplies in England and Wales, with the Chalk providing about 60% of public water supply (Downing, 1998). The Chalk aquifer derives its high transmissivity from a well-developed network of solutionally-enhanced fine and large fractures, bedding plane features and karstic conduits (Allen et al., 1997). In East Yorkshire, where the study area (marked in red on Figure 1.1) is located, the Chalk is the main source of potable water supply for the industries and inhabitants of the area (Edmunds et al., 2001; Smedley et al., 2004; Gale and Rutter, 2006), with the Environment Agency (EA) licensing about 195 million L/day to abstraction (ESI, 2010). Aside from the abstractions, the two most important tributaries that support the ecology of the area and feed the River Hull are almost entirely groundwater sourced from the study area (Foster, 1974; ESI, 2010; National River Flow Archive (NRFA), website <https://nrfa.ceh.ac.uk/data/search>).

In spite of the usefulness of the Chalk aquifer for East Yorkshire, it is vulnerable to contamination from nitrate and organic agrochemicals such as atrazine, DCM (dichloromethane) and trihalomethanes (Smedley et al., 2004). The Chalk aquifer is characterised by a high storage but low permeability matrix, with low storage but high permeability secondary flow features. The secondary flow features control the bulk of the water flow both in the saturated and unsaturated zones (Foster and Milton, 1974; Price, 1987; Younger and Elliot, 1995). On the other hand, the fine matrix structure controls the diffusive exchange of solutes and storage especially in the unsaturated zone (Barker and Foster, 1981). In East Yorkshire, the Chalk outcrop and recharge area of the aquifer which is heavily dominated by agricultural activity, is characterised by thin soils and a

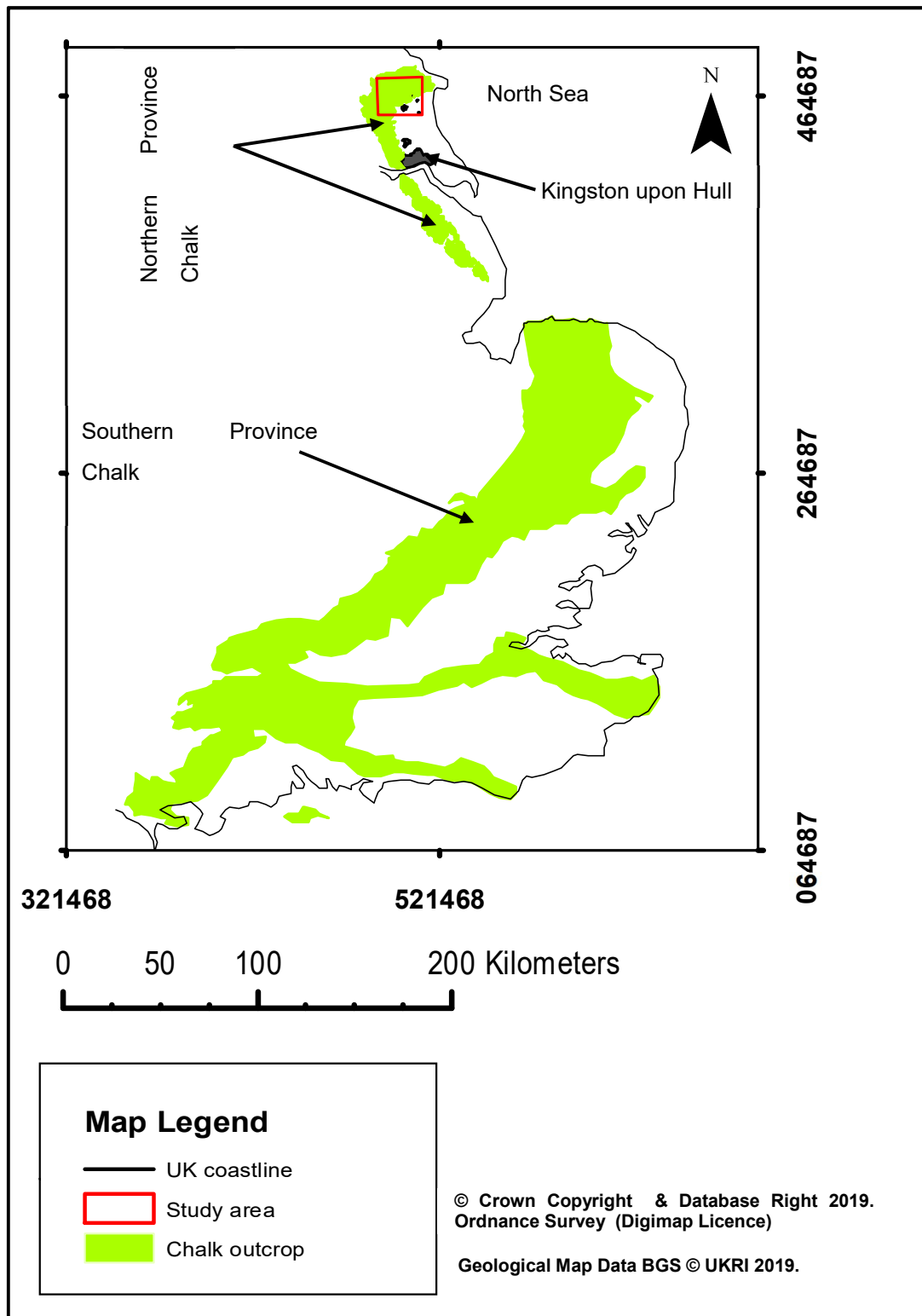


**Figure 1.1:** Chalk outcrop in the UK with the study area marked in red. See Figure 1.2 for the location map of the study area.

thick unsaturated zone. The combination of the agricultural activity, thin soils, matrix and fracture behaviour makes the aquifer vulnerable to contamination by agrochemicals especially nitrates via transport from the unsaturated zone to the

water table. The diffusive exchange between the matrix and fracture results in attenuated and delayed but prolonged release of solutes to the saturated zone, whereas the fracture dominated flow in the unsaturated zone can also rapidly transport contaminants to the saturated zone. Characterising and predicting water quality in the aquifer then requires an appreciation of the key flow and transport processes that occur within the hydrogeologic continuum via input from the unsaturated zone, throughput in the saturated zone and output to springs and abstraction.

## **1.2 Nitrate contamination history, its impacts and management practices**

Increasing nitrate concentrations since the mid-twentieth century and more recently the detection of persistent pesticides like atrazine, DCM and trihalomethanes in the study area (Smedley et al., 2004) has made the hydrogeology of the East Yorkshire Chalk and Kilham area (Figure 1.2), the subject of active research.

On the East Yorkshire Chalk,  $\text{NO}_3^-$  concentrations  $< 2$  mg/L are indicative of natural baseline conditions (Foster et al., 1982; Foster, 2000), so that  $\text{NO}_3^-$  concentrations  $> 2$  mg/L are seen as anthropogenically derived. In the area, nitrate concentrations in groundwater above the WHO drinking water limit of 50 mg/L as  $\text{NO}_3^-$  or 11.3 mg/L as N is mainly from the increased post second world war (1956 – 1971) diffuse application of nitrogenous fertilizers to farmlands (Foster and Crease, 1974; Lawrence et. al, 1983; Buss et al., 2005). Post-war application of fertilizers to farmlands drastically increased by four and half times ( $93 \text{ kg N ha}^{-1} \text{ yr}^{-1}$ ) that of pre-war values, ( $20 \text{ kg N ha}^{-1} \text{ yr}^{-1}$ ) ( Figure 1.3). Foster and Crease (1974) used fertilized and unfertilized unsaturated zone soil profiling to show that post-war landuse change was responsible for increased nitrates concentrations under fertilized farmlands. The driver for Foster and Crease (1974)'s profiling was in response to increasing nitrate concentrations in abstraction wells and springs on the East Yorkshire Chalk (Figure 1.4). Prior to the 1970s, N concentrations on the East Yorkshire Chalk aquifer ranged between 2.5 – 4.5 mg/L, but post 1974 concentrations increased to between 7.5 – 11.5 mg/L. This nitrate time lag effect (nitrate time bomb concept) is a

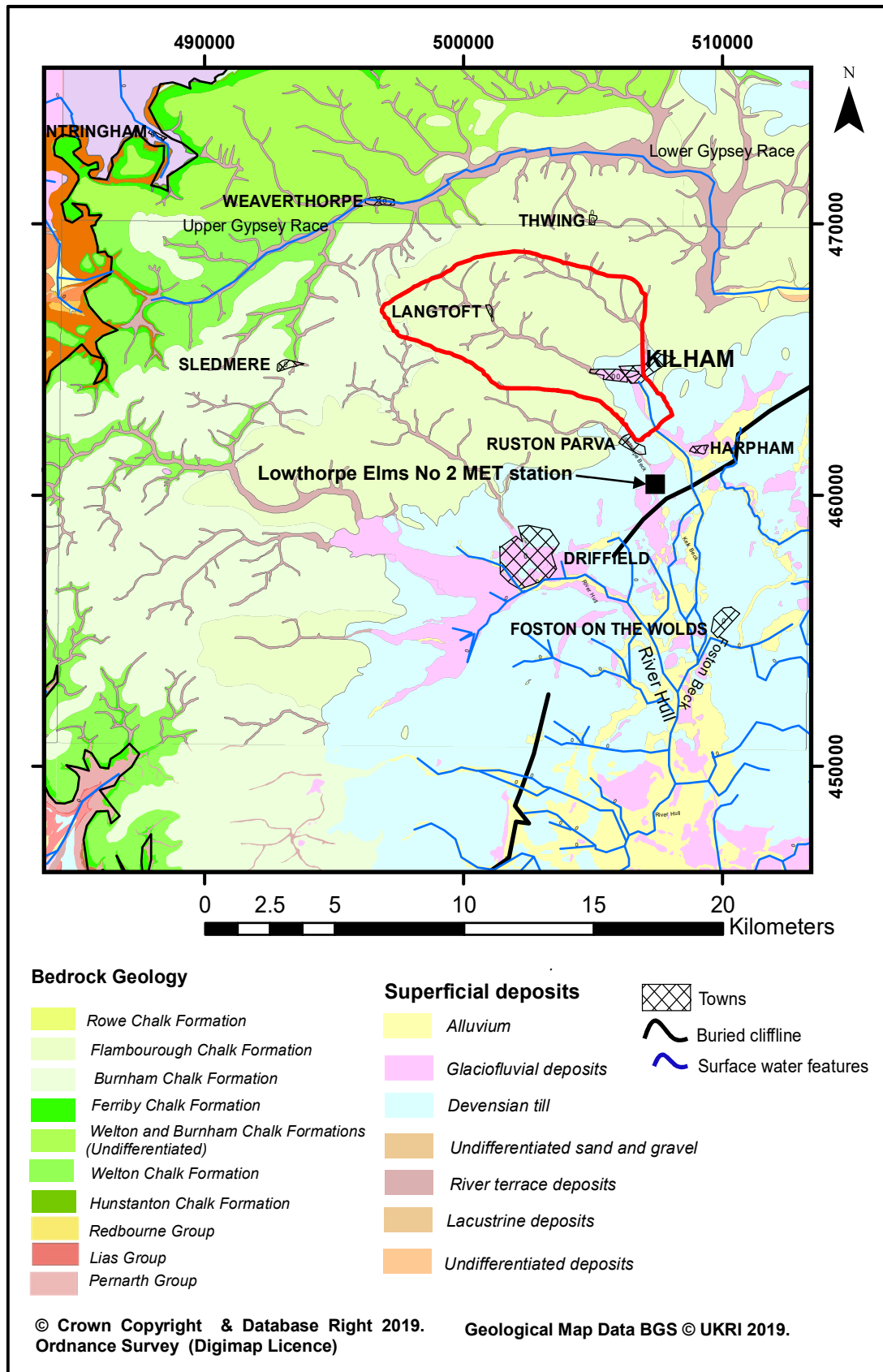


**Figure 1.2:** Location map of study area on geology, with Kilham Catchment, based on topographic highs, marked in red.

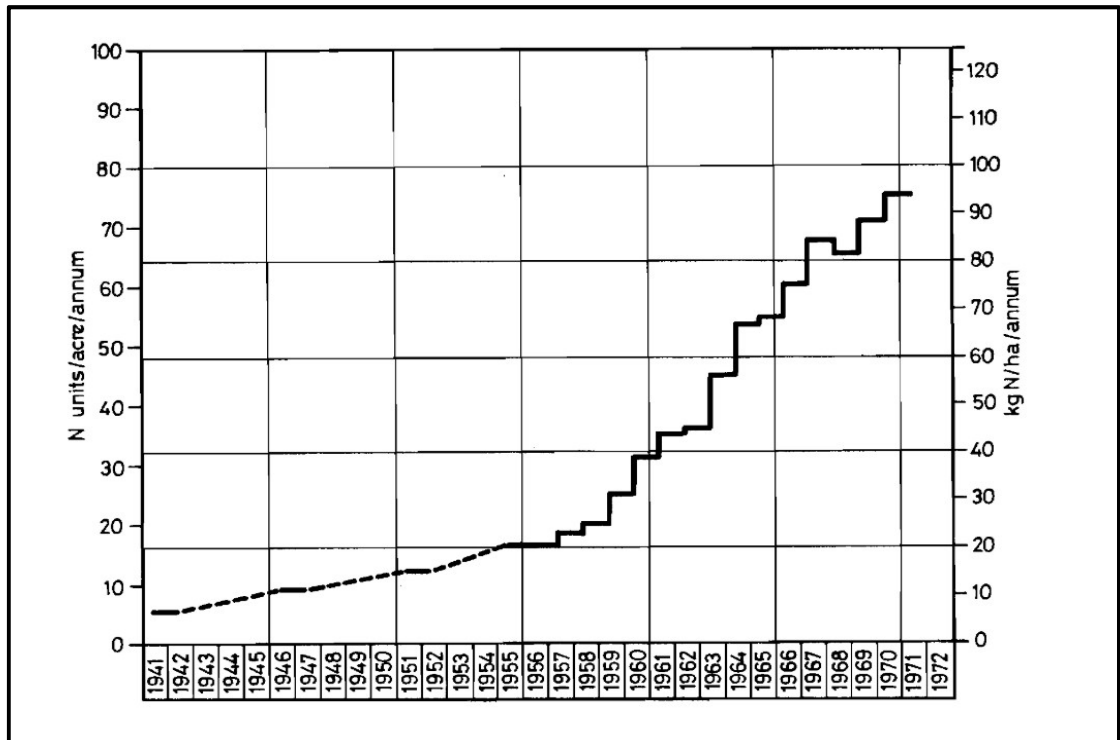


Figure 1.3: Fertilizer nitrogen application rate between the years 1941 – 1972 for the East Yorkshire Region. From Foster and Crease (1974), page 191.

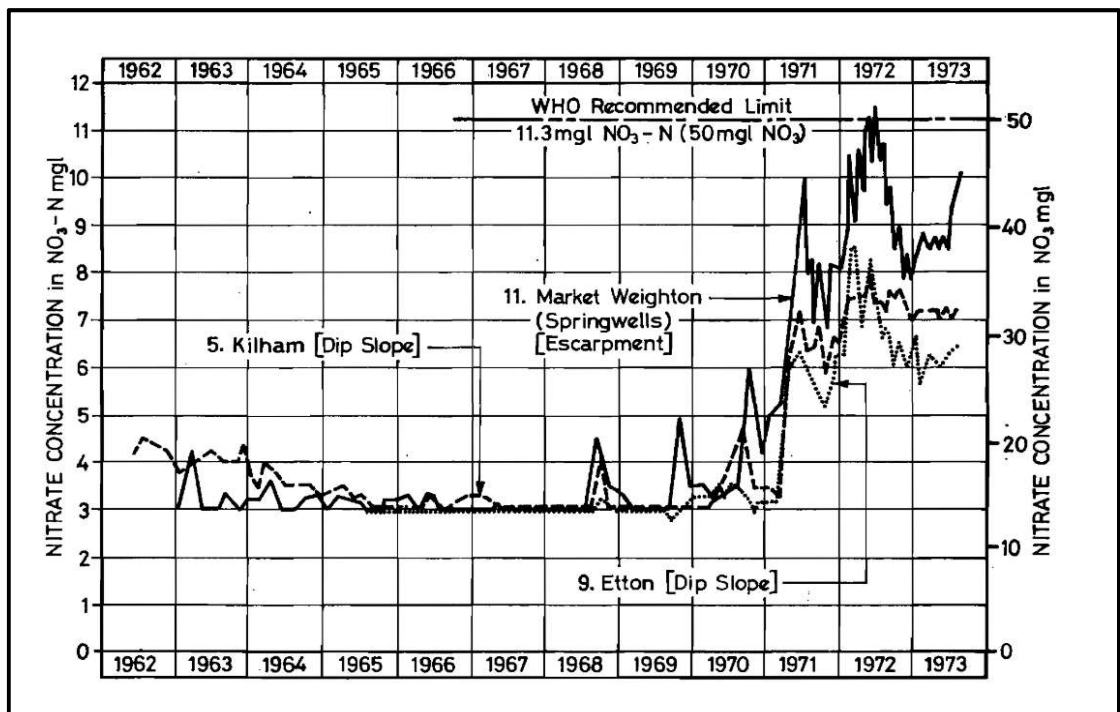
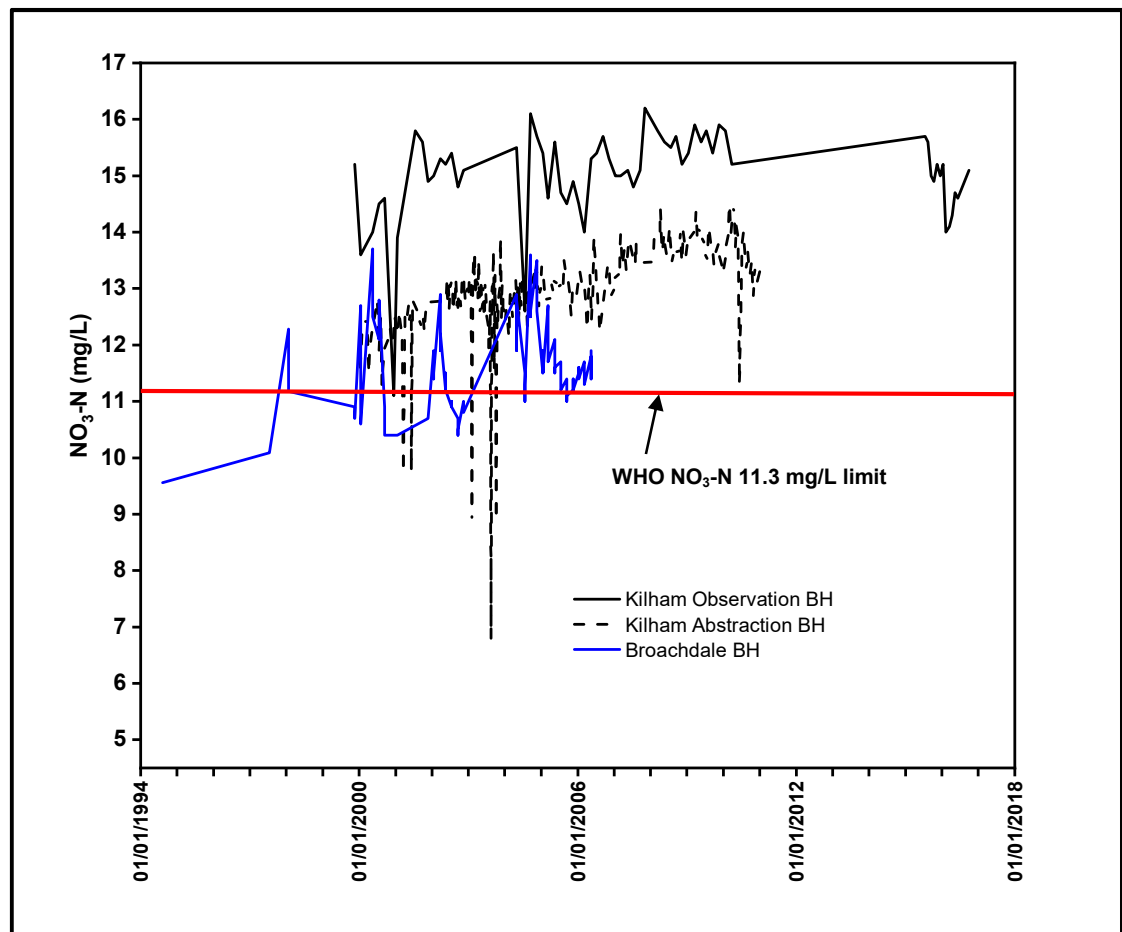


Figure 1.4: Trend of increasing nitrate concentration in some selected wells and springs in East Yorkshire. Foster and Crease (1974), page 181.

function of the thick unsaturated zone, slow downward movement of  $\text{NO}_3^-$  due to diffusive exchange between the fracture and the chalk matrix. The implication of this time lag is that it is difficult correlate nitrate in groundwater with application rates on the land surface. Foster and Crease (1974) predicted that N concentrations in groundwater would keep rising to exceed the WHO limit of 11.3 mg/L in the early 1990s. Recent (1994 – 2016)  $\text{NO}_3\text{-N}$  in groundwater concentrations (Figure) show that N concentrations have exceeded the WHO guideline and have stabilised (Figure 1.5), suggestive of a constant term source.



**Figure 1.5.** Recent nitrate trends in wells in the study area, from EA archived geochemical dataset.

Nitrate in surface water and groundwater has health, economic, ecological and management implications on the resource. Nitrate when reduced to nitrite in the human gut binds with haemoglobin to deprive the body of oxygen resulting in methaemoglobinaemia, which can lead to death in new-borns (Greer and Shannon, 2005; World Health Organisation, 2011). Treatment of nitrated water to acceptable drinking water standards costs a huge amount of money to the UK water industry and ultimately impacts on the consumer. Between 1992 – 1997 water treatment cost amounted to about £16 million per annum (Dalton and Brand-Hardy, 2003). More recently, Defra estimated in 2015 that in England, the water industry and businesses spend about £5 billion annually to protect the water environment and public health from against nitrate contamination (UKWIR, 2018). Treating nitrate polluted water is also energy and carbon intensive. Wells with excessive nitrates can also be abandoned in the process leading to loss of the resource (Knapp, 2005). Excess nitrates can also cause eutrophication of surface water bodies, leading to algal growth and enrichment of streams, rivers and ponds. Low oxygen levels from nutrient enrichment can also cause fish and invertebrates to die. Eutrophication can also cause objectionable and undesirable effects like increased turbidity, offensive odours and discolouration of surface water sources ([www.fwr.org](http://www.fwr.org)).

The increase in nitrate concentrations resulted in the delineation of the East Yorkshire Chalk aquifer as a Nitrate Vulnerable Zone (NVZ), in accordance with the European Commission Nitrate Directive, European Commission (1991). The contamination in the unconfined area and abstraction pressures in the confined part of the aquifer has ultimately resulted in the classification of the aquifer as being in 'Poor' status in terms of quality and quantity under the European Water Framework Directive (EU WFD) (ESI, 2010). More recently, a series of hydrogeological studies and modelling work for the East Yorkshire Chalk and the study area were commissioned by the Environment Agency (EA) to:

- i. inform effective decision making for the management of the resource and;

- ii. meet the EU WFD directive (European Commission, 2000), by providing evidence to support the institution of measures to restore the resource to good status / reverse trends.

The known preventive and management methods for nitrate contamination are via a combination of land retirement from production, highly effective and efficient agricultural management practices, provision of evidence via water quality monitoring (Ford and Williams, 2007), effective development planning and land-use regulation, and catchment delineation (Keim, 2013). Catchment delineation requires the characterisation of catchment flow regimes and knowledge of the hydrogeologic continuum with respect to the input, throughput and output functions of the aquifer (Misstear and Brown, 2007; 2013).

### **1.3 The importance and relevance of this work**

Because of the importance of the Chalk aquifer with its vulnerability to contamination, the East Yorkshire Chalk especially the area around Kilham has been a place of active hydrogeological research since the 1970s. Section 3.1 discusses these previous works and how they underpin the current work. Section 3.2 also throws light on the peculiar characteristics of the study area and the Kilham Catchment and justifies the reasons for the choice of the Study Catchment for this thesis. However, here in this current section, a general overview of the previous works will be presented to justify the relevance and importance of this current research.

Knowledge about the hydrogeologic continuum between the input, throughput and output functions within a fractured aquifer like the Chalk is very important as it provides the information on where, how and when to focus attention for effective resource management and protection. Unsaturated zone studies provide information about the source (Foster et al., 1982; Lawrence et al., 1983), amount, residence time of water and contaminants (Smith et al., 1970; Zaidman et al., 1999; Allshorn et al., 2007; Keim et al., 2012) and chemical signature and evolution (Pitman, 1978a) of recharge to the saturated zone. Saturated zone or throughput studies provide information on the groundwater velocities, flow horizons and borehole connectivity (Buckley and Talbot, 1994; Ward et al., 1998; West and Odling, 2007; Parker et al., 2010) and residence

times, resource volumes and evaluation (Foster, 1974; Foster and Milton, 1974; Foster and Crease, 1975; Foster and Milton, 1976), the key transformation reactions that influence resource chemistry and contaminant transport within the saturated zone (Pitman, 1978a; Pitman, 1986; Elliot et al., 2001; Smedley et al., 2004). Characterising springs that discharge from fractured aquifers provide a wealth of information about aquifer structure, geometry and whether the saturated zone is active or passive in determining the chemistry of the output from the aquifer (Kresic, 2010).

The reasons for the relevance of the current work are presented below.

Firstly, the previous research works in the study area only examined parts of the continuum in isolation without integrating the relationships between input, throughput and output processes. The current work however, sets out to develop a continuum model that provides information on the key hydrogeological processes and provides a link and relationship between the parts of the continuum by drawing on findings from previous unsaturated zone studies and conducting fieldwork activity and monitoring on aquifer throughput and output processes. The model then goes on to provide information on where, when and how to focus effort for aquifer protection and management for the study catchment.

Secondly in spite of the numerous springs that discharge from the aquifer, springs have rarely been studied to provide information about the aquifer structure and geometry. In this study, spring specific electrical conductivity (SEC) and temperature signature are monitored to provide information about aquifer recharge mechanism, geometry and structure. In addition, major ion chemistry monitoring of springs from spring sampling is undertaken as this is a very informative way of analysing how the aquifer responds to seasonality and input and output stressors.

Thirdly, previous unsaturated zone studies in the area (Zaidman et al., 1999; Allshorn et al., 2007; Keim et al., 2012) have shown evidence of rapid bypass flow in the unsaturated zone. However, because most of these studies were conducted very far above the water table, there is no direct conclusive evidence to show that bypass flow reaches either the water table or springs very quickly. This study however, monitored and logged temperature and

specific electrical conductivity (SEC) at the springs and known flow horizons in boreholes every hour with the objective of detecting the rapid bypass flow to the saturated zone and springs.

Additionally, for a fractured aquifer like the Chalk, knowledge of preferential flow horizons, the form and pattern of connectivity between boreholes and the vertical head gradients in wells enables the design and development of abstraction wells, as it determines position for the placement of casing and screens (Gossell et al., 1999). Also, the knowledge enhances groundwater flow model results and enables the effective targeting of horizons to sample and pump water from (Moir et al., 2014; McMillan et al., 2014). Vertical head gradients are especially important in groundwater level and flow direction interpretation (Saines, 1981; Brassington, 1992; Dalton et al., 2006; Weight, 2008) and in analysing well water chemistry data (McMillan et al., 2014). A lot of information about the geometry and flow structure can also be gleaned from well connectivity and flow horizon distribution in the aquifer. Previous works like Foster and Milton (1974), Buckley and Talbot (1994; 1996), Southern Science Ltd (1994) and Parker (2009) have shown flow occurring at discrete horizons and the occurrence of vertical head gradients in boreholes. This current work uses the uniform and point ambient open-well dilution tests, in conjunction with previous well characterisation tests and tracer tests to constrain the flow horizons, flow geometry, velocity and structure for the study area and the Kilham Catchment.

Finally, the study area and the Kilham Catchment are known to be geologically complex with several faults traversing the area, but the impact of these faults on groundwater flow is not known. Recently, Farrant et al. (2016) mapped a number of faults in the area, and postulated that these faults have the potential to impact on groundwater flow both on the local and regional scale. This current study is comparing the distribution of transmissivities obtained from archived pumping test data in relation to the location of identified and mapped faults in the area. The objective of doing this is to correlate the location of faults with the distribution of transmissivities for the study area.

## **1.4 Project aim and objectives**

With the relevance of the current work presented in section 1.3 above, this project has the overall aim of gaining insight into the flow forms, patterns, velocities and regimes of the study area and the Kilham catchment, in the East Yorkshire Chalk aquifer.

A number of hydrogeological field monitoring and literature review activities were undertaken to meet the project aim via a series of four (4) main objectives as:

- A. Characterisation of flow geometry and topology in the saturated zone;
- B. Characterisation of the response of boreholes (throughput) and springs (output) to recharge and rainfall events (input);
- C. Characterisation of the effects of faults on groundwater flow in the study area;
- D. Development of a hydrogeological conceptual model to improve catchment processes and management.

The sub-objectives under the main objectives are now itemised as follows.

### **A. Characterisation of flow geometry and topology between wells in the saturated zone, and to the aquifer output.**

- A1:** To conduct ambient open-well dilution tests for the determination of flow horizons, flow velocities and vertical head gradients in wells;
- A2:** To re-interpret previous tracer tests and well characterisation in association with sub-objective A1 for the determination of borehole connectivity, local scale flow velocities and flow topology;
- A3:** To use flow geometry and topology of the catchment to inform saturated zone flow processes;
- A4:** To validate single well test approaches for obtaining groundwater velocity against well-to-well test data.

### **B. Characterisation of the response of boreholes (throughput) and springs (output) to recharge and rainfall events (input).**

- B1:** To undertake borehole flow horizon specific electrical conductivity (SEC) and temperature monitoring in order to “see” recharge events;
- B2:** To analyse composite groundwater head and Foston Beck ( discharge hydrograph and then use the monitoring data to correlate with rainfall events;
- B3:** To monitor spring SEC and temperature via loggers;
- B4:** To collate and analyse rainfall data from UK Meteorological Office Weather Station at Lowthorpe Elms No. 2 (TA 074 611), about 3.5 km south of Kilham Village;
- B5:** To collate and analyse rainfall chemistry data at High Muffles (SE 775 939), a UK air quality monitoring site during the study period;
- B6:** To sample and characterise spring major ion chemistry within the study period;
- B7:** To review major ion water chemistry characteristics as a framework for interpreting input signals to the aquifer.

**C. Characterisation of the effects of faults on groundwater flow in the study area.**

- C1:** To review previous literature on transmissivity distribution in the Kilham Catchment;
- C2:** To analyse archived pumping tests in the Kilham area;
- C3:** To compare the location of the transmissivities from C2 with fault traces in the Kilham area.

**D. Development of a hydrogeological conceptual model to improve catchment process understanding for effective catchment management.**

- D1:** To use the findings from objectives A to C develop a hydrogeological conceptual model, describing and characterising the input, throughput and output functions of the aquifer in the study area.
- D2:** Describing and commenting on the implications of the findings from the current work on catchment management practices.

## 1.5 Thesis layout

This thesis is made up of eight Chapters.

**Chapter 1** presents a brief overview of the relevant issues pertaining to this thesis. The Chapter outlines the hydrogeologic importance and vulnerability of the Chalk. Project aims and objectives and thesis layout are also described.

**Chapter 2** is a literature review of the Northern Chalk and the Study Catchment. The geology, hydrogeology and topography are described with the aim of linking the structure and functioning of the aquifer with its geology and topography.

**Chapter 3** focuses on the peculiar characteristics of the study area and the Kilham Catchment and presents a justification of the choice of the Study Catchment for this thesis. Details of previous relevant work and archived data about the study area undertaken by several stakeholders and how these works support the current work are described to position the current work.

**Chapter 4** concerns the open-well dilution tests and results. The chapter discusses the importance, field methodology and theory of the open-well dilution testing in the characterisation of fractured aquifers. Then results of the ambient open-well dilution tests used in the charactering wells in this work are presented, interpreted and compared with other previous relevant well characterisation works with the aim of identifying areas of divergence and convergence of interpretation. The chapter ends with a summary of main findings.

**Chapter 5** presents spring and well monitoring results. The theory and hydrogeological importance of springs discharging from fractured aquifers are discussed. Then the theory underlying the use of specific electrical conductivity (SEC) and temperature as natural groundwater tracers in the hydrogeological characterisation of fractured aquifers is presented. Following this, results of spring and well temperature and SEC monitoring and sampling are presented and discussed. Also groundwater level and Foston Beck discharge hydrograph monitoring and their correlation with rainfall data results are presented and discussed. The discussion focusses on the understanding of key hydrogeological processes and mechanisms gleaned from: the sources of

major ions in the aquifer and springs, the seasonal thermal and SEC characteristics, and the relationship between well and stream hydrograph with respect to rainfall patterns. Then the chapter ends with a summary of findings.

**Chapter 6** synthesises findings from the current and previous works. The chapter starts by combining and re-interpreting previous tracer tests, well logging characterisation and open-well dilution tests in the study area for an improved understanding of well connectivity, flow geometry and topology. The validation of the open-well dilution method for determination of groundwater velocity against velocity from well-to-well tracer tests is discussed, and the generic findings are critically assessed. Then transmissivity distribution is reiterated. The chapter then ends with a summary of findings.

**Chapter 7** develops and draws a hydrogeologic conceptual model by drawing on the findings from the previous chapters. Two complementary models are developed: a physical and a chemical model. In these models, the contributing findings from this current work to catchment understanding are stated. The chapter ends by discussing the hydrogeological implications of the findings from this current work.

**Chapter 8** concludes this Thesis. The chapter starts by comparing the current findings vis-à-vis the aim and objectives of this work. Then recommendations to direct further research with the aim of building on and improving the current work and its findings are given.

## **Chapter 2 Literature Review of Study Area**

To understand the physical and chemical hydrogeology of the Chalk, its geology has to be appreciated. This literature review has the aim of presenting the geological factors that affect groundwater flow in the Chalk of East Yorkshire, with a focus on the Kilham catchment. The literature review starts by presenting the geology of the Chalk by highlighting its depositional, Quaternary and tectonic histories, lithology and diagenesis. Secondly, the effects of these geological factors on aquifer behaviour for unsaturated and saturated flow processes are discussed. The effects of the relatively low matrix permeability, large fracture permeabilities and porosity and solute diffusion will be discussed with respect to recharge potential, resource assessment and contaminant fate and transport from the unsaturated zone to the saturated zone. Then flow layering and aquifer heterogeneity with regards to transmissivity and resource estimation are discussed. Finally the effects of geology on surface water features and groundwater geochemistry are considered.

### **2.1 Study area**

#### **2.1.1 Physiography, catchment economic activity and surface water hydrology**

The catchment under investigation is in the unconfined and semi-confined portions of the East Yorkshire Chalk Aquifer (Figure 2.1 and Figure 2.2). Soil cover on the Chalk outcrop is made up of thin, light textured, calcareous free draining, brown silty rendzinas of thickness ranging from 0.2 to 1.0 m (Foster and Crease, 1974). In the confined and semi-confined areas, heavy clayey loams overlay the superficial deposits. The clay content causes drainage problems and seasonal waterlogging in the Hull valley and Holderness Plains (Smedley et al., 2004). Arable farming dominates economic activity in East Yorkshire with wheat and barley as the dominant arable crops in the area. The land is also cultivated for pasture, oil seed rape, sugar beet, potatoes, vegetables, peas and beans. In terms of animal farming, dairy and beef production is also significant in the area (Smedley et al., 2004)

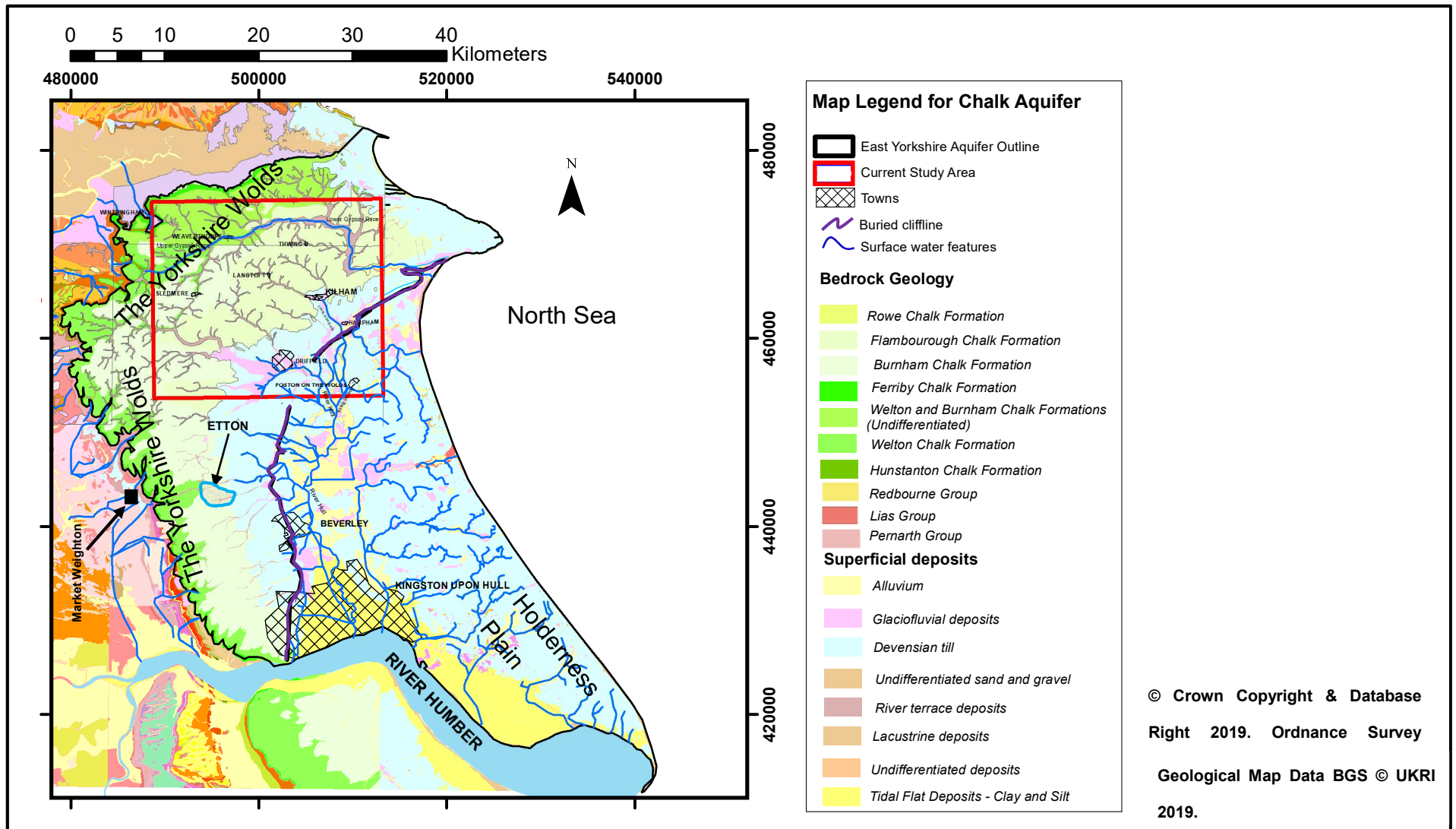
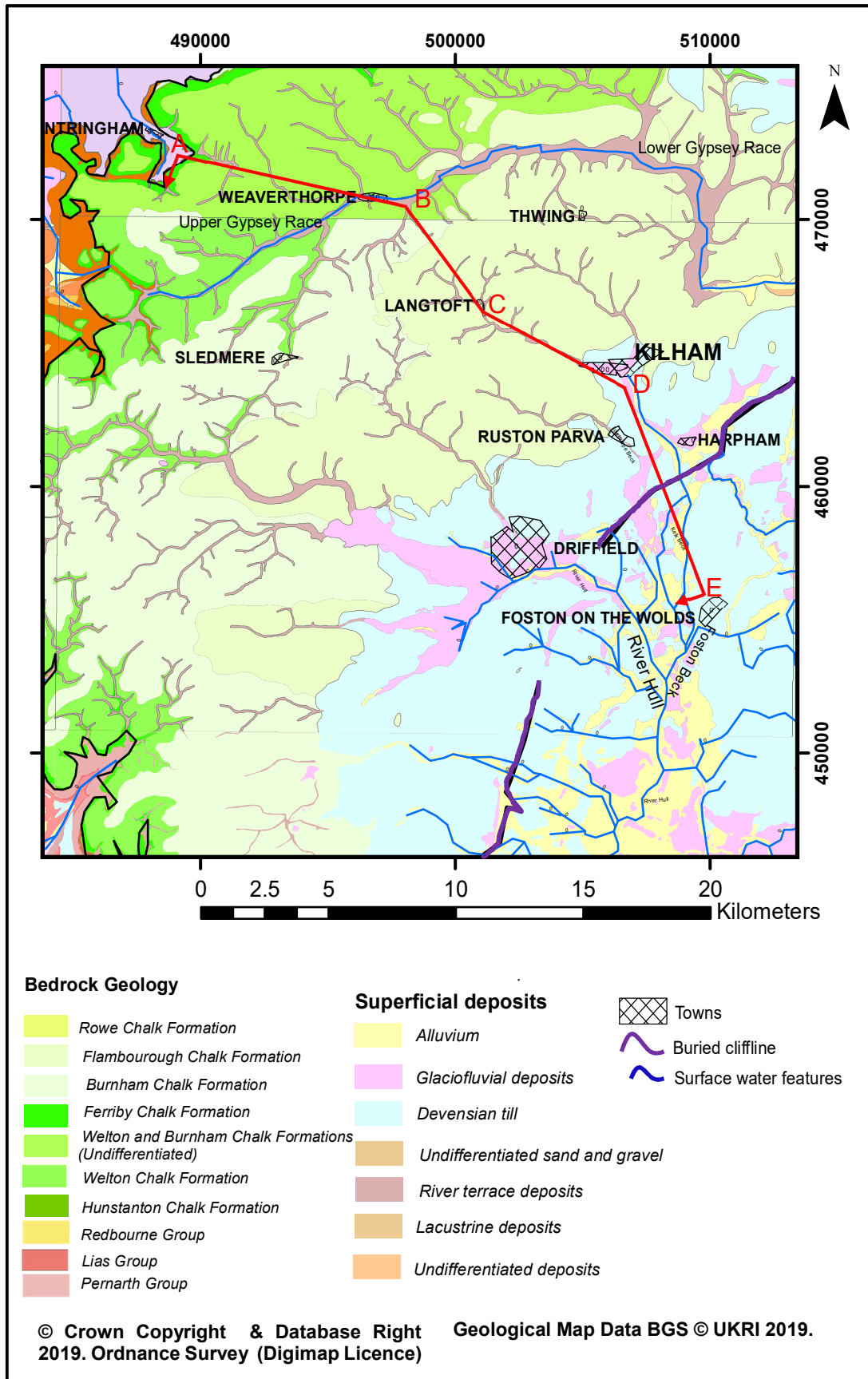


Figure 2.1: Bedrock and superficial geology map of the Chalk Aquifer of East Yorkshire showing the current study area (red square).



**Figure 2.2:** Bedrock and superficial geology of the study area. Section ABCDE cut through profile (Figure 2.4) where borehole information on BGS GeoIndex is available.

The Chalk crops out in the west and north of East Yorkshire, where the scenic, rolling and treeless Yorkshire Wolds has an altitude of up to 220 mAoD (Figure 2.3), forming a characteristic west facing escarpment and an east facing dip slope ( Figure 2.4 ) (Smedley et al., 2004). The elevations reduce through the semi-confined edge of the aquifer to form the flat plains of the Hull Valley and Holderness Plains with elevations reducing to as low as 10 m AoD. In the study area, the highest elevations are found on the south-western and northern areas, on the Yorkshire Wolds, which forms the main recharge area of the aquifer. The elevations reduce sharply to form a tableland between Sledmere, Langtoft, Weaverthorpe and Thwing with some characteristic dry valleys around the plateaus. Then the elevations reduce gently amid the rolling topography towards Kilham, which forms part of the lower edge of the dip slope, reducing elevations to about 35 mAoD. From Kilham, the elevations reduce gently towards Harpham, to about 22 mAoD around the Harpham area, then flatten off to around 10 mAoD around Foston on the Wolds, where the Foston Beck joins the West Beck to form the River Hull. On the scarp side of the area, the elevation exhibits a steep slope with elevations falling sharply from the highs to about 40 mAoD.

Surface water occurrence on the Wolds is rare, but for the Gypsy Race, a stream that flows for its entire length from around Duggleby to Bridlington only when groundwater levels are high (Allen et al., 1997). Springs occur at the confined aquifer edge, although there are some springs up to 5km into the superficial cover. The springs flow into streams that feed the 2 main tributaries of the River Hull. These main tributaries are the West Beck and the Foston Beck. The tributaries join at North Frodingham to become the River Hull. There are also escarpment springs that occur at the contact between the Chalk and the underlying Jurassic strata (Foster and Milton, 1976).

The Gypsy Race is divided into the Upper and Lower reaches. The upper reach starts from escarpment slopes around Duggleby, decreasing in discharge whilst flowing about 10km before typically ceasing to flow at

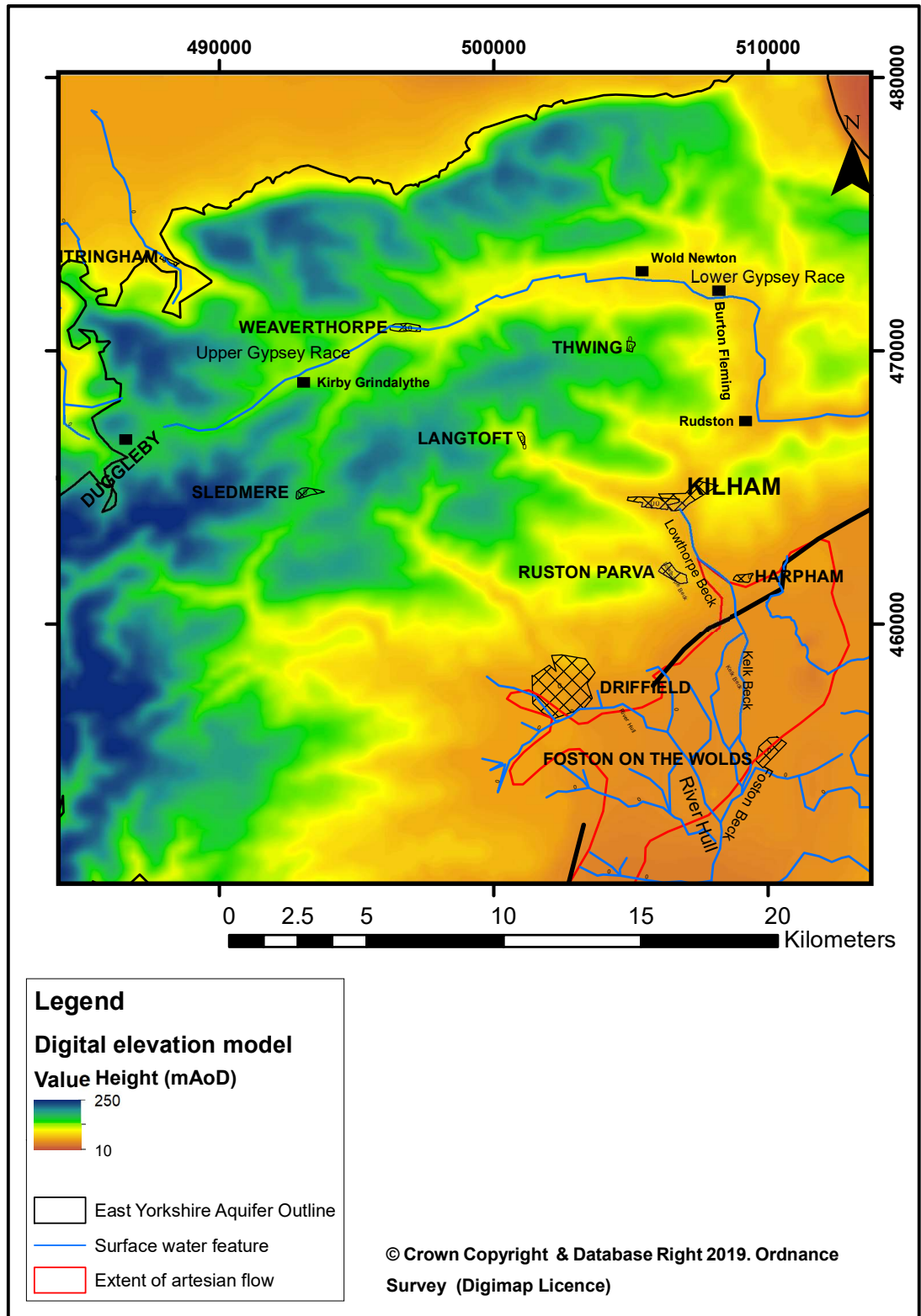


**Figure 2.3:** Digital terrain elevation model of study area showing elevation highs (deep blue) to topographical lows (brown) with the main surface water and drainage features.

Weavertorpe due to bed leakage. At Kirby Grindalythe it has a summer and winter flow of  $5.2 \times 10^3$  and  $17 \times 10^3 \text{ m}^3 \text{ d}^{-1}$  respectively. When groundwater

levels are high, the Upper Gypsey Race flows to join the Lower Gypsey Race before discharging into the North Sea at Bridlington. The Lower Gypsey Race emanates from springs around Wold Newton, Burton Fleming and Rudston. The Lower Gypsey Race is both effluent and influent along its reach at different times and at different locations (Allen et al., 1997).

The River Hull is the dominant surface water body that drains the catchment. The Hull is fed by its groundwater streams Foston Beck and West Beck, although during high precipitation, surface drainage and bank storage also contribute to flow in the tributaries (Foster, 1974). The River Hull flows through areas which are mostly at sea-level for which reason the Hull is embanked to prevent flooding of the low lying areas. Drainage from the low-lying field drains around the embanked River Hull is pumped upwards into the Hull River. The Hull flows across the Holderness Plain, through Kingston-upon-Hull to join the Humber. The River Hull is tidal below Hempholme Lock.

### **2.1.2 Chalk formation and lithology**

The Cretaceous Chalk in the United Kingdom occurs in the north-eastern to the south-eastern part of England. There are two provinces of the Chalk: the Northern and Southern Provinces (Figure 1.1). The catchment under study is located in East Yorkshire and falls under the Northern Province (Figure 2.1 and Figure 2.2). The Northern Province Chalk rests unconformably on the deposits from the Jurassic (Lower Lias) and Lower Cretaceous Speeton Clays. The Chalk in East Yorkshire reaches over 500m thick (Gale and Rutter, 2006), but it is up to 800m thick offshore (Bloomfield and Shand, 1998; Gale and Rutter, 2006).

Between 66 – 145 million years ago, over a 35 million years period, when the area surrounding the current North Sea was located at a latitude 10° degrees further south than its current position, average temperatures were warmer than today and the sea level was several metres higher, soft white microscopic plankton algae and shell fragments from shallow waters were deposited on the seabed, and these deposits hardened through diageneses to form Chalk. The Cretaceous Chalk is an important formation occurring in not only the United Kingdom but in other north-western European countries like France,

Belgium, Netherlands, Germany, Denmark and Sweden (Downing et al., 1993).

Chalk is a fine grained pure soft biogenic limestone (with calcite making up 80 – 92% of the Chalk) derived from the coccolith mud generated from plates of coccolithophorids (Patsoules,1989). In addition to coccolith mud, the Chalk also contains clays of which smectite is the most dominant and coarse fraction (10–100 µm) which includes foraminifers, ostracods, bryozoans, echinoid plates and bivalve fragments (Hancock, 1993).

The chalk-ooze was deposited with an initial porosity of 70% to 80% but the processes of intrinsic and non-intrinsic diagenetic processes like bioturbation reduced both the porosity and permeability of the matrix (Hancock, 1993). The final state of burial diagenesis was influenced by both mechanical compaction and pressure solution. During early diagenesis, mechanical compaction is dominant reducing porosity to 35-50% for 250m overburden, with a slight reduction of porosity to 30-40% at depths of 1000m, after which pressure solution which depends on pore fluid chemistry and grain to grain contact dominates. Pressure solution would result in porosity of 15-20% for 1500-2000m overburden, but achieves a similar porosity if sediment is flushed by fresh water at burial depths of 300-500m (Scholle,1977; Hancock, 1993; Bloomfield,1997). Pressure solution effects are also known to reduce permeability of the Chalk (Hancock,1993), of which stylolites horizons is an example (Gale and Rutter, 2006). Non-intrinsic diagenesis also causes hardgrounds, which are also horizons of reduced permeability. Hardgrounds result when coccolith supply stops or reduces, and bottom currents prevent them from settling, and if exposed on the seafloor for sufficient time become glauconitized and/or phosphatized (Hancock, 1993).

Also abundant in the Northern Chalk are marls and flints. Unlike the Southern Chalk, zone fossils are rare or absent in some places, so the marl and flint bands are usually used for zonation (Barker et al., 1984; Buckley et al., 2001). The upper Chalks are purer, with the lower Chalks (Hunstanton and Ferriby Formations), being more marly. Marls contain magnesium-rich smectite derived from volcanic or terrigenous detritus and are deposited on erosional surfaces. Marl bands in the Chalk can be several centimetres thick, with some

being persistent laterally (Hancock,1993) and can therefore be very useful for stratigraphic correlations (Buckley and Talbot,1996).

Flint is a very hard, brittle, siliceous material that is formed from the infilling of burrow holes of crustaceans or molluscs with transported quartz or siliceous sponges, radiolarians and diatoms that dissolve in alkaline solutions, and later reprecipitate in acidic conditions (Clayton,1986). On the local scale, flints form crosscutting vein cylinders with a burrow at the middle (Hancock, 1993). Flints normally accumulate on bedding planes where they occur as tabular layers or discrete nodules (Mortimore and Wood,1986). Tabular flints can persist laterally, which in association with other lithological features can be used for correlation. However this requires tremendous experience and skill to undertake stratigraphic correlation (Hancock, 1993).

### **2.1.3 Stratigraphy of the Solid Geology**

Sumler (1996) classifies the Northern Province Chalk Formations from the oldest to the youngest as the:

- i. Hunstanton
- ii. Ferriby
- iii. Welton
- iv. Burnham
- v. Flamborough and
- vi. Rowe Formations.

The description of the stratigraphy that follow is by Sumler (1996)'s account. Also included is the areal outcrop occurrence of the different formations in the study area (see Figure 2.2 ) and a developed cross-section showing the Chalk stratigraphy ( Figure 2.4 )

**The Hunstanton Chalk Formation (Albian age)** is also known as the Red Chalk, is made up of marls and iron stained rubbly massive chalk. The Hunstanton forms the basal unit of the Chalk group. The upper part is less marly, and more massive than the lower portion and is paler in colour and prone to discolouration. It is 3 m thick in the south of the region, but increases to 25 - 30 m in the Cleveland Basin.

**The Ferriby Chalk Formation (Cenomanian age)** is flintless and 20-25 m thick in the south but thins out to 10 - 15 m over the Market Weighton Formation and correlates with the Lower Chalk of the Southern Province. The Ferriby Formation has a narrow outcrop area as it crops out on the steep escarpment of the Wolds. The Ferriby Formation cannot be used as an aquifer (Gale and Rutter, 2006) because it has more marls than its overlying counterparts. The Ferriby Formation weathers to a buff colour when exposed, producing marly soils.

In the study area, the Hunstanton and Ferriby Formations are found and outcrop at the western edge of the study area. Part of the Ferriby Formation is overlaid by superficial deposits, whereas the entire Hunstanton Formation crops out at the base of the scarp slope (Figure 2.2).

**The Welton Chalk Formation (Upper Cenomanian – Upper Turonian age)** is thickly bedded, with flint nodules. Its thickness ranges between 40-55 m. The base of the Welton Chalk is marked by the Black Band which is an eroded surface that is stained by glauconite and iron minerals. Above the eroded surface is the Plenus Marl Member, which is about 0.5 – 0.6 m thick and made up of green and brown marls and marly chalk. Above the Plenus Marls lie beds rich in shelly debris and chalk pebbles with marls. Overlying the shelly chalk are pure, soft and flint bearing chalk beds, that are distinctly different from the overlying hard Burnham Formation. There are several marl seams and flint nodules that serve as correlation and marker beds, examples of which include Barton and Grasby Marls.

In the study area, the Welton Formation outcrops at the northern, north-western and western border of the study area (Figure 2.2).

**The Burnham Formation (Turonian – Coniaciana age)** is hard and thinly bedded in comparison with the Welton Chalk. The Burnham Formation has a thickness of 85 -140 m and outcrops on an extensive portion of the Wolds. Its soils have angular chalk and flint debris. As compared to the nodular flints in the Welton Formation, the Burnham Formation is characterised by 0.3 m or more thick tabular flints bands. The base of the Burnham is distinguishable by hard chinks that are particularly flinty, with thick, closely spaced, tabular flints. Just like the Welton Formation, there are some known marl seams and

tabular flints that serve as marker and correlation beds for the formation examples of which include Kiplingcotes and Little Weighton Marls.

The Burnham Formation outcrops in the Southern to the middle portion of the study area, to form a boundary with the Flamborough Formation outcrop on the Wolds around the Langtoft and Octon Cross-roads area. Part of the Burnham Formation is overlaid by superficial deposits in the south of the study area (Figure 2.2).

**The Flamborough Chalk Formation (Santonian – Campanian)** is the youngest of the outcropping formations. The basal 160m of this Formation is exposed between Flamborough Head and Sewerby. The Formation extends to about 220 m thick above the base of the Chalk. The Formation is flintless and softer than the Burnham and Welton Formations. Less is known about the Flamborough Formation stratigraphy because its upper portion is mostly covered by Quaternary superficial deposits, and also because of the difficulty in correlating its coastal section inland due to a paucity of comparatively exposed type sections. The Formation has marl seams of about 1-3 cm thick that can be used as marker bands if they persist laterally.

The Flamborough succession is divided into 3 members by (Whitham, 1993a) as the:

- i. South Landing
- ii. Danes Dyke
- iii. Sewerby Member.

The South Landing Member is about 21 m thick, and is made up of hard, massive chalk with infrequent thin marl seams. The Danes Dyke is about 67 m thick, and is thinly layered, alternating with stylolites and marl seams. It is less hard than the South Landing. The Sewerby Member is the youngest, and is exposed at the coast and is predominantly made up of massive chinks with lower thinly bedded chinks with stylolites.

The Flamborough Chalk outcrops in the central and north-eastern corner of the study area. The majority of the Kilham catchment is located on the Flamborough Chalk. Towards the east and south, the Formation is confined by superficial deposits.

Geological and geophysical evidence indicates that the Flamborough Formation is overlaid by a flinty Chalk formation called **the Rowe Formation**. The Rowe Formation is 70 m thick and continues offshore under the North Sea. The Rowe Chalk forms part of the eastern border of the study area, but is completely confined by superficial deposits to the east.

The summary of the stratigraphy and cross-section through Wintringham to Foston on the Wolds is shown in Table 2.1 and Figure 2.4 respectively.

**Table 2.1.** Chalk stratigraphic summary

<b>Formation</b>	<b>Thickness(m)</b>	<b>Bedding</b>	<b>Lithology</b>
Rowe	Min. 70		Flinty
Flamborough	220 - 280		Marly
Burnham	140 - 150	Thin	Flinty
Welton	40 - 53	Thick	Flinty with marls at its base
Ferriby	10 - 35		Marly
Hunstanston or Red Chalk	1 - 30	Rubbly and massive	Marly

#### **2.1.4 Paleogene and Quaternary influences**

During the Tertiary, there was uplift and folding of the Chalk. The Wolds underwent prolonged denudation leading to removal and reduction of their height. The Chalk was subaerially eroded during the late Paleogene, when drainage was towards the North Sea (Goudie, 1990). Ice invasion in the Quaternary resulted in glacial erosion and periglacial weathering. The frost shattering which is most pronounced in the Hull Valley is responsible for high permeability on the surface, with permeability reducing with depth because of reduced aperture and water circulation. The effects of glaciation are deposition confinement and burial of the Chalk surface get pronounced to the east of the study area (see Figure 2.2 and Figure 2.4).

Quaternary deposit distribution was affected greatly by the topography of the land during deposition. The dominant deposits are of the Devensian and Holocene age, but older deposits occur under these in the Holderness Plain

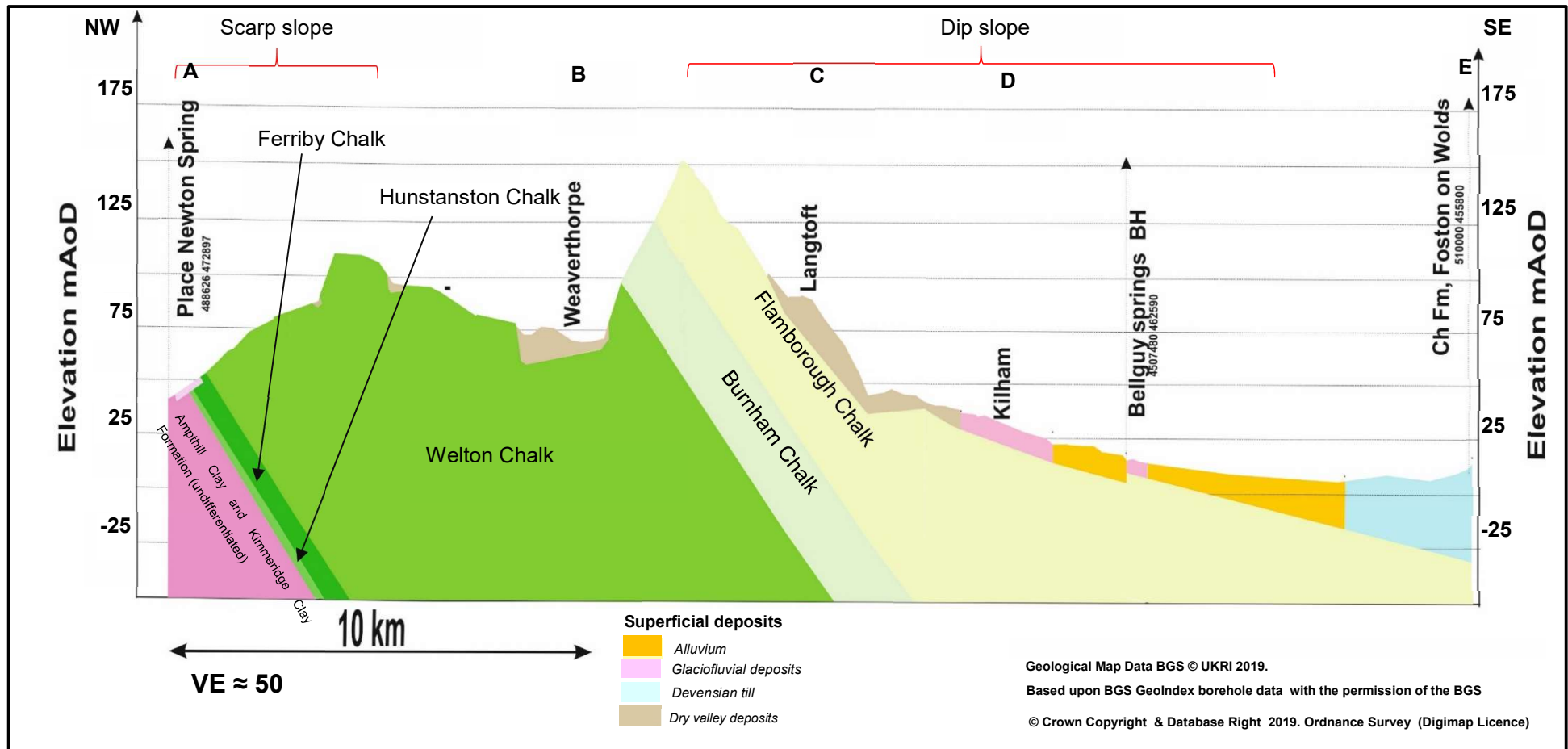


**Figure 2.4.** Geologic cross-section through the study area, from Place Newton Springs (at Wintringham) (A), through Weaverthorpe (B), Langtoft (C), Kilham (D), to Foston on the Wolds (E) showing the steep scarp and gentle dip slopes. The Chalk group lies unconformably on Amphil Clay and Kimmeridge Clay formations. Refer to section 3.3.1. on the methodology for the development of cross-section.

area. The Chalk is exposed at the Wolds, but is covered by thickening Quaternary deposits of Devensian Glacial Till towards the east (Figure 2.2 and Figure 2.4). Scattered remains of Quaternary deposits occur on the Wolds, but are often less than 1m thick. The deposits range in thickness from 10m from the west of an Ipswichian buried cliffline (Figure 2.1 and Figure 2.2) increasing to a thickness of 20m in some places and 50m in the Holderness Plain. Glacial sands and gravels are also common on the Chalk (Berridge and Pattison, 1994) ( Figure 2.1).

The Ipswichian cliff line and a number of buried channels exist beneath the deposits. The buried Ipswichian cliffline runs from Bridlington, along the Wold eastern boundary to the east of Hessle and Barton in the Humber (Figure 2.1 and Figure 2.2). Although the existence of the buried channels is accepted, there is a debate about their origin. Whilst Foster and Milton (1976) attribute the buried valleys to sub-aerial erosion, Rawson and Wright (1992) on other hand suspect them to be interglacial meltwater channels. Some of the buried valleys seem to be eastward extensions of the dry valleys on the Wolds, suggesting that the valleys existed before deposition of the Devensian tills.

Pleistocene cryoturbation, solifluxion and recent weathering processes have also imparted greatly on the Chalk surface resulting in extensive fissuring of the matrix (Price, 1987; Younger, 1989). This is responsible for upper surface increase in joint frequency and opening. Recharge and infiltration into the Chalk is greatly affected by this fragmented surface layer (Gale and Rutter, 2006).

### **2.1.5 Tectonics and Chalk structure**

The Chalk has been affected by two major tectonic activities. The first which occurred in the Late Cretaceous resulted in the deposition and the second which was in the early Oligocene and early Miocene caused folding and faulting (Hancock, 1993).

Firstly, the subsidence of the North Sea Basin in the Late Cretaceous and Early Paleocene, resulted in the deposition and filling of the basin with Chalk (Kirby and Swallow, 1987). The next significant tectonic activity was basin inversion caused by Alpine compression resulting from Africa pressing against

Europe during the Alpine Orogeny (Kirby and Swallow, 1987; Peacock and Sanderson, 1994; Starmer, 1995).

The structure contours and the faults in the Chalk are shown in Figure 2.5 and Figure 2.6 respectively..

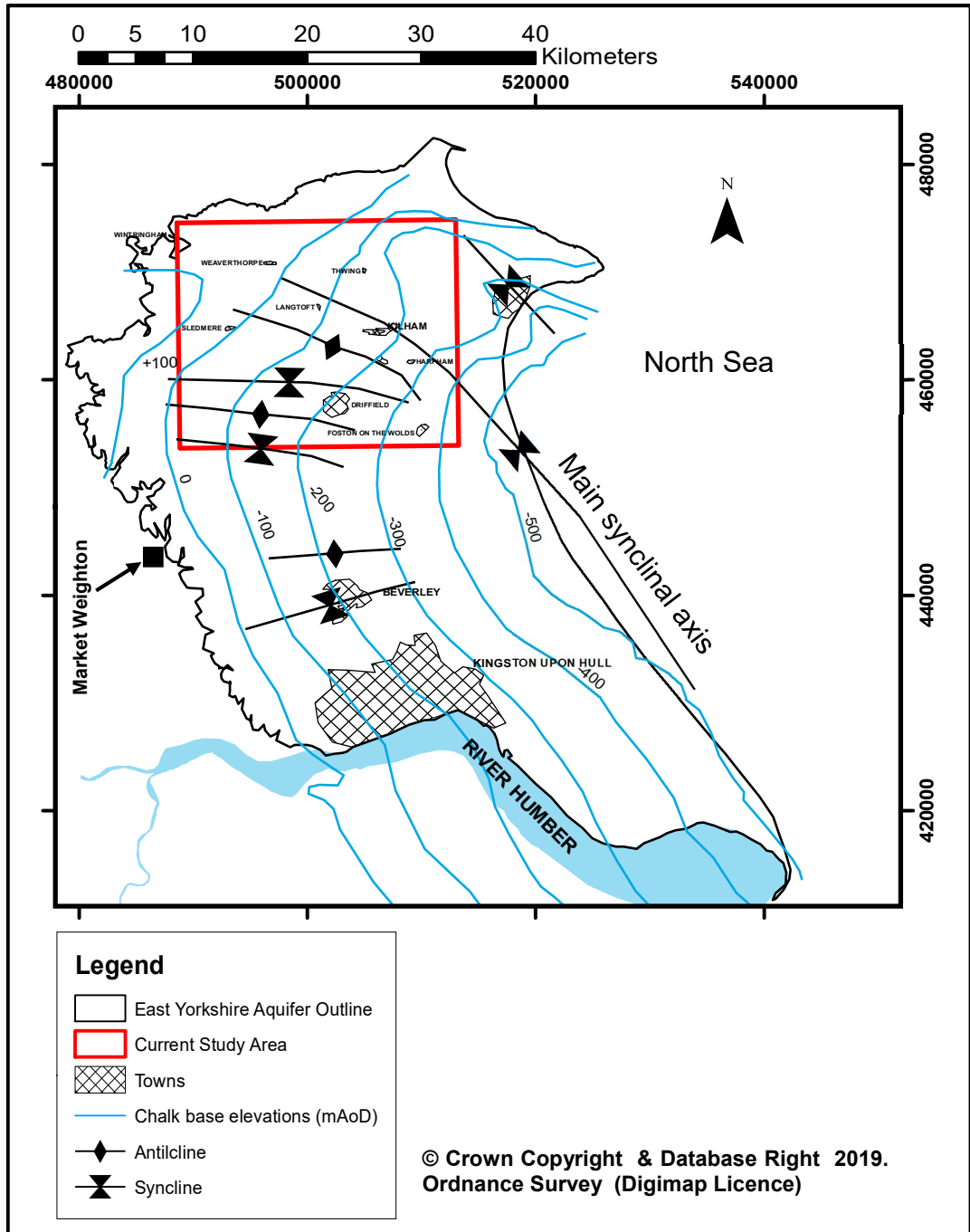


**Figure 2.5:** Structure contours on the base of the Chalk Group showing the main synclinal axis through Kilham. Redrawn from Gale and Rutter (2006) and superimposed on Edina digimap data.

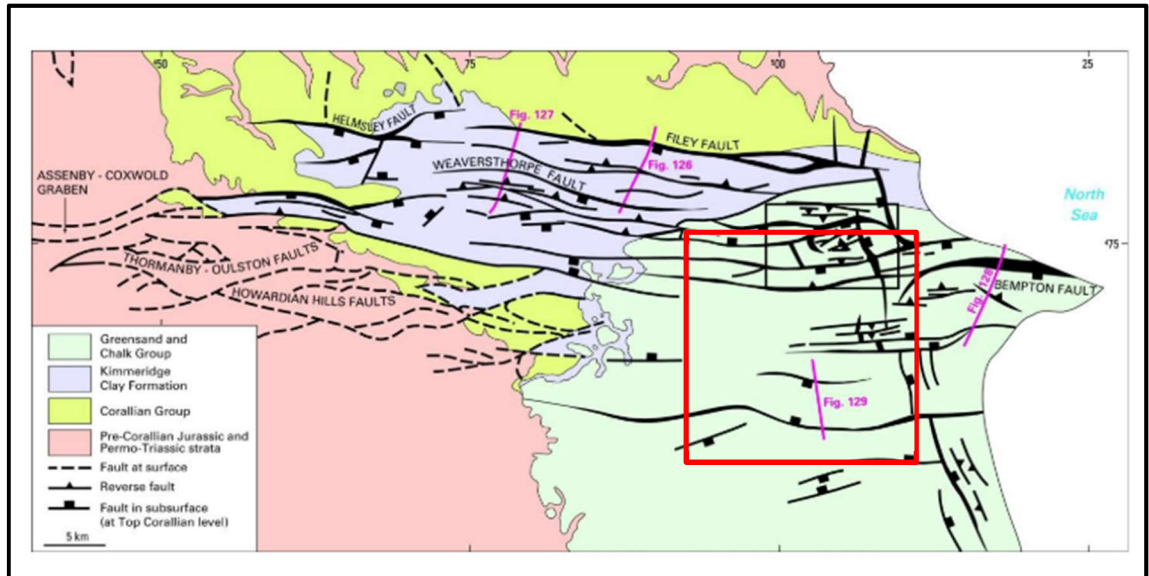


**Figure 2.6:** The Howardian Hills-Flamborough Head Fault zone (at Top Corallian level) as determined from seismic data from Chadwick and Evans (2005). The approximate study area is outlined in red. Figs 126-129 relate to Chadwick and Evans (2005).

The compression caused the Chalk to fold into an extensive open syncline, plunging gently at 2-5° to the south-east on an axis between Driffield and Bridlington. The southern and central portion of the region, form the south-western limb of the syncline dip uniformly at 1° away from the Wolds escarpment into the North Sea (Gale and Rutter, 2006) The north-eastern limb of the syncline abuts against the Flamborough anticline, dipping to the southwest. Aside the main syncline, Foster and Milton (1976) also describe other minor folds axes that have concordant plunge with the main syncline structure.

In the northern part of the region exists a zone of heavy faulting and flexuring. In this zone, the Howardian- Flamborough Fault Belt runs from Flamborough across the Wolds to Malton, part of which is seen at Selwicks Bay. It relates to the late Cretaceous and early Paleogene uplift of the buried southern basin margin of the Cleveland Basin. In the north of the Howardian-Flamborough belt lies the Bempton Shatter Zone, which has contortions of steep dips (Kirby and Swallow, 1987; Peacock and Sanderson, 1994). Foster and Milton (1976) also used borehole evidence to suggest the existence of a large fault of unknown lie around Burdale and Thixendale. Little is known about the

character of the faults and folds in the northern part of the region, because the features are buried beneath the Chalk with few exposures in quarries (Gale and Rutter, 2006).

In comparison with the Southern Chalk, the northern Chalk is more fractured because it is harder, more thinly bedded and fractures cleanly. The hardness is attributable to the double calcite cementation within the pores of the sediments (Allen et al., 1997). Bloomfield (1996) identifies 3 types of fractures that impact on fluid flow in the Chalk. These are joints, faults and bedding plane fractures (Figure 2.7).

The joint system of the Chalk developed during the late Neogene to Recent in response to Alpine compression in north-west Europe (Bevan and Hancock, 1986). Joints developed in response to the regional principal stress direction and are

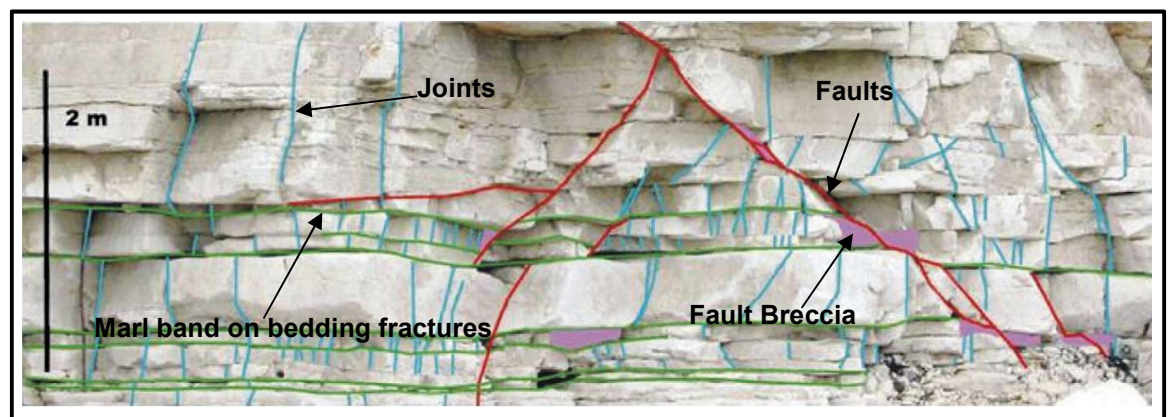


**Figure 2.7:** Fracture types in the Northern Chalk, mapped at Flamborough Head. Adapted from Hartmann et al. (2007).

orthogonal to the least principal stress (Gale and Rutter, 2006). Jointing generally does not persist across a bed (Downing et al., 1993), but with a few exceptions (Hartmann, 2004). Pastoules and Cripps (1990) used a 4 to 10 m coastal scanline at Selwicks Bay and High Stacks to categorise the joint system into five different joint sets, with the dominant sets aligned between 100 and 130°. They associated the dominant joint set with some faults along the south margin of the North Sea, and suggested that these joint sets were formed from the reactivation of the faults. They also recorded joint spacings between 0.15 and 0.33 m, joint trace lengths between 0.5 and 2.5 m with joint apertures normally less than  $10^{-3}$  m. Average joint spacing within a set is

proportional to bed thickness (Ladeira and Price, 1981; Narr and Suppe, 1991; Bloomfield, 1996), with thicker beds showing larger joint spacing and vice versa for smaller beds. The depth to which the regional joint set is developed is unknown and may be different at different areas depending on lithostratigraphy, burial and uplift history, and proximity to faults. However, jointing to depths of 100 m below ground level have been observed in a fracture log of a borehole at Carnaby Moor (Gale and Rutter, 2006). For joint characterisation in the current study area, Zaidman et al. (1999) characterised the joints systems in Ruston Parva (TA 069 616) and Nafferton Wold (TA 048 612) Quarries. They identified at least four major steeply dipping joint sets, the majority of which are stratabond, with joint spacing ranging between 0.3 – 0.5 m, with maximum joint apertures of 10 mm. The joint trace lengths ranged between 0.65 – 2.5 m. They suggested that since the low angles and similar dips of the strata in these two quarries mimic that from drilled boreholes in the Kilham area, the joint systems could be extended to the Kilham area.

Faults are known to exist in the East Yorkshire Chalk, but there is limited information on them because of few exposures at outcrop, quarries and slope face. The shattered zone in and around fault planes can form a zone of local fracture porosity, acting as zones of preferential flow for groundwater. Farrant et al. (2016) used the preponderance of vein calcite to trace faults in the catchment. These vein calcites are supposed to act as flow barriers, but they can also provide local flow paths for preferential flows. In studying the minor faults in the Howardian- Flamborough Belt, Peacock and Sanderson (1994) pinpointed the existence of numerous minor extensional fault displacements between 0.005 – 6 m. These minor faults combine to form conjugate faults, that act to create zones of complex fracturing. Gale and Rutter (2006) report normal and conjugate faults in the Ruston Parva Quarry (see Figure 2.8 for location) of up to a maximum length of 15m, with maximum displacements between 0.1 and 0.2 m. The faults are also high angled without any patterned orientation.

Chadwick and Evans (2005) used seismic data to postulate the existence of major faults in the study area. Recently, Farrant et al. (2016) (Figure 2.8) used digital elevation, seismic and field mapping data to confirm the existence of these major faults. They also used the same methods to find additional faults,

not known of in previous studies. Their field mapping methodology involved the mapping of calcite veins on the field to identify fault traces. In other situations also, digital elevation models were also used to hypothesize on the location of faults in the area. For the confirmed major faults, some had slight

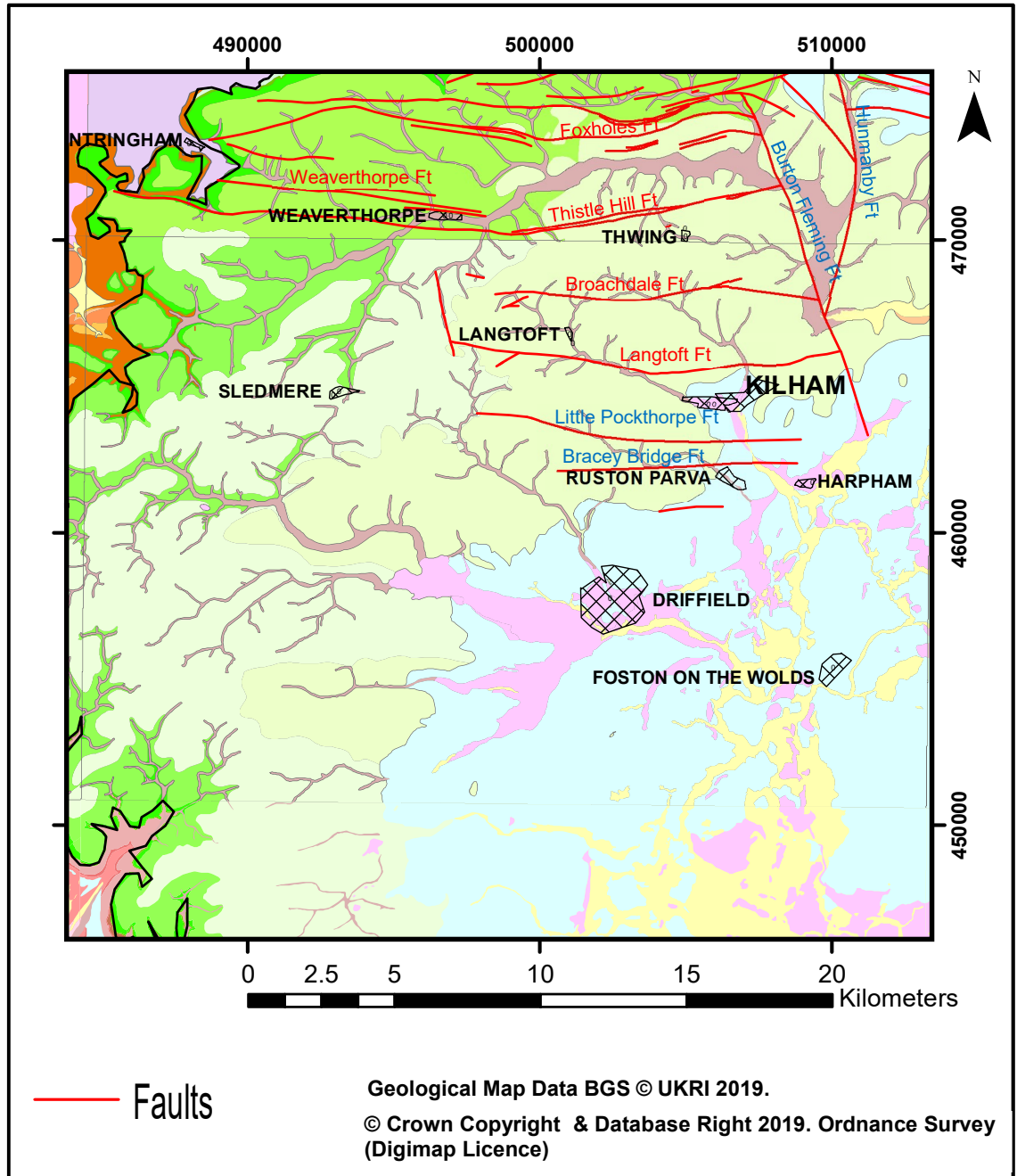


**Figure 2.8:** Map of main faults in the study and Kilham area. Fault line shapefiles were obtained from Farrant et al. (2016). Faults labelled in red were confirmed on the field, those labelled in blue were found from desk study.

offsets from the previously known locations. They mapped major east-west trending faults like Langtoft, Broachdale, Thistle Hill, Weaverthorpe, Foxholes

and Fordon Faults that lie to the north of Kilham Village, and Little Pockthorpe lying to the South of Kilham. The north-east of Kilham was also mapped for the numerous faults that are associated with the Burton Fleming and Hunmanby Faults that are two known major NNE-SSE trending Faults.

Bedding plane fractures are parallel to the strata and are caused by stress release during erosion and uplift (Higginbottom and Fookes, 1970). The bedding plane fractures range from large apertures for massive beds to zones of intense fracturing for marly, thin beds. The fractures are persistent laterally, with apertures exceeding 10 cm in some beds, making bedding plane fractures important for groundwater flow and contaminant transport (Bloomfield, 1996; Waters and Banks, 1997). Marl is found on some of the bedding planes (Hartmann, 2004) and this marls may act as barriers to vertical flow, thereby concentrating flows along the bedding planes (Gale and Rutter, 2006), causing solutional enhanced secondary bedding plane flow features.

## **2.2 The effects of geology on the hydrogeology of the Chalk**

This section sets out to discuss the effects of geology on the aquifer properties of the Chalk. The deposition and lithology, diagenesis, tectonic structure and Quaternary history influences the recharge processes in the unsaturated zone and saturated zone flow processes.

### **2.2.1 Unsaturated zone flow processes and recharge**

The Chalk lithology, diagenesis, structure and Quaternary deposits affects unsaturated zone processes. The unsaturated zone of the Chalk is important for two reasons:

- i. it influences the recharge and subsequently the resource estimation; and
- ii. it also determines the fate and transport of contaminants to the aquifer from the surface.

The small particle sizes of the Chalk matrix implies that the aquifer material has very small pores with very small effective pore throat diameters ranging between 0.1 – 1  $\mu\text{m}$ . This matrix characteristic results in a vadose zone that

is usually close to saturation all year round because of high air entry pressures. Hilly topography and high permeability from fractures in the unsaturated zone results in thick unsaturated zones and flat hydraulic gradient. The factors that affect recharge are the matrix hydraulic conductivity, distribution of fine and large permeability fractures, time and intensity of recharge events and previous moisture content before the recharge event. For recharge to occur, an infiltration rate exceeding  $3\text{-}5\text{ mm d}^{-1}$ , maintained over several days is required so that the matrix hydraulic conductivity is exceeded for the fissure system to fill and drain water to the saturated zone. The influence of evapotranspiration and matrix suction creates a zero flux plane (ZFP), which is a front of moisture movement that varies with season as shown in Figure 2.9.

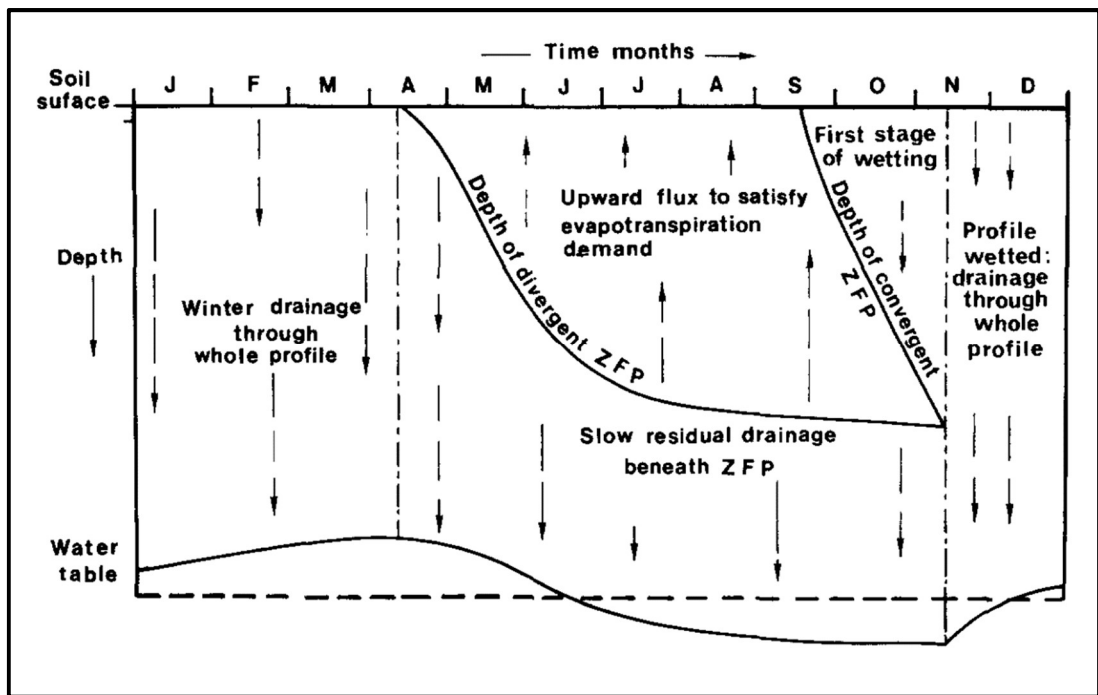


**Figure 2.9:** Seasonal variation of water flux through the unsaturated zone to the water table (Wellings and Bell, 1980).

In the early 1970s, it was thought that rapid fracture flow was the dominant mode of recharge and solute transport to the saturated zone of the Chalk. This was evidenced from:

- i. the often rapid rise in groundwater levels in response to precipitation events (Headworth, 1972; Downing et al., 1978);
- ii. observation of cloudy Chalk well water containing soil bacteria and particles thought to have been rapidly washed from the soil zone via fractures to the saturated zone (Mclean, 1969).

The fracture recharge concept was called into question when Smith et al. (1970) used tritium profiling in the unsaturated Chalk of Hampshire to conclude that the most dominant recharge mechanism (85 %) was by piston displacement through the matrix at a rate not exceeding 0.9 m/yr, whilst fractures accounted for 15% of recharge. However, Foster (1975) alternatively proposed that the diffusion gradient between fissure water and the matrix water explains the tritium peak delay. He did so by distinguishing between fracture flow of water to saturated zone and slow solute transport via diffusive exchange in the unsaturated zone. Foster (1975) also argued that it would be impossible for no development of surface run-off on the chalk even for areas of shallow water table during times of excessive precipitation should piston displacement be the dominant recharge pattern. In spite of the divergence of thought at the time both works showed the potential and importance of the unsaturated zone in attenuating contaminants and/or rapidly transmitting contaminants to the water table.

Later works like Wellings (1984); Wellings and Bell (1980); Cooper et al. (1990); Van den Daele et al. (2007) amongst others confirmed the slow water flux rates and dominance of the matrix flow contribution to recharge. Cooper et al., (1990) also showed that higher matrix conductivity can inhibit the initiation of fracture flows, when the matrix acts as a buffer and slowly releases water to the fracture. There is still a lot of debate about when, how and what level fracture flow is initiated in the unsaturated zone. On the Brighton Chalk, Downing et al. (1978) showed that after high intensity rainfall events, tritium concentrations in well water was higher than in rainfall, indicating the pressure displacement of solutes from the unsaturated zone through fractures to the saturated zone. However, Downing et al. (1978) concluded ambivalently, as other findings also reflected piston flow.

On the Northern Chalk, where this catchment falls, several studies by the University of Leeds have shown that rapid bypass flow occurs during times of

high intensity rainfalls. Zaidman et al. (1999) used electrical resistivity imaging to monitor the movement of distributed saline solution on ground surface into the unsaturated zone at a site near Kilham. They found high saline concentrations near the ground surface indicative of solute diffusion into the matrix, but also observed high solute concentrations at depth especially during periods of rainfall events indicative of rapid bypass flow through fractures. Allshorn et al. (2007) studied tracer fluxes, whilst Keim et al. (2012) measured soil moisture and discharge at a site south of the study area in the Burnham Formation in the exposed face of a tunnel, that lies between 30 – 45 m below the ground surface. These two other studies also confirmed rapid preferential flow bypassing the soil matrix to the water table under high hydraulic loadings. The three studies also found that ponding, saturation and concentrated flows on horizons with impermeable marls or flints or on beds with poor vertical communication with other beds. There was also evidence of rapid bypass flow on steeply dipping strata, fractures or faults with rapid transmission from the surface to deeper depths.

Although the studies above were conducted far above the saturated zone, their findings have direct implication for resource assessment and contaminant fate and transport. Ponding and restricted flows on marls, flints and impermeable beds can lead to delayed yield in times of soil deficit, and cause local perched groundwater tables that will cause slow recharge to the aquifer. This will lead to resource estimation and modelling parameter value errors. Ponding can also result in permeability enhancement in the unsaturated zone via fracture dissolution and enlargement. In addition, should ponding persist long enough, solutes will have enough time to diffuse into the matrix, to be released in times of high hydraulic loading or solute mobilization when the solute concentration gradient reverses for the fracture and matrix. This diffusion delay will cause attenuation but long residence time of contaminants within the aquifer.

Steeply dipping fractures and faults with effective communication from the surface to deeper depths also increase the vulnerability of the aquifer, because of their potential rapid bypass flows from the surface towards the water table.

In the area of study, the recharge areas are characterised by deep depths to groundwater, enabling the unsaturated zone to have a buffering effect on recharge water, resulting in a well defined Chalk water chemistry before the water reaches the saturated zone (Pitman, 1978a).

The Quaternary history and deposits also have a major effect on recharge. The type of cover material overlying the Chalk influences both the fracture development, recharge potential and discharge. In the recharge area, the parts of the Chalk that are covered by glacial sands and gravels allow infiltrating water to reach the saturated zone.

### **2.2.2 Porosity and effective storage**

The porosity in the Northern Province Chalk decreases with burial depth (Bloomfield et al., 1995) due to the interplay of sedimentary characteristics and diagenetic processes (Bloomfield, 1997). Storage in the Chalk is by combination of the matrix, finer fractures and large fracture networks, and in some localities even karstic features (Price, 1987), resulting in a description of its porosity as a double-dual-porosity (Price et al., 1993). The  $K_m$  of the matrix ranges between  $3 - 5 \times 10^{-3} \text{ m d}^{-1}$ .

A lot of work has been done to constrain aquifer porosity both on the regional and local scale with respect to the study site. On the regional scale Barker (1994) found porosities ranging between 12% for the Welton and 34% for Burnham Formations of Humberside and Lincolnshire. Bloomfield et al. (1995) also used 256 samples to find porosity ranging between 3% and 45%, with hardgrounds usually recording porosities less than 10%. On the local scale, Zaidman (1999) found porosities ranging between 14% and 23% at the Ruston Parva Quarry, located on the Flamborough Chalk.

Despite the large porosities in the Chalk matrix, the effective storage is within the fracture networks because the narrow pore throats within the Chalk prevent drainage of the stored water (Price, 1987; Price et al., 2000). Specific yield within the Chalk is contributed by the fracture network with drainage occurring earlier in the larger fractures and subsequently from the smaller fractures resulting in delayed drainage. A collation of aquifer properties by Allen et al. (1997) states storage coefficients ranging between  $1.5 \times 10^{-4}$  and  $1.0 \times 10^{-1}$  with a geometric mean of  $7.2 \times 10^{-3}$  and interquartile range of

between  $1.2 \times 10^{-3}$  and  $1.8 \times 10^{-2}$ . They also state coefficients of  $1 \times 10^{-3}$  and  $5 \times 10^{-3}$  for the confined zone, but indicate that these could also be related to the influence of sand and gravel deposits directly overlying the Chalk in the vicinity of the test boreholes. Foster (1974) used recession analyses of the West Beck discharge to obtain specific yield values ranging between  $5.0 \times 10^{-3}$  and  $1.0 \times 10^{-2}$ . Foster attributed this storage to the fracture network and horizontal layering. Jones et al. (1993) conducted pumping tests at the Yorkshire Water Kilham Abstraction site, and used the pumping test data to obtain specific yield values ranging between  $(3.0 - 6.7) \times 10^{-3}$  at the 90% confident interval using the British Geological Survey Software for analysing pumping test data in large diameter wells (Barker and Herbert, 1989).

### **2.2.3 Hydraulic conductivity variation with depth and flow layering**

The Chalk is an aquifer because of storage in its matrix and flow through its solutionally enhanced fracture network (Price, 1987). In the saturated zone, the matrix contributes negligibly to hydraulic conductivity as the matrix conductivity is only between  $3 - 5 \times 10^{-3} \text{ m d}^{-1}$ . The increased hardness from pressure solution diagenesis of the Northern Chalk makes it more brittle, making it break easily resulting in the proliferation of fractures, with a higher bulk hydraulic conductivity in comparison to the Southern Chalk.

The Chalk like any fractured aquifer is characterised by flow heterogeneity and anisotropy. In the saturated zone, anisotropic flow occurs because the majority of flow in the Chalk occurs on solutionally enhanced bedding plane features, vertical and inclined joints and fractures, and faults. Marls and flints restrict flow on top of bedding flow features resulting in discrete solutionally enhanced horizontal and sub-horizontal flow pathways. Geophysical logging in the Carnaby Moor borehole, located southwest of Bridlington by Bloomfield and Shand (1998) identified five significant depth horizons characterised by marl bands and stylolitic horizons. Flow logging results from Buckley et al. (2001) on the unconfined Southern Province Chalk at Brighton, indicate that flints can also concentrate flows in the Chalk in the saturated zone.

Flow layering in the Northern Chalk has been studied and characterised by several researchers. Foster (1974) used the correlation between groundwater levels and West Beck discharges to suggest flow layering in the unconfined

area of the Northern Province Chalk. Foster and Milton (1974) also documented flow layering by analysing geophysical logs and pumping tests for times of high and low groundwater levels in the Etton recharge area. From the above works, a “two productive layer model” of flow layering was proposed for the unconfined aquifer. The first layer was in the zone of present day water table fluctuation, and the second was at -20 mAoD.

Later works however showed other permeable horizons in the Chalk, refuting the two layer model. This works will be briefly presented here, as they will be dealt with in detail in section 3.2. Buckley and Talbot (1994;1996) analysed historical geophysical logs in the Kilham area to determine flow layering and also to draw a connection between different wells in Kilham. At the borehole scale, they found discrete flow horizons defined by a relatively narrow zone of solutionally enlarged features developed between 5 and 30 mAoD and within 30 m of the land surface. Their detected flow zones were within the zone of water table fluctuation and other flow horizons on top of strata with flints and marls, outside the two model layer previously proposed by Foster and Milton (1974). Buckley and Talbot suggested from their findings that the flow zones were bedding controlled, following the dip of the strata. In spite of their findings, they gave a caveat about the inconsistencies in the logging methodology of the synthesized geophysical logs. They recommended the running of new geophysical suite of logs at suitable scales using recent and consistent methods to define stratigraphic horizons. They also suggested that flow logging be done under both ambient and pumped conditions to constrain the flow horizons and their relative contribution to flow in the wells. Southern Science Ltd (1994) also run geophysical suites of caliper, impeller, gamma, resistivity and fluid conductivity under natural flow conditions for well catchment delineation. Southern Science confirmed several discrete flow zones in the Kilham area, and drew a qualitative conceptual model of flow horizons at borehole scale. Expanding on the number of previous boreholes characterised in terms of flow layering for the Northern Chalk, Parker (2009) and Parker et al. (2019) used both ambient and pumped flow tests in the unconfined zone and confined zone zones respectively, to characterise discrete flow horizons in wells. Vertical flow variation with depth results in the wells were used to develop a model of hydraulic conductivity. Parker’s work

showed very strong evidence for flow layering both at the confined and unconfined zones of the aquifer. Her model identified flow zones at the borehole scale, with hydraulic conductivities ranging from very low flow zones in some superficial deposits to high zones influenced by water table fluctuation, or close to flint and marl bands. The above works demonstrate the anisotropic nature of the Chalk Aquifer, with discrete flow horizons occurring both within the zone of water table fluctuation and at depth in boreholes.

Flow variation with depth in the Northern Chalk is caused by the geology and geologic history of the Chalk. Flow variation with depth has implications for resource evaluation in terms of pumping test data evaluation and interpretation. For resource estimation, the effective aquifer thickness is restricted to only the permeable zone and not the full saturated thickness of the Chalk. Secondly, water table levels and time of season has to be considered in transmissivity estimations as transmissivities increase by a disproportionately large amount between low and high groundwater levels on the unconfined Chalk. Foster and Milton (1976) for example report a transmissivity of  $1000 \text{ m}^2\text{d}^{-1}$  during minimum groundwater levels, and later reporting  $2200 \text{ m}^2\text{d}^{-1}$  during a time when groundwater levels rose by 7m in the borehole. Thirdly, in modelling, it will be appropriate to represent flow horizons based on knowledge of discrete flow horizons and location characteristics with respect to recharge or discharge areas.

#### **2.2.4 Heterogeneity and spatial transmissivity variation of the Chalk Aquifer**

The Chalk Aquifer is heterogenous with lateral variation of transmissivity on both the local and regional scale. Lateral variation of aquifer transmissivity in the Chalk is affected by superficial deposit distribution and their effect on the confinement of the aquifer, topography and faulting.

Figure 2.10 shows the distribution of transmissivity in the Chalk. Transmissivity ranges from  $1 \text{ m}^2\text{d}^{-1}$  to  $10,000 \text{ m}^2\text{d}^{-1}$ , with a mean transmissivity of  $1258 \text{ m}^2\text{d}^{-1}$  (Allen et al., 1997). From Figure 2.10, higher transmissivities are recorded to the west of the buried cliffline away from the Quaternary confining layer and notably towards Kilham, where the transmissivity increases are attributed to concentrated discharges that have caused solutional enlargement and enhancement of fractures. However, transmissivity values

are low east of the edge of the Quaternary cover. Foster and Milton (1976) reported transmissivities of less than  $50 \text{ m}^2\text{d}^{-1}$  beneath the Holderness Plain, where the low transmissivities are attributed to little groundwater circulation

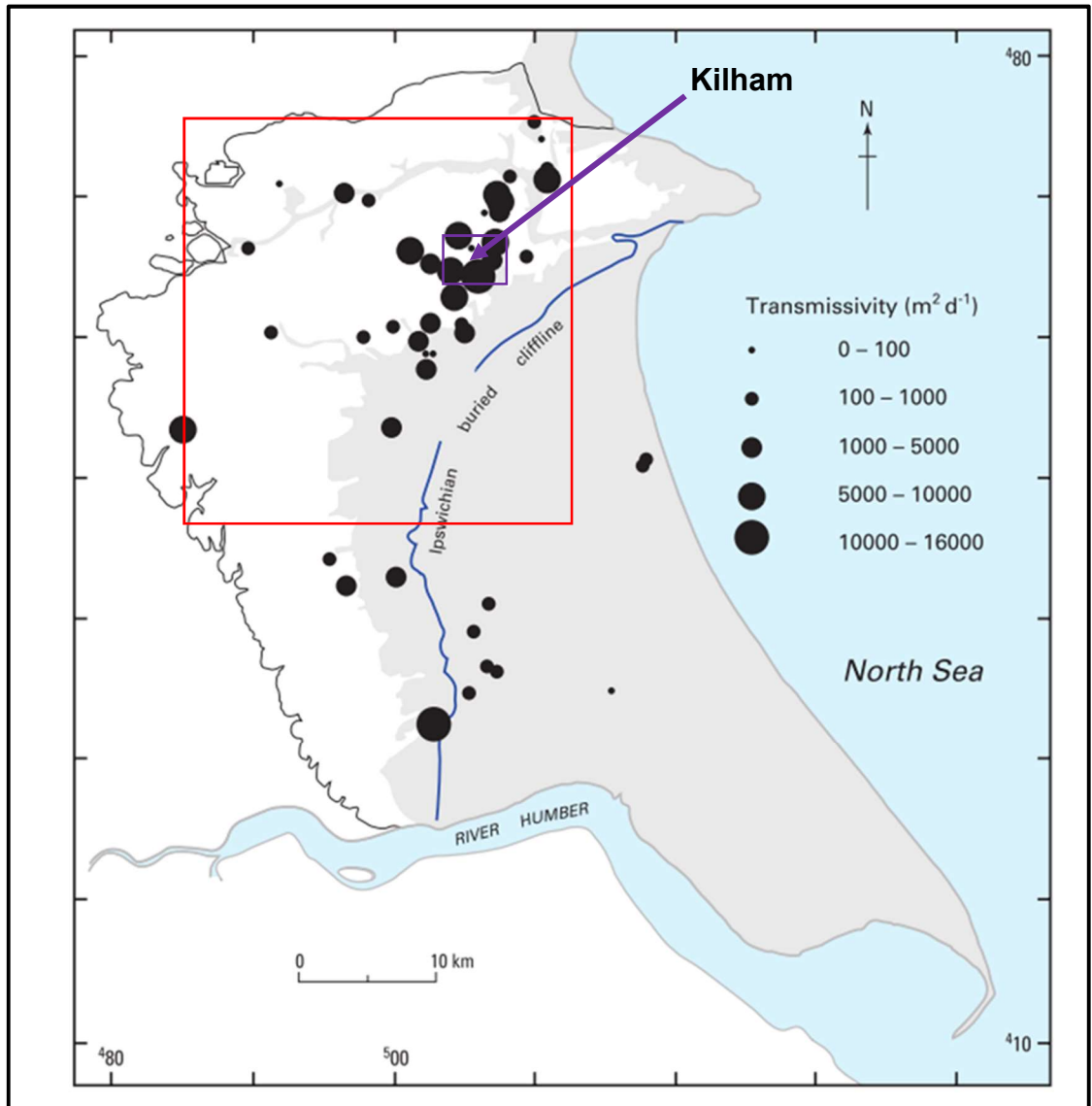


**Figure 2.10** Distribution of transmissivity values measured in the Chalk aquifer, study area (red square) from Gale and Rutter (2006), page 19. Large transmissivities in and around Kilham (purple square and arrow).

resulting in limited scope for the enlargement of fractures by solution. Transmissivities are very variable on the local scale as well. Ward and Williams (1995) for example, present transmissivity values ranging between 17 and  $11,028 \text{ m}^2\text{d}^{-1}$ , with wells in close proximity showing great variability in transmissivity in the Kilham area.

Topography plays an important role in lateral transmissivity distribution in the Chalk. Transmissivity is highest in the valleys than on the interfluves of the Chalk. For example, higher transmissivities are recorded in the Great Wolds Valley and the Kiplingcotes Valley. Most of the wells in the catchment were purposely drilled in the valleys for water resource evaluation rather than for research purposes, partly resulting in a bias of the recorded high transmissivities for the valleys than the interfluves (Allen et al., 1997). In the Southern Chalk, fracture frequency is higher in and around the valleys (Price, 1987; Price et al., 1993) than the interfluves although Younger (1989) dispute the concept, attributing the phenomenon to effective stress release. The high transmissivities recorded in the valleys of the Northern Province Chalk could be one or a combination of reasons adduced from studies from Southern Chalk. These reasons are:

- i. valleys are zones of structural weakness (Price et al., 1993);
- ii. valleys serve as zones of effective stress release by erosion of the valley zone (Younger, 1989; Price, 1987; Price et al., 1993);
- iii. valleys serve as zones of flow concentration dissolution due to mixing of recharging waters of different chemistry (Price et al., 1993);
- iv. periglacial freeze-thaw shattering of valley chalk, resulting in opening up of fractures to depths to several metres (Higginbottom and Fookes, 1970).
- v. the presence of chalk bearings (coarse breccia-like chalk deposit formed through periglacial processes) in valleys (Younger et al., 1997).

Faulting and folding especially in the disturbed north-eastern part of the study area (Figure 2.8) has the potential to result in areas of enhanced hydraulic conductivities or faults could act as flow barriers. For example, In 1982, the BGS conducted a large scale pumping test (further details provided in section 3.2) in the area and showed large transmissivities in the Broachdale and Langtoft Valleys, and into the Kilham and Harpham areas, where artesian conditions exist. The test also suggested the existence of boundary effects on the north western and north eastern parts of the catchment probably from either the barrier effects of the Burton Fleming / Humanby faults or recharge

to the Gypsy Race Valley, or a combination of both effects. Folding in the catchment may also lead to increased fracturing, which may become solutionally enlarged by dissolution. However, less permeable members may also lead to reduced permeability where they occur in surface anticlines on interfluvial and synclinal valleys (Allen et al., 1997). The effect of the folds and faults on the hydrogeology of the region is not very well characterised, because of the paucity of monitoring wells in faulted and folded areas of the catchment (Gale and Rutter, 2006).

Tracing groundwater velocities between wells in the Kilham catchment has shown rapid and karstic flow in the area (details in section 3.2). Ward and Williams (1995) and Ward et al. (1997) used tracers to determine bulk groundwater velocities of up to between 50 and 480 m d<sup>-1</sup> in the area, with the interesting phenomenon that flow circumvented boreholes lying on a straight path between injection and recovery points, whilst connecting boreholes downstream. The tracer tests thus demonstrate the heterogeneity of flow in the Chalk aquifer.

### **2.2.5 Flow patterns in the Chalk**

Figure 2.11 shows the cross-section through the study area with the minimum and maximum composite groundwater level marked, demonstrating the thick unsaturated zone in the recharge area. The groundwater in the Northern Province Chalk is derived from recharge on the Yorkshire Wolds, which occurs mainly in the months October to March at an approximate rate of 300 mm/yr (Foster and Crease, 1974). However, occasional minor recoveries of groundwater levels in June and July suggest that minor recharge events may occur at other times, even when there is a significant soil moisture deficit (Foster and Milton, 1976).

Recharge amount is dependent on: the effective precipitation, the thickness and conductivity of surficial deposits, unsaturated zone thickness and flow mechanism; and rapid bypass flow potential (Gale and Rutter, 2006). Rainfall infiltrates through the thick unsaturated zone of the unconfined Chalk in the Wolds. Marl layers in the unsaturated zone can act as vertical flow barriers, resulting in interflow along bedding planes, before recharging at the band edge (Barker et al., 1984). Effective storage within the Chalk is via the solutionally enhanced fracture network.

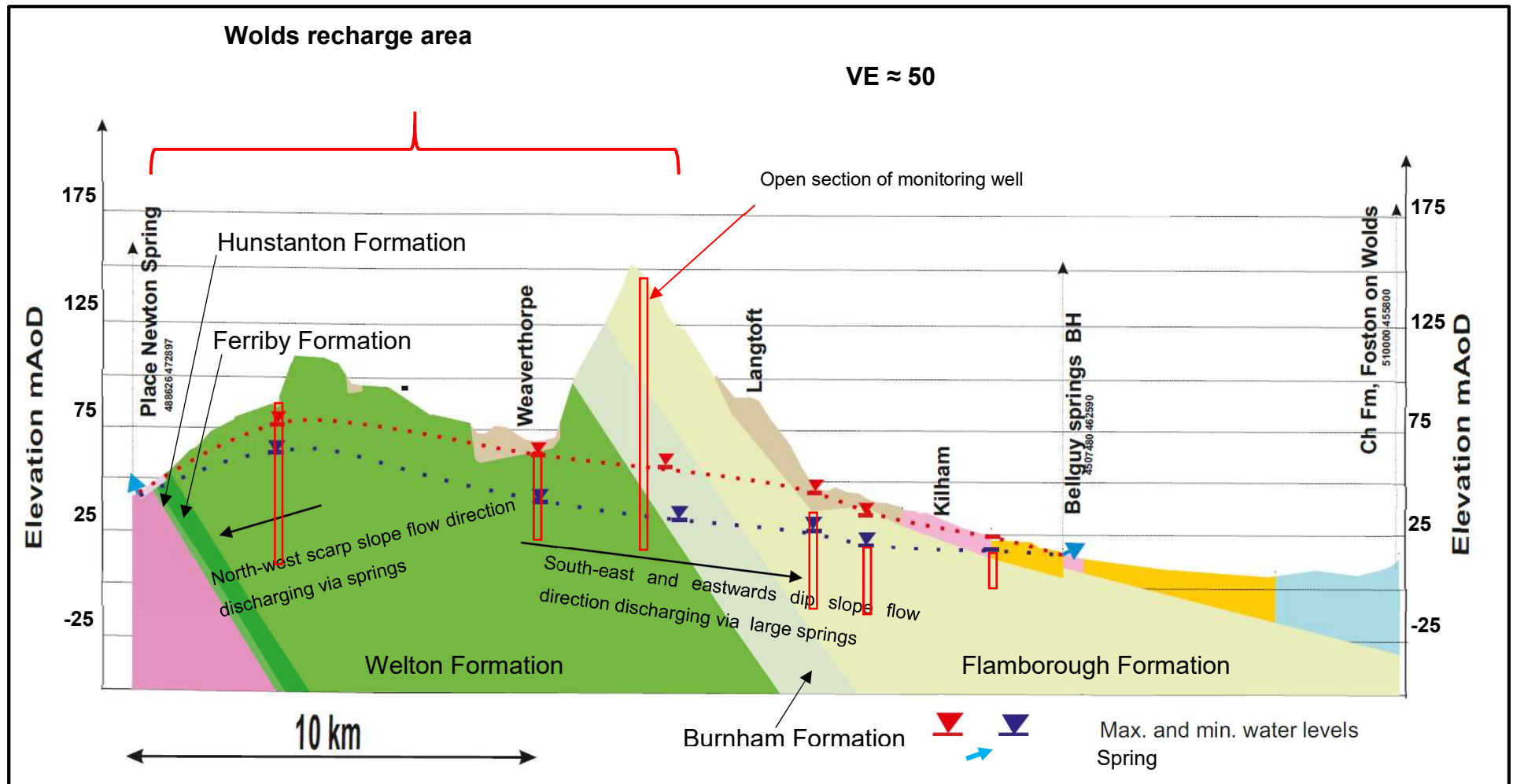


**Figure 2.11.** Geological cross-section of study area showing maximum and minimum groundwater levels, thick unsaturated zone of recharge area and groundwater flow direction on scarp and dip slopes. Groundwater levels data obtained from archived EA monitoring wells marked as red rectangles.

When groundwater reaches the saturated zone, groundwater flow is via the small and large fractures and solutionally enhanced fractures (West and Odling, 2007; Parker, 2009; Parker et al., 2010). Natural groundwater flow direction is eastwards and southwards away from the Wolds along the dip slope towards the edge of the superficial deposits and artesian area. Between the Wolds and the fully confined portion of the Chalk lies the dip slope semi-confined zone of artesian overflow, where the majority of the aquifers dip slope groundwater discharge occurs via numerous sizable springs which form the source of the River Hull and its tributaries. The groundwater level flattens towards the Kilham area and the artesian discharge zone due to the large transmissivities in the area from solutional enhancement of fracture apertures / conduit development. The Chalk also discharges via springs on the Wold escarpment on the west, at the boundary with the underlying Speeton Clay strata (ESI, 2010).

Due to the superficial deposits cover on the Holderness Plain, groundwater flow is sluggish resulting in reduced fracture enlargement (Gale and Rutter, 2006). Foster and Milton (1976) indicate that the Chalk might probably be discharging to surface drains, because drain water had Chalk signature. The natural regional groundwater flow direction on the dip slope is south-east and east wards discharging naturally via the major and large springs in the semiconfined and artesian area. However, this flow direction is altered by major local abstraction in places. In the Kilham area, the Kilham abstraction is not large enough to offset the hydraulic gradient, possibly due to the high transmissivity in the Kilham discharge area (ESI, 2010). On the scarp slopes, flow direction is south-west discharging via relatively minor springs at the contact of the base of the aquifer and underlying clays.

### **2.2.6 Geochemistry of the Northern Chalk Aquifer**

Ninety-eight percent of the Chalk is made up of calcite and low magnesium calcite (Pitman, 1986). Also present as minor constituents of the Chalk are clay minerals (illite and smectite), pyrites (Hancock, 1975), iron oxide, flint bands and clastic limestone (Smedley et al., 2004). Phosphate minerals are also present as concretions. Organic matter content of the Chalk is very low, ranging between 0.01 – 0.1%.

Pitman (1978) used leachates from lysimeters to show that about 76 – 87 % of initial solution occurs within the first metre of infiltration in the unsaturated zone, suggesting rapid equilibration of infiltrating water with respect to calcite. It also showed that recharge water has a well defined chalk-like groundwater chemistry before getting to the saturated zone. Evidence from Pitman (1978) and solute profiling in the unsaturated zone ( eg. Foster, 1976; Foster et al., 1982; Lawrence et al., 1983) also showed nitrate concentrations above the natural baseline value of less than 2 mg/L (Foster et al., 1982), suggesting anthropogenic input from agricultural sources.

From previous studies of the hydrochemistry of the aquifer (Howard and Lloyd, 1983; Pitman, 1986; Hiscock and Lloyd, 1992; Elliot et al., 2001), the saturated zone of the Chalk has two distinct geochemical zones classified as:

- (i) the western oxidising unconfined / semi-confined zone (the study area of this work); and
- (ii) the reducing confined portion east of the buried cliffline where the waters become saline.

A well buffered (pH 7.0 – 7.5) and relatively dilute groundwater is found in the oxic unconfined part of the aquifer, with  $\text{Ca}^{2+}$  and  $\text{HCO}_3^-$  controlling the water chemistry. Elevated nitrate, sulphate and chloride concentrations in this portion of the aquifer signify young recharged waters and anthropogenic inputs from agricultural activity (Smedley et al., 2004; Gale and Rutter, 2006). Relatively older but dilute groundwater is found in the semi-confined zone, with similar chemistry to water in the unconfined part of the aquifer, but with low nitrate contamination because of the protection from the semi-confining layer.

To the east of the buried cliffline, in the confined portion of aquifer, the waters become anoxic characterised by below detection nitrate concentrations. There are two water types in this confined area. The first water type in the confined zone show higher magnesium, potassium and strontium concentrations than unconfined groundwater with very low sodium and chloride concentrations, which indicate long residence time, with no sea-water influence. The second water type is located in the coastal confined portions of the aquifer, which exhibit elevated total dissolved solids (TDS). Elevated

sodium and chloride concentration signify sea-water intrusion and waters of long residence time.

### **2.3 Summary of the geology and hydrogeology of the Chalk**

- The Chalk of the East Yorkshire aquifer is a very important source of water for the region. An understanding of the aquifer properties requires an appreciation of the geologic history and processes.
- The Chalk was deposited during the Cretaceous and underwent tectonic compression and uplift during the Late Cretaceous and Tertiary periods. The compression resulted in faulting, folding and uplift of the Wolds to its current elevation and terrain. Quaternary glacial erosion and deposition from the ice-sheets and meltwaters affected the topography, resulting in further fracturing and confinement of the of the aquifer on the Holderness Plain.
- The lithology, structure and superficial deposits affect the hydrogeology of the Chalk. The physical hydrogeologic properties affected by the geology are permeability and transmissivity, storage and recharge.
- The Chalk is an aquifer because of the storage and flow of water in its fracture network in both the saturated and unsaturated zones. Fracture flow is important not only for the resource evaluation and estimation, but for predicting contaminant transport in the aquifer.
- In the unconfined aquifer, permeability and transmissivity are highest at the zone of seasonal water table fluctuation, although there are some discrete deeper flow horizons. Infiltrating and recharging water is responsible for solution enhancement of fractures in the unconfined aquifer.
- In parts of the confined aquifer, frost shattering which is most pronounced in the Hull Valley is responsible for high permeability on the surface, with permeability reducing with depth because of reduced aperture and water circulation. Marl and flint bands that are existent in both the unsaturated and saturated zones cause concentrated flows in the fractures, causing Chalk dissolution and fracture enlargement.

- In the lateral direction, transmissivities are higher in the unconfined zone and the artesian areas, reducing towards the confined area, which has superficial cover resulting in sluggish flow as a resultant of low fracture enhancement. Transmissivities are also known to be higher in the valleys as compared to the interfluves.
- The hydrogeology reflects directly on the distribution of surface water courses in the area. In the semiconfined zone, the aquifer discharges to numerous springs that feed the River Hull. The intermittent Gypsey Race, which is the only water course on the Wolds is also impacted by the geology and hydrogeology of the Chalk, flowing its full length only at times of high water levels.
- The geology defines the dominance of  $\text{Ca}^{2+}$  and  $\text{HCO}_3^-$  in the oxic groundwater of the unconfined and semi-confined zones. High nitrate, sulphate and chloride concentrations signify the vulnerability of the unconfined portion of the aquifer to anthropogenic inputs. Matrix and fracture diffusive exchange and rapid bypass flow in the unsaturated zone results in rapid transport and long residence time of contaminants. To the far east and coastal areas of the aquifer, reducing conditions result from Quaternary deposit confinement and sluggish flows that prevent the aquifer from freshening. Anthropogenic activity is also at play in the coastal areas of the aquifer, where over-abstraction of groundwater has led to saline intrusion.

## **Chapter 3 Kilham Catchment and Previous Relevant Work**

In this chapter, the reasons for the choice of the Chalk / Kilham Catchment for this work will be justified, followed by the historical context of previous relevant work undertaken by the British Geological Survey (BGS), Environment Agency (EA), the University of Birmingham (UoB) and University of Leeds (UoL) in the study area. Archived data obtained from the BGS and EA, Yorkshire Water (YW) and the UK Meteorological (MET) Office and how they were treated and used in this work is also presented. Also, noteworthy in this chapter is the presentation of the analyses of archived pumping test data for the Kilham area from the EA with the aim of determining the distribution of transmissivities, and their relation with respect to the location of faults in the area.

### **3.1 Justification of the catchment of study**

The study area, which is part of the East Yorkshire Chalk aquifer, with the Kilham Catchment, based on topographic highs is marked out in Figure 3.1. On Figure 3.1 are also marked the springs and boreholes used for the current study.

The catchment of study was chosen because of its resource importance and risk of contamination, previous hydrogeological investigations undertaken in it and it being a typical fractured limestone aquifer.

The Chalk Aquifer is very important at the UK scale. In East Yorkshire, the Chalk is the main source of potable water supply for the area, with the EA licensing about 195 million L/day to abstraction. Aside from the abstractions, more than 80 – 95% of flows (National River Flow Archive (NRFA), website <https://nrfa.ceh.ac.uk/data/search>) for the springs and streams that support the ecology and the conservation Sites of Special Scientific Importance (SSSI) of the River Hull headwaters are groundwater derived from the Kilham catchment and Driffield area (ESI, 2010). In spite of the importance of the aquifer, it has been plagued by diffuse pollution by agrichemicals especially from nitrates that started getting into groundwater from the 1970s onwards

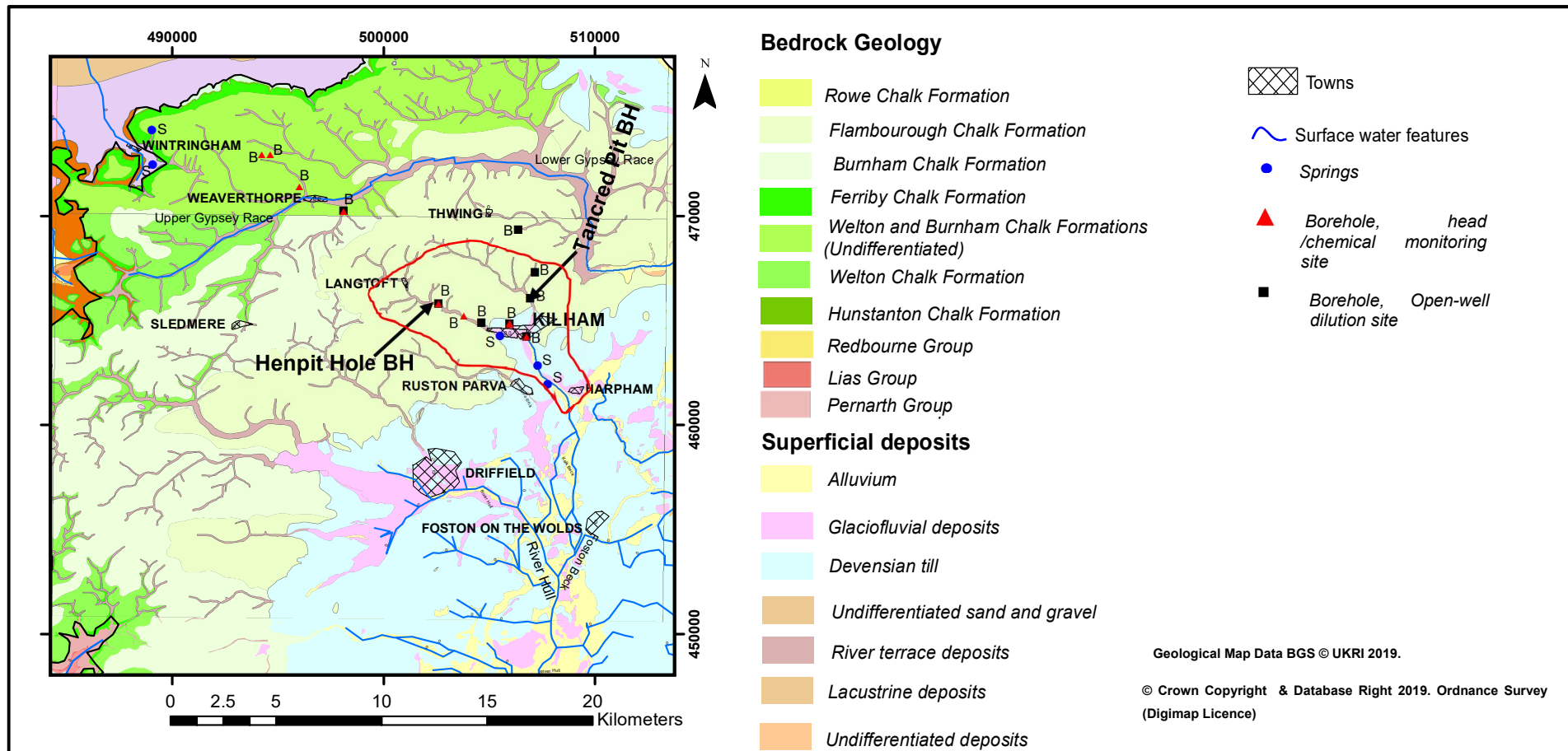


**Figure 3.1.** The general study area (grid boundaries), with the Kilham catchment marked in red on topographic highs and the springs and borehole sites used for this study marked out. Further details on location are presented in chapters 4 and 5.

(Foster and Crease, 1974; Foster et al., 1982; Lawrence et al., 1983) and more recently by persistent pesticides (Smedley et al., 2004) resulting in the delineation of the East Yorkshire Chalk outcrop as a Nitrate Vulnerable Zone (NVZ). The contamination and abstraction pressures on the aquifer has ultimately resulted in the classification of the aquifer as being in “Poor” status in terms of quality and quantity under the European Water Framework Directive (EU WFD) (ESI, 2010).

Secondly, the Kilham catchment was chosen because it is regionally important for two reasons. Although Kilham is a typical Chalk catchment, in comparison to adjoining catchments like the Driffield and Kirby Grindalyte, the Kilham catchment is structurally complex and contorted with important basement faults and folds traversing the catchment (subsection 2.1.5). There are the Burton Fleming and Hunmanby Faults, that are the two major NNE-SSE trending faults with other several minor E-W trending faults in the area. Also, there is a main regional open syncline plunging at 2 - 5° through Kilham village on an axis between Driffield and Bridlington, with several minor E-W folds (subsection 2.1.5). These structural complexities have the potential to influence groundwater flow both on the local and catchment scale. Understanding the influence of the structural complexity on groundwater flow will enable source delineation for springs and wells in the catchment.

Finally, several previous hydrogeological investigations have been undertaken on the Kilham catchment. More recently (2010 to date), the EA has chosen the catchment for both chemical monitoring and hydrogeological characterisation. The findings from the previous and ongoing studies by the EA in the study area will provide a background and conceptual context for constraining the findings from this current project.

### **3.2 Previous hydrogeological investigations in the study area**

Majority of previous investigations on the catchment were undertaken by the BGS. The BGS undertook these works on their own, in partnership with the EA or for the EA. Other players in the area include Yorkshire Water (YW) and the

Universities of Birmingham (UoB) and Leeds (UoL). The following paragraphs will start with unsaturated and saturated flow characterisation undertaken in the area by the BGS, after which other works undertaken in the area by the other players will be presented.

Prior to the 1970s, British hydrogeological thought and focus was on resource potential assessments, with the mindset that aquifer chemistry depended solely on interaction between water and aquifer materials only (Foster, 2000). Also, as a result of works such as Mclean (1969), Headworth (1972) and Downing et al. (1978), it was also thought that solute transport through the unsaturated zone to the saturated zone was solely via rapid fracture flow. But in the early 1970s, these perceptions were to change. Firstly rising nitrates in major aquifers led to the linking of agricultural activities and landuse with aquifer contamination. Secondly, Smith et al. (1970), used environmental tritium (resulting from thermonuclear testing in the 1950s and 60s) profiling to suggest a mechanism of slow downwards piston flow of about 0.9 m/year. But Foster (1975) presented an alternative explanation to the interpretation of Smith et al. (1970) by demonstrating the importance of the unsaturated zone in either attenuating or rapidly transmitting contaminants to the water table (sub-section 2.2.1). This paradigm shift in British hydrogeological thought led to several unsaturated zone solute profiling and characterisation studies (eg. Foster, 1976; Foster et al., 1982; Lawrence et al., 1983) of which the Chalk and East Yorkshire Chalk featured very prominently, showing high nitrate concentrations in the unsaturated zone under tilled land. This evidence of nitrate contamination and rising nitrate concentrations under tilled land showed the threats anthropogenic activities posed to groundwater resources.

The initial water resources assessment investigations on the Chalk were started by the BGS in the 1970s, with physical hydrogeological appraisals of groundwater resource evaluation (eg Foster and Milton, 1974; Foster and Crease, 1975) for the feasibility of a river augmentation project using the Chalk aquifer. The hydrogeological appraisals include pumping tests in the East Yorkshire Chalk and the study of the correlation of chalk stream discharge characteristics with groundwater level variation. A pumping test ( $Q = 324 \text{ m}^3\text{d}^{-1}$  for about 7 days) in 1970 in the Etton area, south of the Kilham catchment

provided evidence of laminar flow towards pumped wells and supporting the use of conventional pumping test analyses on the Chalk aquifer (Foster and Milton, 1974). The Etton pumping tests also showed the effect of groundwater table fluctuation on transmissivity estimation in the unconfined part of the aquifer. In 1982, the BGS undertook a 3 months long ( 5<sup>th</sup> July to 6<sup>th</sup> October 1982) large scale pumping test at Nine Dikes and Cottage Farm (Figure 3.2) aimed at determining the long term borehole yields and also investigating the effects of pumping on rivers and streams in the area. The boreholes were pumped at a combined average rate of 11.2 tcmd (thousand cubic metres daily), yielding a recorded maximum drawdown of 0.5 m in 10% of the area influenced by the test, showing an unconfined aquifer of high transmissivity. This study showed large transmissivities in the Broachdale and Langtoft Valleys (Figure 3.1), and into the Kilham and Harpham areas (Figure 3.2), where artesian conditions exist. The test also suggested the existence of boundary effects on the north western and north eastern parts of the catchment probably from fault effects, or from recharge boundary effects in the Gypsey Race Valley, or from a combination of both preceding factors.

For flow and permeability variation with depth in the aquifer, West Beck stream discharge correlation with groundwater level fluctuation during a recession period (Foster, 1974) and geophysical logging in the Etton area (Foster and Milton, 1974) gave the first line of evidence of hydraulic layering in the aquifer. In the 90s, the BGS (Buckley and Talbot, 1994) compiled and examined archived suite of geophysical logs undertaken in 12 boreholes. The aim of the compilation was the examination of the possibility of correlating fissured horizons between boreholes in the Kilham area for the planning and interpretation of tracer tests for delineation of the catchment and source protection zone (SPZ) demarcation for the Kilham Abstraction. Amongst the logs, they found the caliper, resistivity, heat pulse and flow impeller logs as the most useful for stratigraphic correlation whereas gamma, fluid EC and temperature were not useful. The difficulty resulted from arbitrariness and non-consistency of measurements across different institutions and techniques, effects of artifacts in logs due to tightness of scales on reproduction and digitisation and difficulty in calibrating the logs due to improvements in techniques over the 20 years. In spite of the difficulties and some lack of

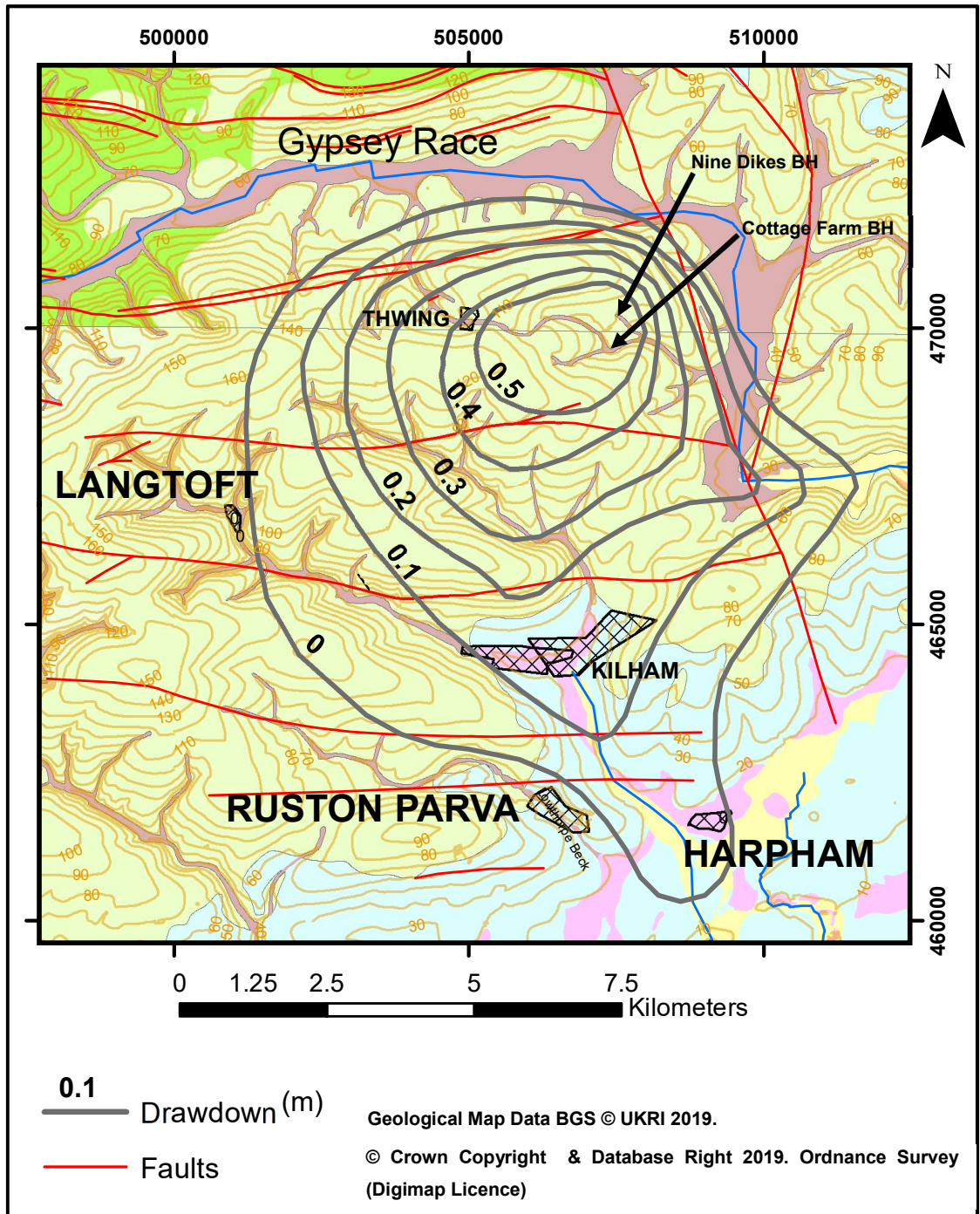


**Figure 3.2.** Drawdown of 3 months duration large scale pumping test superimposed on faults mapped by Farrant et al (2016). Large transmissivities exist in the Broachdale and Langtoft valleys and south of Kilham whilst probable boundary effects are indicated by closeness of the groundwater contours in north-eastern and northern part of area of influence.

of confidence in the geophysical logs, they found provisional flow horizons lay within -11 and 34 mAoD, with a majority lying within 30 m below the land surface. They also found caliper enlargements fell within the zone of groundwater table fluctuation. In some of the boreholes (eg. Tancred Pit and Henpit Hole boreholes located in the Broachdale and Langtoft valleys respectively, see Figure 3.1), they also found flowing features at deeper depths outside the previously stated depths. From these observations, they gave provisional flow horizons in each borehole but had difficulties correlating flow between boreholes because of the unavailability of definite and distinctive lateral and continuous stratigraphic markers like marls or flints. They tried constraining flow horizons by bedding across the area, but this did not fit all the boreholes, casting some doubt on correlation via bedding and recommended geophysical logging of the observation boreholes using newer and better calibrated methods to constrain and define bedding and lithological features more accurately. Using the provisional flow horizons of Buckley and Talbot (1994), the BGS (Ward and Williams, 1995; Ward et al., 1997; Ward et al., 2000) undertook two rounds of tracer tests in the area between and within the Langtoft and Broachdale Valleys with the aim of establishing connections between boreholes and springs in the area. The aim was to provide evidence to the EA for the delineation of source protection for the Kilham abstraction and springs in the Kilham area. The tracer tests showed connection between some of the wells in the area, with fast flows in up to 100s of  $\text{m d}^{-1}$  between the boreholes and springs.

Aside from the previous geophysical works used by Buckley and Talbot (1994), the EA also commissioned Southern Science to undertake a suite of geophysical logs in 14 boreholes in the Kilham area. The main aim was to provide design information for the installation of piezometers in the area by the EA for the monitoring of water quality variation with depth in the aquifer. Secondly, it was also to support the tracer tests undertaken by the BGS stated in the preceding paragraph. Southern Science Ltd, (1994) undertook Closed Circuit Television (CCTV), temperature, conductivity, impeller, caliper, natural gamma, resistivity and gamma-gamma logs the boreholes under ambient conditions. The logging confirmed previous flow horizons in some of the

boreholes, with the production of qualitative borehole flow analyses from the CCTV inspection.

In the EAs bid to effectively manage and regulate groundwater resource in the East Yorkshire aquifer and also meet the European Water Framework Directive (EU WFD) of characterising the physical and chemical status of groundwater resource bodies, the EA commissioned ESI Ltd in 2009 to develop a numerical hydrogeological model of the East Yorkshire Chalk aquifer. The project scope included the development of a 3D geological model of the aquifer and spot gauging of flows in streams sourced from springs draining the Chalk escarpment (ESI Limited, 2010). Farrant et al. (2016) provided data for the refinement and recalibration of the initial ESI model, for the assessment of the impact of faults on groundwater flow in the Kilham catchment. Farrant et al. (2016) undertook geological deskstudy and fieldwork, and literature review of previous flow characterisation in the Kilham area with the aim of producing an improved conceptual geological model of flow for input into the ESI second round of modelling. They mapped faults on the field hitherto not identified, confirmed previously known faults and also used previous tracer tests and flow logging data to characterise flow horizons in several wells in the area. Flow focussing and high transmissivities were found at depth, suggesting that the standard VKD model used in the previous ESI numerical model was not appropriate for the catchment. Also they tried correlating flow horizons between boreholes and mapped the Flamborough and Burnham boundaries, but these were fraught with uncertainties because of the unavailability of standard geophysical logs for wells in the area, poor lithostratigraphic and biostratigraphical control between Flamborough Head and inland exposures (Whitham, 1993b).

Recently, during the 2015/16 and 2016/17 hydrological years, the EA undertook a series of geochemical sampling and borehole geophysical logging of Weaverthorpe, Weaverthorpe Slack and Bartondale boreholes. The aim of sampling was to monitor seasonal variation of groundwater quality in springs and wells on the Chalk, whereas the borehole logging was to monitor groundwater quality and flow variation with depth, and also to estimate the age of groundwater at the various depths. The geophysical tests include caliper,

natural gamma, fluid temperature and conductivity, impeller flowmeter and optical imaging logging. The findings of the geophysical tests are reported in Butcher and Townsend (2017).

In terms of aquifer data and information, the BGS in collaboration with the EA have compiled detailed geological and hydrogeological information of the aquifer in investigations like Allen et al. (1997), Smedley et al. (2004), and Gale and Rutter (2006). Allen et al. (1997) provides a physical characterisation of the aquifer in terms of flow conditions and resource potential. Smedley et al. (2004) and Gale and Rutter (2006) are baseline condition reports. Smedley et al (2004) analysed and interpreted spatial, temporal and depth quality trends in groundwater chemistry of the East Yorkshire Chalk aquifer and is a very useful document for understanding the groundwater chemistry of the East Yorkshire Chalk.

The UoL have undertaken previous research on the Northern Province Chalk and the Kilham catchment with a focus on unsaturated zone transport, saturated zone flow structure and geometry. Zaidman et al. (1999) used geophysics to map the downward movement of an applied saline tracer from the ground surface into the unsaturated zone. Allshorn (2008) and Keim (2013) studied tracer fluxes, and soil moisture and discharge respectively to the exposed face of a tunnel. The three unsaturated zone studies confirmed preferential flow bypassing the chalk matrix to the water table during times of high hydraulic loadings. Hartmann (2004) and West and Odling (2007) also used the concentration profiles of injected tracers near a pumped borehole to characterise fracture network properties and the identification of flow zones in boreholes at the Wilfholme Landing site (NGR TA 062 472), which is in the confined area of the aquifer. Parker (2009) developed a conceptual model to better characterise vertical and lateral hydraulic conductivity variation, flow variation in wells from literature (eg. Buckley and Talbot, 1994,1996; Bloomfield and Shand, 1998) and new results from borehole dilution testing and flow logging for 26 boreholes under both ambient and pumped states on the East Yorkshire Chalk. Her model identified flow zones at the borehole scale, with hydraulic conductivities ranging from very low in some superficial deposits to high in both zones influenced by water table fluctuation, or close to flint and

marl bands. More recently, Azeez (2017) used recession analysis, chemical and numerical methods to characterise flow structure and geometry in the Driffield and Kirby Grindalyte catchments. The catchments were found to be drained by double and one reservoir systems respectively.

### **3.3 Data obtained for the current studies**

#### **3.3.1 EA/BGS**

##### ***Pumping test data analyses***

Archived pumping test data from the unconfined zone of the Kilham Catchment from the EA were obtained and analysed using AquiferWin32 software. The re-analyses aimed at using a consistent method for obtaining aquifer transmissivity values for the assessment of aquifer parameter distribution and also using drawdown data to understand flow regime in the aquifer. The pumping test data were for constant discharge tests for the period 1971 to 1985 for 11 wells (Figure 3.3).

The test duration, discharge and drawdown for each test site are shown in Table 3.1. Generally, most of these tests were single well tests for well yield assessments rather than for aquifer parameter determination requiring no observation boreholes. The unavailability of observation wells made the determination of specific yields impossible for these analysed pumping tests. The highly transmissive nature of the aquifer also resulted in very low drawdowns, as the discharges and pumping durations were not large enough to cause substantial drawdowns. The lack of observation boreholes and the highly transmissive nature of the aquifer made the assessment of boundary effects by faults impossible. The data is of poor quality in some of the wells because discharge rates were not constant, and also the water levels were manually monitored.

Because of the highly fractured nature of the Chalk, the very low drawdowns recorded as compared to the saturated thickness of the aquifer and previous linear relationship between yield and drawdown shown by Foster and Milton (1974) at the Etton boreholes, the concepts of representative elementary

volume (REV) for radial flow and the classical Theis (1935) and Cooper and Jacob (1946) approaches and their assumptions were used in the AquiferWin 32 software for the analyses. The head data (metres) and time (minutes) were inputted into the programme and the units were set (time in minutes, discharge

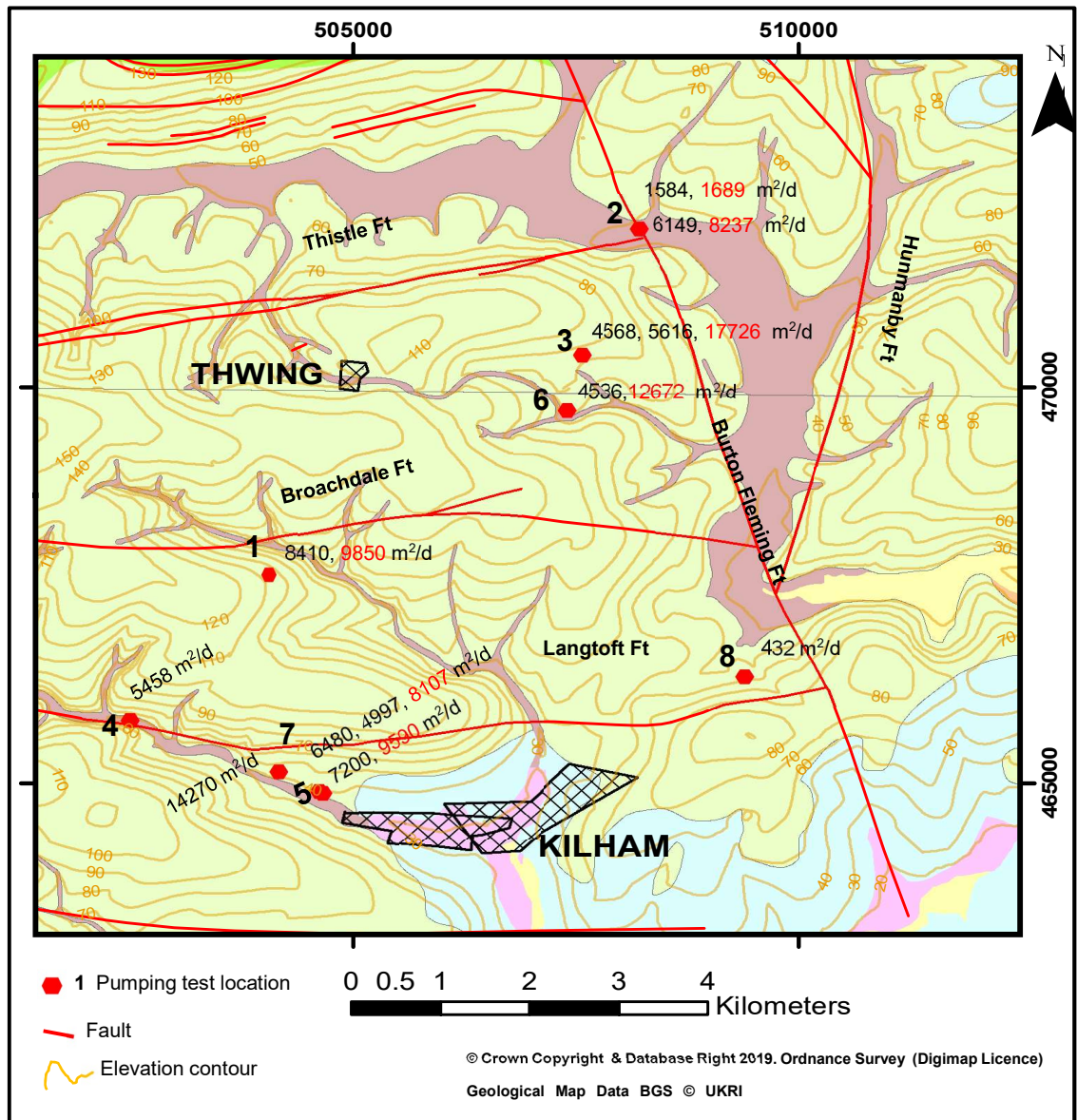


**Figure 3.3.** Transmissivity, fault and contour map superimposed on geology of the Kilham area. Red transmissivity values are from recovery analysis, whereas black text are from C&J, Theis and Neuman analyses. Purple dashed lines are faults from Farrant et al (2016).

in m<sup>3</sup>/min, transmissivity in m<sup>2</sup>/min, and length in metres). The analyses were run for both pumping and recovery periods for available data that were amenable for analyses by the methods stated above. Most of the data were

difficult to analyse using the Theis curve approach as the drawdown versus time curve was relatively flat due to the very small drawdowns.

For the Cooper and Jacob (C-J) straight line analyses, the regression line was fitted for late time data so as to avoid the possible well bore storage effects. This was a constraint of the approach because of the unavailability of observation boreholes to determine the limiting time i.e.  $u \leq 0.01$  value. For the Theis recovery analyses, the data was fitted to late time, when the time ratios were small and approaching 2 when it is expected that the well bore storage effects were negligible. The software output of transmissivity were in  $\text{m}^2/\text{min}$ , and were converted to  $\text{m}^2/\text{d}$ .

The results for these analyses are presented in Table 3.1 and on Figure 3.3. The attached map has the locations, transmissivity values and confirmed/mapped faults from Farrant et. al (2016). Transmissivity values from recovery tests are of the same order of magnitude for transmissivities from the C-J, Theis and Neuman methods for the drawdown phase but generally the recovery phase values are higher for all the locations. This could be due to two possible reasons. The first has to do with the discharge rate used in the recovery phase analyses, which was normally taken to be the last discharge rate at the time the pump was stopped. Had the discharge sequences been timed for the pumping duration, an average and corrected discharge could have yielded a smaller transmissivity for the recovery phase analyses. Secondly, a backflow from the discharge line into the well at the time pumping stops can result in artificial recharge resulting in large transmissivity values for recovery tests. To prevent this, check valves could have been used during pumping tests to cut out backflow to the well. There was no information about the methodology used to collect the drawdown data analysed in this study.

In the current analyses, the distribution of the transmissivity locations is not dense enough for a spatial correlation, but the values are biased towards the valleys as the wells are mostly concentrated in the valleys and increase towards the Kilham area. Bias towards the valleys is mostly because most of these wells were drilled for yield assessments rather than aquifer property characterisation. It is difficult to determine the effect of faults in the area because there were no observation wells near or straddling faults. Also the low pumping rates used in

**Table 3.1.** Pumping test characteristics and Transmissivity estimations in the Kilham Catchment

Label number	Site and date of test	Coordinates from BGS geoindex/distance to nearest fault	Diameter (m)	Borehole depth/ casing bottom / RWL bgl (m)	Q (m <sup>3</sup> /min)	Maximum drawdown (m)	Pumping duration (min)	Transmissivity, T (m <sup>2</sup> /day)		Best T stated by Farrant et. al. 2016
								Drawdown phase	Recovery	
								C & J <sup>1</sup> / Theis <sup>2</sup> / Neuman <sup>3</sup>	Theis recovery	Obtained from different sources
1	Broachdale (Sept. 1978)	504500,467850 420m	0.2	85/7.5/33.3	0.874	0.279	480	<b>8410<sup>1</sup></b>	<b>9850</b>	<b>N/A</b>
2	Burton Fleming (Mar. 1977)	508200,472000 133 m	0.2	30/12/25.5	0.415	0.41	480	<b>1584<sup>1</sup></b>	<b>1699</b>	
2	Burton Fleming (Feb. 1985)	508200,472000 133 m	0.2	30/12/25.5	1.164	0.41	1800	<b>6149<sup>1</sup></b>	<b>8237</b>	<b>N/A</b>
3	Cottage Farm (Sept. 1981)	507400,469700 1.5 km	0.15	60/7.5/27.4	1.400	0.875	120	<b>4536<sup>1</sup></b>	<b>12672</b>	<b>5000</b>
4	Henpit Hole (Aug. 1978)	502500,465800 160 m	0.2	65/13/18.3	0.638	0.225	540	<b>N/A</b>	<b>5458</b>	<b>11028</b>
5	Little Kilham Farm 4 <sup>r</sup> well (Aug. 1978)	504660,464880 1.2 km	0.1	30/8/16.1	0.462	0.044	420	<b>6480<sup>2</sup>, 4997<sup>1</sup></b>	<b>8107</b>	<b>7698</b>
5	Little Kilham Farm 8 <sup>r</sup> well (Aug. 1978)	504620,464900 1.2 km	0.2	50/8/16.1	0.500	0.214	570	<b>7200<sup>1</sup></b>	<b>9590</b>	
6	Nine Dikes (Jul. 1978)	507570,470400	0.2	82/7.5/44.5	2.500	0.19	1140	<b>4568<sup>3</sup>, 5616<sup>1</sup></b>	<b>N/A</b>	<b>9800</b>

**Table 3.1. continued**

6	Nine (Sept. 1981)	Dikes	507570,470400	0.2	82/7.5/44.5	0.831	0.22	390	<b>N/A</b>	<b>17726</b>	
7	Middledale (Aug. 1978)		504170,465140 400m	0.2	55/25/19.3	0.939	0.035	480	<b>14270<sup>1</sup></b>	<b>N/A</b>	<b>6318</b>
8	Manor (Oct. 1984)	House	509390,466350 309m	0.2	50/10/27.1	0.590	0.72	180	<b>432<sup>1</sup></b>	<b>N/A</b>	<b>N/A</b>

comparison with the aquifer transmissivity may have made it difficult to detect faults more remote to the pumped wells.

Table 3.1 also contains the best estimates values of transmissivity values from Farrant et al. (2016) obtained from the EA excel summary of transmissivities for the catchment, transmissivities values stated by Allen et. al. (1997), Ward et al. (1997) and other sources. Their values are given here for comparison purposes only, as there are no dates and the exact borehole coordinates for the pumping tests because there are several boreholes on the same site. Their estimates are mostly within the range of values obtained for this current analyses and are of the same order of magnitude. The differences between this current analyses and the values of Farrant et al. (2016) could be due to differences in season of test, analytical method methods used, analytical subjectivity and how the tests were performed.

#### ***Borehole geophysical log data***

Between February and April 2017, hardcopies of borehole geophysical logs undertaken in the area by Southern Science, Water Research Centre, BGS, UoB were retrieved from the EA archives. The aim of obtaining the borehole logs was to constrain the interpretation of uniform and point open-well dilution test results for this current work. Qualitative CCTV models and image logs were scanned and aligned with depth of open-well dilution tests. Caliper logs were also scanned and digitised by scaling and tracing the logs in WebPlotDigitizer (obtainable from <https://automerio.io/WebPlotDigitizer/>). The borehole diameters with depth were then plotted in originpro and correlated with open-well dilution results in Chapter 4.

#### ***Historical groundwater levels, BGS geindex and Edina digimap datasets***

Historical groundwater level data from the EA archives and borehole information obtained from the BGS geindex dataset (<http://mapapps.bgs.ac.uk/geologyofbritain/home.html>) were used in planning open-well dilution tests (Chapter 4) and for complementing monitored groundwater levels for this work (Chapter 5). The geindex in combination with Edina digimap geological and ordnance datasets were used to develop

geological and hydrogeological cross-sections in Chapters 2 and 6. The cross-sections with the Formation contacts were initially plotted in the BGS Groundhog® Desktop GIS software, and imported to Corel Draw, to be drawn over. This was because at the time of the section development, the BGS software was in beta mode and had functional weaknesses.

### ***Geochemical sampling data***

Borehole and spring geochemical sampling data for the 2015/16 and 2016/17 hydrological years for the Kilham catchment were obtained from the EA groundwater quality archive (from <https://environment.data.gov.uk/water-quality/view/landing>). This data provided a context for comparing yearly geochemical time series for the wells and springs in the study area with the aim of understanding the factors that affect the major ion geochemical seasonal variability. Nitrate data from Kilham and other abstraction boreholes were also taken from YW for the same purpose as the EA geochemical dataset. Both datasets are presented and discussed in Chapter 5.

### ***Foston Mill Gauging Station data***

Stream flow data from Foston Mill Gauging Station (TA 093 548) (Figure 5.7), which measures groundwater discharge from the Kilham catchment was also obtained from the EA to enable a correlation of stream flow data with groundwater level data. The aim of doing this was to get an understanding of the similarities and differences of groundwater fluctuations and Chalk groundwater discharge for a catchment scale analyses. This dataset is presented and discussed in Chapter 5. Details of the gauging station are obtainable from <https://nrfa.ceh.ac.uk/data/station/info/26003>.

### **3.3.2 UK MET Office Data and UK Air Information Resource (UK AIR) rainfall chemistry data.**

Hourly pressure, rainfall and temperature data for Leconfield (TA 015 436), Bridlington (TA 185 678) and Lowthorpe Elms No.2 (TA 074 61) weather stations were obtained from the UK MET Office for the study period. The data was compared with spring temperatures, groundwater levels and used as a barometric check on the barometric pressure readings for this study in Chapter 5. Double mass analysis (Willis, 1999) of the monthly average rainfall

average data for the stations using Lowthorpe Elms No.2 as control station showed that the stations behaved similarly with  $R^2$  of 0.9997 and slopes of 1.02 and 1.08 for Leconfield and Bridlington stations respectively. Lowthorpe Elms No. 2 (TA 074 611, elevation 20m AoD) data was used as proxy for the Kilham area, because it is the closest station to the observation boreholes in Kilham and also due to the similarities of rainfall across the catchment. However, in spite of the rainfall similarities, orographic effects in the catchment has the potential to cause local variation in precipitation events and amounts, and atmospheric pressure distribution in the area. Rainfall chemistry data for the years 2014 to 2018 were obtained for High Muffles (SE 775 939), from the UK Air Information Resource (UK AIR), UK Eutrophying and Acidifying and Precipitation Network (UKEAP) website. This site because was used because it is the closest to the study area and since the main economic activity of the area is agriculture, High Muffles is considered representative of the rainfall chemistry.

### **3.4 Chapter summary**

- Justification has been given for the choice of the study area and Kilham catchment.
- The study area was chosen because of its water resource importance and pollution threat, its structural complexity and how it affects flow and previous and current ongoing work and how they provide constraints to the findings of this work.
- An overview of relevant work that underpins the current work has been presented.
- How archived data was obtained from the EA/BGS, YW, WRC, Southern Science, UoB and MET Office and how they were treated and used has been presented for the continuing chapters.
- Undertook the analyses of archived pumping test data with the aim of determining the distribution of hydraulic properties and their relation to faults in the area.
- The transmissivities (430 – 14270 m<sup>2</sup>/d) determined showed an aquifer which is variable even at the local scale. Because of the nature of the

pumping tests (mostly single well tests), the effects of faults on the transmissivities was not determined.

## **Chapter 4 Open-well dilution testing and the characterisation of flow variation with depth**

### **4.1 Hydraulic conductivity and flow variation with depth in the Chalk**

The Chalk is a fractured, anisotropic and heterogeneous aquifer (Allen et al., 1997) with flow occurring in a network of solutionally-enhanced (karstic) fractures and conduits (Tate et al., 1970; Buckley and Talbot, 1994; Maurice et al., 2012) resulting in flow variation with depth and hydraulic head differences between different flow zones. Knowledge of flow variation with depth is important for catchment delineation and the evaluation of groundwater resource potential (Pedler et al., 1990; West and Odling, 2007; Moir et al., 2014) and in abstraction well design and development (Gossell et al., 1999; West and Odling, 2007). Flow variation with depth information also enhances groundwater modelling results and enables the determination of the fate and transport of contaminants for effective design of a remediation scheme (Moir et al., 2014) in pinpointing locations to sample and pump water from (McMillan et al., 2014). For the East Yorkshire Chalk in particular, knowledge of ambient vertical flow components in wells is a prerequisite for the interpretation of groundwater levels (Saines, 1981; Price, 2009; Post and von Asmuth, 2013) and for planning groundwater sampling (McMillan et al., 2014) and tracer tests (Maurice et al., 2010).

The methods used to characterise hydraulic flow variation with depth in a borehole include core sampling (Shuter and Teasdale, 1989), conventional geophysical logging (Keys, 1990), caliper logging (Paillet and Pedler, 1996), packer testing (Quinn et al., 2011), flow logging (Molz et al., 1989; Parker et al., 2010), borehole CCTV (Zemanek et al., 1970; Paillet, 1991) and open-well dilution testing (Tsang et al., 1990; Tsang and Doughty, 2003; West and Odling, 2007; Maurice et al., 2010; Parker et al., 2010) amongst others. Core logging and sampling to determine the hydraulic conductivity variation with depth is not representative of a heterogeneous medium like the Chalk which has flow dominated by fractures. Also sampling and coring for laboratory tests

results in disturbed samples. Conventional borehole geophysics include the techniques that use the borehole wall or fluid properties to indirectly infer flow properties and these includes neutron, gamma and resistivity logging. Caliper logs measure the borehole diameter, and show borehole wall enlargement. The enlargements coincide with fractures (which may or may not be flowing features) and/or may be caused by drilling effects. Borehole flow logging is a direct borehole logging method used to evaluate hydraulic conductivity and flow variation with depth in a borehole that is open to the aquifer and can be done under both pumped or ambient conditions. Flow logging measures profiles of cumulative flow with depth during logging. An increase in flow signifies an inflowing feature, whereas a decrease in flow marks an outflowing feature. However, flow logging is expensive, requires the caliper log for interpretation and has a lower detection limit of  $10^{-2} \text{ ms}^{-1}$ , whereas ambient horizontal flow velocities in open boreholes can be as low as  $10^{-4} - 10^{-6} \text{ ms}^{-1}$  (Pitrak et al., 2007). Flow logging is also not able to detect pure horizontal crossflows in boreholes (Paillet and Pedler, 1996; Maurice et al., 2010). Packer tests are expensive, time consuming and require a priori information about the subsurface for interpretation of results. Packers also sample only a small volume of the aquifer at the borehole wall. Borehole CCTV and image logs provide a view of borehole wall properties by showing horizontal and vertical fractures, but not all fractures detected are flowing features. Also, image logs are variable in quality and can be very difficult to interpret especially in turbid groundwater.

Open-well dilution testing, also known as hydrophysical logging (eg. Pedler et al., 1992; Kobr, 2003; Paillet et al., 2012) is a technique used to characterise borehole hydraulic properties and flow variation with depth in uncased boreholes via the interpretation of specific electrical conductance (SEC) contrasts between aquifer formation fluid and borehole fluid column resulting from the introduction of a tracer in the well (Tsang et al., 1990; Pedler et al., 1990; West and Odling, 2007; Maurice et al., 2010). Open-well dilution testing can be undertaken under pumped or ambient conditions. The open-well dilution method as compared to the other methods is cheap and easy to undertake, and can also resolve very low vertical flow velocities that occur in

wells under ambient flow conditions. It also lends itself to an improved interpretation from image and caliper logs (Kobr, 2003; Maurice et al., 2010).

Ambient open-well dilution testing was the preferred method in this study because: i. it is cheap, easy to use, and it is done using simple equipment and logistics; ii. the method can resolve very low flows under ambient conditions (Maurice et al., 2010), (iii) the water levels in the majority of the study area > 10m BGL, which makes pumped approaches expensive and impracticable. The following subheadings will provide details about the strengths and weaknesses, operating principles of the method and results obtained from the method. The results are integrated with caliper and image log information where available to provide a better interpretation of the open-well dilution test.

## **4.2 Theory of regional scale groundwater flow**

In order to understand and contextualise the findings from the open-well dilution tests from this chapter and groundwater monitoring in Chapter 5, the theory of groundwater flow on the catchment scale is briefly presented. In a fractured aquifer like the chalk where permeability varies with depth, this theory is important for understanding groundwater flow.

Regional groundwater flow theory thereafter called the Tothian model (of topographically and gravity driven flows) has developed from mathematical, analytical and numerical studies undertaken by authors like Hubbert (1940), Tóth (1962;1963); Freeze and Witherspoon (1967;1968). More recently, main aspects of the concept have been summarised in Tóth (2009). Liang et al. (2010) used a sand box model to demonstrate the concept for the first time.

Regional groundwater flow theory argues that groundwater on the catchment scale divides flow into hierarchical flow cells that separate recharge and discharge areas. Groundwater movement in recharge areas is downwards, whereas discharge areas are marked by upwards movement of groundwater. Between the two are transition areas that have dominant horizontal flows, because there no or little vertical head differences in such areas. Recharge and discharge areas are separated by regional, intermediate or local flow systems. Regional flow systems are characterised by long residence time and deeper flows that sustain perennial springs. Local flow systems on the other

hand drain short residence time and shallower flows that supply springs that are only activated at times of high groundwater levels. Intermediate systems fall in between the local and regional flow cells.

The relative position of recharge and discharge areas, and flow patterns on the catchment scale depend on topography, geology, geometry, stratigraphy and water table configuration of the catchment. Groundwater tables that mimic the rolling terrain in steeply dipping stratified aquifers produce more complicated flow cells with deeper penetration depths of circulation, whereas a flat terrain with flat water tables and low dipping stratified aquifers produce relatively flat, simple flow and shallower systems.

### **4.3 Theory of open-well dilution tests and field methodology used**

#### **4.3.1 Strengths and drawbacks of the technique**

The open-well dilution method has advantages as compared to other borehole investigation techniques. The method is sensitive to very low ambient flows that cannot be resolved by flowmeters (Tsang et al., 1990; West and Odling, 2007) and can also detect crossflows under both ambient and pumped conditions (Doughty and Tsang, 2005; West and Odling, 2007; Maurice et al., 2010). It is also less expensive in relation to packer tests (Tsang et al., 1990; Tsang and Doughty, 2003; West and Odling, 2007) and flowmeter logging, and as compared to flowmeter logging, and it does not always require caliper logging for interpretation (Tsang et al., 1990; Pedler et al., 1990).

The weaknesses of the method are that:

- i. open-well dilution is only applicable to unscreened wells (Tsang et al., 1990).
- ii. the curve fitting techniques used in some of the applications can be time consuming (Löv et al., 1994; Moir et al., 2014) providing non-unique aquifer parameters (West and Odling, 2007);
- iii. specific electrical conductance (SEC) that forms the basis of the technique can be masked by dispersion and inflow effects (Tsang et al., 1990; West and Odling, 2007);
- iv. errors in tracer concentration measurements can also introduce errors in the estimated parameters (Brainerd and Robbins, 2004; West and Odling, 2007); and
- v. in wells where there are substantial inflows, the flowmeter logging method is superior over the borehole dilution method because results from borehole dilution become difficult to interpret due to masking of minor inflow fractures that might be present by the large inflows (Tsang and Doughty, 2003).

#### **4.3.2 Method and set-up**

The open-well dilution method can be done for both ambient (eg. Drost et al., 1968; Ward et al., 1998; Pitrak et al., 2007; Maurice et al., 2010) and pumped states (eg. Tsang et al., 1990; Pedler et al., 1992; Brainerd and Robbins,

2004; West and Odling, 2007; Moir et al., 2014). Under natural hydraulic head conditions, the ambient uniform injection test is conducted to infer inflow, outflow and crossflow zones whereas the ambient point injection test is used to characterise the previously mentioned flow zones and vertical flows and their direction. On the other hand, the pumped test is done to infer inflows and out flows only and also for the determination of layer transmissivity and storativity in conjunction with pumping test data (Doughty and Tsang, 2005). Further details will be provided for the ambient test as this is the main method used in this work in subsequent subsections.

Generally, the procedure for the open-well dilution test can be summarised as follows. First a background electrical conductivity with depth log of the well is done using a conductance logger. Then a tracer of known concentration and conductivity is placed uniformly into the well or to a specific zone of interest by the use of a riser pipe whilst the borehole is either pumped or is in the ambient state. The conductance logger is then used to measure specific electrical conductance (SEC) with depth immediately after the tracer placement. Then sequential SEC logs are obtained with time under ambient conditions for the ambient test, whereas the monitoring is done whilst slugging or constantly pumping the well for the pumped test. The difference in the background electrical conductance and the sequential logs (caused by the inflow of contrasting SEC formation water) is used to locate the hydraulically conductive zones within the borehole. Finally, mass techniques and approaches such as the advective-dispersion-equation (ADE) encoded in analytical models are then used to infer layer flow variation with depth in boreholes.

For the pumped condition, the method can also be repeated for different pumping rates (the multirate test, like in Doughty and Tsang, 2005), and logging can also be undertaken using multiple boreholes (see West and Odling, 2007) to enable the determination of far field hydraulic properties and fracture interconnectedness.

Several tracers can be used for the open-well dilution method. These tracers include common salt (West and Odling, 2007; Maurice et al., 2010; Moir et al., 2014), deionised water (Pedler et al., 1990; Tsang et al., 1990), fluorescein

(Lewis et al., 1966) and food dyes (Pitrak et al., 2007). The choice of a tracer for the open-well dilution test depends on the background SEC of formation water, cost, toxicity, solubility, non-reactivity with aquifer material and potential for density settling, measurement method and detection limit (Ward et al., 1998).

### 4.3.3 Open-well dilution testing principles and analytical techniques

One technique is based on the solution to the 1-dimensional advection dispersion equation (ADE) and mass conservation theories. After SEC logs are obtained, inflow/outflow / feedpoints are located by examining the location of peaks (in deionised water injection) and kinks (saline water injection) in the SEC logs caused by contrasts in formation water and tracer filled well water.

The rate of change of tracer concentration with respect to time is based on the solution to the 1-dimensional ADE used by West and Odling (2007) as:

$$\frac{\partial C(z, t)}{\partial t} = -\frac{\partial(Cu(z, t))}{\partial z} + \frac{\partial}{\partial z} \left[ \alpha_B u(z, t) \frac{\partial C}{\partial z} \right] - \frac{CQ_o(z, t)}{\pi r_w^2} \quad (4.1)$$

where  $C(z,t)$  is the concentration at time  $t$  after tracer injection at elevation  $z$ ,  $u(z,t)$  is vertical velocity in the borehole,  $Q_o(z,t)$  is the volumetric inflow rate of formation water of zero tracer concentration per unit depth of well per unit time,  $r_w$  is the well radius, and  $\alpha_B$  is the longitudinal coefficient of dispersivity. The first term on the right of Equation (4.1) represents vertical advective effect of the flow in the well bore. The second term describes 'Fickian' dispersion of tracer. The last term represents dilution effect of inflowing formation water.

The assumptions for solving the ADE are that: longitudinal dispersion within the borehole is Fickian, i.e. the solute distribution is Gaussian; well bore diameter is small compared to the length; and density-driven effects are negligible in the well. For mass conservation, the cumulative sum of the discharge and solute mass for a set of fractures is equal to the total flow and mass at a point just above the fractures of interest (Tsang et al., 1990; Doughty and Tsang, 2005; Brainerd and Robbins, 2004).

There are four (4) main methods for analysing open-well dilution tests. These are analytical, modelling/curve fitting, integral and combined methods. The

analytical methods use the mass balance of solute to infer feedpoints from early and late time data for pumped wells (Tsang et al., 1990), and for the special ambient horizontal crossflow situation (Drost et al., 1968; Lewis et al., 1966; Ward et al., 1998; Pitrak et al., 2007). The analytical techniques provide useful information when used in conjunction with other types of complementary analyses, but on their own are overly simplistic for real world problems (Doughty and Tsang, 2005; Ward et al., 1998).

The modelling approaches use inversion by fitting the field SEC log to the 1-D ADE model (Doughty and Tsang, 2005) by specifying fracture feedpoints, varying the fracture and concentration discharge (BORE codes, I & II in Tsang et al., 1990), and varying flow velocity and dispersivity until there is a good fit between the field data and the ADE (West and Odling, 2007). Modelling approaches are time consuming, complex and can result in superfluous parameters (Evans, 1995). They require expensive algorithms that can only be suitable for a few experienced modellers (Moir et al., 2014). It is also known that the ADE fails to conserve mass in numerical models (Szymczak and Ladd, 2003).

Integral methods like that by used by Löw et al (1990) and Evans (1995) can provide automated feedpoint parameter iteration for providing an initial good fit to the BORE code. Another integral method that holds a lot of promise is that developed recently by Moir et al. (2014), which uses an excel method based on calculus and error analysis and in the process removes subjectivity in open-well dilution analyses. Although the integral approaches reduce computation time, they depend only on inflow points and are not applicable to horizontal crossflows under ambient conditions.

The last method is the combined approach which models the ADE based on the appreciation of feedpoint signatures that are attributed to the physical processes in the well. Doughty and Tsang (2005) used the distinctive signatures produced by inflow and outflow points under pumped conditions to give a physical insight into flow properties in a well. The understanding was then used in efficiently setting parameters for models like BORE code I and II, and in the process reducing the amount of time and labour used in iterative modelling. Maurice et al. (2010) also developed a spreadsheet based

computer simulation of profile patterns and signatures produced by inflow, outflow, crossflow and vertical flow in wells under ambient state. The model was then successfully used in characterising flow in real wells in the Southern Chalk of the UK. The combined approaches are simple to use, more efficient and require less time and effort but are subjective and sometimes non-unique.

In this chapter, the signature (a subset of the combined approach) and analytical procedures for analysing ambient open-well dilution tests will be used, the details of the which are provided in section 4.3.4.

#### **4.3.4 Analytical and field procedures used in this chapter**

The two kinds of ambient open-well dilution test undertaken for this chapter are the uniform and point emplacement tests, the details of which will be given in the section below.

Depending on the location of a well in a catchment of a fractured aquifer like the Chalk where flow occurs at discrete horizons separated by low permeability matrix, ambient flows can be dominated by lateral horizontal crossflows, vertical flows or a combination of both. Figure 4.1 presents the tracer profiles of a uniformly injected tracer into a well under horizontal crossflow. For uniform diffuse horizontal crossflow, the tracer is lost uniformly with parallel vertical profiles (Figure 4.1a). In a uniformly horizontal flow but with a discrete horizontal flowing fracture at point e (Figure 4.1b) having a much faster crossflow compared to the rest of the well, the tracer profiles are still parallel but marked with a distinctive kink at the location of the inflow point (e). In a scenario where horizontal flow is faster in the upper part of the well as compared to the lower part (Figure 4.1c), a boundary between the two profiles (depths  $d_1$  and  $d_2$ ) is shown at point f, with the upper part of the borehole undergoing faster tracer dilution with time. Doughty and Tsang (2005) and Maurice et al. (2010) presents simulations of several scenarios, but the most basic was presented above to give a better understanding of the uniform injection/horizontal crossflow case.

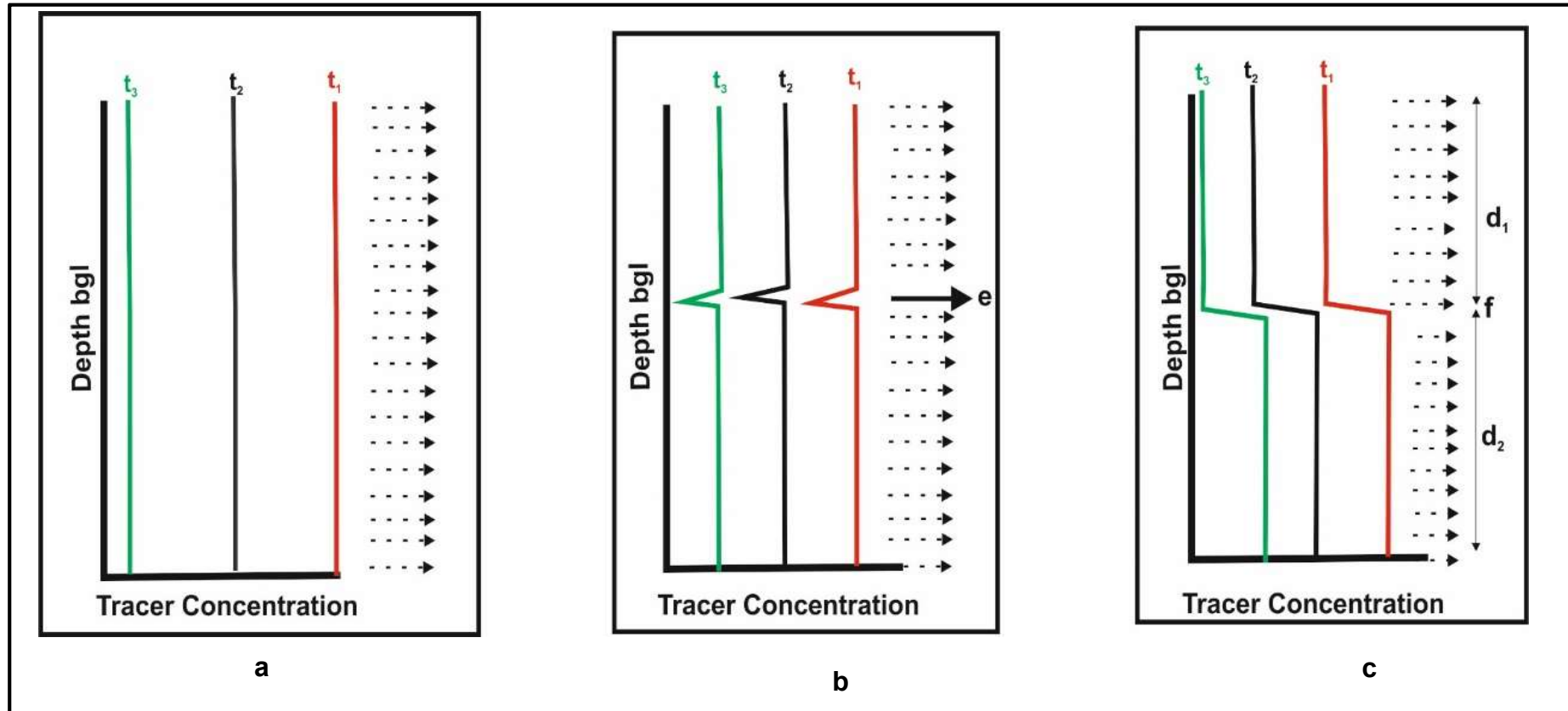


**Figure 4.1** Tracer profile evolution with time for simple horizontal flow case: (a) uniform diffuse horizontal flow; (b) diffuse uniform flow but with a discrete flowing fracture with a comparatively higher flow; (c) different diffuse flow zones. Adopted and amended from Maurice et al. (2010)

In ambient uniform open-well dilution testing in wells dominated by horizontal crossflow case presented above, and at a particular crossflow well interval where the following assumptions apply that:

- i. the concentration within the borehole is uniform and equal to concentration exiting the borehole;
- i. there are no vertical flows;
- ii. the flow is under steady-state;
- iii. the tracer is non-reactive,

then the first and second components of equation (4.1) are negligible, (4.1) then becomes:

$$\frac{dC}{dt} = \frac{-Aq_w C}{V} \quad (4.2)$$

$$\frac{dC}{C} = \frac{-Aq_w \cdot dt}{V} \quad (4.3)$$

$$\text{and } q_w = \alpha q_f \quad (4.4).$$

where  $q_w$  is the horizontal specific discharge or Darcian flux through the dilution interval in the well,  $q_f$  is the specific discharge through the formation that gets constricted into the dilution interval of the well,  $\alpha$  is the dimensionless correction factor that accounts for flow convergence and distortion from the formation into the open section of the well as a result of drilling disturbance (Drost et al., 1968; Gustafsson and Anderson, 1991), defined by the ratio of the aquifer width contributing to flow to the well to the well diameter (Figure 4.2), and ranges between 0.5 to 8 (Hall, 1993; Ward et al., 1998),  $V$  is the dilution volume in the well interval,  $A$  is the cross-sectional area of the well test interval perpendicular to flow in the direction of undisturbed groundwater flow (product of well diameter and dilution depth) and  $C$  is concentration at any time  $t$  after injection of tracer.

$\alpha = 2$  has sufficed for laboratory scale experiments but real aquifers have been found to have higher values of up to between 7 – 8 (Hall, 1993), and even values  $> 10$  have been recorded by Kearl (1997). The discrepancy in  $\alpha$  values in the two test scenarios is because in comparison to real aquifers, laboratory experiments are small and made up of uniform and well sorted porous media which have no disturbance from well drilling effects. Gustafsson

and Anderson (1991) used  $\alpha = 2 \pm 1.5$  for fractured granitic rock in Sweden. For this studies,  $\alpha = 2$  was used assuming there is little disturbance from drilling.

Integrating (4.3) and using the boundary conditions of C from  $C_0$  to  $C_t$ , and time from 0 to time, t and moving the  $\ln C_0$  term to the right yields,

$$\ln C_t = - \left( \frac{Aq_w}{V} \right) t + \ln C_0 \quad (4.5)$$

$$\ln C_t = - \left( \frac{2q_w}{\pi r_w} \right) t + \ln C_0 \quad (4.6)$$

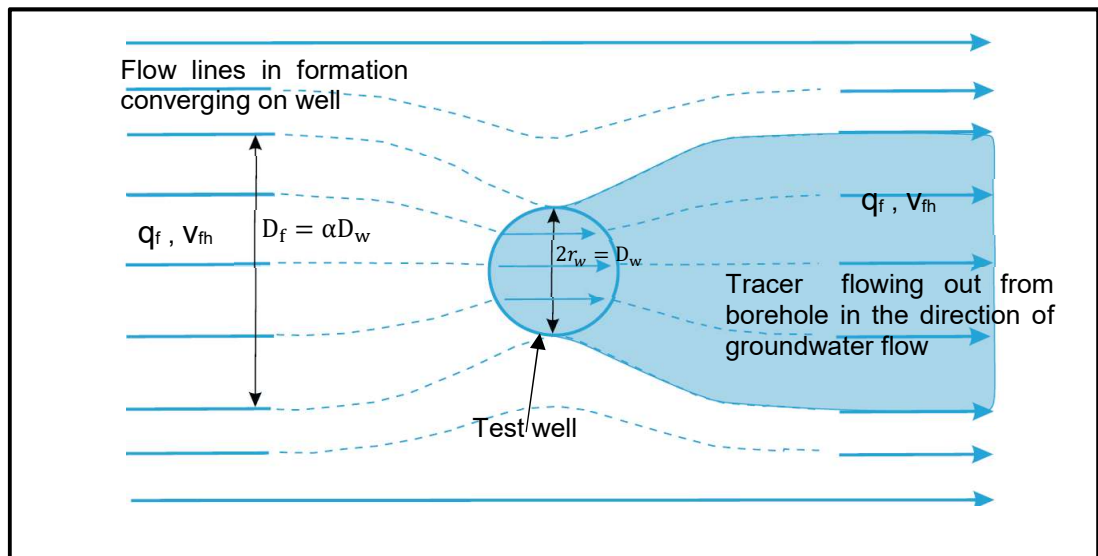


**Figure 4.2.** Plan view of ambient open-well dilution experiment showing flow line distortion and convergence from the formation width  $D_f$ , into the test well of diameter  $D_w$ , resulting in an artificial increase of flow through the well by a factor of  $\alpha, \approx 2$ , dilutes and washes away tracer from the test interval of the well in the direction of groundwater. Adopted and redrawn from Freeze and Cherry (1979) and Maldaner et al. (2018).

Equations (4.5) and (4.6) are valid for all tracers and represent the natural decay of tracer concentration with time in the well dilution interval. From (4.6) data analysis is done by plotting the natural logarithm of concentration versus time assuming tracer dilution is from horizontal crossflows at depth of interest

(Figure 4.3). Then the slope,  $m$  of the tracer decay line is proportional to  $q_w$  as:

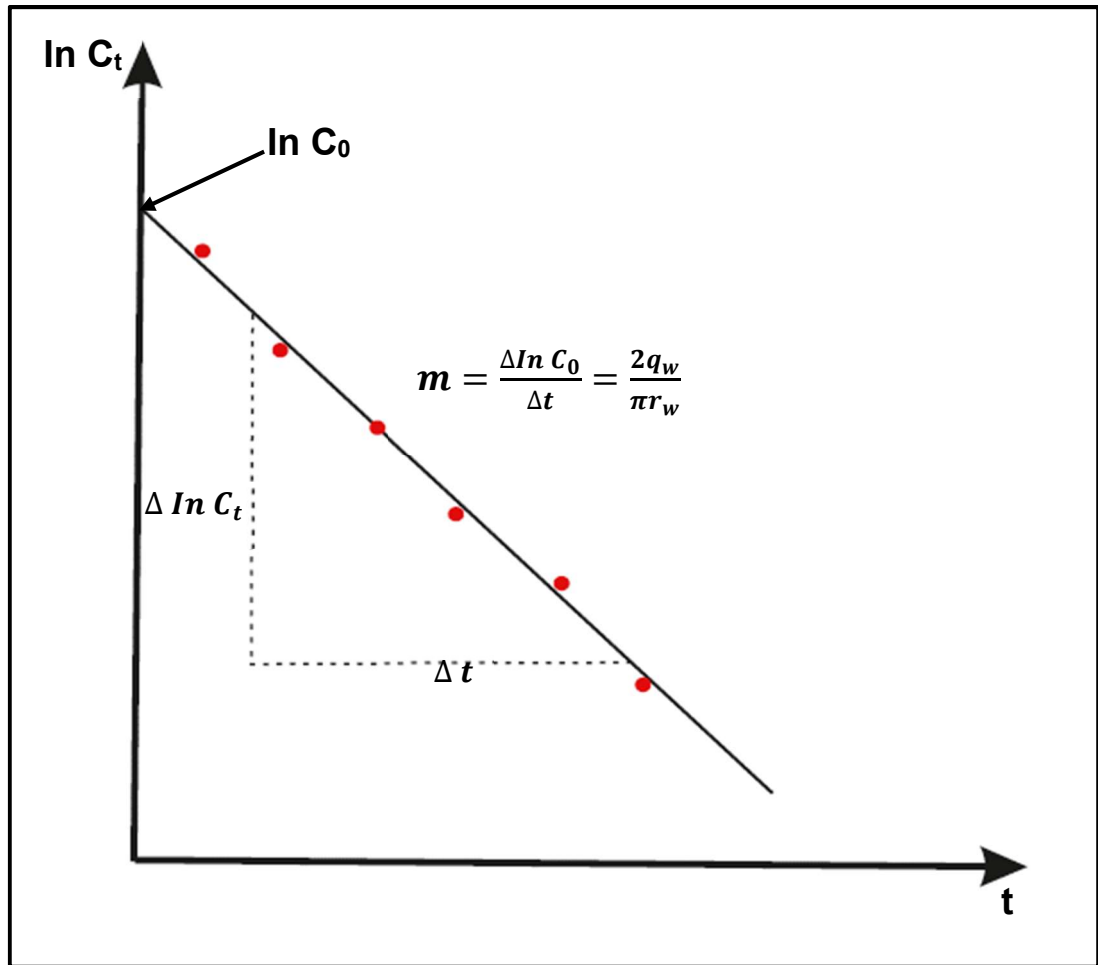


**Figure 4.3.** Tracer concentration decay plot versus time graph for a uniform open well dilution test for a specific sampling depth, at which tracer decay occurs by horizontal flows. The slope of the line is directly related to the darcy flux through the well, and the y-intercept is the natural log of the initial concentration.

$$q_w = \frac{m\pi r_w}{2} \quad (4.7).$$

The slope,  $m$  increases for rapid tracer dilution, representing faster flows and reducing for slow dilution and slower flows.

But from (4.4),  $q_f$  is what is desired for the formations is given as:

$$q_f = \frac{q_w}{\alpha} = \frac{m\pi r_w}{2\alpha} \quad (4.8).$$

Dividing equation (4.8) by the flowing or effective porosity,  $\phi_e$  then yields the average linear velocity of groundwater in the formation as :

$$v_{fh} = \frac{q_f}{\phi_e} = \frac{m\pi r_w}{2\phi_e \alpha} \quad (4.9).$$

In wells with dominant or substantial vertical flows, plots of the natural logarithm of concentration versus time are not linear because of additional dilution from vertical flows (Drost et al., 1968; Ward et al., 1998; Pitrak et al., 2007; Piccinini et al., 2016). In that case, a uniformly injected tracer (Figure 4.4a) in the borehole will show dilution at inflow points marked by kinks ( points d and e) but with a progressive movement of the freshwater front along the vertical axis of the borehole to an outflow point (point f). For this well, after assessing the fit of equation (4.5), the uniform profiles are qualitatively evaluated using signature methods to inform further tests with targeted point injection of tracer with a known mass of solute (say at or above point d). The point injection test (Figure 4.4b) in a vertically flowing zone shows the tracer profile peak moving upwards (or downwards) with a reduction in peak due to dispersion (spreading in the absence of mass loss) to the outflow point. The resultant model from analysing the uniform and point injection is shown in Figure 4.4c. The injected tracer slug is then observed with time for mass (and hence flow) losses. The mass of solute under any profile, in a borehole of radius,  $r$ , is determined by integrating the area under the profile given by the expression from Doughty and Tsang (2005) as:

$$M = \int [C(z) - C_0] \pi r_w^2 dz \quad (4.10)$$

The distance between the profile centroid and log times of profiles are used to determine velocity of vertical flow,  $u_v$ . Using the profile velocities and borehole radius from caliper logs where available, vertical discharge  $Q_v$  is computed (Kobr, 2003) as:

$$Q_v = \pi r_w^2 u_v \quad (4.11)$$

Then plotting  $Q_v$  with depth yields the vertical flowrate variation with depth. The signature analyses of the logs and mass and flow conservation analyses are then used to infer a flow model for the tested well.

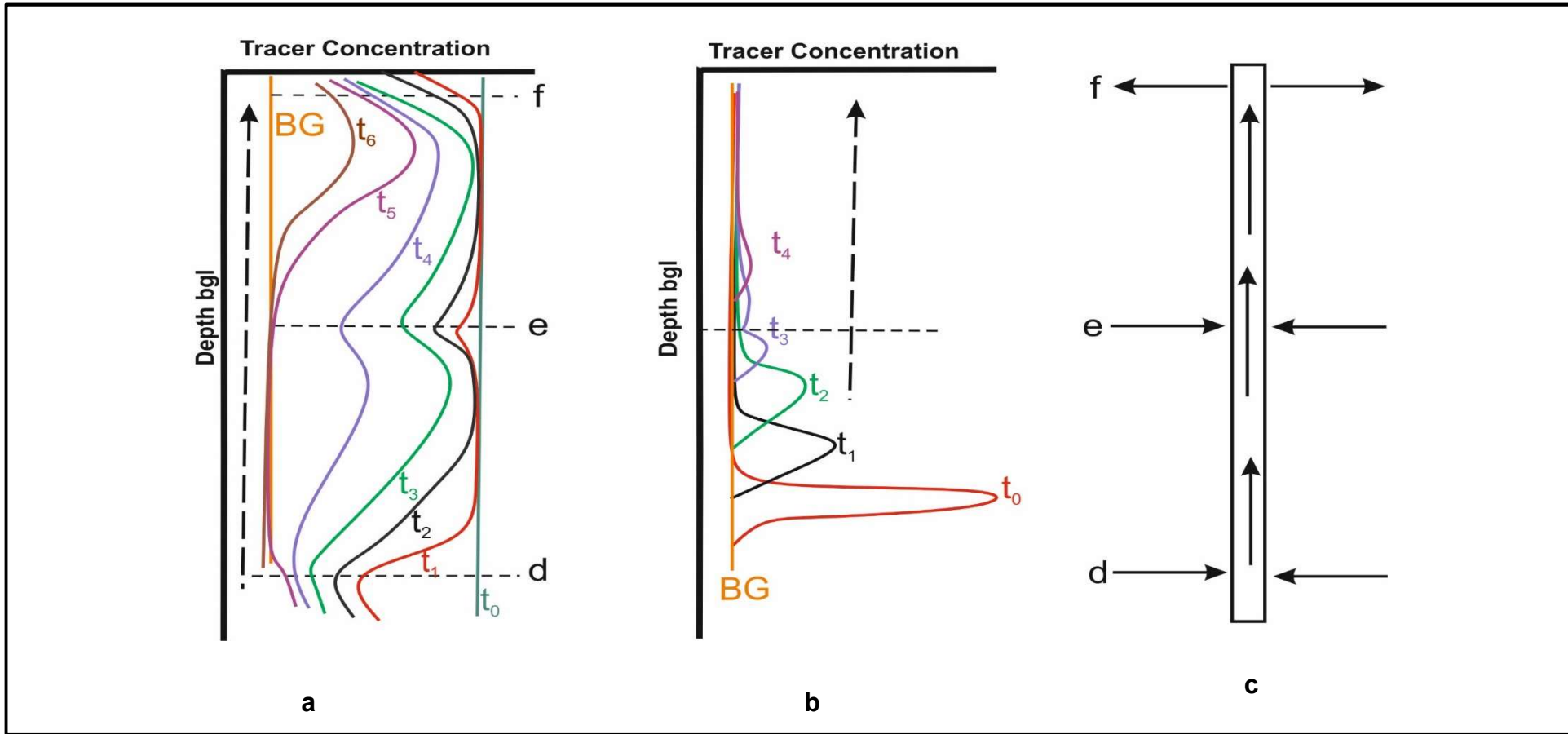


**Figure 4.4** Schematic of injected tracer evolution for a well with vertical flow: (a) uniform injection with an upward moving fresh water front; (b) point injection ; (c) flow model, **d** and **e** are inflow points, **f** is outflow.

#### 4.4 Field Methodology used in this chapter for ambient open-well dilution testing

Common salt was chosen as a tracer because it is inexpensive, readily available, easy and safe to handle and non-toxic to humans and the environment. Also because the salt background levels in the aquifer are also very low, common salt caused a contrast for SEC measurement but because of the small volumes used, did not cause a deterioration of the aquifer water quality. In terms of monitoring, salt concentration is also easily monitored with a conductivity meter (Ward et al., 1998).

Due to the dual porosity nature of the chalk, it was important to check whether the salt concentration dilution in the wellbore space was solely from dilution by inflow water and not from diffusion into the matrix block. The characteristic fracture diffusion time,  $t_{cf}$  is defined by Barker et al. (2000) as the time for a tracer to diffuse through a matrix volume equal to the fracture volume in a flat slab model and is given as:

$$t_{cf} = \frac{a_f^2}{4\phi_m D_e} \quad (4.12)$$

where  $a_f$  is the fracture aperture,  $D_e$  is the effective diffusion coefficient and  $\phi_m$  is the matrix porosity. Representing the borehole as an equivalent fracture, the fracture aperture value considered is 101.6mm, because that is the smallest well diameter in this study. Hartmann (2004) measured bromide effective diffusion co-efficient in chalk as  $(1.9 - 3.2) \times 10^{-11} \text{ m}^2\text{s}^{-1}$ , for matrix porosity of 33 – 37% on samples of the Northern Province Chalk from East Yorkshire. The  $D_e$  for chloride is same as bromide (Schwartz and Zhang, 2003) and thus these values were used in determining  $t_{cf}$ . Inputting these parameters into equation (4.12) yields a minimum time of 2,523 days for the salt concentration to drop to 50% of the initial injected concentration. But since the time for the tests in this chapter to drop to background levels is 7days,  $\lll 2,523$  days, the salt dilution in the wells can be attributed to groundwater flow in the wells.

Two kinds of ambient flow open-well dilution tests were undertaken: uniform (see Ward et al., 1998; West and Odling, 2007; Maurice et al., 2010) and

point emplacement tests (see Tate et al., 1970; Kobr, 2003; Maurice et al., 2010).

Since the initial aim of this chapter was to test wells in the Kilham catchment and its surrounding areas with the current method, a comprehensive review of available wells in the catchment was undertaken to obtain information about the kinds of borehole characterisation tests performed on the wells in previous works and their findings. Then well completion details were obtained from the EA and BGS onshore borehole log data from the BGS Geindex at <http://mapapps.bgs.ac.uk/geologyofbritain/home.html>. Twenty-four (24) wells were identified at the end of the desk study process. After the desk study exercise, several field feasibility and reconnaissance visits were undertaken for an assessment of the field conditions. After the visits however, sixteen (16) wells were ruled out because of: their use (the EA had instrumented some with loggers which would be difficult and tedious to remove eg. Nine Dikes Road borehole), location (some were in fields without access, whilst others could not be found because they had either been decommissioned or filled in eg Cottage Farm and West End Farm boreholes), state (some were feasible but on day of the test were dry holes eg. Nine Dikes Barn borehole). Figure 4.5 and Figure 4.6 shows the distribution of the wells and Table 4.1 presents the completion and testing parameters and details for the tested wells. For both tests, the borehole was first logged for background specific electrical conductance (SEC). For the uniform tests, volume of tracer to be injected,  $V_{ij}$  was determined by using the testable depth,  $h_t$  (from water table to well bottom) and injection tube diameter,  $d_{inj}$  in the expression:

$$V_{ij} = \frac{\pi(d_{ij})^2 h_t}{4} \quad (4.13)$$

Salt of known mass based on the criteria that concentration in injection tube does not exceed 120 g/L to avoid density settling, was then dissolved in the determined volume of water from equation (4.13) in a 25 L plastic container via vigorous shaking (see Table 4.1 for the injection parameters). After this, a 25 mm injection tube weighted with scaffold pole was attached to a rope that was secured to an immovable structure on the surface to ensure that the set-up was not lost to the well. Then a funnel was attached to the bottom of the weighted hose to act as a mixer and disperser. After this, the injection

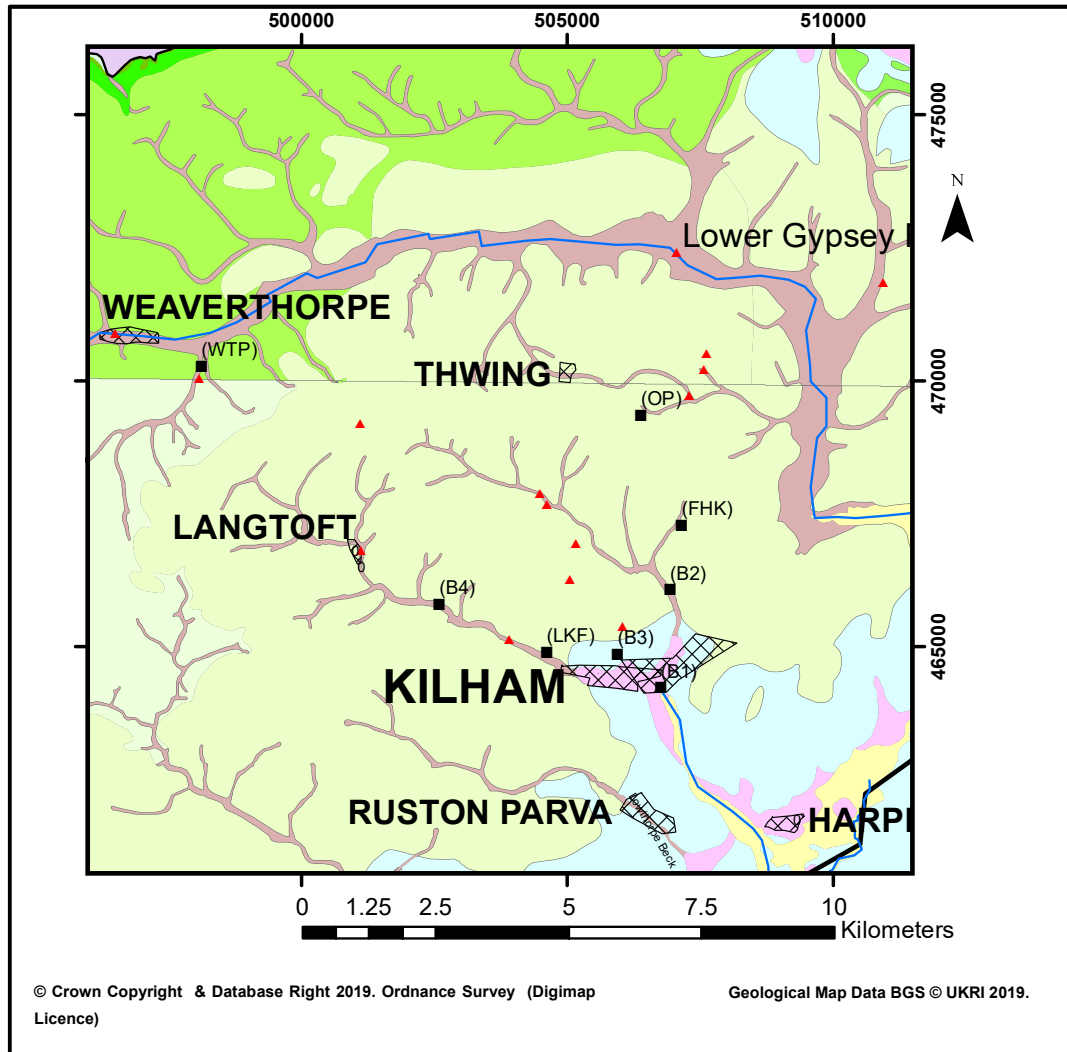


**Figure 4.5.** Map of wells in the Kilham catchment and surrounding areas initially targeted for open-well dilution testing. Black squares for tested wells and red triangles for untested wells

tube was inserted into the well, and the tube was fed with the salt solution via a funnel at the top of the well. For wells with water level within the casing, the tube section within the casing was filled with fresh water. The injection period was timed, after which the hose pipe was slowly pulled out of the well aiming to produce a uniform concentration via mixing with the well water via use of a disperser attached to the bottom of the hose. Then sequential logs of SEC with depth were measured. See Figure 4.7 for the set-up of the uniform injection test. Using a calibration equation and chart (Figure 4.8) produced by dissolving known masses of table salt in chalk water of known volume by

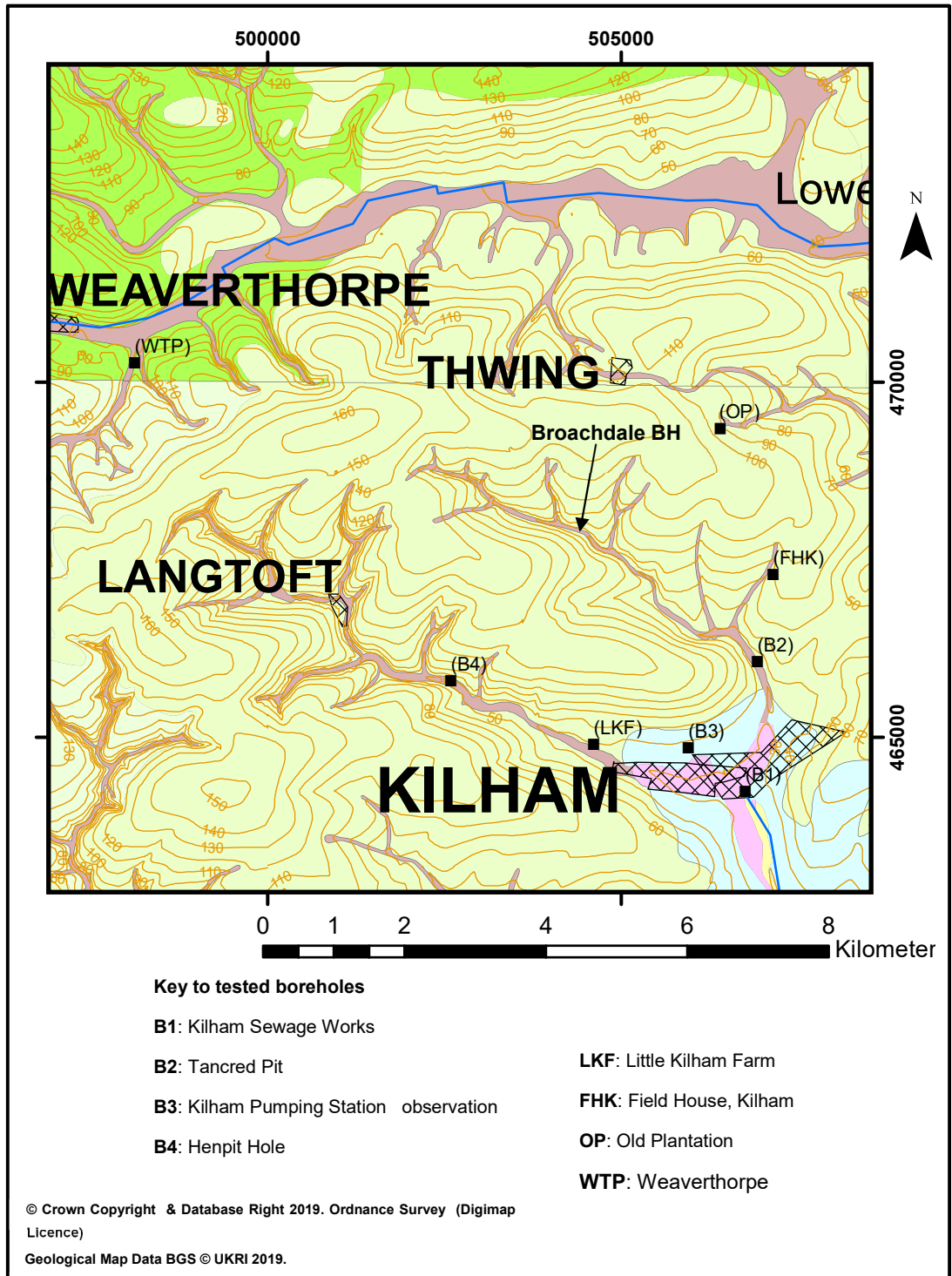


**Figure 4.6.** Open-well dilution tested wells location superimposed on geology and elevation contours of the Kilham catchment.

**Table 4.1.** Borehole details and injection parameters of the 8 tested wells

Well name	NGR	Well ground elevation (m AoD)	Well depth (m)	Casing bottom bgl (m)	Top diameter (mm)	Kind of test performed	Date of tests	Mass of Salt injected for uniform/point tests (g)
Kilham Sewage Works (B1)	TA 067 642	24.13	15.96	9.0	101.6	Uniform and point	12/05/2016 27/06/2016	1000/75
Kilham Pumping Station Observation (B3)	TA 059 648	36.33	20.00	9.0	150	Uniform and point	20/07/2017 23/11/2017	250/75
Little Kilham Farm (LKF)	TA 046 649	39.96	50.00	8.0	202	Uniform and point	20/07/2017 24/11/2017	900/75

**Table 4.1** continued

<b>Well name</b>	<b>NGR</b>	<b>Well ground elevation (m AoD)</b>	<b>Well depth (m)</b>	<b>Casing bottom bgl (m)</b>	<b>Top diameter (mm)</b>	<b>Kind of test performed</b>	<b>Date of tests</b>	<b>Mass of Salt injected for uniform/point tests (g)</b>
Henpit Hole (B4)	TA 025 658	48.54	65.00	13.0	230	Uniform and point	09/06/2017 17/11/2017	3400/75
Tancred Pit (B2)	TA 069 660	36.40	50.00	13.0	220	Uniform and point	13/05/2016 28/06/2016	2500/75
Field House Kilham (FHK)	TA 071 672	68.66	67.00	8.0	208	Uniform	09/08/2017	450/75
Old Plantation (OP)	TA 063 693	94.42	100.00	7.5	203	Uniform	10/08/2017	500/75
Weaverthorpe (WTP)	SE 981 702	71.00	45.72	5.5	152.4	Uniform and point	03/08/2017 24/11/2017	650/75

the use of a Solinst TLC 107 conductivity meter and handheld conductivity meter, the SEC profiles were converted to sodium chloride concentration profiles. The Solinst TLC meter reads depth readings better than 1 cm (Post and von Asmuth, 2013). Following qualitative and signature interpretation of the logs, tests showing horizontal crossflow signatures were tested and analysed using the method of Pitrak et al. (2007) for the production of a specific discharge versus depth plot. For profiles with signatures of vertical flows, further point emplacement tests were planned to better resolve vertical flow.

For point emplacement tests, target injection points within the wells were identified from the signature and quantitative analyses of the uniform tests. Then, 75 g of sodium chloride (NaCl) from a  $150 \text{ gL}^{-1}$  NaCl solution was fed into a 0.5 L compartment of a 1.2 m long x 70 mm diameter point injection barrel ( Figure 4.9). The barrel was then lowered to the target depth of interest and the salt solution was released by operating a connected Rothenberger

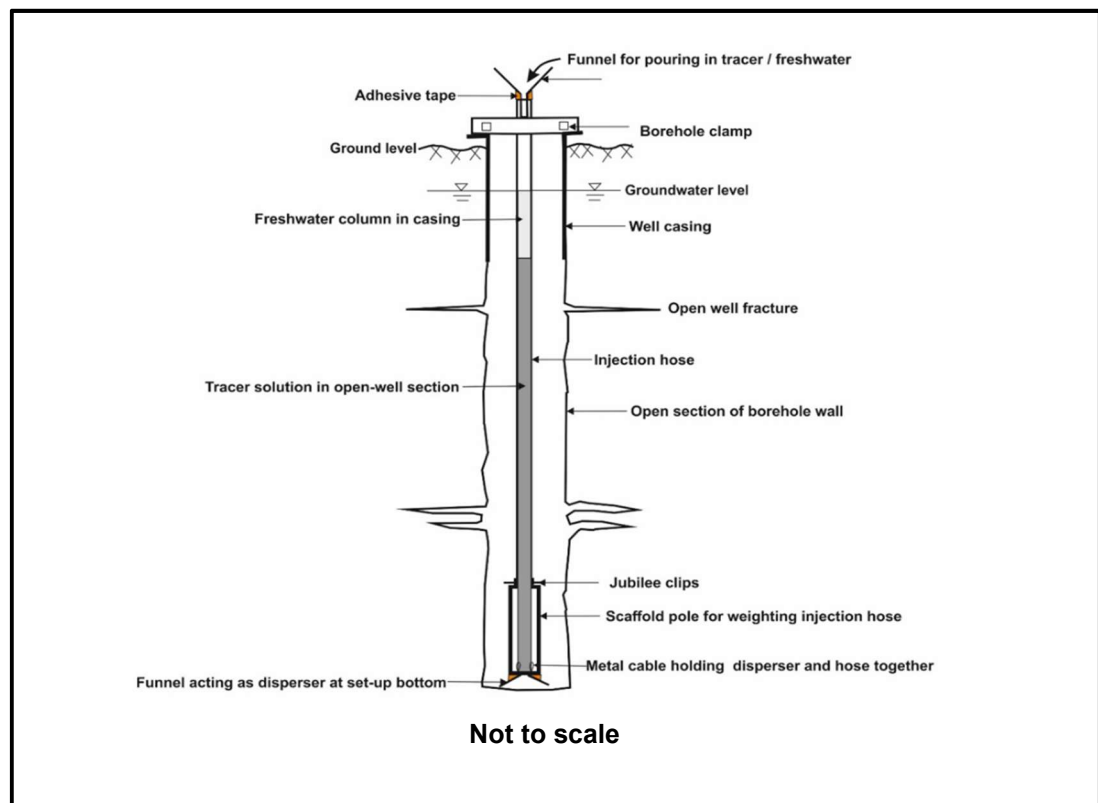


**Figure 4.7.** Uniform open-well dilution test set-up

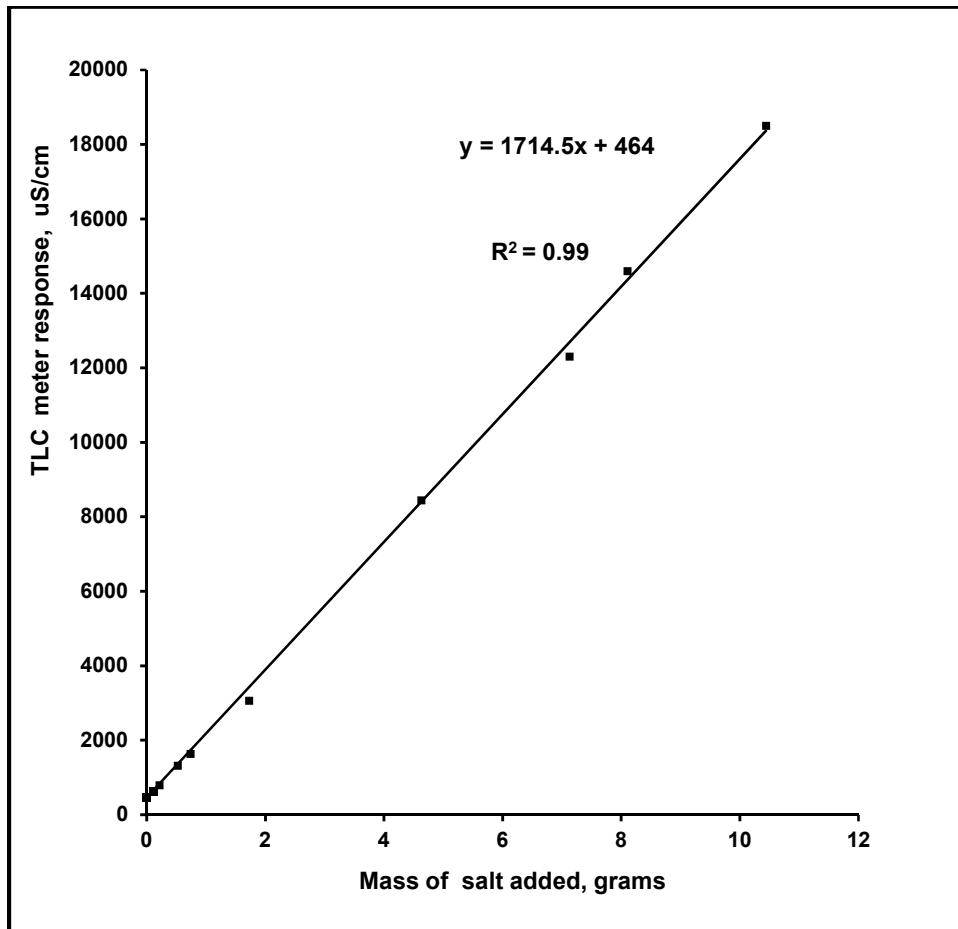


**Figure 4.8** Solinst TLC logger response versus salt concentration calibration chart

Test pump at ground surface. After the injection and barrel withdrawal, sequential SEC measurements were made to monitor vertical migration and attenuation of the resulting sodium chloride slug within the well. The logs were then analysed using the methods described in Doughty and Tsang (2003), Kobr (2003) and Maurice et al. (2010) to determine the vertical flow velocity, tracer loss and tracer dilution to infer inflow, outflow and crossflow zones in the wells.

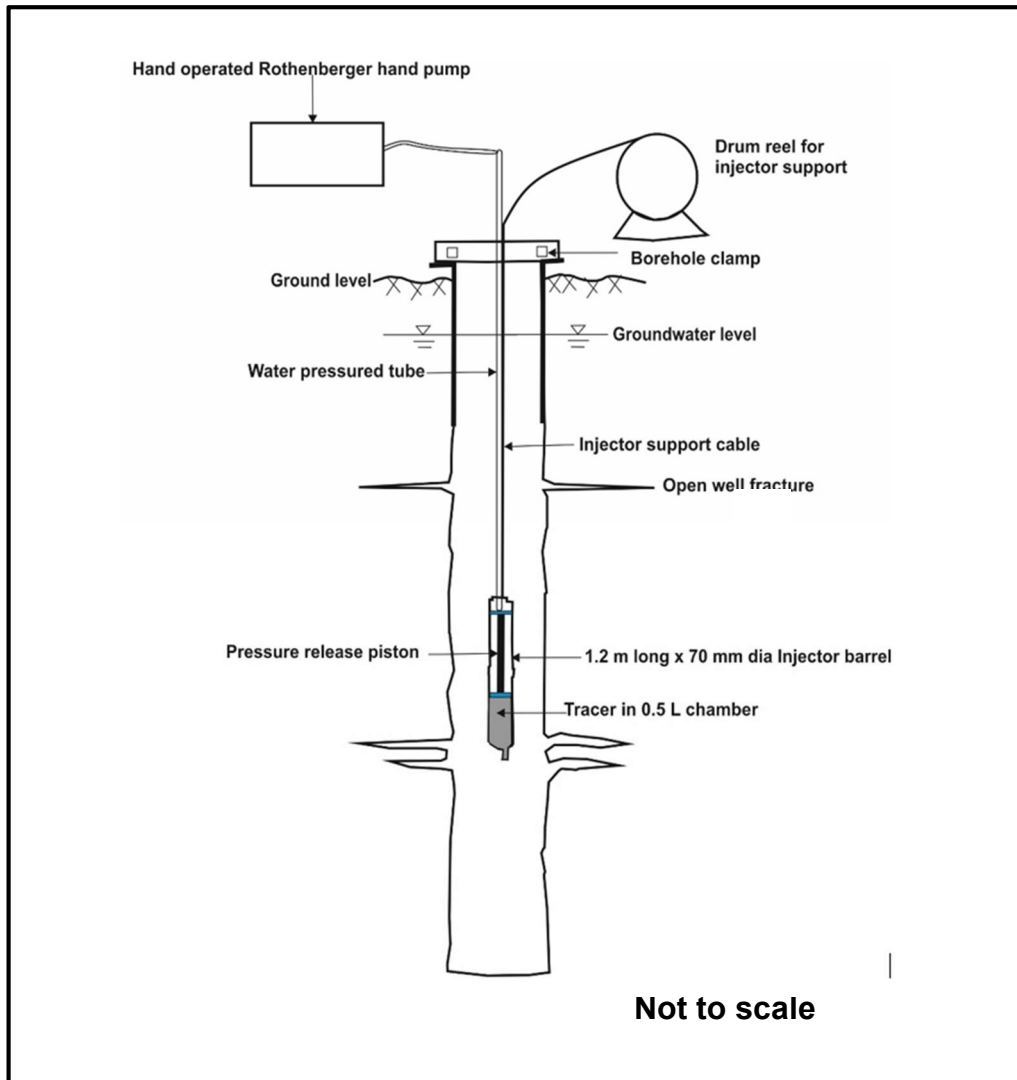


Figure 4.9 Point injection set-up

## **4.5 Ambient open-well dilution tests results and discussion**

### **4.5.1 Results and discussion of uniform and point emplacement open-well dilution testing**

#### **Kilham Sewage Works Borehole**

The results for a uniform test for the Kilham Sewage Plant borehole is shown in Figure 4.10. In Figure 4.10a, times 1-7 and 17-24 minutes after the tracer injection were not used in characterising flow in the borehole because of improper mixing and density settling at the bottom of the well. In the first profile that shows good mixing i.e. 54 – 67 minutes, uniform salt concentration of  $4.8 \text{ gL}^{-1}$  remains at depths 9.2 m to 15.5 m, reducing to  $4.5 \text{ gL}^{-1}$  at the well bottom. The  $4.8 \text{ gL}^{-1}$  concentration is consistent with the injected concentration. The logs show faster dilution at the well bottom with dilution reducing upwards towards depth 9 m. There are minor kinks in the logs, but they are not persistent through time for flow feature marking, suggesting diffuse flowing features.

An example plot of the natural logarithm of the concentrations with time for depth 11.5 mbgl is shown in Figure 4.11. The regression information for the other depths are as shown in Table 4.2. The range of the slope and coefficient of correlation of the concentration plots are  $0.0003 - 0.0007 \text{ gL}^{-1}\text{min}^{-1}$  and 0.91- 0.99 respectively. The slopes increase down the well, whereas the coefficient of correlation reduce down the well. The specific discharge with depth averaged over 0.6 m depth intervals, derived from the slopes of concentration decays using the Pitrak et al. (2007) model is shown in Figure 4.10b. A lowest computed discharge of 0.04 m/day is at the top of the profile doubling to 0.08m/day at the bottom of the well. Results of a follow up point injection at the well bottom for vertical flow determination is shown in Figure 4.12. The tracer was static during the first 3 hours after injection of the tracer. Returning to the borehole after twenty-three hours, the tracer had reduced to background levels. Using the uniform tests signature which does not show the movement of a fresh water front, non-consistent kinking in profiles, the linearity of the Pitrak et al. (2007) model, and the high  $R^2$  values and non-vertical movement of the point injected tracer at the well bottom suggests that

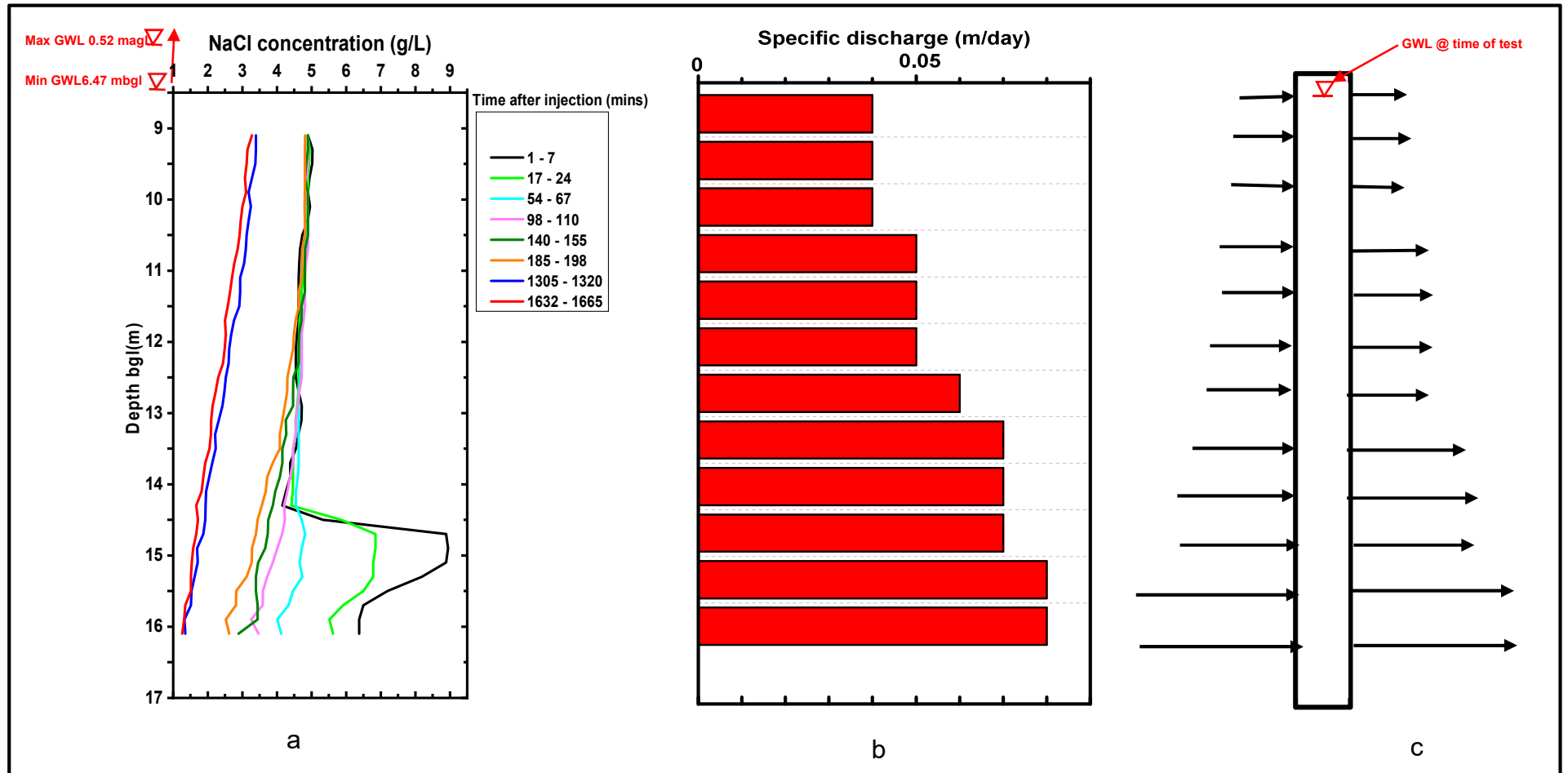


**Figure 4.10.** Kilham Sewage Works results: (a) uniform injection profiles; (b) specific discharge with depth plot; (c) borehole crossflow model (ambient).

diffuse horizontal crossflow dominate over vertical flow in the well. Flow concentration at the well bottom is consistent with its location at a discharge area of the catchment. The dominance of horizontal crossflow through the well is also consistent with its location as it could be laterally connected to Lowthorpe Beck stream, which is about 5 m away from the well. The proposed horizontal flow model of the borehole is shown in Figure 4.10c.

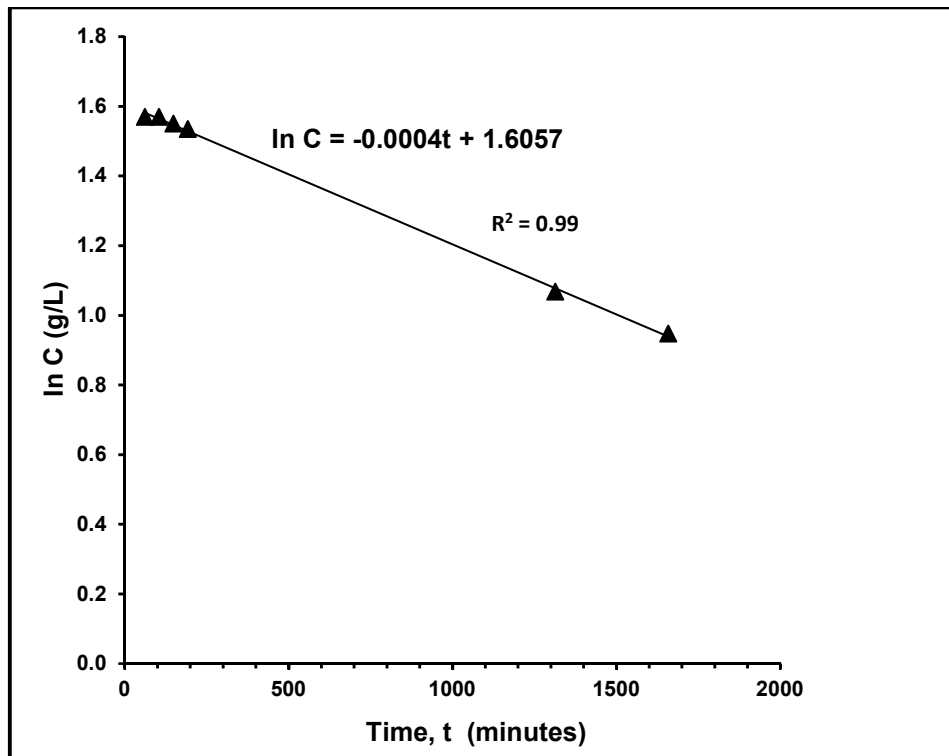


**Figure 4.11.** Kilham Sewage Works borehole sample plot of linear regression for the determination of specific discharge for depth 11.5 m bgl.

**Table 4.2.** Kilham Sewage Works borehole horizontal flow model test parameters

Depth (m)	slope $\text{gL}^{-1} \text{min}^{-1}$	$R^2$
9.1	0.0003	0.99
9.3	0.0003	0.99
9.5	0.0003	0.99
9.7	0.0003	0.99
9.9	0.0004	0.99
10.1	0.0004	0.99
10.3	0.0004	0.99
10.5	0.0004	0.99

Table 4.2 continued

Depth (m)	slope gL <sup>-1</sup> min <sup>-1</sup>	R <sup>2</sup>
10.7	0.0004	0.99
10.9	0.0004	0.99
11.1	0.0004	0.99
11.3	0.0004	0.99
11.5	0.0004	0.99
11.7	0.0004	0.99
11.9	0.0004	0.99
12.1	0.0004	0.98
12.3	0.0004	0.99
12.5	0.0004	0.99
12.9	0.0005	0.99
13.1	0.0005	0.99
13.3	0.0005	0.98
13.5	0.0006	0.97
13.7	0.0006	0.99
13.9	0.0006	0.97
14.1	0.0006	0.98
14.3	0.0006	0.98
14.5	0.0006	0.96
14.7	0.0006	0.95
14.9	0.0006	0.95
15.1	0.0006	0.95
15.5	0.0006	0.91
15.7	0.0007	0.94
15.9	0.0007	0.91
16.1	0.0007	0.92

### **Kilham Pumping Station Observation Borehole**

The results for Kilham Pumping Station observation borehole is shown in Figure 4.13. This is an EA observation borehole, that is about 20 m away from two main Yorkshire Water Kilham abstraction boreholes. The uniform injection (Figure 4.13a) resulted in an initial concentration of ~6 gL<sup>-1</sup>. The profiles are smooth, with a faster tracer dilution at the water table, with downward freshwater movement front to depth 19 m, with the freshwater front reaching depth 15 m between 1235-1239 minutes. There is a distinctive kink at 19.2 m, which is a boundary, with greater depths showing slow tracer dilution. Below 19.2 m, the profiles are vertical reducing in concentration with time although the freshwater front has not reached the well bottom, indicative of uniform crossflow across the well bottom.

The result from a point injection test at depth 13.6 m profile and mass and centroid results are shown in Figure 4.13b and Figure 4.14 respectively. The initial calculated mass of 79 g, which is more than the injected mass of 75 g, is possibly due to improper mixing after injection. The profile peaks and

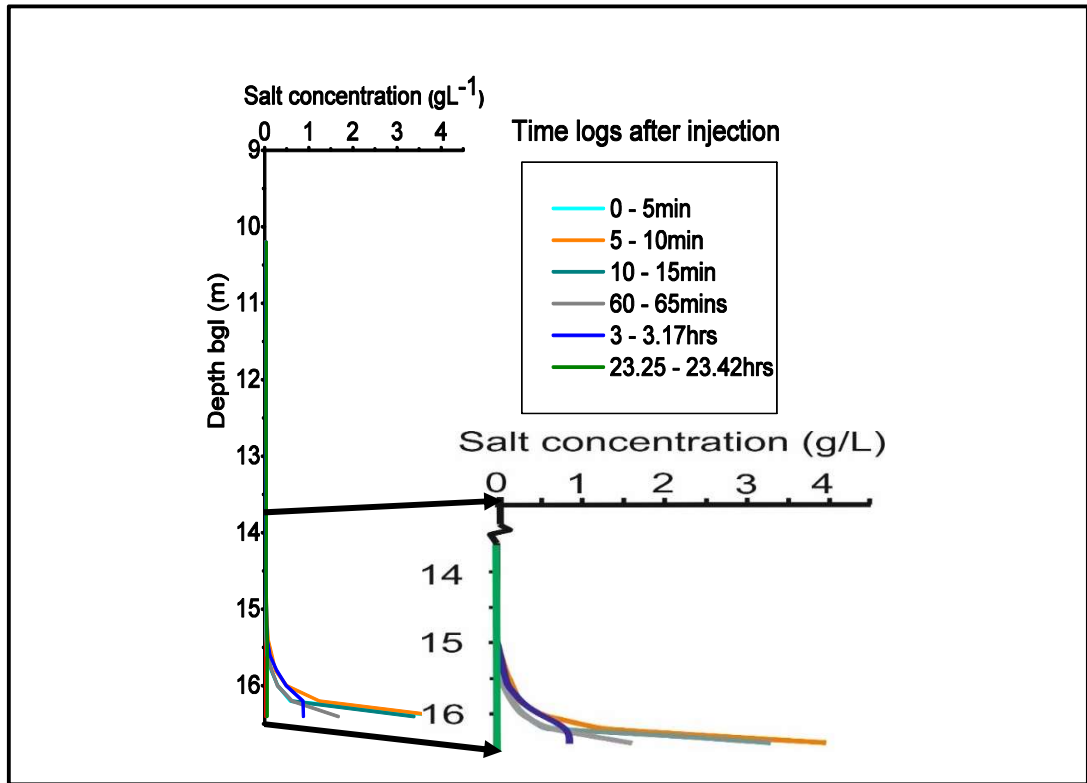


**Figure 4.12.** Kilham Sewage Works borehole point injection at depth 15.5 m.

concentrations reduce with time but the mass is conserved with little mass loss during the test time. The profile peaks and tracer leading front also move downwards with time, with little mass loss in between profiles. The tracer dilution is attributed to mixing with water column below the tracer front and tracer dispersion (Figure 4.13b and Figure 4.14). The little mass loss with time during the test time suggests a depth interval of sluggish flow within the borehole. The largest mass loss of tracer (6 g) occurred when the profile (237 – 242) mins leading front reached depth 19.6 m suggesting that the bottom part of the well is possibly an outflow zone as observed in the uniform test. However, it is difficult to reconcile the rapid dilution of tracer at the water table and the distinctive downwards movement of freshwater front in the uniform test, as compared to tracer stagnation and sluggish flow observed in the point

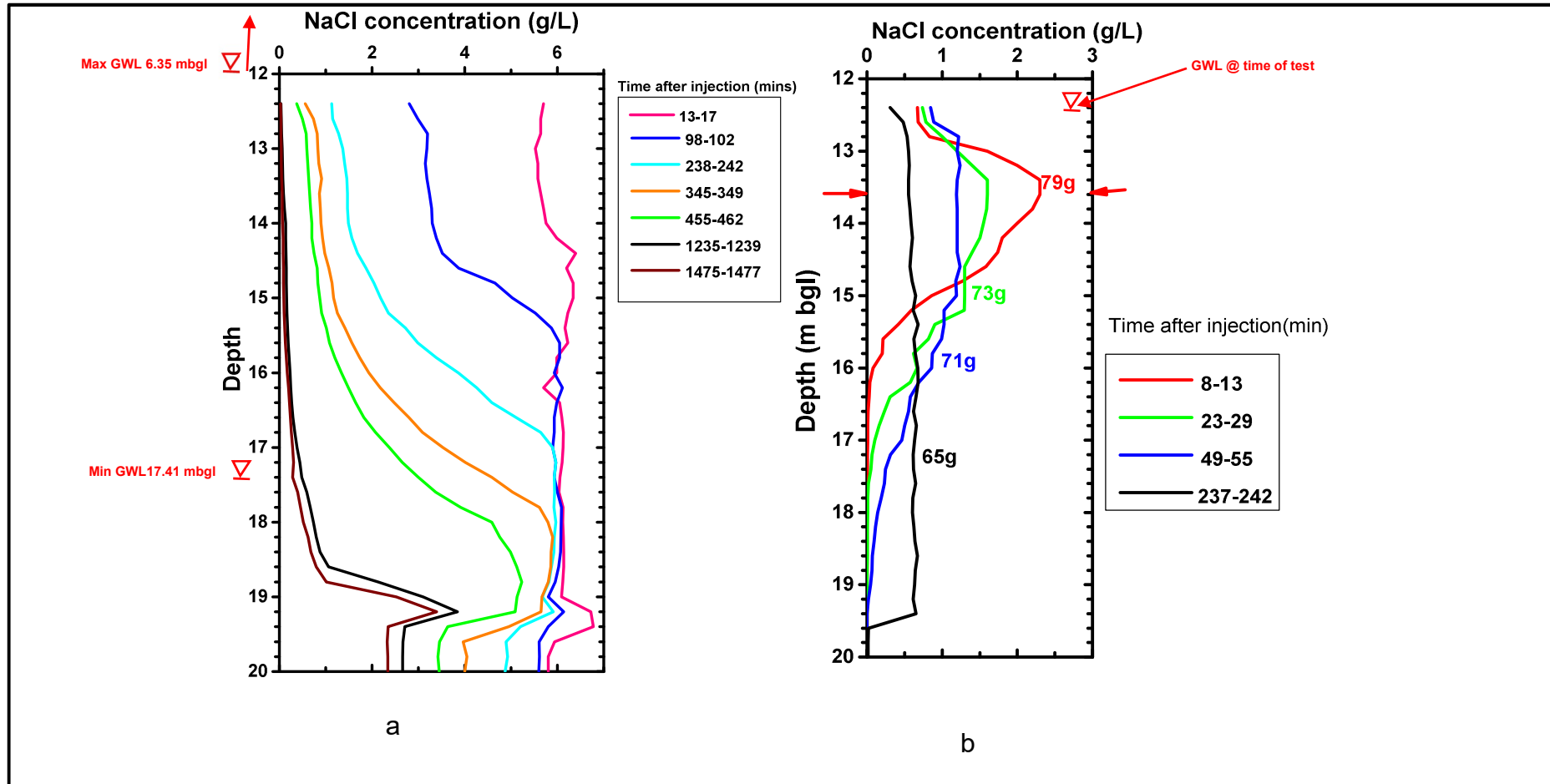


**Figure 4.13.** Kilham Pumping Station borehole results: (a) uniform injection profiles; (b) point injection at depth 13.6 m bgl arrowed in red.

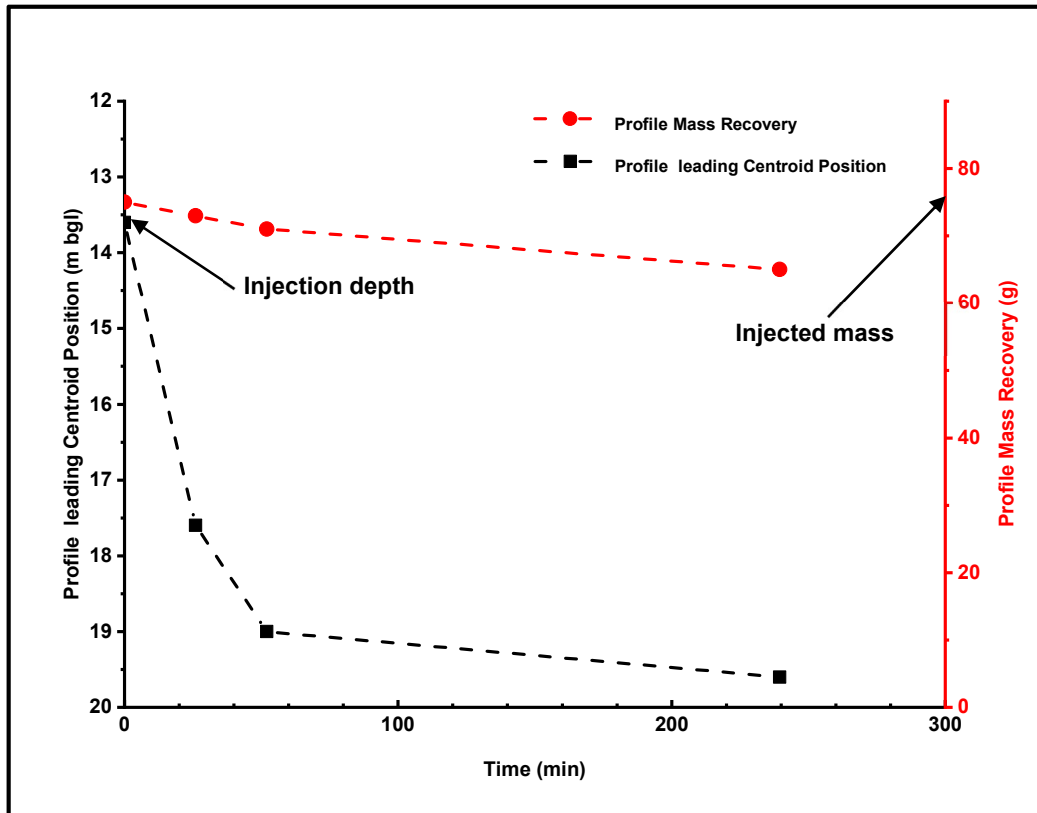


**Figure 4.14.** EA Kilham Pumping Station Observation profile centroid position (black squares) and mass recovery (red circles) with time plot for point injection of 75 g NaCl at 13.6 mbgl

test. This disparity could probably be attributable to different flow regimes at the time of the test as a result of seasonal differences or and/or from the different pumping regimes in the nearby YW abstraction boreholes for the different times of the two tests.

To constrain the flow characteristics in the observation borehole, the findings from a recent geophysical test conducted in Kilham Abstraction BH No.1 by European Geophysical Services (2018) on behalf of Yorkshire Water were used. Figure 4.15 shows the caliper log and ambient flow logging results for Kilham Abstraction BH No.1. Figure 4.15a shows borehole diameter enlargements distributed between the zone of watertable fluctuation (6.35 – 17.41 mbgl) and at depth. The zone of substantial and consistent ambient flow features occur between 23 – 54 mbgl with ambient upward flows from deeper depth outflowing around depth 23 mbgl (Figure 4.15b). The flow

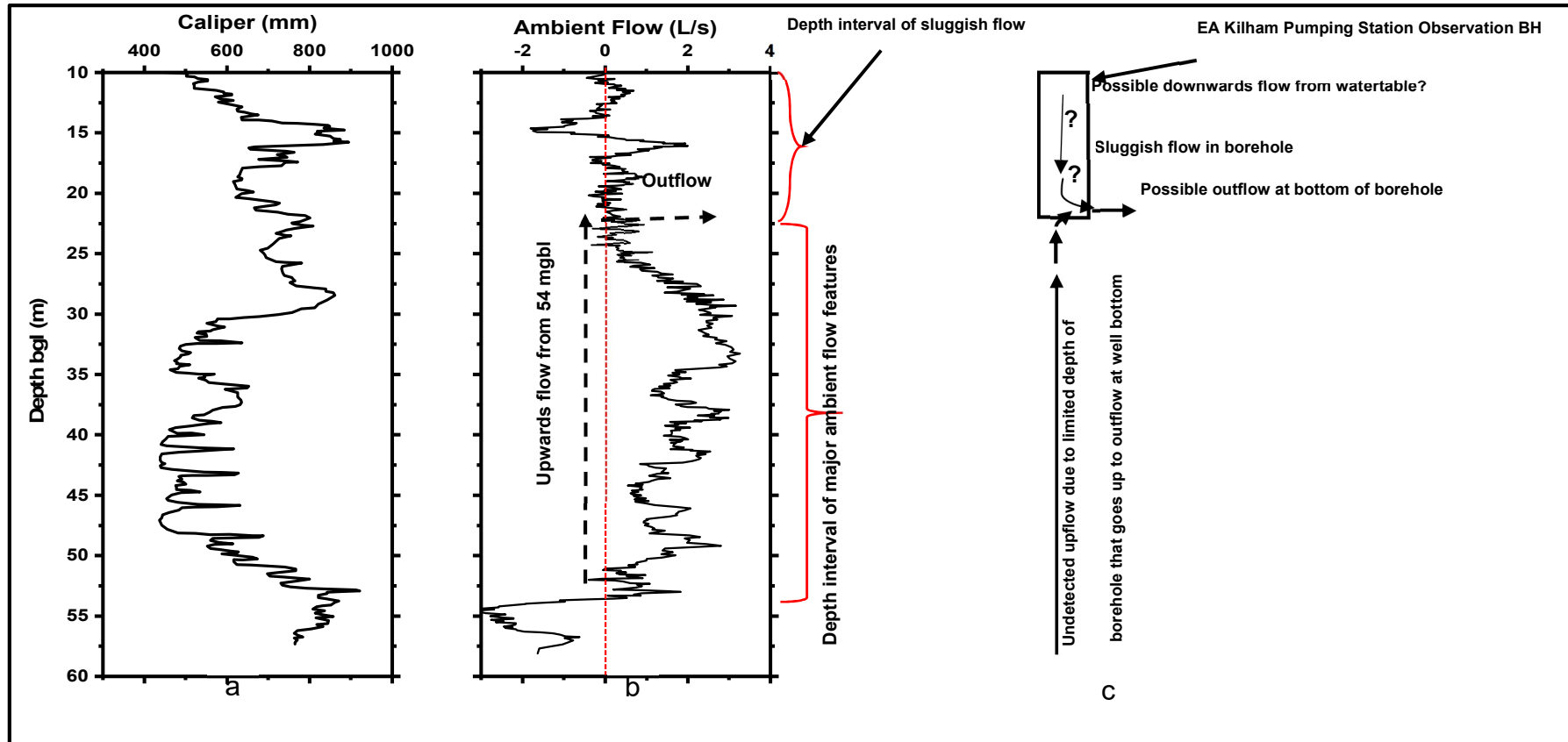


**Figure 4.15.** Borehole geophysics (BH 1) results European Geophysical Services (2018). (a) Borehole caliper with diameter enlargements within watertable fluctuation zone and at depth; (b) Ambient flow results with substantial flows occurring between depth 23 – 54 mbgl with no substantial flows occurring above depth 23 mbgl; (c) Flow model (ambient) in observation borehole.

features also correspond with the diameter enlargements on the caliper log. The depth interval above 23 mbgl has no or small flows, suggesting that the EA Kilham observation borehole used for the open-well dilution testing lies within the zone of slow flows (12 – 20 mbgl), and that accounts for the sluggish flow observed in the point dilution test. In addition, the Kilham area is a discharge zone and so ambient upwards flows from depth to discharge at higher horizons should be the norm, which is confirmed by the results of European Geophysical Services (2018). The discharge and upwards flow in the Kilham discharge area is further discussed in Chapter 6. Information from the point dilution tests and flow characterisation above 23 mbgl is used to model the EA Kilham observation borehole in Figure 4.15c. Flow in the borehole is described as sluggish and slow, with possible outflow at the bottom of the well. Downwards flow from the watertable is uncertain considering the location of the borehole as a discharge location.

#### **Little Kilham Farm Borehole**

The results for the Little Kilham Farm borehole are presented in Figure 4.16. In Figure 4.16a, the well diameter is irregular, ranging from 225 – 460 mm with the majority of the biggest diameters occurring between depths 15m and 26 mbgl reducing with depth to the well bottom. The enlarged diameters at the upper part of the well indicate solutionally enlarged fractures in the zone of seasonal water table fluctuation. In Figure 4.16b, the initial salt concentration is fairly uniform ( $\sim 1.4 \text{ gL}^{-1}$ ) below 27 mbgl but slightly lower above this depth ( $\sim 1.0 \text{ gL}^{-1}$  at the water table). Between the water table and 30 – 37 mbgl, fast uniform dilution occurred, with tracer concentrations approaching background in about 60 min. Below these depths dilution was slower. At the bottom of the well, very slow dilution occurred after about 60 minutes. The profiles also show numerous kinks that are not consistent with depth. The profiles also show some evidence of downward movement of a freshwater front in the well between depths 38.5 and 45 m. Below this depth to the bottom of the well, there is slow dilution.

Profiles 5 - 40 minutes were used in deriving and testing the horizontal flow model parameters for depths 18 to 35m because profiles 60 – 274 minutes

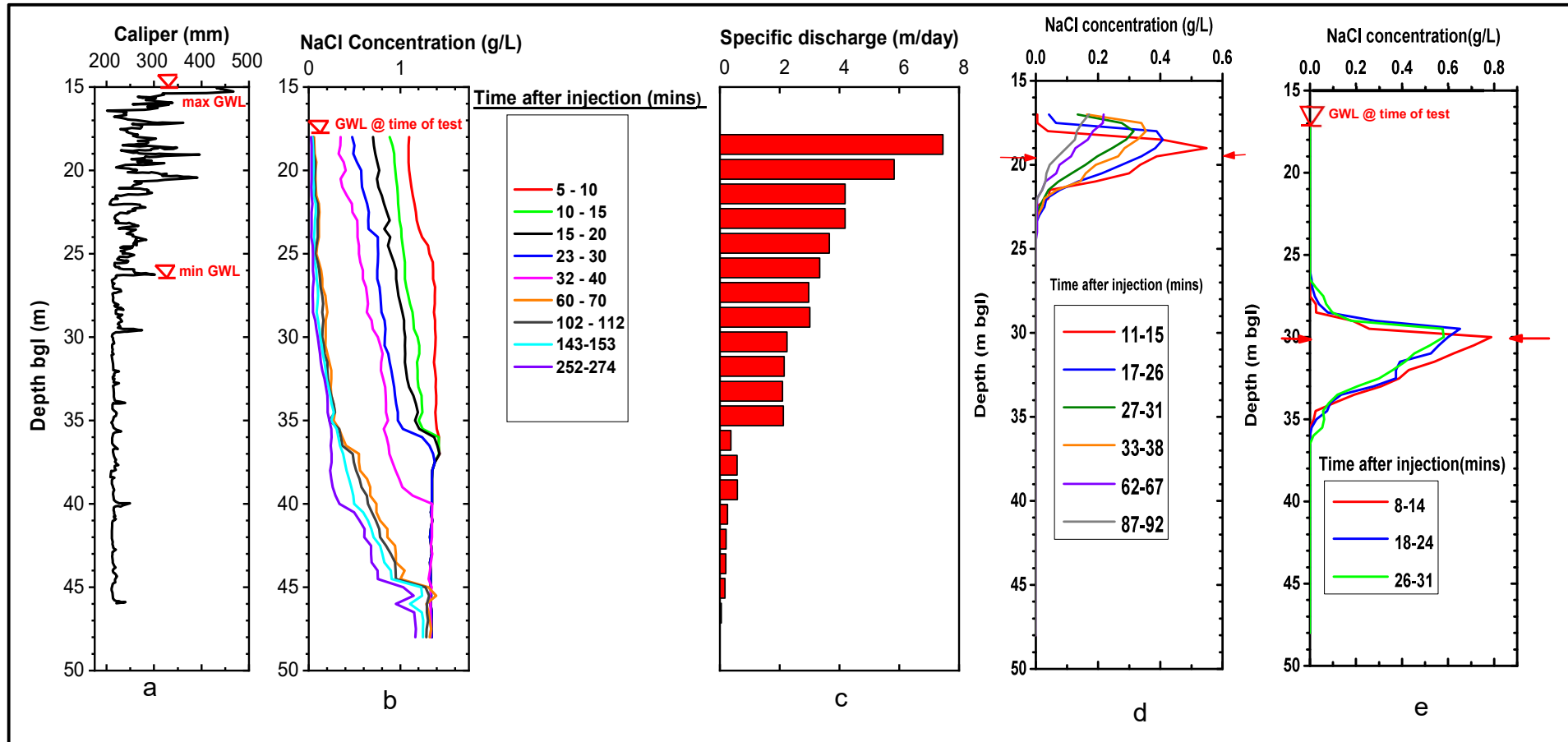


**Figure 4.16** Little Kilham Farm results: (a) caliper log;(b) uniform injection profiles with time;(c) specific discharge with depth plot;point injection (red arrows) profiles for depths (d) 19.5 and (e) 30 mbgl.

are close to the background concentration in the depth interval, and will affect the initial horizontal flow parameters. The horizontal crossflow model test parameters for each depth is presented Table 4.3, with a sample plot for depth 23.5 mbgl shown in Figure 4.17. Below depth 35 m however, profiles 60 – 274 minutes were used since effective dilution only commenced at this depth when the freshwater front got to depth 35m and below. From Table 4.3, the slopes range between 0.0006 and 0.0392, whilst the  $R^2$  range between 0.81 and 0.99. The highest slopes and  $R^2$  occur at the zone of water table fluctuation, suggesting highest crossflows dominate in this zone, whereas the smallest of both parameters occur between depths 35.5 m and well bottom, which corresponds to the zone of vertical dilution, without horizontal crossflows dominance. Figure 4.16c shows derivation of specific discharges using the Pitrak et al. (2007) model for depth intervals of 1.5 m.

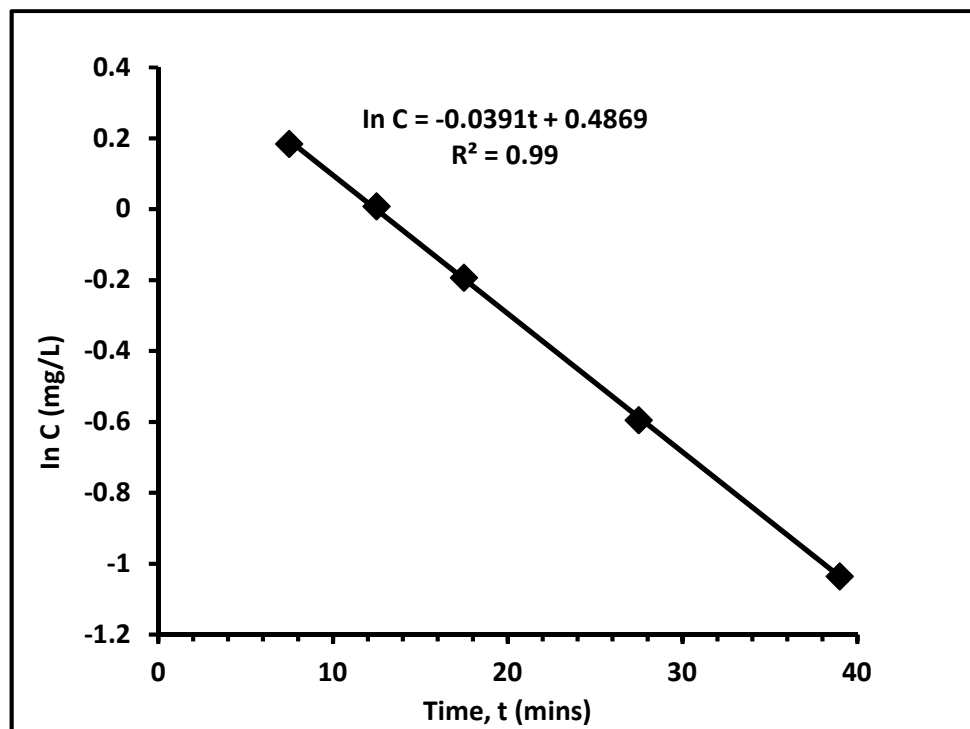


**Figure 4.17.** Little Kilham Pitrak et al (2007) horizontal flow model regression plot for depth 23.5 mbgl

**Table 4.3.** Little Kilham Farm horizontal flow model test parameters. 5 – 40 and 60 – 275 minutes profiles used to determine the parameters for depths 18 – 35 mbgl and 35.5 – 48 mbgl respectively.

<b>Depth (m)</b>	<b>Slope gL<sup>-1</sup> min<sup>-1</sup></b>	<b>R<sup>2</sup></b>
18	0.0367	0.989
18.5	0.0368	0.995
19	0.0392	0.997
19.5	0.0340	0.995
20	0.0317	0.998
20.5	0.0363	0.991
21	0.0351	0.994
21.5	0.0317	0.998
22	0.0281	0.996
22.5	0.0279	0.998
23	0.0256	0.988
23.5	0.0391	0.999
24	0.0217	0.974
24.5	0.0322	0.992
25.5	0.0265	0.977
26	0.0250	0.973
26.5	0.0250	0.973
27	0.0237	0.964
27.5	0.0232	0.969
28	0.0231	0.975
28.5	0.0238	0.990
29	0.0215	0.981
29.5	0.0210	0.981
30	0.0195	0.955
30.5	0.0186	0.929
31	0.0171	0.938
31.5	0.0170	0.958
32	0.0172	0.968
32.5	0.0164	0.962
33	0.0157	0.964
33.5	0.0160	0.979
34	0.0159	0.990
34.5	0.0157	0.972
35	0.0146	0.987
35.5	0.0163	0.987
36	0.0020	0.810
36.5	0.0027	0.810
37	0.0040	0.910
37.5	0.0041	0.920
38	0.0046	0.930
38.5	0.0049	0.950
39	0.0048	0.950
39.5	0.0044	0.910
40	0.0041	0.910

Table 4.3 continued

<b>Depth (m)</b>	<b>Slope gL<sup>-1</sup> min<sup>-1</sup></b>	<b>R<sup>2</sup></b>
<b>40.5</b>	0.0021	0.830
<b>41</b>	0.0017	0.850
<b>41.5</b>	0.0017	0.870
<b>42</b>	0.0017	0.880
<b>42.5</b>	0.0016	0.900
<b>43</b>	0.0017	0.910
<b>43.5</b>	0.0017	0.930
<b>44</b>	0.0016	0.950
<b>44.5</b>	0.0014	0.940
<b>45</b>	0.0014	0.970
<b>45.5</b>	0.0012	0.960
<b>46</b>	0.0012	0.980
<b>46.5</b>	0.0016	0.990
<b>47</b>	0.0007	0.980
<b>47.5</b>	0.0006	0.990
<b>48</b>	0.0006	0.990

The calculated discharges are highest within the zone of water table fluctuation in coincidence with the zone of enhanced diameter seen in the caliper logs, reducing to the bottom of the well, with a marked drop in discharge at depth 35 mbgl. The results suggest solutional enlarged and enhancement of fractures has occurred near the water table, creating the zone of greatest permeability and flow.

To test the vertical flow observed in the uniform profile, point injections for depths 19.5 mbgl (Figure 4.16d) and 30 mbgl (Figure 4.16e) were done. For point injection at depth 19.5 m, the profile peaks and centroids moved slowly upwards with time (~0.01 m/min), with the profile slowly spreading out with mass loss (Figure 4.18) suggestive of rapid mixing and the dominance of crossflows in the zone of enhanced permeability near the water table of the well. For injection at depth 30 mbgl, monitored between 8 – 31 minutes, the profiles spread out with time, but without a rapid mass loss as compared to the top of the well. The monitoring was discontinued because of inclement weather at the time of the test.

Using the results of the open-well dilution testing, flow in the well is dominated by horizontal crossflows, that are strongest near the zone of enhanced permeability in the zone of watertable fluctuation. There is weak downwards

flow from depth 35 mbgl. The model for this work and a previous model from Southern Science Ltd (1994) CCTV view is shown in Figure 4.19b and Figure 4.19c respectively.

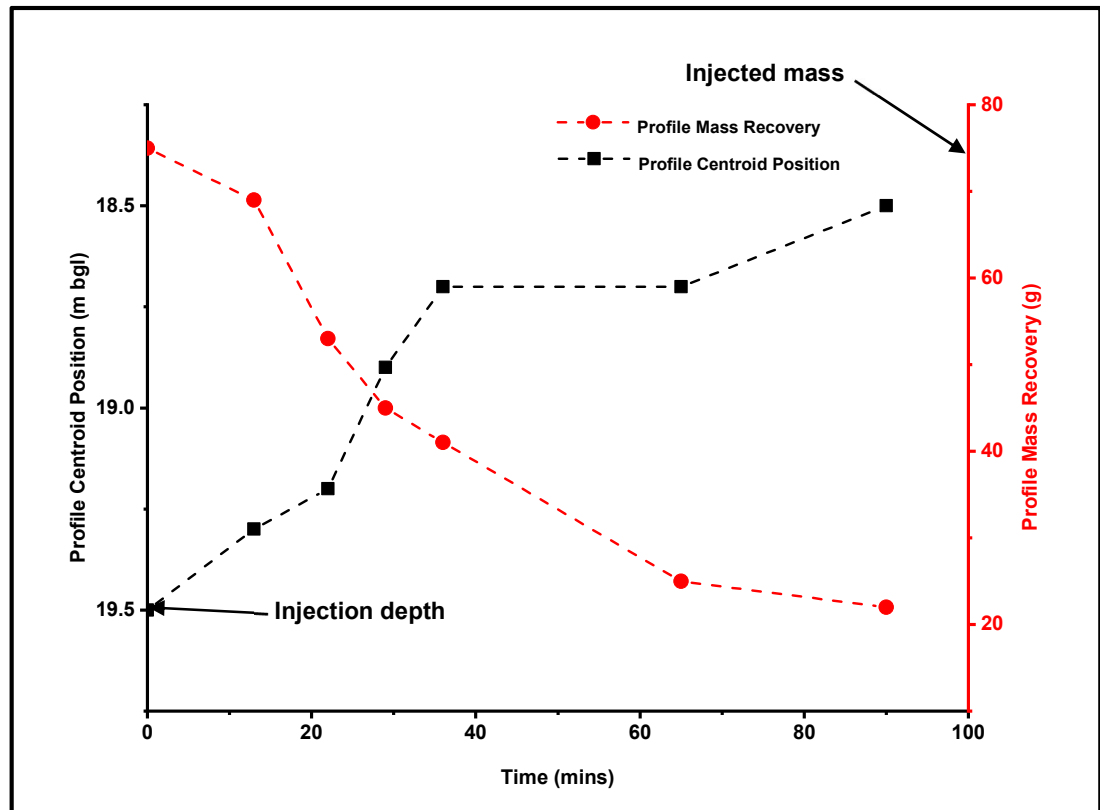


**Figure 4.18** Little Kilham Farm centroid position (black squares) and mass recovery (red circles) with time plot for point injection of 75 g NaCl at 19.5 mbgl

Like the CCTV model, the current method also identifies dominant crossflows, and small vertical movements but there are contrasts with the direction of vertical flow at the water table and from depths 40m to the well bottom. This could be due to the qualitative nature of the CCTV image log especially in a well like Little Kilham with very slow vertical flow. Ward et al. (1998) found a relatively rapid horizontal tracer dilution between 35 – 45 mbgl for a uniform injection test. However, this rapid dilution could be due to little tracer injection in the depth interval. Also the caliper log in this current work that show the reduction of possible flow features in this depth interval, suggesting that the rapid dilution is an artefact of little tracer injection. Parker (2010) also used uniform injection profiles only to adduce inflows at the water table, moving

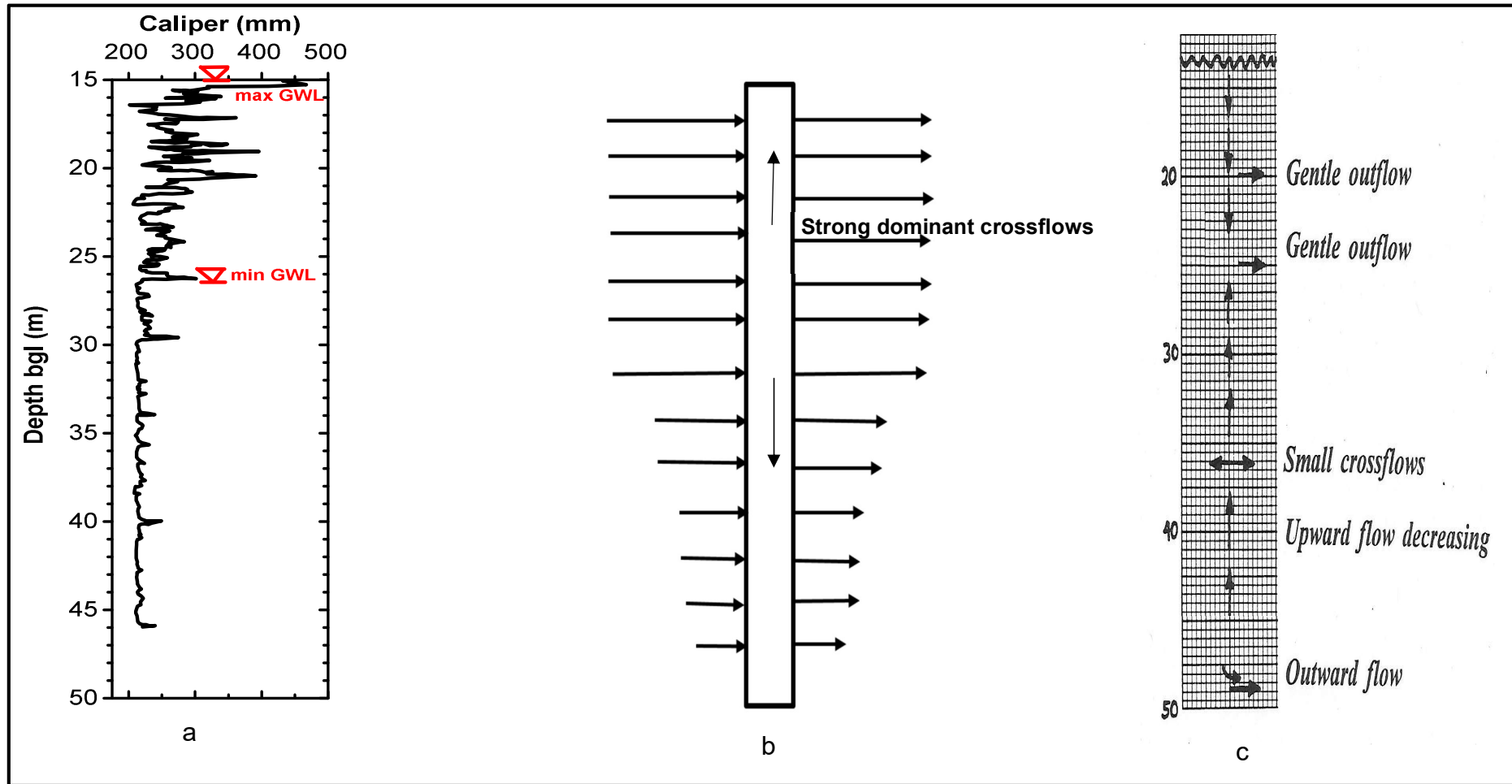


**Figure 4.19.** Little Kilham Farm borehole: (a) caliper log; (b) ambient flow model based on the work presented here with dominant crossflows(thick horizontal arrows) with weak vertical flows (thin arrows);(c) Southern Science (1994) CCTV flow model.

downwards to the well bottom. Parker (2010) stated the existence of some crossflows but did not attempt to quantify dominance or otherwise of crossflow/vertical flow. In this work however, both uniform and point tests were undertaken to assess the most dominant flow component, and gradual mass loss, tracer peak reduction, profile edge spreading suggest small vertical flows. The horizontal flow dominance in Little Kilham borehole is consistent with the relative location in relation to the main discharge zone of the Chalk, as the borehole is located on the flanks of the valley towards the Kilham discharge area (Figure 4.6).

### **Field House, Kilham Borehole**

The caliper log and uniform injection test results for Field House, Kilham borehole is shown in Figure 4.20. The well diameter (Figure 4.20a) ranges between 160 and 165mm, with two minor enlargements between depths 50 - 55 m. The initial tracer concentration ( Figure 4.20b) ranges between 0.85 – 0.99 gL<sup>-1</sup>, with minimum at the water table and the middle part of the profile. There is faster dilution at the watertable with a freshwater front moving downwards, the freshwater front reaching depths 47 and 50.5 m at times 1445 -1456 and 2165 - 2178 minutes respectively. The smoothness without kinks suggest that horizontal flows are not dominant.

Just like the current work, Parker (2009) also showed inflows at water table, moving downward towards the well bottom. She however states some additional crossflows based on poor fitting of the field profiles to the ADE model used. However, this could be due to the non-uniform injection of tracer in the well, resulting in density and solute settling in the well. In this current work, the use of the caliper log shows little fracture enlargement rules out the dominance of horizontal flows in the well. Also, the position of the well on the interfluvium and the recharge zone supports the dominance of downwards flow in the well.

### **Old Plantation Borehole**

The caliper log and uniform injection test results for the Old Plantation borehole is shown in Figure 4.21. The borehole diameter (Figure 4.21a) is generally irregular, ranging between 220 – 250 mm, with diameter enlargements between

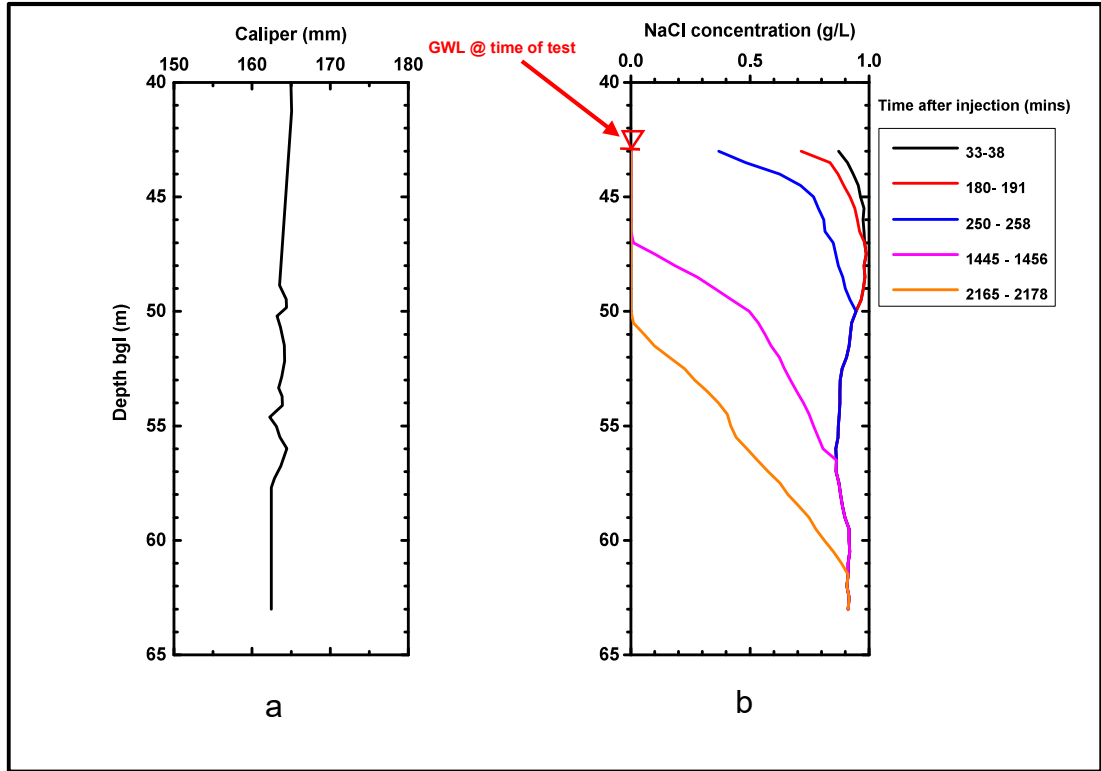


Figure 4.20. Field House, Kilham borehole results: (a) caliper log; (b) uniform injection profiles.

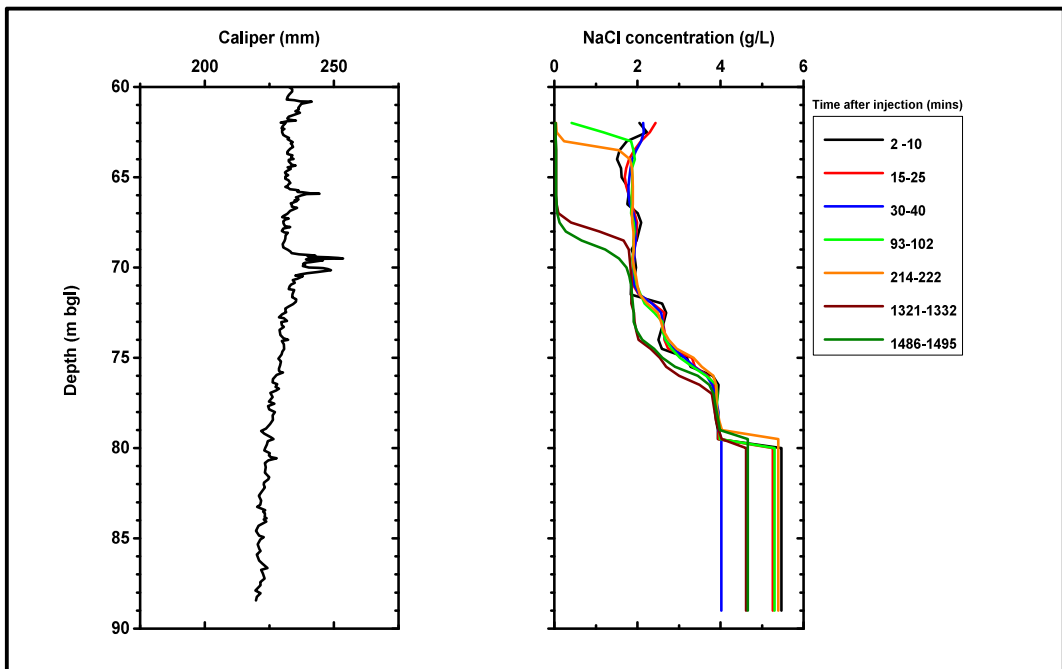


Figure 4.21. Old Plantation results: (a) caliper log; (b) uniform injection profiles.

depths 60 – 70 m, with major enlargements at 61, 66, 69.5 and 70.5 m. Below depth 70.5 m, the diameter reduces towards the borehole bottom.

During the uniform injection test, the injector got stuck at depths 72 and 80 m, for which the injector had to be turned and twisted for about 20 minutes before the injector was freed and pulled up. The initial uniform profile concentration (Figure 4.21b) ranges between 2 and 5.5 gL<sup>-1</sup>. The initial concentration is 2 gL<sup>-1</sup> from the water table to 72 m, then increases gently to 5.5 gL<sup>-1</sup> at 80 m, and then stays same to the well bottom. The initial non-uniform injection tracer distribution could possibly be attributed to irregular injection and density settling because of the injector getting stuck at the two depths 72 and 80 mbgl. In spite of the irregular tracer distribution, there is slow dilution at the water table, with a freshwater front moving downwards seen at 63 and 67 m, at times 214-222 and 1486-1495 minutes respectively. The smoothness of the profiles without kinks suggests that horizontal crossflows are not dominant and a possible outflow is postulated for the depth 70 mbgl. Apart from the archived geophysical logs used in addition to the uniform injection test, the well has not been previously characterised. The location of the well, which is high up the Wolds, supports the downward movement of water, since this is a recharge zone.

### **Henpit Hole Borehole**

The results for caliper log and a uniform injection at Henpit Hole is shown in Figure 4.22. The borehole diameter (Figure 4.22a) is very irregular, ranging between 220 and 380 mm, reducing towards the well bottom. The largest diameter enlargements occur between 20 – 35 m bgl, with some other enlargements occurring at depths 37.5, 49 and 55 mbgl. The uniform injection (Figure 4.22b) shows rapid dilution of the injected tracer, with freshwater front moving upwards, reaching depths 44 m and 18 mbgl (water table) between 3 – 15 and 15 – 18 minutes respectively after injection. Using the distance between the well bottom and the mid time of total logging time yielded an upward velocity of 4.3 m/min. To test for vertical flow, the point injection was done at depth 45 m but all the tracer was washed out within 3 minutes after injection and was not detected by the Solinst logger. The CCTV view from Southern Science (1994)(Figure 4.22c) confirms the presence of heavy

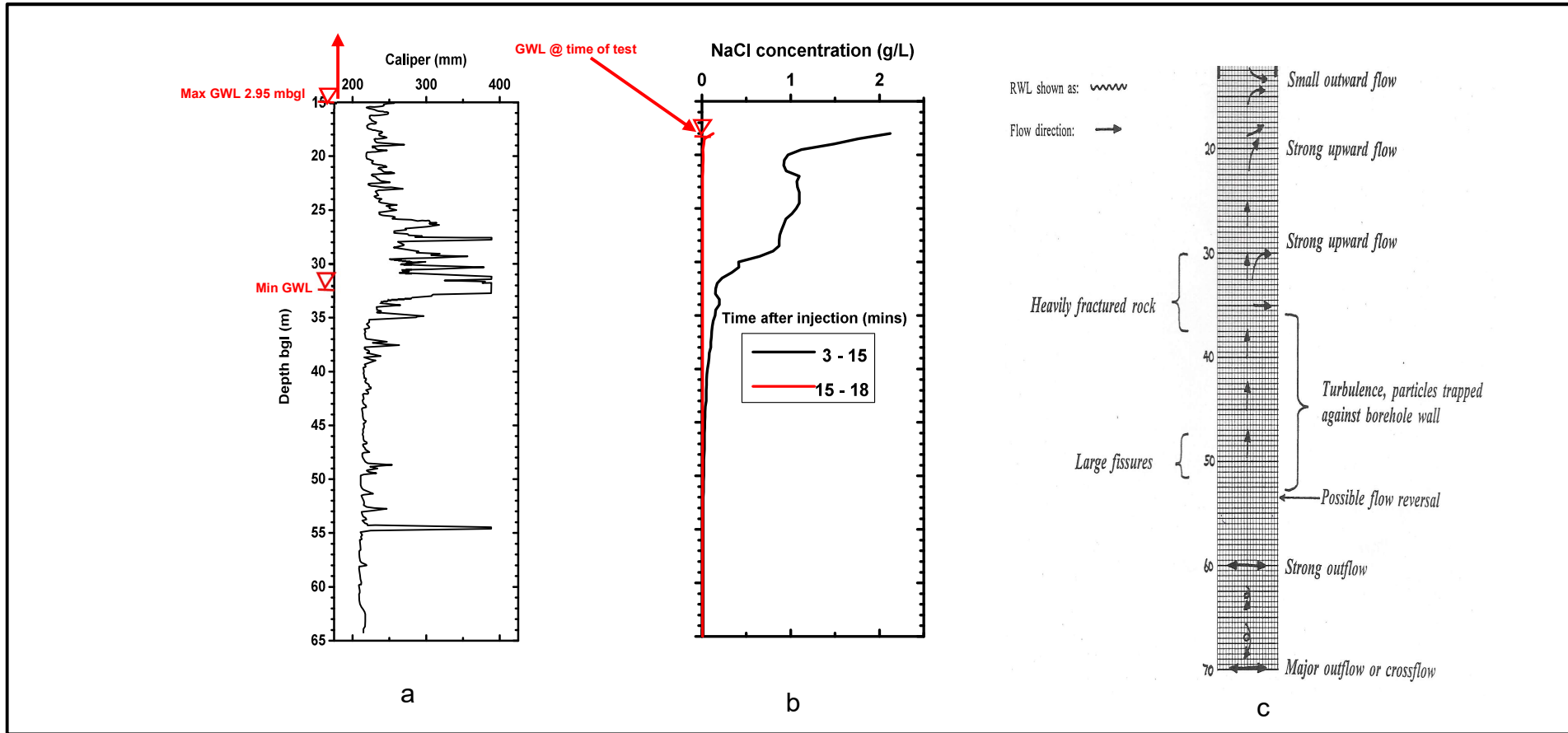


Figure 4.22 Henpit Hole borehole results: (a) caliper log; (b) uniform injection profile; (c) Southern Science (1994) CCTV flow model.

fracturing and large fractures with strong upwards flow and outflows towards the water table.

Just like previous works, the current work was able to show strong upwards flows, but was not able to infer inflow and outflow points because of the rapid tracer dilution, due to fast flows. Parker (2009) used flow impeller to determine ambient upwards velocity of 4 m/min which is in agreement with the current work. She also determined an inflow at 64 m bgl and an outflow at 14 m, which agrees with the Southern Science (1994) model above. Because Henpit Hole is located in a valley surrounded by high recharge areas, the rapid upflow in Henpit Hole is possibly due to the inflow zone tapping higher recharge areas with higher hydraulic heads.

### **Tancred Pit Borehole**

The results for Tancred Pit borehole is shown in Figure 4.23. The borehole diameter (Figure 4.23a) is highly irregular, ranging between 200 and 480 mm, with the largest enlargement occurring between casing bottom and 29 mbgl. The diameter is largest beneath the casing, reducing towards the well bottom but with enlargements at depths 34.5, 38.5 and 43.5 mbgl. The uniform injection (Figure 4.23b) shows a rapid dilution of tracer, with an upward moving freshwater front moving from the well bottom to reach depth 24 mbgl within 5 – 20 minutes. By the second log time (20-37minutes), the concentration profile in the well had returned to background levels, and so the subsequent profiles lie on each other. The plots show rapid dilution in the well.

To test the vertical flow in the well, tracer was injected at depth 45 mbgl and monitored. Figure 4.23c shows results from point injection at 45 mbgl. Details about the centroid position, mass and velocity of the profiles for the point injection at depth 45 mbgl are provided in Table 4.4 and plotted in Figure 4.23 d.

The point injection profiles show the profiles moving upwards from the depth of injection to the area of enlarged diameter at the bottom of the casing whilst losing tracer mass (Figure 4.23). The recovered mass for 0-3 mins profile is 84 g, which is higher than the injected mass of 75 g. This is due to a signal artefact because of incomplete mixing of the tracer just after injection. In spite

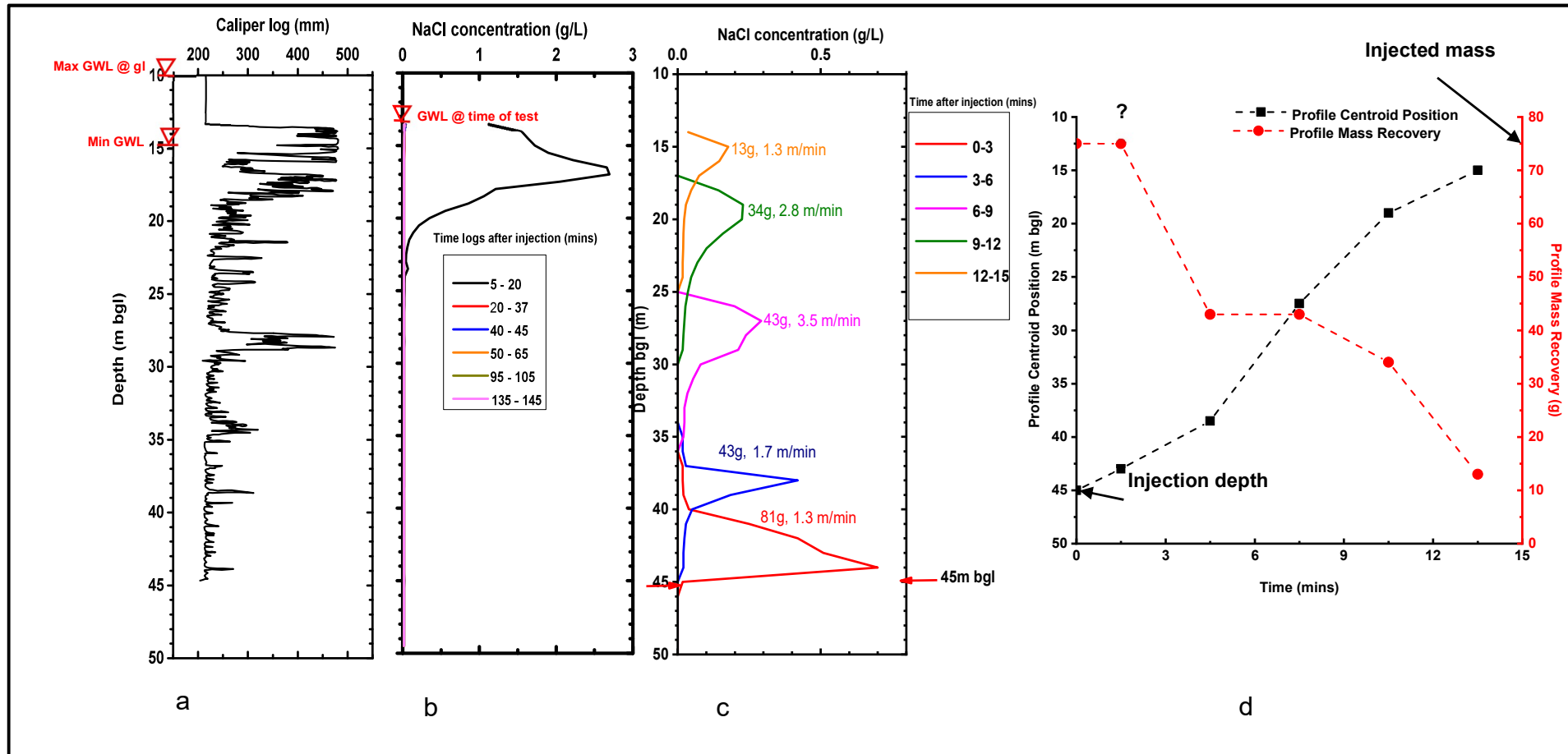


**Figure 4.23.** Tancred Pit borehole results: (a) caliper log; (b) uniform injection profiles; (c) profiles for point injection (red arrowed) at depth 45 mbgl; (d) centroid position (black squares) and mass recovery (red circles) with time plot for upwards moving profile of point injection of 75 g NaCl at 45 mbgl

of this, the resultant profiles provide data about flow in the borehole. The injected tracer moved from the point of injection (45 mbgl) to depth 43 mbgl with a velocity of 1.3 m min<sup>-1</sup>. The centroid then moved to depth 38.5 mbgl and then to depth 27.5 mbgl with velocities of 1.7 and 3.5 m min<sup>-1</sup> respectively between the depth intervals, whilst maintaining tracer mass of 43 g in each profile in the process. The tracer mass lost from the injection depth to depth 38.5 mbgl is then 32 g, without any tracer loss from depth 38.5 to 27.5 mbgl. The profile moves upwards from 27.5 to 19 mbgl with a velocity of 2.8 m min<sup>-1</sup>, whilst losing 9 g of tracer. Finally, the profile moves from 19 mbgl towards the zone of enhanced permeability at the bottom of the casing with a reduced velocity of 1.3 m min<sup>-1</sup> whilst losing 21 g of tracer in the depth interval. The average upwards velocity from the tracer injection point to the bottom of the

**Table 4.4.** Details of point injection of tracer at depth 45 mbgl and profile properties in Tancred Pit borehole

Profile time (min)	Depth of profile centroid (m bgl)	Velocity between centroid (m/min)	Profile mass recovered (g)	Mass loss between profiles (g)
0	45		75 <sup>1</sup>	
		1.3		?
0-3	43		84 <sup>2</sup>	
		1.7		32
3-6	38		43	
		3.5		0
6-9	27.5		43	
		2.8		9
9-12	19		34	
		1.3		21
12-15	15		13	

<sup>1</sup> 75 g of NaCl injected at depth 45 mbgl

<sup>2</sup> Reason or higher mass of recovered tracer than injected is explained in text

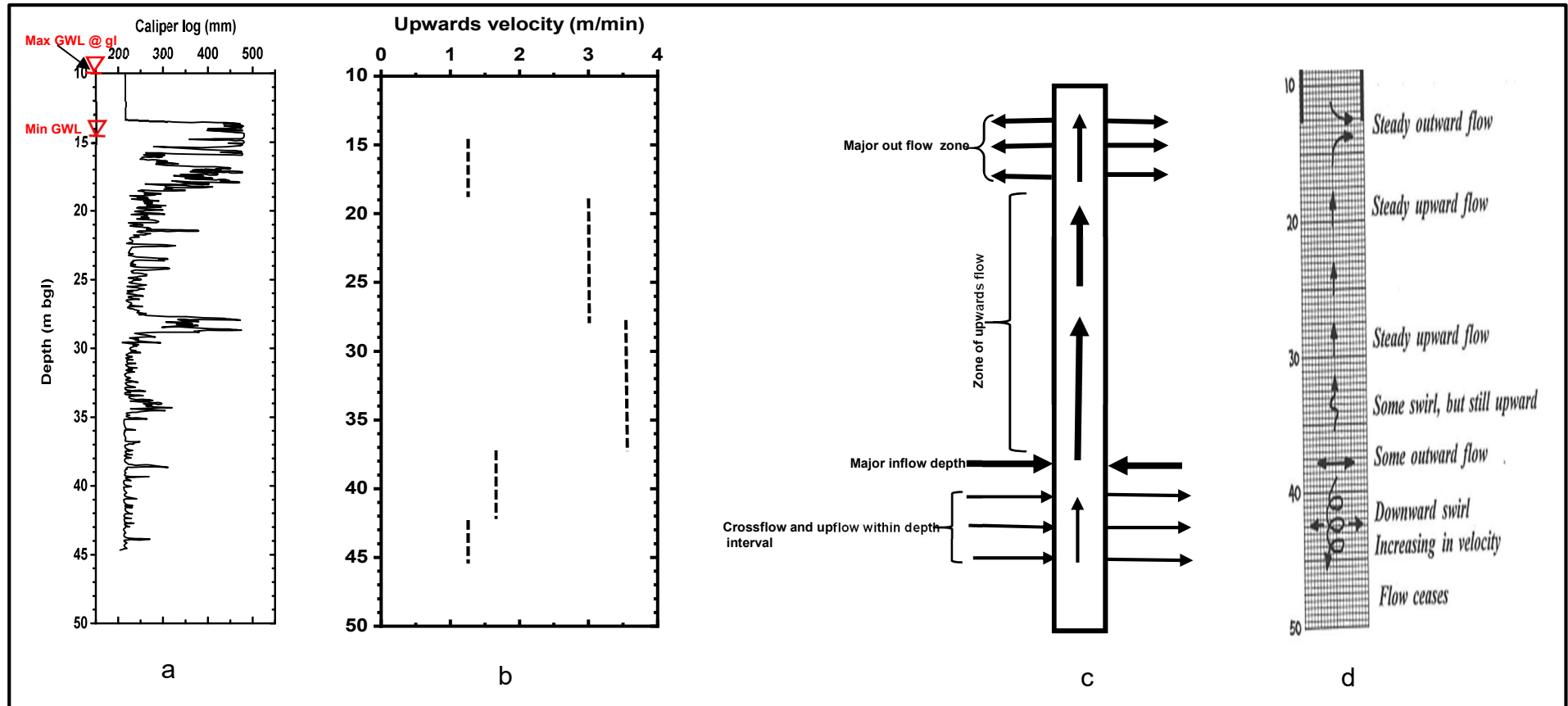


**Figure 4.24.** Tancred Pit borehole results: (a) caliper log; upwards (b) velocity profile for depth intervals marked by profile centroid positions (c) current work flow model (ambient) ; (d) Southern Science (1994) CCTV flow model.

casing is  $2.1 \text{ m min}^{-1}$ . The derived velocities described above are plotted in Figure 4.24b with depth.

The large mass loss (32 g) between depth 45 and 38.5 mbgl initially suggests an outflow zone. But the increase in velocity in the 43 – 38.5 mbgl depth interval suggests a washout zone, with component of the flow moving upwards, indicative of crossflowing features with some upflow. This interpretation is evidenced by the caliper log between the depth interval, as additional flows will result in velocity increase because the diameter of the well remains almost the same in the depth interval. Another reason for the velocity increase could be due to a constriction or borehole wall collapse in the depth interval at the time the open-well dilution tests were undertaken. The depth interval 38.5 to 27.5 mbgl records an increased velocity of  $3.5 \text{ m min}^{-1}$  (from  $1.6 \text{ m min}^{-1}$  in depth 43 to 38.5 mbgl) suggests that there are major inflow features in the depth interval that increase the velocity in the depth interval. This interpretation is premised firstly on no tracer loss in the depth interval. Secondly, should the flow from below the depth interval be constant, then the increased well diameter at depths 38.5, 34 and 28 mbgl within the depth interval should result in velocity reduction rather than an increase. A relook at the profile (6 – 9 mins) shows a smooth profile, without kinks. This then shows that the major inflow depth is possibly at 38.5 mbgl and not above it.

The profile (9 – 12 mins) reducing in flow velocity within the 27.5 to 19 mbgl is in consistent with the increased well diameter in the depth interval. The profile losing 9 g of tracer possible occurred at the front of the profile around 17 mbgl. Should there have been outflows before the tracer front, these would have produced kinks on the profile. From 17 mbgl to the zone of enhanced permeability near the bottom of the casing, which coincides with a zone of enlarged fractures, the flows and mass reduce drastically suggesting large major outflows in this depth interval.

The interpretation for the uniform and point injection in Tancred Pit well produces a flow model shown in Figure 4.24c. A comparison of the current flow model (Figure 4.24c) with the Southern Science (1994) CCTV model (Figure 4.24d) show a similarity in showing inflows, upflows, crossflows and outflows. Previous works like Southern Science (1994) and Parker (2009) also

showed upwards flow from the well bottom to the water table. Parker (2009) determined an ambient upward flow speed of  $2 \text{ m min}^{-1}$  using a flow impeller. Inflow zones identified by previous works ranged between 42 and 44 mbgl, whilst the diffuse outflow zone ranged between 20 mbgl to the casing bottom. Parker (2009) also found major outflows between depths 27 and 29 mbgl, and at 20 mbgl corresponding to 27.5 m and 20 mbgl respectively in this current work. The current work was able to detect crossflows at 38.5 – 45 mbgl depth interval, which agrees with the findings of the Southern Science (1994) CCTV image log. However Parker (2009) was not able to detect the crossflows from impeller logging as has been identified in this current work.

The rapid inflow fractures in Tancred Pit borehole have been shown by a tracer test undertaken by Ward and Williams (1995) (see link with section in Chapter 6 for details of the tracer tests and its reinterpretation), connects with Broachdale borehole (see Figure 4.6 for relative location of the two boreholes), which has a relatively high hydraulic head due to its relatively higher elevation.

### **Weaverthorpe Borehole**

Figure 4.25 to Figure 4.27 show the results of the Weaverthorpe borehole. Figure 4.25a shows the image log, with horizontal fracture traces distributed at different depths of the well coinciding with borehole enlargement on the caliper log (Figure 4.25b). The diameter of the well (Figure 4.25b) is irregular, ranging in diameter from 100 and 155 mm, with the largest enlargements occurring in the zone of seasonal water table fluctuation. The diameter reduces towards the well bottom.

Figure 4.25c shows uniform injection resulted in an initial salt concentration of  $2.75 \text{ gL}^{-1}$  at the well bottom and near the water table, but has very large distinctive reductions at 33.5 and 40 mbgl for the first profile (2 – 8 mins), and these kinks persist through the rest of the profiles. The distinctive and persistent kink observed at depth 40 mbgl, which shows background concentrations for all the profiles is indicative of a main inflow / crossflow fracture. A freshwater front from the fracture at 40 mbgl then drives flow up the well, with the tracer peak initially seen at 38 mbgl moving upwards and attenuating at depth 33.5 mbgl. Fairly rapid dilution occurs between the water

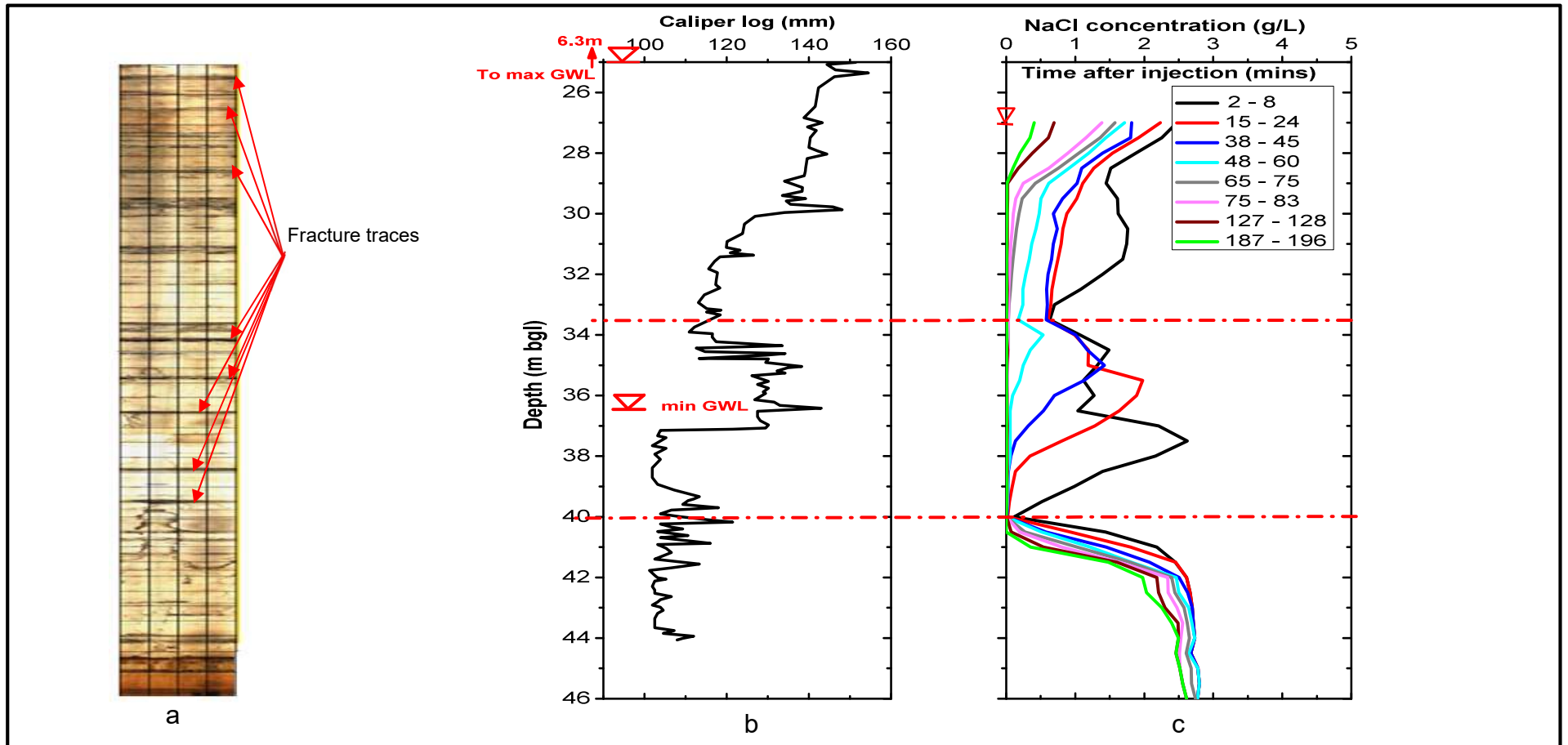


**Figure 4.25.** Weaverthorpe borehole results: (a) borehole image log with fracture traces; (b) caliper log; (c) uniform injection profiles.

table and 33.5 mbgl, with the dilution rate increasing with depth in this depth interval. Depth 33.5 mbgl is a possible crossflow fracture because of the kink and freshwater front from this fracture that flows upwards to depth 29 mbgl after the tracer peak from below 33.5 mbgl had passed the depth between 65 – 75 mins. The uniform nature of the profiles between 29 – 27 mbgl indicates an outflow between this depth interval. Between depths 40 – 42 m, there is a slow but uniform dilution, whilst below 42 mbgl tracer dilutes very slowly indicative of little flow to the bottom of the well.

To constrain the flow features from the uniform injection, point injections were undertaken at depths 39.5, 33.5 and 41.5 mbgl. Figure 4.26a show results from point injection at 39.5 mbgl. Details about the centroid position, mass and velocity of the profiles for the point injection at depth 39.5 mbgl are provided in Table 4.5 and plotted in Figure 4.27a.

The calculated recovered tracer mass from the 1-7 mins profile of 81.0 g, is more than the injected mass of 75.0 g, indicating incomplete mixing with the water column. The tracer profile centroid moves upwards (Figure 4.27a) from the point

**Table 4.5.**Details of point injection of tracer at depth 39.5 mbgl and profile properties in Weaverthorpe borehole

Profile time (min)	Depth of profile centroid (m bgl)	Velocity between centroid (m/min)	Profile mass recovered (g)	Mass loss between profiles (g)
0	39.5		75 <sup>1</sup>	
		0.50		?
1-7	37.5		81 <sup>2</sup>	
		0.13		10
7-13	36.7		65	
		0.18		6
19-27	34.4		59	
				31
27-33	34.2		28	

<sup>1</sup> 75 g of tracer injected

<sup>2</sup> Reason for a higher recovery amount explained in text

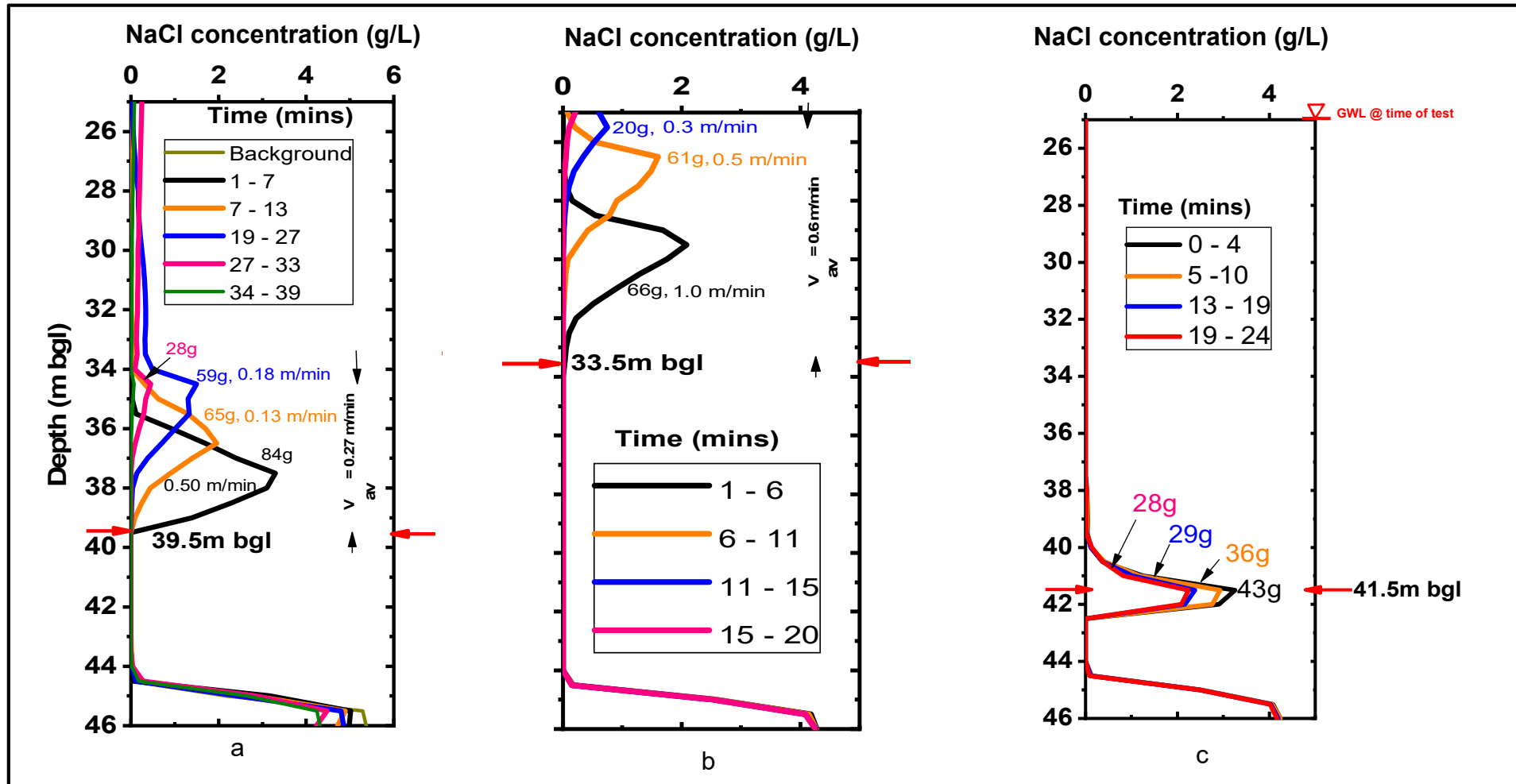
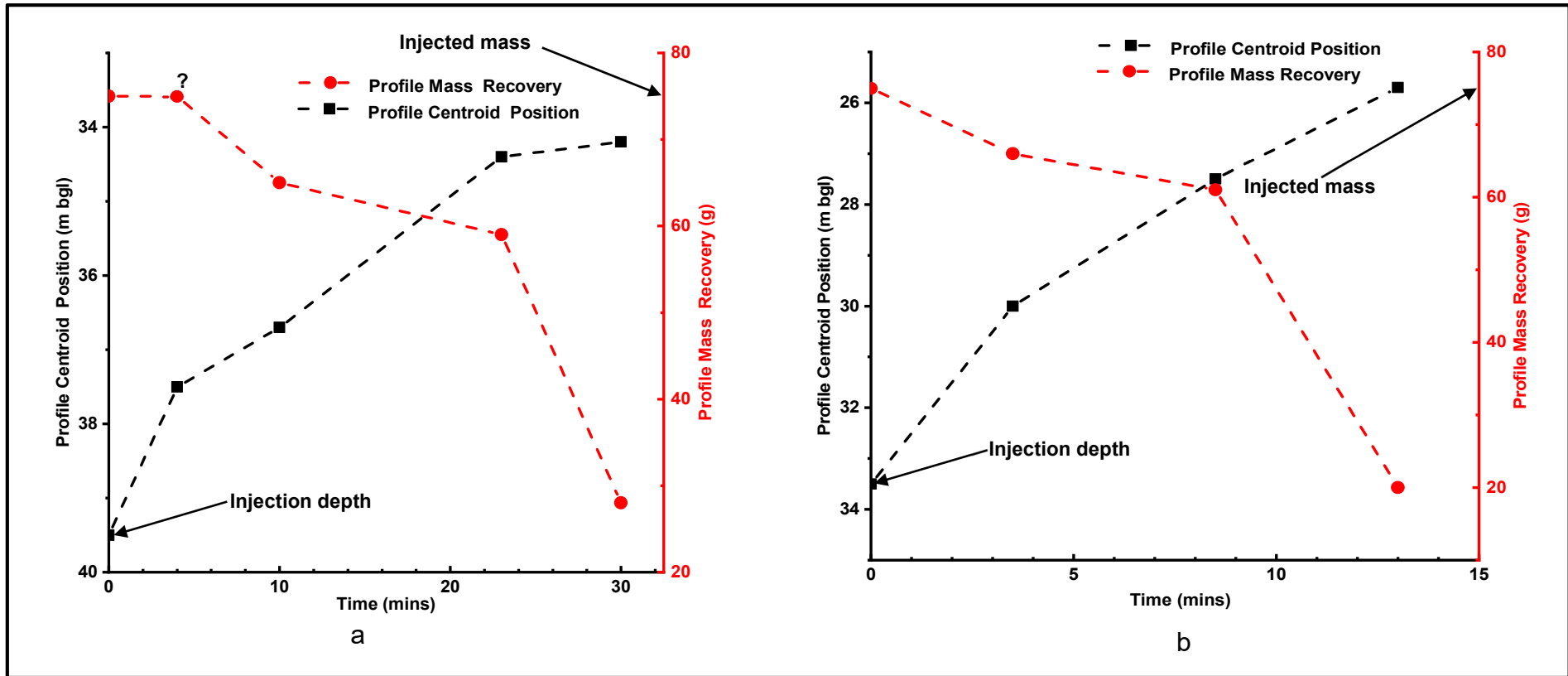


Figure 4.26. Weaverthorpe borehole point injection (red arrowed) for depths: (a) 39.5 m; (b) 33.5 m and (c) 41.5 mbgl.



**Figure 4.27.** Weaverthorpe borehole centroid position (black squares) and mass recovery (red circles) with time plot for upwards moving profiles of point injection of 75 g NaCl at: (a) 39.5 m and (b) 33.5 m bgl.

of injection to depth 37.5 m (1-7 mins) with a velocity of  $0.50 \text{ m min}^{-1}$ . The profile centroid then moves to depths 36.7 m (7 – 13 mins) and 34.4 m (19-27 mins) with velocities of  $0.13$  and  $0.18 \text{ m min}^{-1}$ , which is in agreement with the diameter increase from the caliper log (Figure 4.25b) for the depth interval. The profiles also lose 10.0 and 6.0 g of tracer respectively. The profile centroid then moves to depth 34.2 m (27- 33 mins), with tracer spreading upwards through to depth 26.5 m, whilst losing 31 g of tracer. The average upward velocity of tracer centroid is  $0.27 \text{ m min}^{-1}$  between depths 39.5 to 34.4 mbgl.

The 10.0 g loss for the 7-13 mins profile probably occurred around the depth of injection (39.5 mbgl), which is close to the 40 mbgl kink area as evidenced by the smoothness of the profile, without kinks. Also the profile had not reached the 33.5 mbgl (the next major kink point) at the time of logging. The 6.0 g (19-27 mins) and 31.0 g (27-33 mins) loss possibly occurred at or above the 33.5 mbgl kink point.

To resolve the flow features above depth 33.5 mbgl, another point injection test was undertaken at the 33.5 mbgl kink point. Figure 4.26b show results from point injection at depth 33.5 mbgl. Details about the centroid position, mass and velocity of the profiles for the point injection at depth 33.5 mbgl are provided in Table 4.6 and plotted in Figure 4.27b. The 1 – 6 mins tracer profile moves upwards at a velocity of  $1.0 \text{ m min}^{-1}$  between the injection point to depth 30 m, whilst losing 9 g of tracer. The increase in velocity for this profile (1-6 mins) in comparison to that below depth 33.5 mbgl is in consonance with the decreased diameter above 33.5 mbgl. The tracer centroid then moves upwards to depths 27.2 mbgl (6-11 mins) and then to 25.7 mbgl (11-15 mins) with reduced velocities of  $0.5$  and  $0.4 \text{ m min}^{-1}$  respectively, in consonance with the enlarged diameters on the caliper log. The tracer lose masses of 5 and 41 g for 6-11 mins and 11-15 mins profiles respectively. The average velocity between the depth of injection and the water table is  $0.6 \text{ m min}^{-1}$ .

The 9.0 g mass loss for the 1-6 mins profile occurred possibly at the depth 33.5 mbgl, indicating that the kink at 33.5 mbgl is a possible outflow / crossflow feature. The large mass loss (41 g) and reduction in velocity between the 6 – 11 mins and 11 – 15 mins profiles suggests an outflow zone between 27.5 –

25.7 mbgl depth interval, which corresponds to area of enlarged well diameters.

**Table 4.6.** Details of point injection of tracer at depth 33.5 mbgl and profile properties in Weaverthorpe borehole.

Profile time (min)	Depth of profile centroid (m bgl)	Velocity between centroid (m/min)	Profile mass recovered (g)	Mass loss between profiles (g)
0	33.5		75	
		1.0		9
1-6	30.0		66	
		0.5		5
6-11	27.5		61	
		0.4		41
11-15	25.7		20	

Figure 4.26c shows results from point injection at 41.5 m bgl. The peaks for each log remains at the same depth, but reduce with time. A small amount of tracer migrated upwards creating asymmetrical peaks. The tracer mass calculated from the first log (0-4 min) is 43 g – much less than the 75 g injected indicating that either the highest tracer concentration was missed (as SEC was logged only every 0.5 m), or due to incomplete mixing within the water column. The masses for subsequent logs are 36, 29 and 28 g. This uniform dilution behaviour most likely indicates a crossflow at the depth of investigation.

The resulting velocity variation with depth is plotted in Figure 4.28b. The results and interpretation of the uniform and point tracer injection for the Weaverthorpe well have been used to produce a flow model in (Figure 4.28c).

The current work is compared with Parker (2009)'s characterisation of the Weaverthorpe borehole (Figure 4.29). Parker used uniform injection only to infer inflows at 40 m and 21 mbgl ( at a time of higher water table in the well),

with an outflow at 35 m bgl (Figure 4.29b). Parker's model showed the flows moving upwards from 40 m, and moving downwards from 21 m to converge and exit at 35 m bgl. This is in contrast to the current work which used both uniform and point injection to infer upwards flow only from 40 m, towards the zone of enhanced permeability at the water table (27 and 25 m for uniform and point testing respectively), with evidence of crossflows, major outflows and diffuse outflows at different sections of the well. Comparing the flow convergence model of Parker (2009) and the current work suggests that there is a possible flow regime pattern switch / changes in the well depending on the head difference between the fractures that feed the enhanced permeable zone near the water table and the fractures in the 33.5 - 35 m bgl depth interval. At high groundwater levels, flow moves downwards from the high permeable zone at the water table to exit at 35 mbgl, whereas at low groundwater levels, discharge is towards the enhanced permeable zone at the water table. The flow regime switch / change could possibly be in response to relative catchment size variation at relatively high and low ground water levels, which activate different hydraulic heads and fracture flow systems in the formation.

Weaverthorpe borehole's location in a valley is similar to that of Henpit Hole and Tancred Pit, and so the reason for the upwards flow from the deeper fractures is attributable to connection with higher recharge areas. However Weaverthorpe is different in terms of flow modelling because of flow regime switch / changes between 35 m and the zone of enhanced permeability at the water table. This characteristic observed in the Weaverthorpe borehole has implications for aquifer management, groundwater sampling and hydraulic head data interpretation and this is discussed in Chapters 5, 7 and 8.

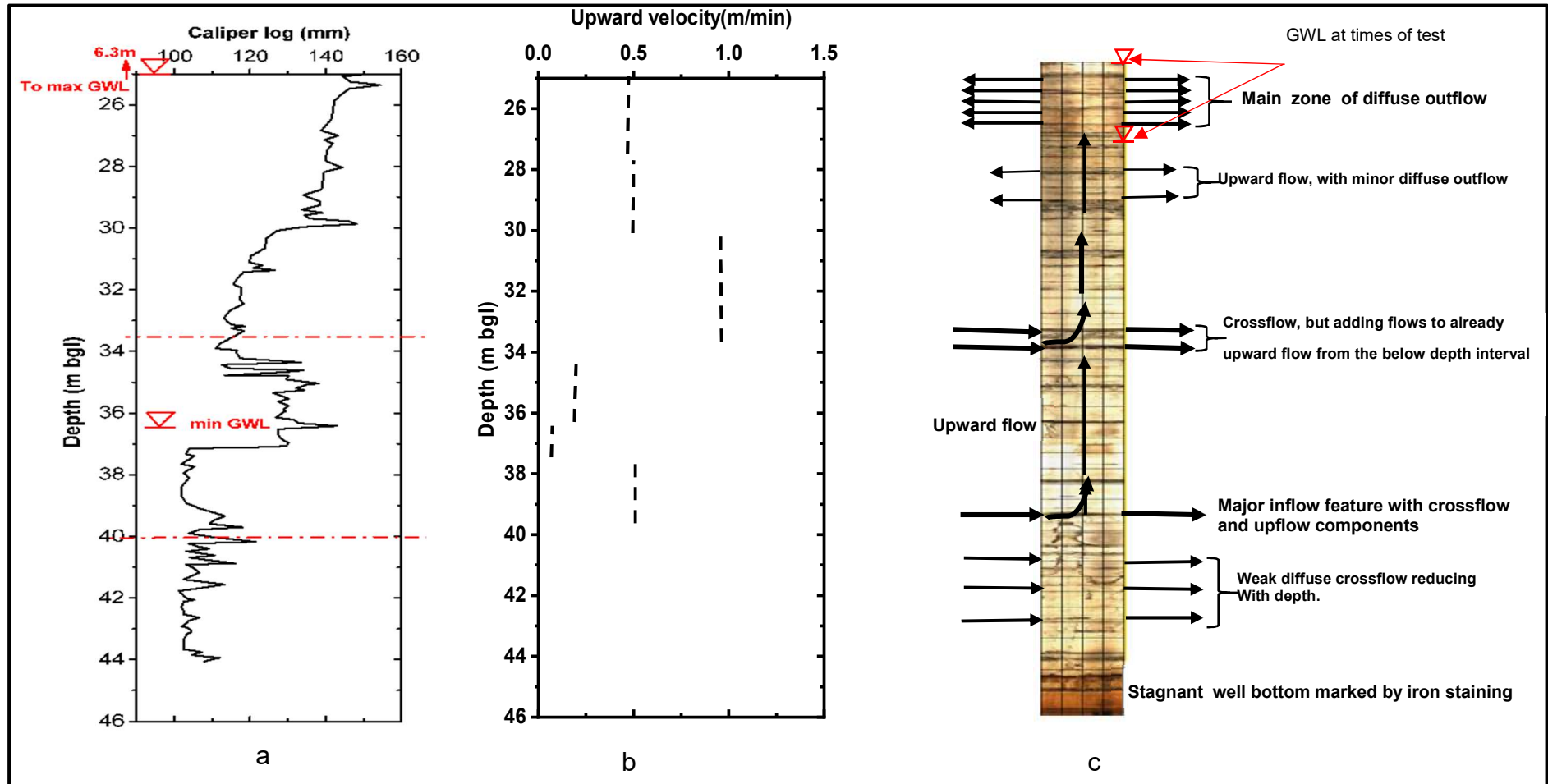


**Figure 4.28.** Weavertorpe borehole: (a) caliper log; (b) velocity profile for depth intervals marked by profile centroid positions; (c) well flow model (ambient)

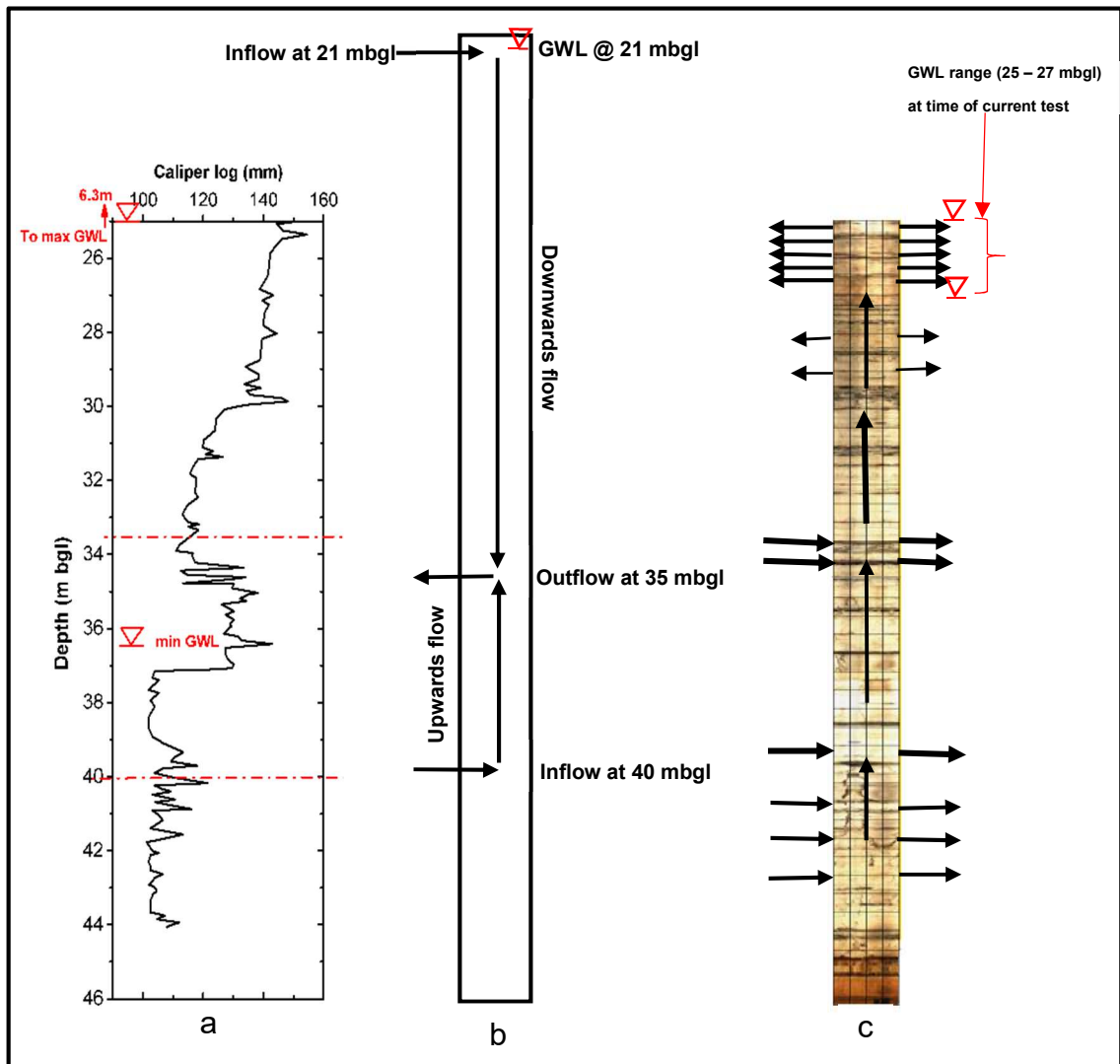


**Figure 4.29.** Comparison of the flow models for the Weaverthorpe borehole. (a) Caliper log; (b) Flow model of Parker (2009) upflow and downflow converging to outflow 35 mbgl; (c) current ambient flow model from this work

#### 4.6 Summary of findings

- This chapter has shown the effective use of the open-well dilution testing in conjunction with image, caliper and CCTV image to better resolve flows for the development of flow models at the borehole scale.
- The combination of point and uniform dilution tracer injections can resolve flows in open wells in a fractured Chalk aquifer. For an effective

use of the technique, uniform injections should be used initially, followed by point injections at selected depths based on the uniform test results where needed.

- The open-well dilution method has been used to infer inflow, outflow, crossflow, and vertical flows in wells in the catchment. The open-well dilution method has been used to identify flow on discrete horizons, which confirms flow and permeability variation with depth in the catchment, with the implication that a general model of flow variation with depth in boreholes in the Chalk must consider the specific location of the borehole in the catchment.
- Comparison of the current findings in this chapter with previous characterisation via impeller logging showed good agreement, and even showed better resolution in some cases. For instance, flow logging cannot see crossflows, but the open-well dilution approach used was able to detect crossflows. Also, open-well dilution was able to see the very low ambient flows that are not detectable by flow logging.
- The open-well dilution method has some limitations. Firstly, the method can be difficult and inapplicable in wells with rapid flows. This was shown in Henpit Hole and Tancred Pit because of rapid dilution and washout of the tracer after injection. Secondly, for wells with dominant horizontal flows, the computed horizontal velocities are not entirely due to horizontal flow dilution, but also due to some vertical flow, resulting in an overestimation of the horizontal velocities. Thirdly, the SEC and concentration profiles on which the method depends is prone to error due to dispersion effects that cause smearing of the tracer resulting in some level of subjectivity in identifying conductive zones.
- The method would have benefited from continuous rather than point SEC measurements, because of the tendency of the meter to miss the tracer at non-measured depths and zones of incomplete mixing. In addition, the method is prone to density driven mixing effects.
- Findings from this chapter will be incorporated with other previous findings to describe flow topology in chapter 6, which will then be used in chapter 7 to build a conceptual model for the study area.

## **Chapter 5 Spring and well monitoring and results**

In this chapter, the use of specific electrical conductivity (SEC), temperature, major ion chemistry and groundwater level monitoring in springs and wells will be used to characterise the Chalk aquifer. In fractured carbonate aquifer studies, it is apt to use springs rather than boreholes because spring discharge represents the gross behaviour of the aquifer whereas boreholes have a very low probability of intersecting relevant flow features even at intuitively logical locations (Worthington et al., 1992; Worthington et al., 2000; Ford and Williams, 2007). Temperature and SEC lend themselves to easy, automatic and continuous measurement with the potential to detect the memory and temporal effects of input signals at the springs for characterisation of recharge and flow regime in the aquifer. Reliable groundwater level data is also very useful for understanding catchment scale behaviour. First the theory of specific electrical conductivity (SEC), temperature and groundwater level monitoring and instrumentation is presented. Then the field methods used and their results are discussed and summarised.

### **5.1 Springs and their importance in fractured carbonate aquifer studies**

Carbonate springs are important for their groundwater resource potential and also for hydrogeological studies for aquifer characterisation. Large springs form the discharge routes for fractured carbonate aquifers, serving not only as sources of water supply but also support for the ecology and ecosystem of their catchments (Ford and Williams, 2007; Kresic, 2010). In hydrogeological studies, spring discharge and quality characteristics through time provide hydrogeological information about the recharge and transport mechanisms of the aquifers for effective resource and aquifer management (Manga, 2001; Desmarais and Rojstaczer, 2002; Birk et al., 2004; Ford and Williams, 2007; Kresic, 2010; Covington et al., 2011; Doucette and Peterson, 2014; Luo et al., 2018). The recharge and transport properties of carbonate aquifers depend on the type and area of recharge, geology, water residence time, size and degree of interconnection between fractures and flow features (Dreiss, 1989;

Vandike, 1996). For this reason, a sound catchment hydrogeologic framework is needed in understanding the flow characteristics of carbonate springs.

In the past seven decades, a lot of work focusing on the analyses of spring discharge and quality parameters over time (termed chemograph by Ford and Williams, 2007 ) to determine recharge type and mode, residence time of flow and proportion of flow components in carbonate aquifers have been done. Figure 5.1 shows the basic concepts of these studies. Their main assumptions are based on on: i. the short lag time between input events like storms and initial response in spring discharge, and ii. the relatively long response memory of discharge and quality parameters at springs (Dreiss, 1989).

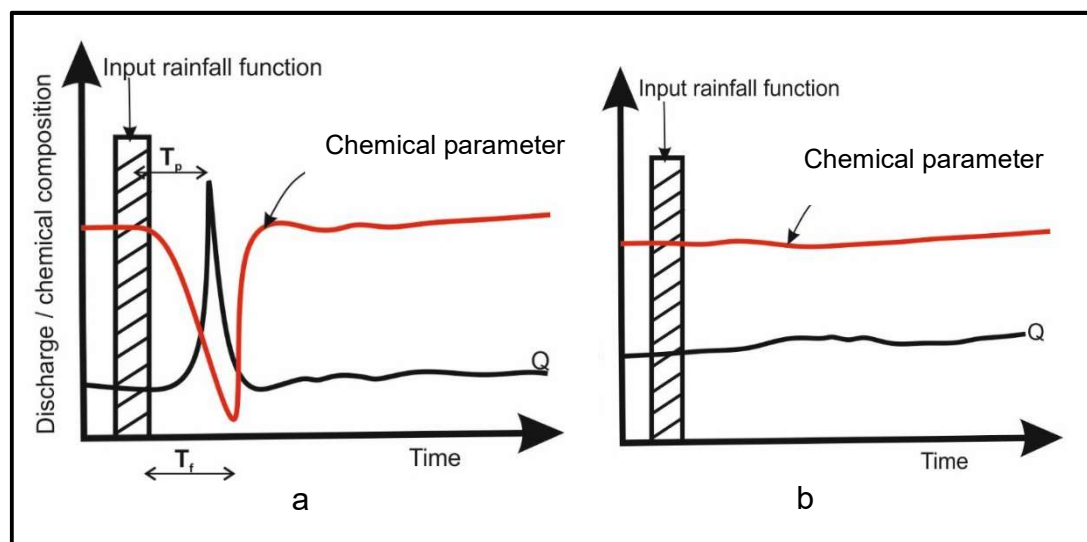


**Figure 5.1.** Schematic of a carbonate fractured aquifer's spring response to input events: (a) rapid recharge and flow via conduits; (b) diffuse homogenised recharge

In Figure 5.1a, a fractured carbonate aquifer spring fed by rapid bypass flow via conduits and short residence time results in a relatively quick pressure pulse transmission through the aquifer, in time  $T_p$ , resulting in an increase in spring discharge. However, the input event takes time to travel (memory effect of the aquifer) to the spring in time  $T_f$ , which is the flow through time or residence time of the aquifer, signified by the reduction in the chemical parameter of the spring. In Figure 5.1b, due to the diffuse nature of recharge or long residence or flow through time and flow homogenisation in the aquifer,

the input recharge event is masked and cannot be easily seen in either the spring discharge or chemical parameter.

Pulse through time method development to date has proceeded as follows below. Ashton (1966) introduced the flood pulse train concept and a binary deductive thinking approach for inferring pulse form and aquifer response to the pulse. The method was found to be difficult to apply in practice for interpreting aquifer response, but it did set the tone for future work in that direction. Refinements of the pulse train technique happened two decades later. Christopher (1980) used the chemograph of chemical analytes and snow melt pulses to characterise the hydrology of the Russett Well system, in Derbyshire. Smart and Hodge (1980) also used Rhodamine WT dye injection and recharged water to the Cheddar spring (Carboniferous Limestone) from a pump shut off at a waterworks to describe the vadose zone structure and water transfer mechanism to the saturated zone.

Development continued with Pitty (1968) who used seasonal calcium content variation in limestones and the temperature peak signals at springs to infer source area and flow through time in the Pennines. Shuster and White (1971;1972) and Ternan (1972), in Pennsylvania, US and Pennines, UK respectively differentiated between rapid conduit and slow diffuse flow types in karst aquifers using the seasonal variation of hardness, temperature, Ca to Mg ratios, calcite and dolomite saturation indices. They found that the hardness variation for the diffuse flow type was small (<5%) whereas the conduit flow type had hardness variations >10%. Scanlon and Thrailkill (1987) found similar seasonal variations in temperature,  $\text{Ca}^{2+}$ ,  $\text{Mg}^{2+}$ ,  $\text{HCO}_3^-$  and hardness of two groups of springs with dissimilar physical characteristics in the shales and limestones of the relatively flat Bluegrass Region. Dreiss (1989) and Vandike (1996) used a year's temperature and SEC log, discharge,  $\text{Ca}^{2+}$ ,  $\text{Mg}^{2+}$ ,  $\text{HCO}_3^-$  and precipitation data for the Maramec Spring, discharging from the dolomitic aquifer on the Eminence Formation of Missouri to characterise recharge mechanism, pulse travel time and the residence time. They used the lag time between the precipitation event and discharge increase and reduced analyte concentration to determine pulse travel time of 3-4 days and residence times of 12-15 days. They concluded that the spring discharge characteristic was because of the well developed conduit system in the catchment.

For studies based solely on temperature, Crowther and Pitty (1982) used water temperature variability to differentiate between deep and shallow groundwaters in Malaysia. They found that shallow flows showed greater temperature variability attributable to atmospheric air circulation, whereas waters without atmospheric interaction had constant temperature with time.

In the past two decades, other works have used similar approaches to characterise aquifers. Martin and Dean (1999), Birk et al. (2004) and Liñán Baena et al. (2009) used temperature and SEC on carbonate aquifer in Florida, gypsum karst spring of Urenbrunnen in Germany and karstic (limestone and dolomite) aquifer in southern Spain respectively. In some other places, workers took advantage of the catchment agricultural activity, nitrate application times and seasonal nitrate concentration variations at springs to determine times of recharge and the provenance of spring waters (eg. Menció et al., 2011 on carbonate aquifer of north-east Spain; Toran and White, 2005 on limestone and dolomite karstic aquifer in Pennsylvania ; He et al., 2010 on limestone and dolomite karstic aquifer in China). On the Southern Province Chalk of the UK, Darling et al. (2012) used the hydrochemistry of springs and boreholes through time to study the effect of groundwater level recovery on water after the 1996/97 drought. The recovery did not seem to have any effect on water quality because of the intimate water matrix interaction and flow homogenisation in the aquifer.

## **5.2 Classification of carbonate aquifers: conduit or diffuse flow or a combination of both?**

Shuster and White (1971,1972) and Ternan (1972), in Pennsylvania, US and Pennines, UK respectively differentiated between rapid conduit and slow diffuse flow types in karst aquifers using the seasonal variation of hardness, temperature, Ca/Mg, calcite and dolomite saturation indices. Shuster and White (1971,1972) found that diffuse systems showed little variation in chemical properties through the year irrespective of the season and storm event, with a hardness variation of less than 5% whereas the rapid conduit systems showed a large variation greater than 10% in hardness, and concluded that diffuse and conduit flow are the two extremes of carbonate aquifer types and that the two flow systems account for the hardness variation in carbonate aquifers. Diffuse flow springs were non-flashy, had waters of

long residence time, and discharged from many fractures with laminar flow patterns. On the other hand, conduit flow springs are flashy, with turbulent flow with high velocities to as high as  $1.6 \text{ km day}^{-1}$ .

The statistical method and end member flow classification was found not applicable in all catchments. Scanlon and Thraikill (1987) found similar seasonal variations in temperature,  $\text{Ca}^{2+}$ ,  $\text{Mg}^{2+}$ ,  $\text{HCO}_3^-$  and hardness in springs in the shales and limestones of the Bluegrass Region of Kentucky, and they could not differentiate flow between the two different aquifer end members. They related the similarity to the mode of recharge and attributed this to the peculiar bedrock geology and structure of the Bluegrass area. A paradigm shift in thought in the understanding of hardness variation and its attribution to flow types was shown by Worthington et al. (1992) via a statistical analyses of 39 springs from 6 temperate countries to demonstrate that there was no evidence for hardness variation attribution to flow types as proposed by Shuster and White (1971,1972), but instead that more than 75% of hardness variation was attributable to recharge type.

Other studies also demonstrated the two end member flow type classification i.e diffuse versus conduit flow by Shuster and White (1971,1972), was overly simplistic, and that most carbonate aquifers have a mix of the two kinds with each flow type highlighted depending on the method of study. In the same catchment, an injected tracer test can demonstrate fast conduit flow with rapid velocities with short residence times to springs, whereas the use of environmental tracers like temperature shows slow diffuse laminar flow and long residence times with intimate matrix contact, with little chemical signature variation. For example, Atkinson (1977) studied Cheddar Springs to determine the proportion of flow attributable to diffuse and conduit flow in the Carboniferous Limestone of the UK. The results showed that the aquifer is a double component system, with the majority of flows occurring in the solutionally enlarged conduits, whilst the majority of the storage is contributed by microfractures. Worthington et al. (2000) introduced a triple porosity permeability model for unconfined carbonate aquifers. They tested the proportion of storage and flow between the matrix, fractures and conduits in four contrasting carbonate aquifers from four countries. They found that carbonate aquifers have contributions from the matrix and conduits as well as

from fractures, but all three components contributing to the bulk aquifer behaviour. Concluding, they said that typically at least 96% of storage was from the matrix, whilst 94% and more of flow was via conduits/fractures. Further explanation of the concept is given in Worthington (2007) and in its current state, the concept of triple porosity permeability model is accepted by hydrogeologists for carbonate aquifer studies (Weight, 2008).

### **5.3 Specific electrical conductivity and its theory**

#### **5.3.1 Importance of SEC and its measurement**

Electrical conductance is a measure of the ability of water or any media to conduct an electrical current, and it depends on the type and quantity of dissolved substances in water. The electrical conductance of a media normalised to unit length and unit cross-section at a specified temperature is called specific electrical conductivity (SEC) (Hem, 1982; Wagner et al., 2006). SEC is normally measured to temperature of either 20 or 25 °C. The SI unit for EC and SEC is mS/cm, but  $\mu\text{S/cm}$  prevails in literature and field measurements because of the appropriateness of the scale (Wagner et al., 2006; Weight, 2008).

SEC is a very important water parameter for rapid assessment of water quality and can be used as a proxy for total dissolved solids, but there is no universal relationship between the two parameters (Hem, 1982; Wagner et al., 2006). SEC is measured with conductivity meters which are small, robust, easy to use and give quick measurements reproducible up to  $\pm 2 \mu\text{S/cm}$  (Krawczyk and Ford, 2006). SEC measured in the field ensures that this parameter is measured before there is aeration and temperature change in the sample (Appello and Postma, 2005; Krawczyk and Ford, 2006; Ford and Williams, 2007; Brassington, 2007; Weight, 2008). In continuous monitoring of water parameters, easy to use and set up automatic SEC loggers are available that also measure at set times for data downloads in the future (Wagner et al., 2006). The automatic loggers are particularly important especially in remote sampling sites as they are able to detect the temporal and memory effects at springs and other waters.

SEC has several uses. It is used for determining the salinity (Lewis, 1980) and major solute concentrations (McNeil and Cox, 2000) of natural waters;

checking the accuracy and error source for water chemical analyses (Laxen, 1977; Miller et al., 1988; American Public Health Association, American Water Works Association, 1999; McCleskey, 2011; McCleskey et al., 2012); determining the chemical composition of water for discriminating different water sources for contamination detection (Krawczyk and Ford, 2006).

In this chapter, SEC will be used in two ways. The first method is by continuous SEC data logging at selected spring sites and a flow depth in a borehole, with the aim of “seeing” the types and timing of water discharging at the springs and the flow depth in the borehole. The second approach is by calculating the contribution of the major ions in spring samples to measured SEC at time of sampling. The aim of the second method is to discriminate the water types in the catchment. A full detail about the theory and theoretical considerations for undertaking the calculations is presented below.

### 5.3.2 SEC theory and transport number

SEC depends on the proportions of the major ionic species in the sample, the total dissolved solids and the temperature of the sample (Hem, 1982; McCleskey et al., 2012). Because EC increases between 1 – 3% per °C rise in temperature depending on the electrolytes present (Wagner et al., 2006; Weight, 2008), for comparison of ECs of solutions at different temperatures, EC is determined at a specified temperature to normally 25 °C, to yield SEC. To convert EC at any temperature to  $EC_{25} = SEC$ , the following expression is used, as:

$$EC_{25} = SEC = \frac{EC}{1 + \alpha_T(t - 25^\circ C)} \quad (5.1)$$

where EC is conductivity at solution temperature, t in °C,  $\alpha_T$  is the temperature compensation factor. Most field conductivity meters are programmed to display EC to 25 °C after using a temperature linear compensation factor,  $\alpha$  that varies between 0.019 - 0.020 °C<sup>-1</sup> based on a KCl standard (McCleskey et al., 2012).

Most of the concepts for interpreting SEC data were developed by Kohlrausch. Kohlrausch law states that the equivalent conductivity of an electrolyte at infinite dilution is equal to the sum of the conductivity of the anions and cations.

This means that the conductivity of the solution is then the sum of the conductivity of the anions and cations. Knowing the chemical composition of an aqueous solution, then its theoretical total SEC can be calculated from Eith et al., (2007) as:

$$SEC = \sum \frac{c_i \gamma_i z_i \Lambda_i}{M_i} \quad (5.2)$$

where  $c_i$ ,  $\gamma_i$ ,  $\Lambda_i$ ,  $z_i$  and  $M_i$  are the concentration ( $\text{mgL}^{-1}$ ), activity coefficient (dimensionless), equivalent electrical conductivity of the  $i_{th}$  ion in solution ( $\mu\text{S/cm per meqL}^{-1}$ ), charge in solution (dimensionless) and molar mass ( $\text{gmol}^{-1}$ ) respectively of the  $i_{th}$  ion in the solution.  $\gamma_i$  is apt in equation (5.2) because conductivity meters measure the activity of the ions rather than their analytical concentrations. Activity is the effective concentration of an ion in solution without the effects of electrical attractions, repulsions and ion pairing (Stumm and Morgan, 1996). Activity,  $a_i$  (dimensionless) is related to molal concentration of the  $m_i$  of the  $i_{th}$  ion ( $\text{mol kg}^{-1}$ ) as:

$$a_i = \gamma_i \cdot m_i / m_i^0 = \gamma_i m_i \quad (5.3)$$

where  $m_i^0$  is the standard state of water,  $1 \text{ mol kg}^{-1} \text{ H}_2\text{O}$  (unit molal concentration) and  $\gamma_i$  is defined in the standardised modified version of the Debye-Hückel relation (Appello and Postma, 2005) as:

$$\log \gamma_i = \frac{-Az_i^2 \sqrt{I}}{1 + Br_i \sqrt{I}} \quad (5.4)$$

where  $A = 0.5085$ ,  $B = 0.3281 \times 10^{10}/m$  are constants for water at  $25^\circ\text{C}$  at 1 bar,  $r_i$  is the hydrated ion size in  $\text{\AA}$ , ( $\text{\AA} = 10^{-10} \text{ m}$ ),  $I$  is the ionic strength of the solution (dimensionless). The smaller  $r_i$  is, the more closely oppositely charged species surround and shield it, thereby reducing ionic activity coefficient (Appello and Postma, 2005).

The ionic strength,  $I$  (dimensionless) is a measure of the total concentration of ions, highlighting the non-ideal behaviour of real solutions with ions.  $I$  is calculated as:

$$I = \frac{1}{2} \sum m_i / m_i^0 \cdot z_i^2 = \frac{1}{2} \sum m_i \cdot z_i^2 \quad (5.5)$$

Equation (5.4) is applicable for ideal solutions of  $I < 0.1$  (Appello and Postma, 2005). Other expressions between  $\gamma_i$  and  $I$  that are applicable as  $I$  increases exist. The relationship between  $\gamma_i$  and  $I$  using equation (5.4) for major ions

in groundwater is shown in Figure 5.2.  $\gamma_i$  approaches 1 in dilute solutions, but decreases with salinity increase. It decreases as  $I$  approaches 0.1, resulting from the potential for ion combination. For  $I = 0.1 - 1.0$ ,  $\gamma_i$  decreases in most cases and  $\gamma_i$  for monovalent ions are typically bigger than divalent ions (Ford and Williams, 2007).

Table 1 presents the parameters and constants in equations (5.2) – (5.5).

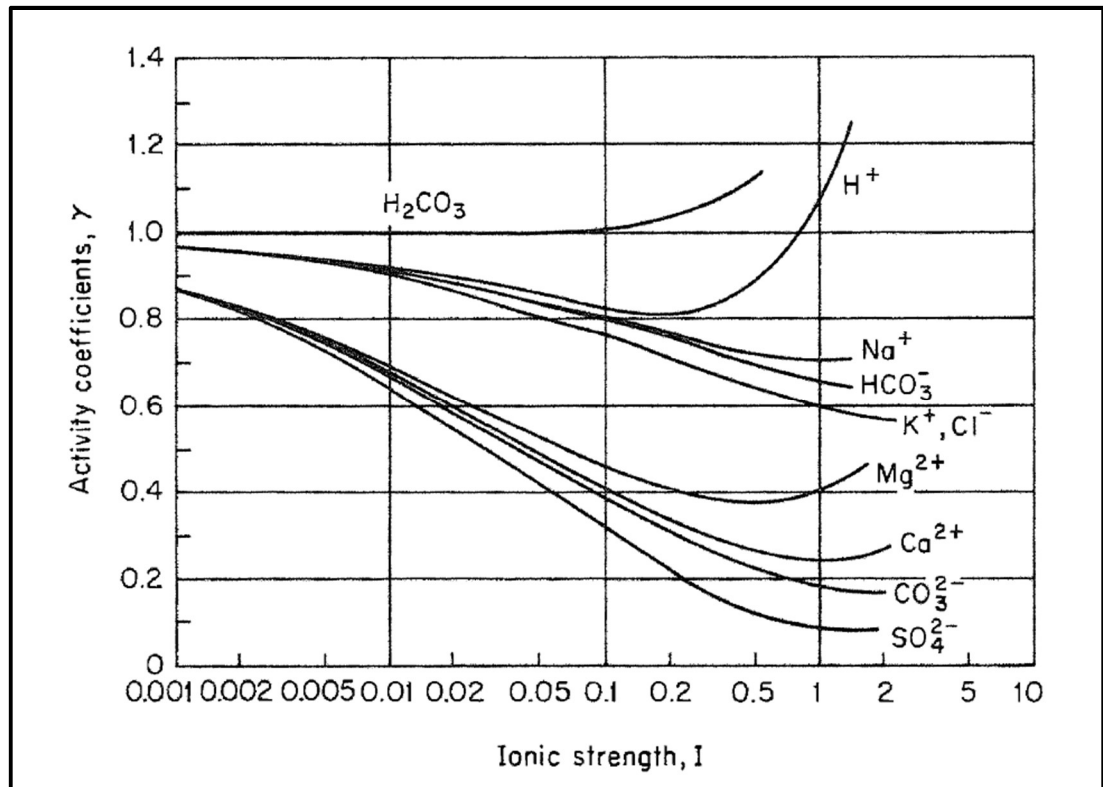


**Figure 5.2:** Relationship between activity coefficient and ionic strength for major ions in groundwater, from Freeze and Cherry (1979).

Another important concept of SEC in the Kohlrausch law is the transport number of an individual ion in solution. The transport number,  $t_n$  is the ratio of the contribution of the  $i_{th}$  ion to the total SEC, ( $SEC_i$ ) to the field measured SEC.  $t_n$  is given as:

$$t_n = \frac{SEC_i}{SEC_{measured}} \quad (5.6)$$

**Table 5.1:** Parameters of major ions used in equations (5.2) to (5.5)

Ion	Specific electrical conductivity (from Appello and Postma 2005; Eith et al 2007) $\Lambda$ ( $\mu\text{S}/\text{cm per meqL}^{-1}$ )	Molar mass ( $\text{g mol}^{-1}$ )	$r$ ( $\text{\AA}$ )
$\text{Ca}^{2+}$	60	40	6.0
$\text{Mg}^{2+}$	53	96	8.0
$\text{Na}^+$	50	23	4.0 - 4.5
$\text{K}^+$	74	39	3.0
$\text{HCO}_3^-$	45	61	4.0 - 4.5
$\text{Cl}^-$	76	35	3.0
$\text{NO}_3^-$	71	62	3.0
$\text{SO}_4^{2-}$	80	96	4.0

The concept of transport numbers is important for knowing which ions contribute substantially to the total electrical conductivity for interpreting SEC data, and also for developing relationships between individual ions for the detection of quality deviation from baseline composition for contamination studies. Krawczyk and Ford (2006) for example used the relationship between calculated SEC taking into account non-ideal solution effects and total hardness to detect contamination in carbonate aquifers. They showed that in uncontaminated waters, the dominant contributors to SEC are  $\text{Ca}^{2+}$ ,  $\text{Mg}^{2+}$  and  $\text{HCO}_3^-$ , which contribute more than 90% to the SEC. However, in waters contaminated by agricultural and industrial inputs,  $\text{NO}_3^-$ ,  $\text{Cl}^-$  and  $\text{SO}_4^{2-}$  contribute between 20 – 40% to the SEC.

### 5.3.3 Carbon dioxide and its effect on SEC in carbonate aquifers

Carbon dioxide gas, ( $\text{CO}_{2(\text{g})}$ ) concentrations and partial pressure,  $P_{\text{CO}_2}$  variation are important for understanding the carbonate process and chemistry (Appello and Postma, 2005; Ford and Williams, 2007).  $\text{CO}_2$  is the most soluble of atmospheric gases, with a solubility that is proportional to its partial pressure and inversely proportional to temperature of the environment (Ford and Williams, 2007).

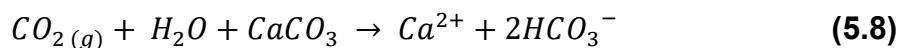
The concentration resulting from its dissolution of CO<sub>2</sub> in water in g/L is given as:

$$CO_2(aq) = 1.963P_{CO_2}C_{ab} \quad (5.7)$$

where  $P_{CO_2}$  is the partial pressure of CO<sub>2(g)</sub>, 1.963 is the weight in grams of 1 L CO<sub>2</sub> at 1 atm and 20 °C, and  $C_{ab}$  is the temperature adsorption coefficient.

Soil CO<sub>2</sub> produced from the respiration of plant roots and soil bacteria is the main agent for enhanced dissolution of carbonate rocks. Groundwater  $P_{CO_2}$  is 2 to 3 times higher than atmospheric CO<sub>2</sub> because of CO<sub>2</sub> uptake in the soil by infiltrating water. CO<sub>2</sub> production in the soil zone varies with temperature, water vapour, land use type, soil structure and texture, bacteria growth and activity and the length of the growing season. Although mean annual temperature has been used to estimate  $P_{CO_2}$ , evapotranspiration has been found to be a better proxy for measuring soil biological activity, and hence a measure of  $P_{CO_2}$  (Brook et al., 1983). In the UK, the soil zone CO<sub>2</sub> concentrations vary with the seasons, with the maximum concentrations occurring in the summer months, when biological activity and evapotranspiration are highest (Pitman, 1978a). Electrical conductivity (EC) for carbonate groundwater is controlled by concentrations of Ca<sup>2+</sup> and HCO<sub>3</sub><sup>-</sup>, which in turn are influenced by calcite saturation which determines calcite dissolution or precipitation (Krawczyk and Ford, 2006). The degree of calcite dissolution is controlled by  $P_{CO_2}$  variation from temperature changes in the environment, CO<sub>2</sub> flux between the soil zone and the saturated zone via the unsaturated zone and the kinetics of calcite dissolution.

The overall reaction of calcite with soil derived CO<sub>2</sub> is given as:



Any factor that increases CO<sub>2</sub> in (5.8) causes dissolution of calcite, resulting in the increase of Ca<sup>2+</sup> and HCO<sub>3</sub><sup>-</sup> concentrations, and consequent EC increase whereas removal of CO<sub>2</sub> causes calcite precipitation, resulting in reduction in EC. Increasing air temperature at the water-air contact surface causes decreasing partial pressure of CO<sub>2</sub>, leading to loss of the CO<sub>2</sub> from solution, whereas temperature decrease has the opposite effect. In unconfined aquifers where the water table is deep and found within the zone of stable temperatures, the temperature effect is often negligible in the aquifer,

but is important at discharge to springs because of surface effects. CO<sub>2</sub> flux from the soil zone to the saturated zone depends on the thickness of the unsaturated zone and its permeability, i.e. the degree of confinement. When calcite dissolution occurs in the presence of constant flux of CO<sub>2</sub> to the saturated zone from soil zone, the groundwater evolves under an open system, resulting in an increase in EC. On the other hand, a disconnect between soil CO<sub>2</sub> and saturated zone results in closed system with respect to CO<sub>2</sub>, where consumed CO<sub>2</sub> is not replaced, so EC does not increase. The open system is often found for shallow groundwater levels or in aquifers with rapid mass transfer between the soil and water table, whereas the closed system is normally found for deeper water table aquifers (Pitman, 1978b). Pitman (1978a) found an open and closed system side by side at Givendale, on the western edge of the Yorkshire Wolds. For aquifers that lie in between shallow and deeper groundwater levels however, the modes may switch in response to the seasonal variation of groundwater levels and recharge fluxes. Aside the above factors, the EC and geochemical evolution in carbonate aquifers can be complex due to calcite dissolution kinetics, pairing and complexation, corrosive mixing and different flow modes (Pitman, 1978a; Ford and Williams, 2007).

#### **5.4 Water temperature as a groundwater tracer**

Temperature is a very important parameter in hydrological studies because it affects the density, SEC, pH of water, chemical reaction rates and biological activity in water (Radtke et al., 2005; Wagner et al., 2006). Temperature can be easily measured using thermometers or by monitoring sensors at programmed intervals. Modern thermometers and thermistors can measure temperature to  $\pm 0.1$  °C (Anderson, 2005; Wagner et al., 2006; Weight, 2008).

Rocks and soils have very low thermal diffusivity because they have a relatively large specific heat capacity and modest thermal conductivity. Because of the low thermal diffusivity, without advecting groundwater, heat pulses from the surface cannot be transmitted very fast to the subsurface. In the UK, solar radiation that heats the earth surface in the summer from elevated air temperatures, propagates to a few meters below the ground

surface, usually marked by a zone of seasonal temperature variation that reduces in amplitude, but with an increase temperature minima and maxima lag time with depth, till ground temperatures become stable (Banks, 2008; Busby et al., 2009). The above described depth is termed the surficial zone. The stable ground temperature reflects the long term annual average air temperature, varying between  $\pm 1 - 2$  °C of the annual average ambient temperature. In mainland UK, the mean annual temperature ranges between 8 – 12 °C from north to south, with a decrease eastwards and northwards from highs in the south-west of England (Busby et al., 2009). Below the surficial zone is the geothermal zone, where without groundwater advection, temperature increases linearly at the rate of 2.6 °C per 100m from heat from the earth's interior (Busby et al., 2009).

Hydrogeologists use groundwater temperature as a tracer in shallow groundwater environments where flows are driven by forced convection by taking advantage of the temperature contrasts between the surface, surficial and geothermal zones to characterise aquifers. Shallow and local waters sourced from the surficial zone show the effect of the seasonal variation with ambient temperatures reflecting the annual average temperatures, whereas regional flows that drain the deep geothermal zone will show slightly higher temperatures (Cartwright, 1968; Parsons, 1970). Anderson (2005) provides a review of the theory of heat transport in groundwater and the use of heat as a groundwater tracer to: characterise aquifers on the basin scale for determining recharge and discharge rates (Cartwright, 1970); determine surface warming and thermal pollution of aquifers by urban heat islands (Taniguchi et al., 1999; Banks et al., 2009; Farr et al., 2017); characterise groundwater-surface water interaction (Silliman et al., 1995; Stonestrom and Constantz, 2003); determine hydraulic conductivity and groundwater flow rate (Bravo et al., 2002; Stonestrom and Constantz, 2003). Groundwater temperature has also been used to trace depth and location of fractures (Kappelmeyer, 1957; Silliman and Robinson, 1989).

Carbonate spring thermal response provides important information about the geometry, conduit structure, recharge source and type, and an indication of the residence times of water in the aquifer that the spring drains. Thermal response of carbonate springs is dependent on the effectiveness of heat

exchange between the advecting groundwater and the conduit or fracture walls. Heat exchange effectiveness along the groundwater flowpath is measured by the Stanton Number ( $S_t$ ), a dimensionless parameter defined as:

$$S_t = \frac{\text{conductive heat flux into the rock matrix}}{\text{convective heat flux along the flow path}} \quad (5.9)$$

$S_t$  relates the heat transfer coefficient to the heat carrying capacity of the flowing groundwater in a conduit or fracture.

Luhmann et al. (2011) used the thermal response of karst springs in Southern Minnesota to classify springs into two end members as discharging from:

i. thermally ineffective pathways and ii. thermally effective pathways.

Thermally ineffective pathways are characterised by small  $S_t$ ,  $\ll 1$ , produced by short flow paths and fast flow through times or large diameter fractures and conduits. Small  $S_t$  spring thermal signals mimics recharge and ambient air temperatures and are in phase with seasonal air temperature variations. On the other hand, thermally effective pathways enable the recharge water to have enough time for thermal equilibration with the rock temperature, and are characterised by large  $S_t$ ,  $\gg 1$  produced from relatively distributed flow paths like flow in small or narrow aperture fractures and intergranular pores, long flow paths or low velocities or diffuse recharge. Thermal response of springs fed by thermally effective pathways do not show input events or recharge water temperatures, and may show either stable or damped signals with minima and maxima that are out of phase with surface seasonal temperature variations. Time lag between surface and signals in thermally ineffective flowpaths is directly related to the residence time of the water in the aquifer, whereas the time lag in thermally effective systems is not related to the residence time, but is a function of the time surface temperature signals propagate to the aquifer depth.

Several works like Crowther and Pitty (1982), Bundschuh (1993), Birk et al. (2004), Martin and Dean (1999), Liñán Baena et al. (2009) used the thermal response of carbonate springs and their similarity or contrasts to the air temperature signals to infer recharge source and type and residence time of water discharging at springs. In addition to the above characteristics Birk et al. (2004) was also able to use the thermal and chemical lags to give an

approximate first-order conduit volume estimate for the karst of southwest Germany.

The aim of reviewing the above groundwater temperature works is to later use the concepts to interpret temperature time series data from chalk springs and wells in this chapter.

## 5.5 Groundwater level measurement

### 5.5.1 Groundwater level measurements and importance

Groundwater level measurements are a very important parameter in all hydrogeological investigations. They are used to determine groundwater flow direction and catchment flow patterns, to assess the impact of stresses on the aquifer and to characterise groundwater-surface water interaction. Groundwater level data is also very important for the differentiation of hydrogeologic units, determination of aquifer properties like transmissivity and the calibration of groundwater flow models (Dalton et al., 2006; Brassington, 2007).

Measurement of groundwater level is used to determine hydraulic head. Hydraulic head is driving force that causes water to move from places of high potential to areas of low potential. Hydraulic head,  $h_i$  is the mechanical energy per unit weight of water at a point in an aquifer (Figure 5.3). It is expressed mathematically as:

$$h_i = Z_i + \frac{P_i}{\rho_i g} = Z_i + h_{pi} \quad (5.10)$$

where  $Z_i$  is the elevation head (m),  $P_i$  is the groundwater gauge pressure at the measurement point ( $\text{Nm}^{-2}$ ),  $\rho_i$  is the density of groundwater ( $\text{kgm}^{-3}$ ),  $h_{pi}$  is the pressure head (m). Equation (5.10) is valid for groundwater flow and direction in constant density water only, but in waters where flow is driven by density differences requires correction of the terms in the equation (Post et al., 2007). The gauge pressure is defined as part of the absolute pressure,  $P_{abs}$  as:

$$P_{abs} = P_{atm} + P_i \quad (5.11)$$

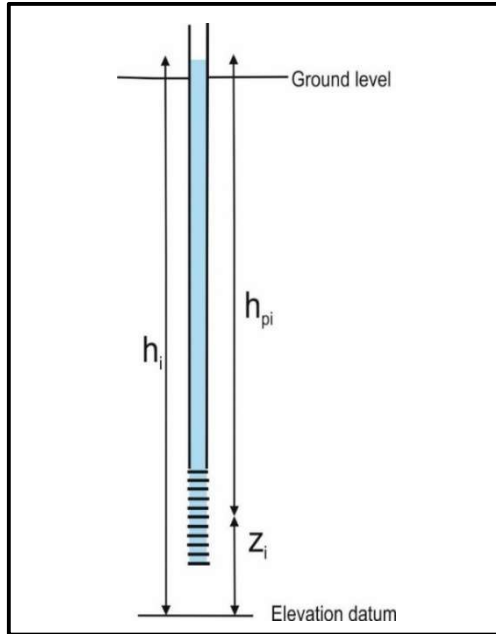


**Figure 5.3:** Schematic for the hydraulic head equation

where  $P_{atm}$  is atmospheric pressure.

At the water table, gauge pressure is zero, and then equation (5.11) becomes:

$$P_{abs} = P_{atm} \quad (5.12), \quad \text{and also from (5.10)}$$

$$h_i = z_i \quad (5.13).$$

From equation (5.10), water table elevation at a particular location equals the hydraulic head at the water table in unconfined aquifers under hydrostatic conditions.

In interpreting and using groundwater levels, aquifer knowledge based on sound hydrogeological framework of the catchment, monitoring well completion and condition, natural and manmade stressors on the aquifer and the method for collecting the groundwater level data are important. The hydrogeology includes the geology and the structural complexity, aquifer types and their heterogeneity and anisotropy, their boundary conditions, lateral and vertical extent, flow and storage characteristics. The monitoring details include well type, construction detail, depth, cased and screened or open depth length, location in relation to recharge and discharge zones. The stressors like storage changes, atmospheric pressure, earth tides,

abstractions, man-made dynamic movements and pipe leaks influence the cycles, amplitudes and patterns of the groundwater level fluctuation.

### **5.5.2 Groundwater level monitoring and measurement equipment**

The measurement of groundwater level requires a monitoring well and a measurement device. A monitoring well could be either a piezometer or an observation borehole. A piezometer is a specially designed monitoring well with relatively smaller diameter casing but with short open slotted section to measure the pressure of water at a particular point in the aquifer. On the other hand, an observation borehole has a relatively bigger diameter with screened, slotted or open borehole, typically over a longer length than a piezometer. In aquifers with varying hydraulic conductivity variation with depth with different hydraulic heads characterised by vertical flows, the head measured in observation boreholes are composite heads of the screened or open depth (Saines, 1981; Brassington, 1992). In stratified aquifers several piezometers can be installed in a single observation borehole to provide a relatively economic and practical way of determining groundwater heads.

Groundwater level is measured with either a dipper / electric tape (E-tape) or by pressure transducers (Figure 5.4). The E-tape is an easy to use device that gives quick groundwater level readings to the nearest cm for periodic measurements, and has been in use since the early 1980s (Brassington, 2007; Weight, 2008). The E-tape has graduated cable, with a probe at its head. Once the probe goes into the well and touches water, an electric circuit is completed between the electrode pins, which is indicated on the surface by a buzzer sound, with or without a light on spool. In using the tape, it is important to take measurements from the same measurement point to have consistent results. Knowing the elevation of an accurately surveyed in measurement point in relation to the datum in the area, the water level determined with the dipper is used to determine the hydraulic head of the wells in the catchment, flow direction and hydraulic gradient. False readings can occur from condensation within the casing with a badly tuned sensitivity knob setting. Substantial errors of the E-tape use results from kinked, wear and non-vertical suspension of the tape. Aside from the E-tape or dipper, other methods for taking periodic water level measurements include the use of

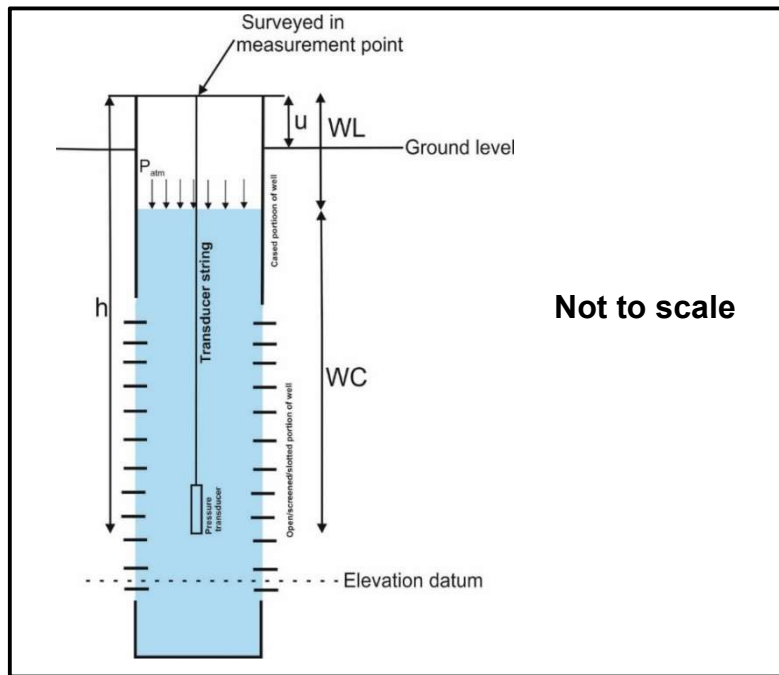


**Figure 5.4:** Pressure transducer in a monitoring well.  $u$  is the upstand above ground level,  $WL$  is depth to water level from measurement point,  $WC$  is the water column depth above the transducer,  $h$  is the depth of sensor below the measurement point

home made / improvised dipper, chalked tape, weighted bowl or bottle, airline submergence, ultrasound method amongst other methods are documented in the hydrogeological literature (eg. Dalton et al., 2006; Brassington, 2007; Weight, 2008).

Since the 1990s, electronic pressure transducers have become the instrument of choice for automatic and continuous groundwater level measurement for hydrogeologists. Pressure transducers measure water level column (from water column pressure) from water level fluctuation from the deflection of a diaphragm resulting from the measurement of electrical resistance generated by strain gauge resulting from water column weight on the diaphragm surface. Pressure transducers are hung below the water surface from a measurement point above the well top by a string or transducer cable. With the column of water above the transducer and the elevation of the measurement point, the water level and hydraulic head is determined.

There are two kinds of pressure transducers (Figure 5.5): the non-vented and vented pressure transducers (Brassington, 2007; Weight, 2008; Price, 2009; Sorensen and Butcher, 2011). The non-vented transducer (Figure 5.5a)

measures the applied absolute applied pressure ( $P_{abs}$ ) on the diaphragm surface because the back of the diaphragm is sealed off from the atmosphere. The water column pressure then is equal to the absolute pressure less atmospheric pressure. Non-vented transducer use therefore requires that atmospheric pressure data either measured directly in the well or from a weather station in the locality with similar topographical and air movement characteristics could be used, although Post and von Asmuth (2013) report the use of weather station data could be a source of error in water column heights. A vented transducer (Figure 5.5b) on the other hand only measures the water pressure head above the sensor, because the sensor's vent allows the application of atmospheric pressure at the back of the diaphragm.

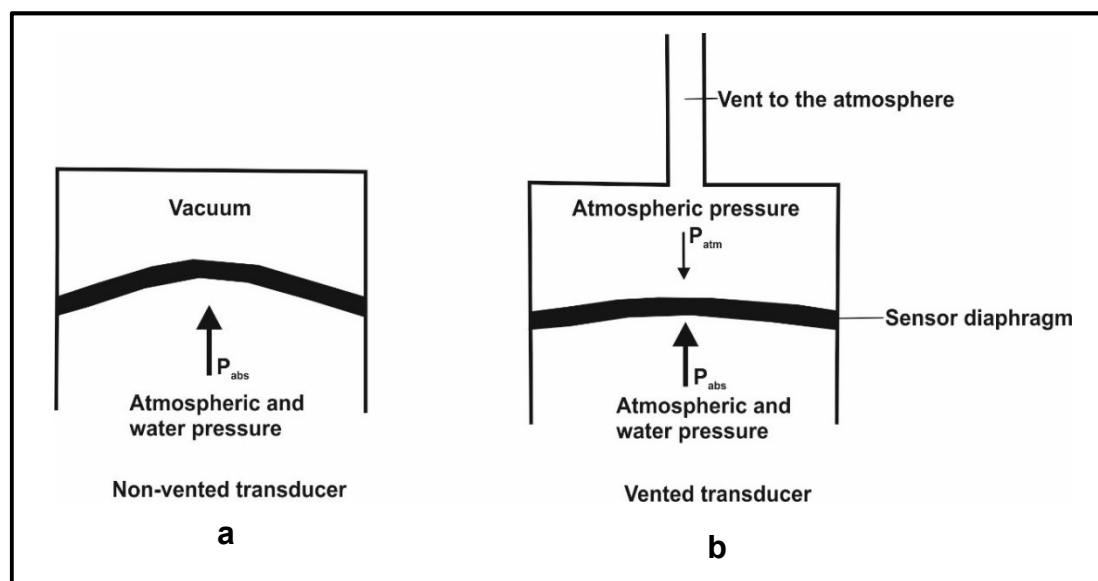


**Figure 5.5:** Difference in working principle of the (a) non-vented and (b) vented pressure transducer. Modified from Sorensen and Butcher (2011).

The choice of a transducer for a particular application depends on the accuracy, resolution or sensitivity and the operating pressure depth range. The accuracy is normally expressed as a percentage (usually 0.1%) of the operating depth range, with the greatest accuracy for the smallest operating depth, reducing with increasing depth range (Brassington, 2007). For a example, a 1 bar (100 kPa, ~10 m of head) transducer has an accuracy of  $\pm 1$

cm, whereas that for 10 bar transducer is  $\pm 10$  cm. The sensitivity is how much groundwater level will fluctuate before it can be detected by the transducer. Sensitivity is also expressed as a percentage of the depth range. A transducer of depth range 0 – 60 m with accuracy 0.1% and sensitivity of 0.01% means that the pressure transducer will measure readings to  $\pm 6$  cm, and will detect water level fluctuations in excess of 6 mm. The operating depth limits the variation of water column depth that the transducer can measure or withstand. For example, if a 12 m water level fluctuation is expected, then a transducer of 1.5 bar can be used to measure the fluctuation if correctly placed within 3 m or so of the lowest water level.

In spite of the usefulness of the pressure transducer, they are liable to sensor drifts which can be corrected with periodic manual measurements (Sorensen and Butcher, 2011). Pressure transducer readings are also prone to errors from time lag and equilibration effects and non-verticality of the transducer (Post and von Asmuth, 2013).

### **5.5.3 Relationship between transducer water column and depth to water level in monitoring wells**

The relationship between water level depth below the measurement point and water column above the transducer (Figure 5.4) will now be developed. This is important in verifying transducer pressure readings and also for determining hydraulic gradients and direction of groundwater flow on the catchment scale.

Figure 5.4 shows an observation well/piezometer with an installed pressure transducer attached from a measurement point above the well top. The depth to water from the measurement point, that can be measured by a dipper is  $WL$  m, and the depth of the column of water above the transducer is  $WC$  m with pressure  $P_{WC}$   $\text{kNm}^{-2}$ . The water surface is open to the atmosphere and under atmospheric pressure  $P_{atm}$   $\text{kNm}^{-2}$  measured with a barometric pressure transducer in the air.  $h$  m is the depth of the transducer sensor below the measurement point and the well water has a unit weight of  $\gamma_w$   $\text{kNm}^{-3}$ .

For the unvented case, the pressure transducer measures  $P_{abs}$  given by:

$$P_{abs} = P_{atm} + P_{WC} \quad (5.14)$$

and  $WC$  is given as:

$$WC = \frac{P_{abs} - P_{atm}}{\gamma_w} \quad (5.15)$$

and as  $WL = h - WC$  (5.16)

$$WL = h - \frac{P_{abs} - P_{atm}}{\gamma_w} \quad (5.17)$$

For the vented scenario, as  $P_{atm}$  is compensated for,

$$WL = h - \frac{P_{wc}}{\gamma_w} \quad (5.18)$$

## 5.6 Spring sampling and well monitoring

### 5.6.1 Spring SEC and temperature monitoring: site and equipment considerations, installation and data retrieval

Onset HOBO conductivity logger model U24-001 was the logger of choice for the SEC and temperature logging. This was based on cost, versatility and applicability, sensitivity, excellent before and after sales customer service and equipment ruggedness. A market survey of applicable industry loggers showed that the HOBO was the most inexpensive for this study. Figure 5.6 shows an image of the HOBO loggers used for SEC and temperature logging.



**Figure 5.6.** Onset HOBO Conductivity Logger Model U24-001 used for logging SEC at the Springs and Tancred Pit borehole.

The HOBO is 16.5 cm long x 3.18 cm diameter, and has EC operating range of 0 – 10,000  $\mu\text{S}/\text{cm}$ , resolution of 1  $\mu\text{S}/\text{cm}$  and an accuracy of 3% of reading or 20  $\mu\text{S}/\text{cm}$ , whichever is greater. Its temperature operating range is -2 to 36  $^{\circ}\text{C}$ , at a resolution of 0.01  $^{\circ}\text{C}$  and an accuracy of  $\pm 0.1$   $^{\circ}\text{C}$ . It also has a response time of 1 s to 90% of change and a clock accuracy of  $\pm 1$  min per month.

After a deskstudy from maps and literature on springs draining the aquifer, three springs: Bracey Bridge, Bellguy and Place Newton were decided on for sampling. See the location map and details of monitored springs and boreholes for this chapter in Figure 5.7 and Table 5.2 respectively. The first two springs drain the dip slope, whereas the third drains the scarp slope. Initial reconnaissance to the springs showed that these three were the most accessible and loggers would be less prone to vandalism and theft. Also,

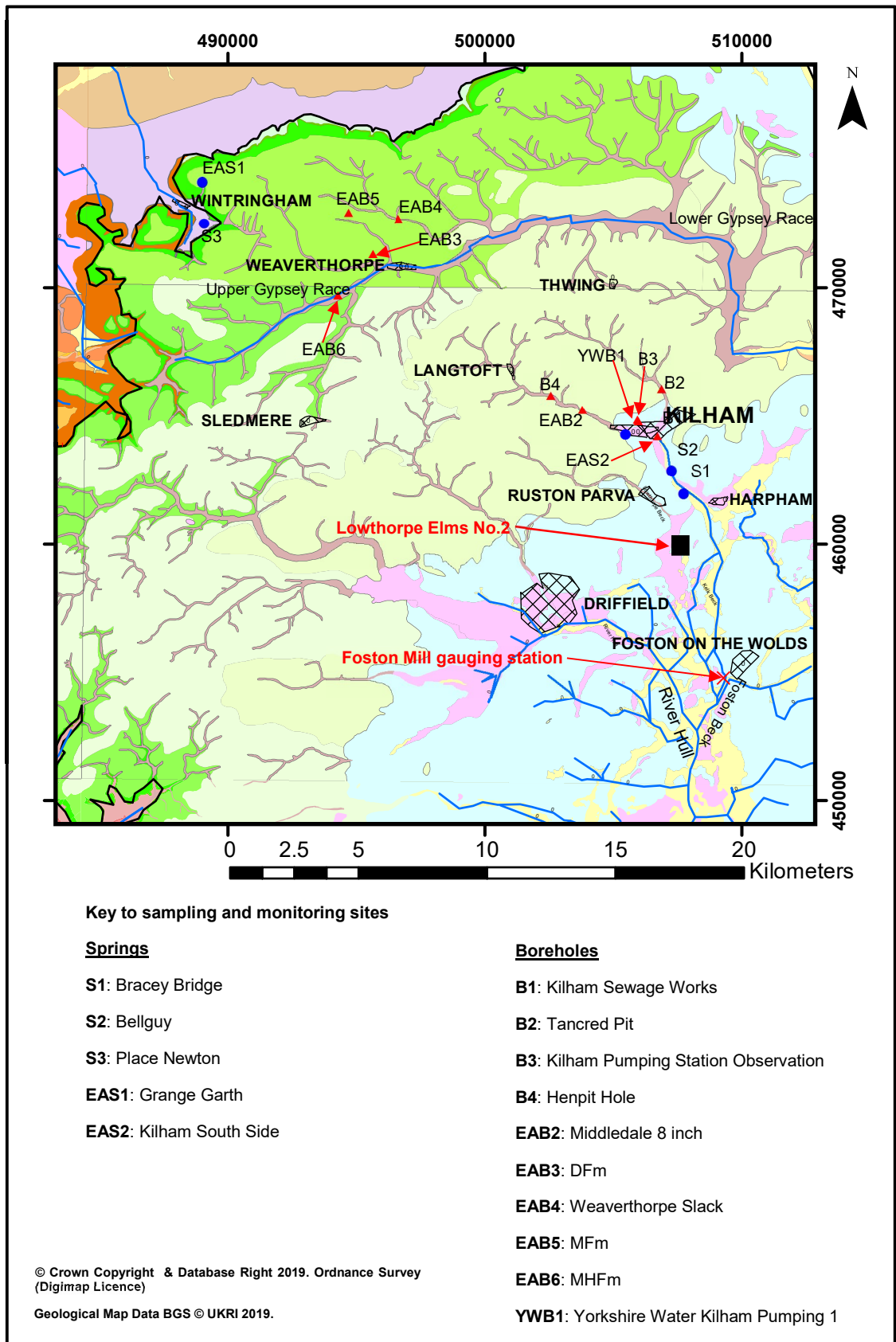


**Figure 5.7.** Location map for monitored sites. S and B coding are for monitored data for current work, EA coding for Environment Agency data, YW coding for Yorkshire Water data.

**Table 5.2** Location data and details for spring and borehole monitoring sites.

<b>Site</b>	<b>NGR</b>	<b>Site details</b>
<b><i>Springs</i></b>		
Bracey Bridge (S1)	TA 077 619	Emergence point is from a metal pipe. Flows and discharges into a pool during the recharge season but becomes static during the dry period, with pool area been only moist without flow. Was only sampled.
Bellguy (S2)	TA 072 628	A perennial spring with a flowing and bubbling emergence point into which logger was placed. Logger placed below column of water.
Place Newton (S3)	SE 886 728	A perennial spring, but flows from slope steep slope face so monitoring at the about foot of the slope, which is about 3 meters from emergence point.
Grange Garth (EAS1)	SE 886 731	Seasonal spring. Chemistry data from the EA archive.
Kilham South Side (EAS2)	TA 054 642	Seasonal spring that only flows when groundwater levels are high. Chemistry data from the EA archive.

Table 5.2 continued

<b>Site</b>	<b>NGR</b>	<b>Site details</b>
<b><i>Boreholes</i></b>		
Kilham Sewage Works (B1)	TA 067 642	Borehole is about 5 m from the Lowthorpe Beck. Monitored for absolute and atmospheric pressure.
Tancred Pit (B2)	TA 069 660	In a field on the Rudston road. It is artesian at times and has spring nearby that flows when groundwater levels are high. SEC and absolute pressure monitored.
Kilham Pumping Station Observation ( B3)	TA 059 648	A borehole near the Yorkshire Water Kilham Station entrance. Borehole used as a monitoring borehole by the EA.
Henpit Hole (B4)	TA 025 658	Located near a farm in the Langtoft valley. Absolute pressure monitored.
Middledale 8 inch (EAB2)	TA 038 652	Near the Middledale Farm at the Raven farm junction fork. Data from EA groundwater monitoring.
Yorkshire Water Kilham Abstraction 1(YWB1)	TA 059 648	Yorkshire Water (YW) abstraction well. Obtained head and chemical quality dataset from the YW.

Table 5.2 continued

<b>Site</b>	<b>NGR</b>	<b>Site details</b>
<b><i>Boreholes</i></b>		
DFm (EAB3)	Confidential site	A farm which is part of the EA monitoring programme.
Weaverthorpe Slack (EAB4)	SE 966 727	Borehole in field located in a valley between Weaverthorpe and Sherburn wolds. Data from monitoring archived monitored data from the EA.
MFm (EAB5)	Confidential site	A private farm in the Wolds with sampling from a tap. Part of EA monitored data.
MHFm (EAB6)	Confidential site	A private farm that is part of the EA monitoring programme.

Bellguy and Place Newton flow all year round. For the scarp site, ESI (2010) water balance and discharge analyses showed that the Place Newton springs is a major discharge for the scarp slope. Bellguy and Bracey Bridge drain to Foston Beck, one of the major tributaries of the River Hull. In addition, these springs had low potential for sensor fouling and loggers running dry during the summer months (Wagner et al., 2006). After these considerations, permission was then sought from landowners on which the springs were located for the assurance of continuous sampling and the security of the loggers. In spite of the attempt to secure the loggers, Bracey Bridge logging was discontinued after 3 months because the logger could not be found in the spring.

The loggers after initial calibration checks in Leeds University were installed at the springs, and secured to trees via strings. At Bellguy and Bracey Bridge, they were installed at the bubbling points to minimise atmospheric effects on the sensor. At Place Newton, because the spring emergence point was on a slope face, the logger was installed in a pool beneath the emergence, the loggers were programmed to log electrical conductance and temperature every hour. Before logger installation and data readout, conductivity and temperature of the springs were measured with a HANNA HI 9033 multirange handheld conductivity meter and thermometer respectively for verification and drift correction in the loggers. Using the spring temperature, electrical conductance was then converted to SEC at 25 °C after correction for drift and then plotted with time.

### **5.6.2 Spring sampling and laboratory analyses**

Springs were sampled on 8/9 occasions between February 2017 to January 2018. Temperature, pH, SEC and alkalinity were measured at the springs. Before taking pH readings, 4.01 and 6.86 capped buffers held in the springs for temperature equilibration were used to calibrate a HANNA HI 9025 pH meter. After this the meter was used to measure pH after it had equilibrated with the sample temperature and readings were stable. SEC was measured with a HANNA 70031 handheld conductivity meter after calibration with a 1,400  $\mu\text{S}/\text{cm}$  standard solution. Temperature was also measured using handheld probes, after the probe had equilibrated with spring temperature.  $\text{CaCO}_3$  alkalinity was measured using a HACH digital titrator by titrating 100 mL filtered spring sample with 1.6 M  $\text{H}_2\text{SO}_4$  titrant, using bromocresol green

methyl red as indicators. The indicator changed from green to purple at the endpoint. Samples for chemical analyses were filtered through 0.45 µm filter and stored as acidified and unacidified splits in high-density polyethylene (HDPE) bottles for cations and anions respectively. The samples were then stored on ice and transported to the University of Leeds Cohen laboratories for storage and refrigeration until analyses. The major cations were analysed with Inductively Coupled Plasma Atomic Emission Spectroscopy (ICP-AES) at Cohen laboratory whilst major anions ( $\text{Cl}^-$ ,  $\text{SO}_4^{2-}$  and  $\text{NO}_3^-$ ) were analysed by Ion Chromatography (IC) at the School of Geography laboratory, University of Leeds.

### 5.6.3 Water level, SEC and temperature monitoring

The choice of SEC loggers has already been dealt with in sub-section 5.6.1. Amongst the wells, only Tancred Pit was logged for SEC and temperature at depth 45 m bgl. This depth was chosen for monitoring so the logger could detect the type of water that enters at that depth since that depth has been identified as a major inflow zone for the well (refer to sub-section 4.5.1 and Parker, 2009), that connects with recharge areas (Ward and Williams, 1995).

In-situ non-vented pressure transducers (Rugged TROLL 100) of different operating head ranges and barometric pressure transducer (BaroTROLL 100) were used to monitor absolute pressures and atmospheric pressure respectively in the wells. A typical logger is shown in Figure 5.8. The logger is 14.4 cm long x 2.62 cm diameter with accuracy and resolution of  $\pm 0.1\%$  and



**Figure 5.8.** In-Situ non-vented pressure transducer (Rugged TROLL 100) for monitoring groundwater level in wells.

$\pm 0.01$  % of full scale reading. Details of wells that were instrumented have already been presented in Figure 5.7 and Table 5.2. No market survey was undertaken for the In-situ loggers as they were already available from previous investigations. Also, the loggers were appropriate for the current studies and easy to set up and use. The completion details of the wells are detailed in Table 4.1. The choice of which transducer to install in each well was based on deskstudy of the 10 years groundwater level fluctuations of the wells from the Environment Agency. The deskstudy was later followed up by a site reconnaissance to assess the accessibility and feasibility of the well sites for monitoring. After this assessment, the transducers were stringed and attached at the well top, and then the transducers were placed below the historic minimum water level to monitor absolute pressure above the transducers in all the monitoring wells. Manual water levels were measured after the initial installation and before subsequent data downloads. The transducers were programmed to monitor absolute pressure every hour. For Kilham Sewage Works borehole, a barometric transducer was also installed for measuring atmospheric pressure for the determination of water column above the transducer. Using equation (5.17), the water columns were verified and corrected for drift if any, then the lowest level for each well was used as reference to calculate a relative column of water above the transducer. These data were then plotted with time.

## **5.7 Spring and well monitoring results and discussions**

### **5.7.1 Results and discussions of well monitoring**

In this subsection, the results from well hydrographs will be presented to characterise well behaviour during recharge and recession times and also their response to local stresses like pumping. Also, the well hydrographs are compared to Foston Mill gauging station (Figure 5.7) daily discharges and daily rainfall amounts for the area with the aim of detecting similarities and differences in well and stream discharge hydrographs.

The well hydrograph, discharge from Foston Mill gauging station and daily rainfall data from Lowthorpe Elms No. 2 (TA 074 611) are presented in Figure 5.9. All the wells apart from Yorkshire Water Abstraction borehole 1 (YWB1),

Weatherthorpe Slack (EAB4) and Middledale (EAB2) boreholes were instrumented as part of this studies. Yorkshire Water supplied data for Yorkshire Water Abstraction borehole 1 (a supply well), whereas data for Weaverthorpe Slack and Middledale were from the Environment Agency.

In Figure 5.9a, the well hydrograph maximum peaks for Kilham Sewage and Weaverthorpe Slack are 2.5 m and 14 m respectively for the 2017/18 year. The well hydrograph rising limb for the 2016/17 year was between December 2016 to end of March 2017 (R16/17), with the recession limb starting from then on but ending earlier than the previous year at early September, 2017. The rising limb for 2017/18 then starts from then on to end in April 2018 (R17/18) but with some dips and peaks through the period. The well hydrographs show similar rising and falling limb patterns with different amplitudes. The hydrographs show two distinct amplitudes for the 2016/17 and 2017/18 hydrologic years, with the latter having a larger peak amplitude. The hydrograph amplitudes increase with increasing distance from the discharge area around Kilham Village. Kilham Sewage works, which is about 5 m away from the Lowthorpe Beck Stream has an amplitude of 1.8 m for the 2016/17 hydrological year, whereas Weaverthorpe Slack, located about 14 km from Kilham, at the recharge area in the Wolds has the highest amplitude of 5.8 m for the 2016/17 year. For the 2017/18 year, the well hydrographs of Tancred Pit, Henpit Hole and Middledale boreholes show pronounced amplitudes, mimicking the peaks in Weaverthorpe Slack. On the other hand, the well hydrographs for the boreholes in Kilham Village show broader and subdued peaks, which is characteristic of the discharge area.

In Figure 5.9b, the Foston Mill daily discharge pattern for the monitoring period mimics the well hydrographs, but with some flashes and spikes corresponding to rainfall events. The peak average daily discharge for 2016/17 is about  $0.85 \text{ m}^3\text{s}^{-1}$ , lower than  $1.8 \text{ m}^3\text{s}^{-1}$ , for the 2017/18 year. The major peaks observed in the well hydrographs also coincide with major peaks in the discharges at Foston Mill gauging station. The rainfall total for the rising limb of the hydrograph for 2016/17 is 171.6 mm, whereas that for 2017/18 is 336.4 mm, which is twice

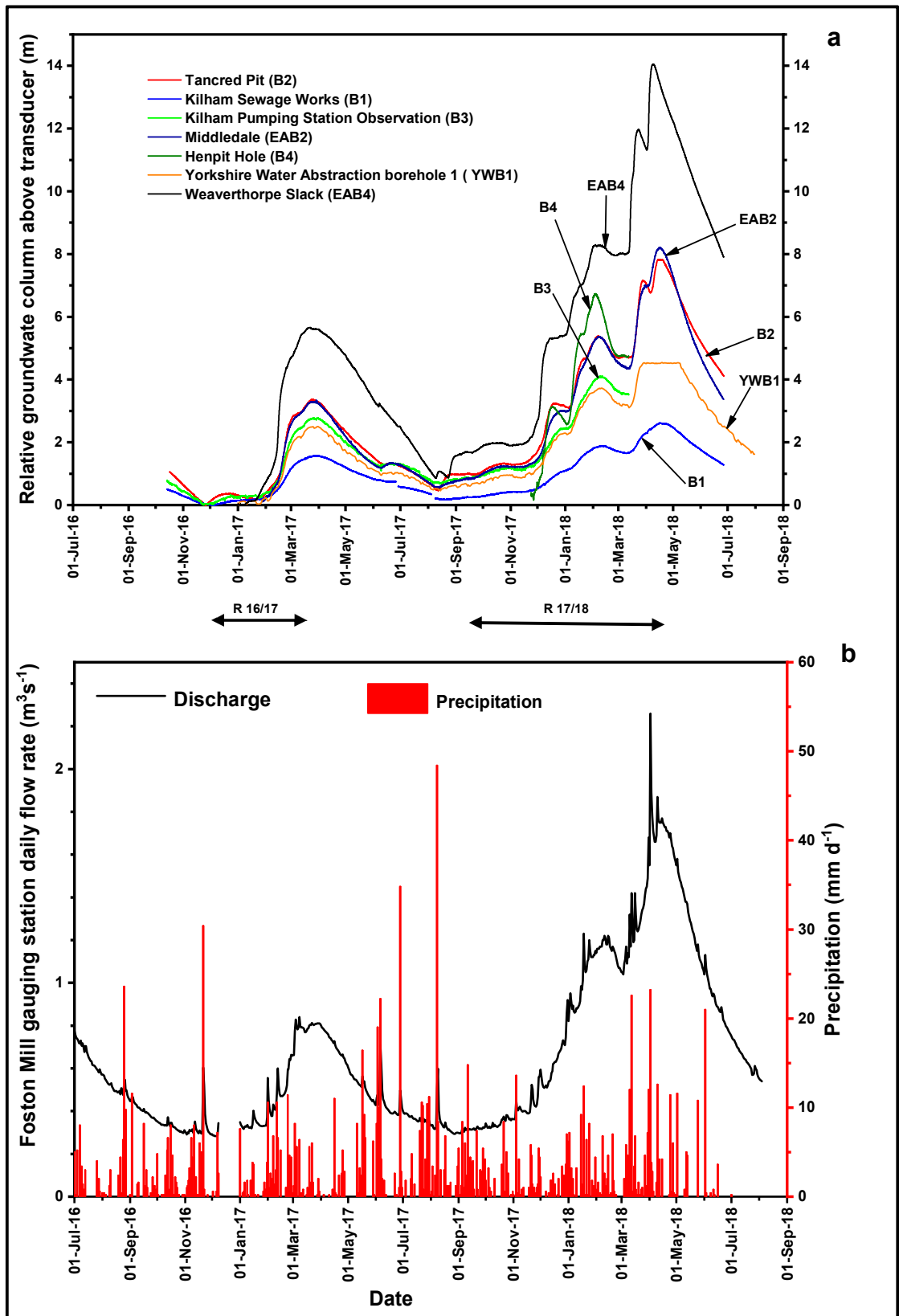


**Figure 5.9.** Comparison of well hydrographs and Foston Mill discharge hydrograph. (a) Well hydrographs with high amplitude for Weaverthorpe Slack (EAB4) located in a recharge zone in comparison to lower amplitudes in the Kilham area (discharge zone). (b) Foston Mill daily discharge hydrograph and daily precipitation data.

the amount for the previous year. The rain days for the 2017/18 recharge period are also more than that for the previous year.

Figure 5.10 shows the well hydrographs only for the Kilham discharge area without that for Weaverthorpe Slack borehole (EAB4). The well hydrographs follow a similar pattern and are generally smooth but for Yorkshire Water Abstraction 1 (YWB1) and Kilham Pumping Station Observation (B3) that show the response of the wells to local abstraction. Kilham Pumping Station Observation borehole (B3) is about 40 m from the Yorkshire Water Abstraction borehole 1 (YWB1), and so the two wells show a similar response to the abstraction cycles by reducing during pumping and recovering after pump shut-down or abstraction rate reduction (example shown in green ellipse), although the response is stronger in YWB1 since it is the pumped well. The steady state hydrograph in the pumping well (YWB1) between late March and mid-May 2018 (ellipsed in orange on YWB1 hydrograph in Figure 5.10) was as a result of the abstraction borehole pressure transducer going out of range because of high groundwater levels during the period (pers com. YW).

From the hydrographs, the other monitored wells are apparently not in the radius of influence of the abstraction at Kilham, since they do not display the dips and recoveries observed in Kilham Pumping Station observation borehole (B3). Comparing the daily rainfall events with well hydrographs, there are no spikes or flashes on the well hydrographs as was seen for the Foston Mill gauging station discharge hydrograph.

The monitored well hydrographs show a similar seasonal pattern for the 2016/17 and 2017/18 hydrological years. The well hydrographs for the 2017/18 increase with the increased rainfall in the area. The increasing amplitude of the groundwater hydrographs with distance away from the discharge areas is consistent with the position of the wells, as wells close to discharge areas experience small groundwater fluctuations, whereas recharge areas show very wide groundwater fluctuation. The smooth nature of the ground water hydrographs without spikes that correlate with rainfall events shows the physical buffering capacity of the aquifer and its ability to mask input signals. Apart from the Kilham Pumping Station borehole, the inability of the other monitored wells to respond to the abstraction regime at

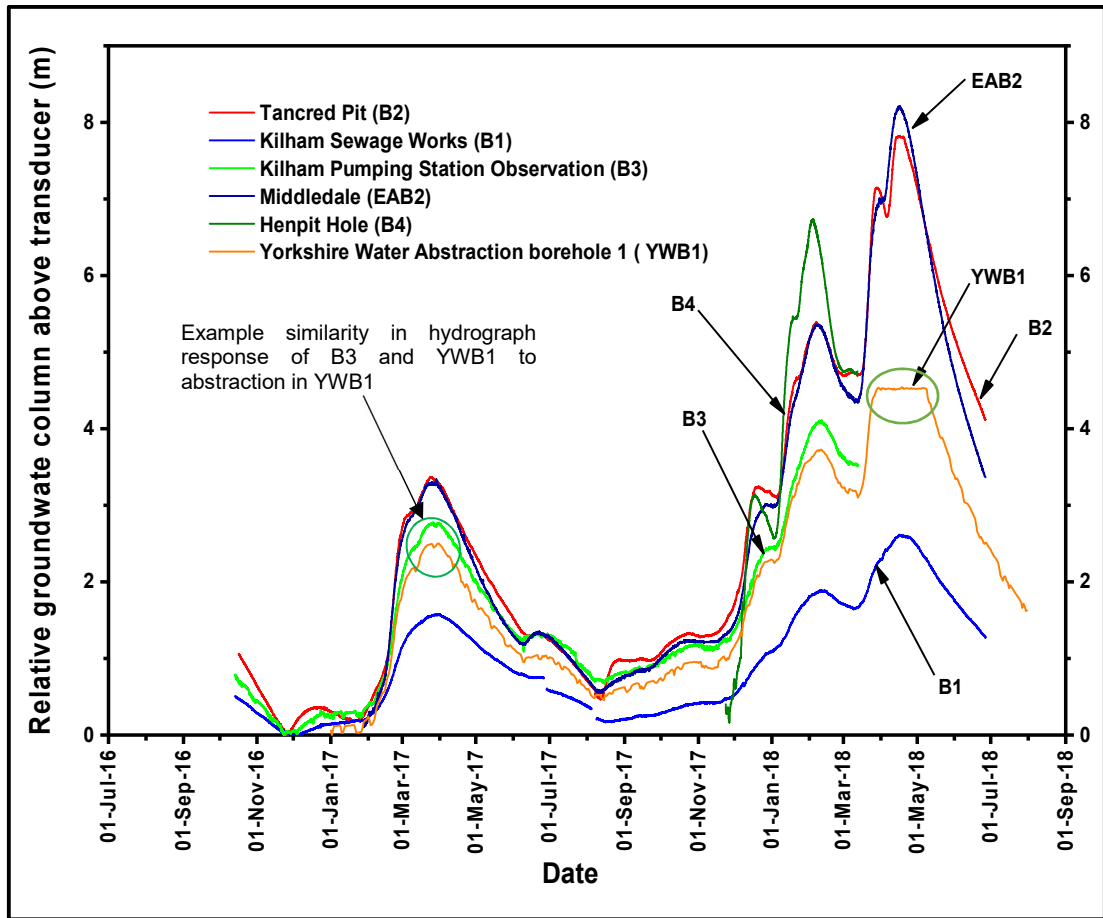


**Figure 5.10.** Well hydrograph general pattern for the Kilham area (discharge zone). Similarity in B3 and YWB1 hydrograph responses to abstraction in YWB1 highlighted (green ellipse and arrowed). Steady state behaviour of YWB1 hydrograph in due to logger going out of measurement range response to high water levels for the period late March to mid May 2018 also highlighted (orange ellipse).

Kilham is consistent with the very large transmissive nature of the aquifer in Kilham and its surrounding areas.

Foston Mill gauging station discharge hydrograph strongly mimics the groundwater hydrograph as about 85 – 95% of its flow is groundwater derived (Foster, 1974). However, as the Foston Beck is a surface feature, and also because of the location of the gauging station on glacial tills, the discharge hydrograph has minor surface runoff contribution shown by the discharge flashes and peaks that correspond with rainfall events, but mimic the groundwater hydrograph pattern after the storm passes.

### **5.7.2 Results and discussions of spring SEC and temperature monitoring**

The thermographs for the air temperature, Bellguy (S2) and Place Newton (S3) springs and Tancred Pit borehole (B2) are shown in Figure 5.11. In Figure 5.11a, a 7-day running average ambient temperature shows large seasonal variability during the monitoring period, with maxima in the summer and minima in the winter months. The ambient temperature ranged between a minimum and maximum of 2.0 and 18.0 °C respectively for the monitoring period, with a yearly average temperature of 10.3 °C and coefficient of variation (CV) of 51%.

In contrast to the air temperatures, the springs and borehole thermographs in Figure 5.11b show little variability. Bellguy records the highest temperatures, ranging between 9.6 and 10.5 °C, with a mean temperature of 10.1 °C, with a CV of 2%. Bellguy thermograph is initially flashy becoming smooth after February 2017. The thermograph shows periodicity recording maxima for the Februaries of 2017 and 2018. The thermograph for Place Newton springs lies between that for Bellguy and Tancred Pit borehole, recording a temperature between 9.2 and 10.1 °C, with a temperature average of 9.8 °C, with a CV of 3%. Place Newton spring thermograph is the most flashy with diurnal variations, mimicking a subdued form of daily ambient temperature, i.e. daily periodicity. Both Bellguy and Place Newton spring thermographs are out of phase with the average ambient temperature, with thermal lags of temperature minimum and maximum shown. In May 2016, both springs record temperature minimums, resulting in a 4.5 months thermal lag ( $TL_{min}$ ) from the averaged ambient temperature signal. For the maximum temperature lags from the averaged ambient temperature signal, Place Newton shows a 3.5 months thermal lag ( $TL_{max}$  S3) occurring in October 2017, whereas Bellguy records a maximum temperature in February, 2018 implying a thermal lag of 7.5 months ( $TL_{max}$  S2).

Comparing the springs and Tancred Pit borehole, the thermograph of the borehole is thermally stable and not variable and does not show phase relation with the averaged ambient air temperatures. Tancred Pit borehole records a constant temperature of 9.2 °C during the monitoring period.

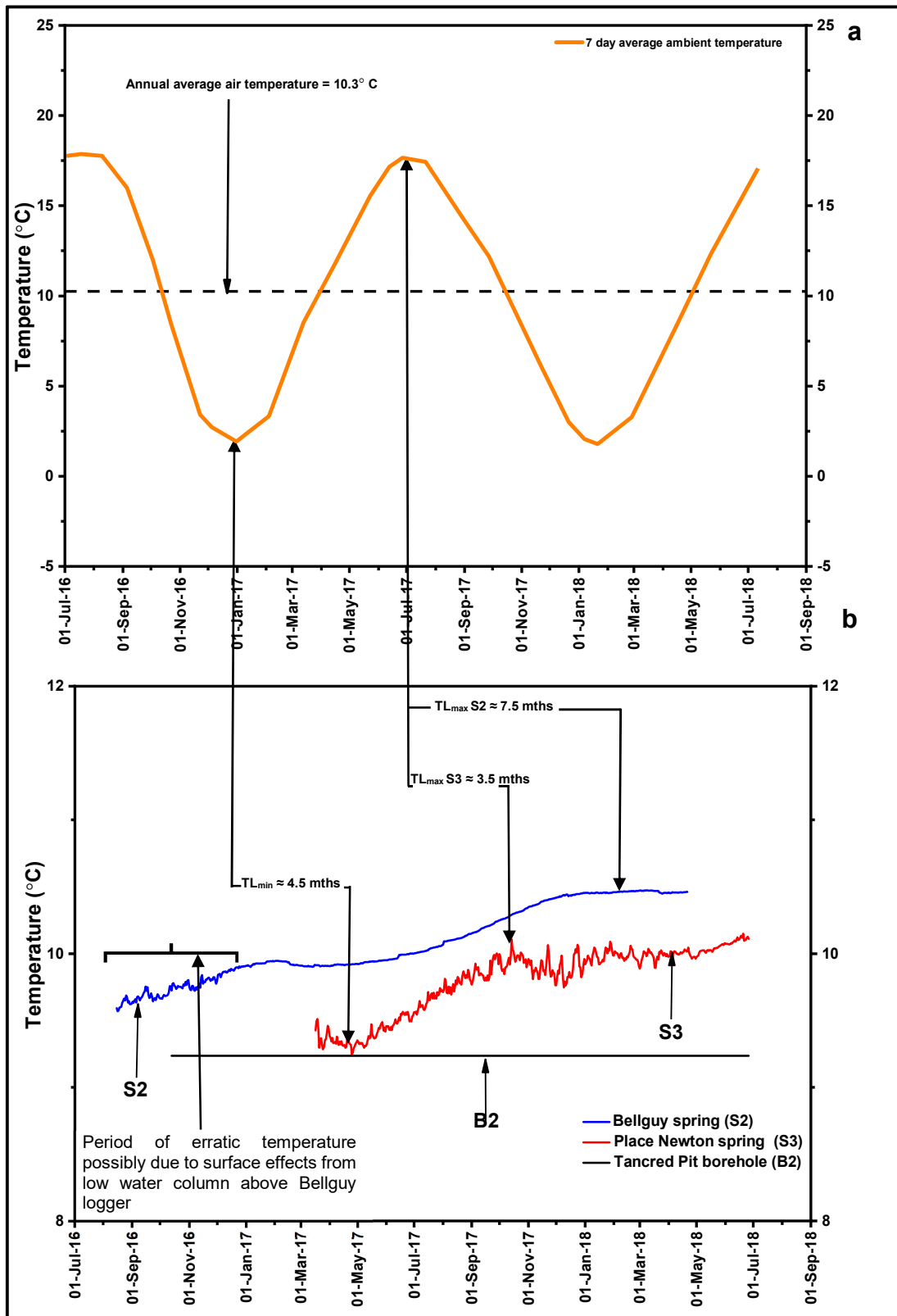


**Figure 5.11.** Comparison of ambient air, spring and borehole temperature. (a) Large seasonal air temperature variation with annual average of 10.3 °C. (b) Springs (S2 and S3) and borehole (B2) temperatures reflective of average ambient air temperature, with S2,S3 and B2 temperatures showing relatively little variation in temperature. Thermal lags between spring and air temperature maximum and minimum also shown.

The mean temperatures of the springs and the borehole water reflects the mean ambient temperature (8 – 12 ° C), implying that the borehole water and the source of the springs are below the surficial zone and outside the influence of surface air temperatures. The low coefficients of variation and mean temperatures of the springs, and borehole temperature indicates that they are sourced from recharge water that has had enough time to thermally equilibrate with the rock. This implies flow in the aquifer is characterised by diffuse recharge, thermally effective pathways and relatively long residence times that masks input temperature signals, suggestive of an aquifer with Stanton Number,  $S_t \gg 1$ .

Tancred Pit borehole water thermal stability is representative of the relatively deeper source environment (45 mbgl in comparison to springs) that has thermally equilibrated with rock temperature in comparison to the springs that most likely discharge a combination of shallower and deeper waters. Place Newton springs sensitivity to ambient air temperature shows the influence of air temperatures on the logger, because of the few centimetres of water depth above the logger. Bellguy on the other hand shows a smooth temperature profile reflective of deeper depth of placement in the spring emergence after an initial influence from ambient air. The thermal lags between ambient temperatures and spring (S2, S3) temperatures cannot be used to determine the residence time of their waters as the lags are essentially a function of the time taken for surface temperature fluctuations to propagate to the depths from which the springs are sourced.

The SEC time series for Tancred Pit boreholes, Bellguy and Place Newton springs, and periodically monitored boreholes is shown in Figure 5.12. Tancred Pit borehole SEC and periodically monitored boreholes plots show stable and non-varying SEC over the monitoring period. Tancred Pit borehole records the lowest SEC of 524 - 530  $\mu\text{S}/\text{cm}$ . In contrast, the springs record periods of low variability and erratic and flashy SECs. For > 99% of the time, Bellguy spring records SEC of 625 - 661  $\mu\text{S}/\text{cm}$ , but also records up to a high of 2150  $\mu\text{S}/\text{cm}$  but then stabilises in February 2017, in correspondence with time of erratic temperatures earlier presented. Unlike Bellguy, Place Newton spring erratic record does not stop but alternates with the stable profile to

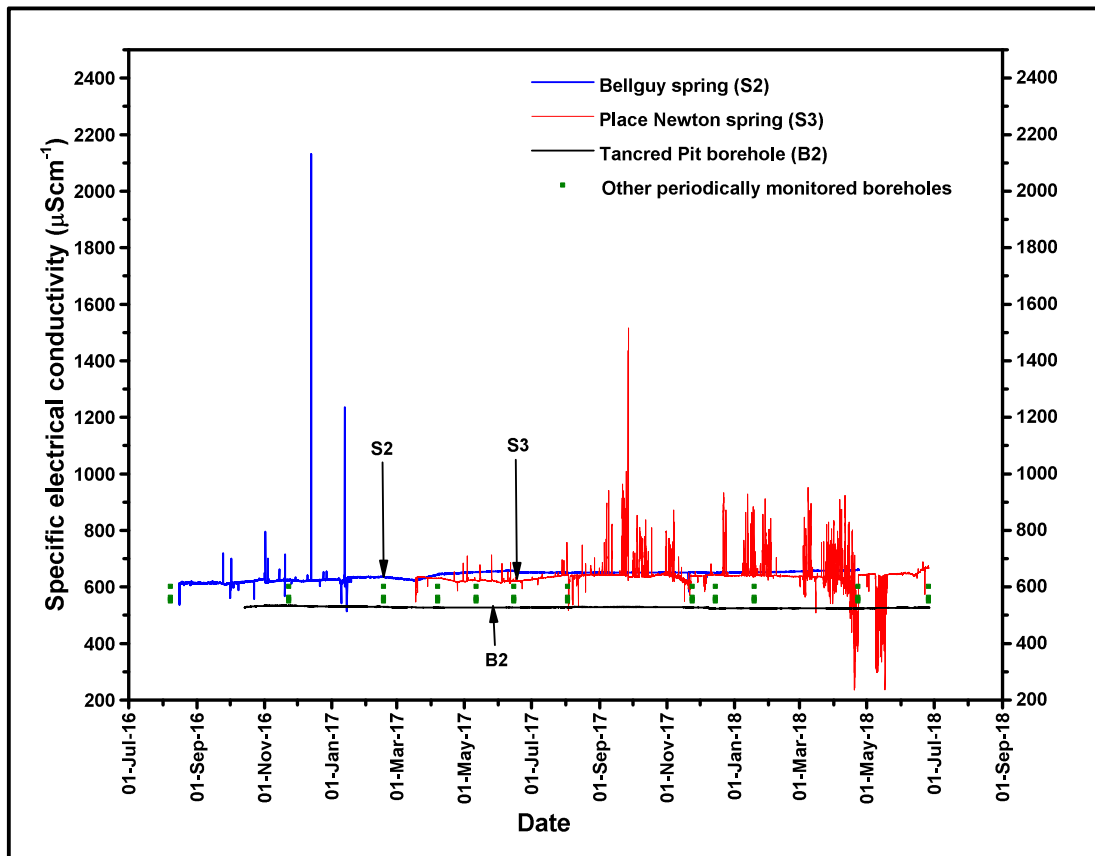


**Figure 5.12.** SEC time series of Bellguy and Place Newton springs, Tancred Pit borehole (B2) and periodically monitored wells.

end of monitoring. Place Newton records SEC of 630 – 670  $\mu\text{S/cm}$  for about 93% of the time, but also records  $> 670 \mu\text{S/cm}$  for about 6% of the time and  $< 630 \mu\text{S/cm}$  for 3% of the time. The maximum and minimum SEC recorded for Place Newton is 1500  $\mu\text{S/cm}$  and 230  $\mu\text{S/cm}$  on 24 September 2017, and 20 May and April 2018 respectively.

The SEC base signal (for the majority of the time) on which are superimposed extremes and flashes for both springs is taken to be the normal water quality that discharges at both springs but the erratic records are further scrutinised to give an indication of their possible source. Firstly, the corresponding end of the erratic signals in both SEC and temperature, for Bellguy in January/February 2017 is likely due to increased water depth above the logger at the spring site suggesting that the erratic logs could be due to ambient air / surface effects on the logger. On the other hand, the Place Newton logger location without substantial water column above it exposes the logger to ambient air effects. Secondly, the hand probe measured SEC and the major

ion characteristics of the sampled springs (to come in the section 5.7.3) did not show SEC extremes and anomaly as shown on the loggers, but showed baseline line chalk signatures as presented in Smedley et al. (2004) and other literature. The above reasons are adduced to show that the erratic records on the springs are noise and disturbance from the logger environment. In spite of the reasons above, other unexplained and unexpected phenomenon like fouling, blockage and algal growth on the sensor and passage of water of a different chemistry can give the erratic SEC signals.

The non-varying SEC signal for Tancred Pit borehole is reflective of a well mixed, homogenised and calcite equilibrated closed carbonate environment, whereas the SEC variation for the springs may possibly be from the switching of the open and closed carbonate system along the flowpath of waters that discharge via the springs. The variation could also be from the mixing and convergence of waters of different saturation levels at the springs.

### 5.7.3 Results of spring sampling

The hydrochemical results are presented in Table 5.3. Sampling temperatures ranged from 9.5 to 12.5 °C, with an average of 10.6 °C, which is representative of the average annual ambient temperature. pH ranged between 6.68 and 7.80, which is typical of Chalk groundwater for the area. Table 5.3 also shows the charge balance errors (CBEs) calculated from the major ions using the expression (Appello and Postma, 2005):

$$CBE = 100 \times \frac{TZ^+ - TZ^-}{TZ^+ + TZ^-} \quad (5.19)$$

where  $TZ^+$  and  $TZ^-$  are the cationic and anionic concentration sums respectively in milliequivalent per litre (meq/L). The CBEs range between - 4.90 and +4.51 %, which is within the  $\pm 5\%$  for analytical accuracy and completeness (Appello and Postma, 2005; Brassington, 2007). The distribution of the CBEs is shown in Figure 5.13. About 52% of the CBEs fall within  $\pm 2\%$ . The laboratory analyses were checked and validated in two ways. Firstly, an added blind sample (Bracey Bridge, 12 May, 2017) to check the precision reported  $\pm 1\%$  for the  $Ca^{2+}$ ,  $NO_3^-$ ,  $Cl^-$  and  $SO_4^{2-}$ , which apart from alkalinity, are critical for understanding the hydrochemistry of the water

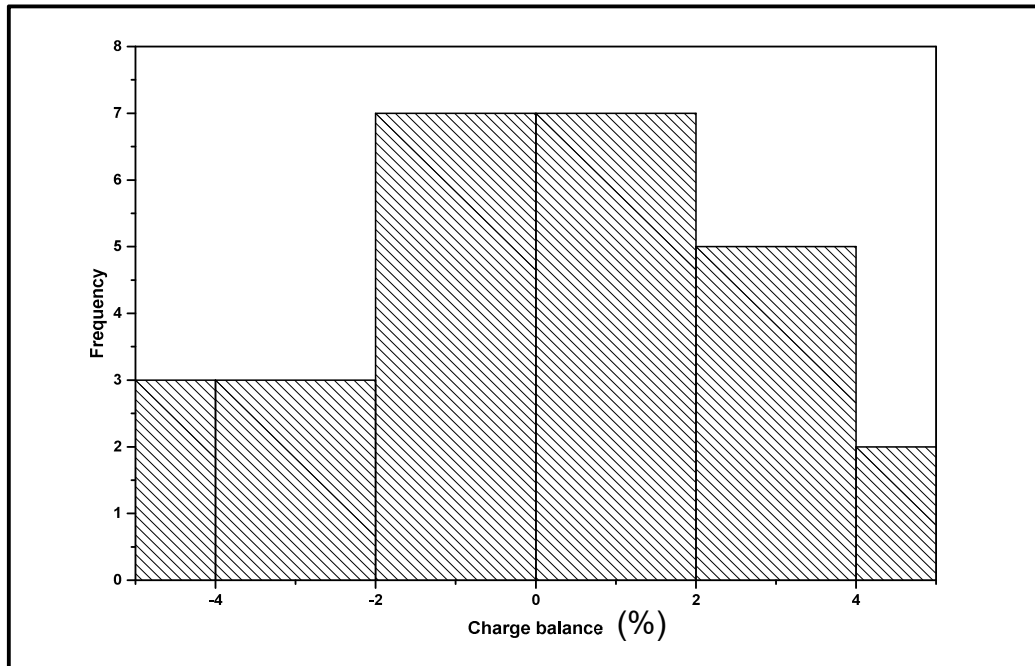


**Figure 5.13.** Distribution of CBEs for sampled springs

in the unconfined chalk. Secondly, the sample duplicates and laboratory standard concentrations supplied with analytical results agreed with actuals to  $\pm 1\%$ . From Table 5.3, the TZ<sup>+</sup> and TZ<sup>-</sup> shows that the most dominant ions are Ca<sup>2+</sup> for cations and alkalinity for anions. Ca<sup>2+</sup> accounts for between 87 to 93% of the TZ<sup>+</sup>, whilst alkalinity contributes between 53 to 61% of the TZ<sup>-</sup>. For the rest of the cations, Na<sup>+</sup> contributes between 5 -10%, > Mg > K. For Bracey Bridge and Bellguy springs anions TZ<sup>-</sup> contributions, NO<sub>3</sub><sup>-</sup>  $\approx$  Cl<sup>-</sup> (14 -17 %) > SO<sub>4</sub><sup>2-</sup>. However, at Place Newton, NO<sub>3</sub><sup>-</sup> (18 – 20%) > SO<sub>4</sub><sup>2-</sup> (12 -14 %) > Cl<sup>-</sup> (9 -12 %).

The time series for the concentrations are provided in Figure 5.14 to Figure 5.16. Bracey Bridge records the lowest Ca<sup>2+</sup> and HCO<sub>3</sub><sup>-</sup> concentrations for the majority of the sampling time, whilst Bellguy and Place Newton springs are consistently higher for HCO<sub>3</sub><sup>-</sup> and Ca<sup>2+</sup>. Place Newton springs records the highest NO<sub>3</sub><sup>-</sup> and SO<sub>4</sub><sup>2-</sup> concentrations, whilst recording the lowest Cl<sup>-</sup>, Na<sup>+</sup> and K<sup>+</sup> concentrations for the monitoring period. Within each site, Ca<sup>2+</sup> and HCO<sub>3</sub><sup>-</sup> account for the greatest variability in terms of analytical concentrations, but in terms of relative standard deviation, K<sup>+</sup>, Mg<sup>2+</sup> and Na<sup>+</sup> are the most

**Table 5.3.** Field measurements and major ion chemistry of monitored springs for this studies

Sample Location and date	SEC μS/cm	pH	Temp °C	Cations (mg/L)				Anions (mg/L)				Charge balance		
				Ca <sup>2+</sup>	K <sup>+</sup>	Mg <sup>2+</sup>	Na <sup>+</sup>	CaCO <sub>3</sub> alkalinity	SO <sub>4</sub> <sup>-2</sup>	NO <sub>3</sub> <sup>-</sup>	Cl <sup>-</sup>	TZ <sup>+</sup> meq/L	TZ <sup>-</sup> meq/L	CB %
<b>17 February 2017</b>														
Bracey Bridge Springs	558	6.80	10.0	80.80	1.17	1.81	10.3	152.0	20.50	50.50	27.90	4.66	5.07	- 4.18
Bellguy springs	636	6.83	10.0	103.00	2.01	1.99	11.7	157.0	28.30	60.30	33.30	5.86	5.65	1.80
Place Newton	630	6.83	9.5	105.00	0.630	2.00	8.65	148.0	38.20	70.10	22.80	5.78	5.52	2.31
<b>17 March 2017</b>														
Bracey Bridge Springs	560	6.83	9.8	90.60	1.12	1.71	9.81	155.0	19.50	52.50	27.60	5.12	5.13	- 0.13
Bellguy springs	625	7.32	9.6	100.00	1.49	1.90	11.1	160.0	27.70	59.10	32.80	5.67	5.65	0.13
Place Newton	630	7.52	9.5	102.00	0.504	1.94	8.34	149.0	37.80	69.40	22.70	5.62	5.53	0.77
<b>07 April 2017</b>														
Bracey Bridge Springs	568	7.20	11.7	94.50	1.11	1.78	10.1	159.0	22.50	53.10	28.50	5.33	5.31	0.23
Bellguy springs	646	7.00	11.6	97.20	1.62	1.83	11.1	181.0	27.30	57.50	32.30	5.52	6.03	- 4.35
Place Newton	630	7.20	9.5	103.00	0.533	1.87	8.39	160.0	38.70	70.10	22.70	5.67	5.78	- 0.92

**Table 5.3** continued

Sample Location and date	SEC μS/cm	pH	Temp °C	Cations (mg/L)				Anions (mg/L)				Charge balance		
				Ca <sup>2+</sup>	K <sup>+</sup>	Mg <sup>2+</sup>	Na <sup>+</sup>	CaCO <sub>3</sub> alkalinity	SO <sub>4</sub> <sup>-2</sup>	NO <sub>3</sub> <sup>-</sup>	Cl <sup>-</sup>	TZ <sup>+</sup> meq/L	TZ <sup>-</sup> meq/L	CB %
<b>12 May 2017</b>														
Bracey Bridge Springs	578	7.50	11.8	92.50	1.13	1.74	9.87	162.0	20.23	52.16	28.39	5.21	5.30	-0.84
(Bracey Bridge check)				93.80	1.02	1.24	7.68	163.0	20.00	52.48	28.74	5.14	5.31	-1.63
Relative standard deviation (%)				-1	10	29	22	-1	1	-1	-1			
<b>15 June 2017</b>														
Bracey Bridge Springs	565	7.66	12.0	93.00	0.80	1.32	7.66	156.0	19.33	52.09	27.71	5.10	5.14	-0.40
Bellguy springs	658	7.80	12.0	110.30	1.76	2.22	13.5	185.0	27.07	62.42	32.26	6.32	6.18	1.08
Place Newton	620	7.80	12.0	101.0	0.33	1.48	6.25	175.0	35.13	72.24	21.22	5.44	6.00	-4.90
<b>03 August 2017</b>														
Bracey Bridge Springs	580	6.80	12.0	92.0	1.20	1.91	11.37	145.0	19.49	52.15	27.66	5.27	4.93	3.39
Bellguy springs	650	6.50	11.8	109.6	1.68	2.21	13.7	184.0	26.99	61.44	32.76	6.29	6.16	1.07
Place Newton	642	6.95	10.5	112.2	0.61	2.27	10.23	165.0	36.53	74.10	22.93	6.25	5.90	2.84
<b>20 October 2017</b>														
Bracey Bridge Springs	568	7.12	12.5	93.50	1.11	1.78	10.50	145.0	20.00	53.00	27.00	5.30	4.93	3.56

**Table 5.3** continued

Sample Location and date	SEC μS/cm	pH	Temp °C	Cations (mg/L)				Anions (mg/L)				Charge balance		
				Ca <sup>2+</sup>	K <sup>+</sup>	Mg <sup>2+</sup>	Na <sup>+</sup>	CaCO <sub>3</sub>	SO <sub>4</sub> <sup>-2</sup>	NO <sub>3</sub> <sup>-</sup>	Cl <sup>-</sup>	TZ <sup>+</sup>	TZ <sup>-</sup>	CB
								alkalinity					meq/L	meq/L
Bellguy springs	652	7.13	10.2	104.0	1.62	2.05	12.5	165.0	28.0	61.0	32.0	5.94	5.77	1.49
Place Newton	635	6.85	11.7	112.0	0.51	1.75	7.44	160.0	36.0	70.0	22.0	6.07	5.70	3.15
<b>08 December 2017</b>														
Place Newton	642	7.11	9.6	112.0	0.70	2.18	9.93	160.0	37.0	71.0	22.0	6.22	5.74	4.03
<b>15 December 2017</b>														
Bracey Bridge Springs	582	6.89	9.8	95.8	1.15	1.77	12.30	149.0	20.0	53.0	27.0	5.49	5.02	4.51
Bellguy springs	650	6.95	9.6	105.0	1.69	2.03	9.10	171.0	28.0	63.0	31.0	5.85	5.89	- 0.40
<b>19 January 2018</b>														
Bracey Bridge Springs	585	6.68	9.8	92.40	1.14	1.76	10.1	163.0	21.0	54.0	28.0	5.22	5.36	- 1.26
Bellguy springs	650	7.14	9.6	100.0	1.68	2.00	11.8	170.0	26.0	61.0	31.0	5.71	5.80	- 0.77
Place Newton	635	7.26	9.5	106.0	0.57	2.11	9.11	189.0	36.0	70.0	21.0	5.87	6.25	- 3.12

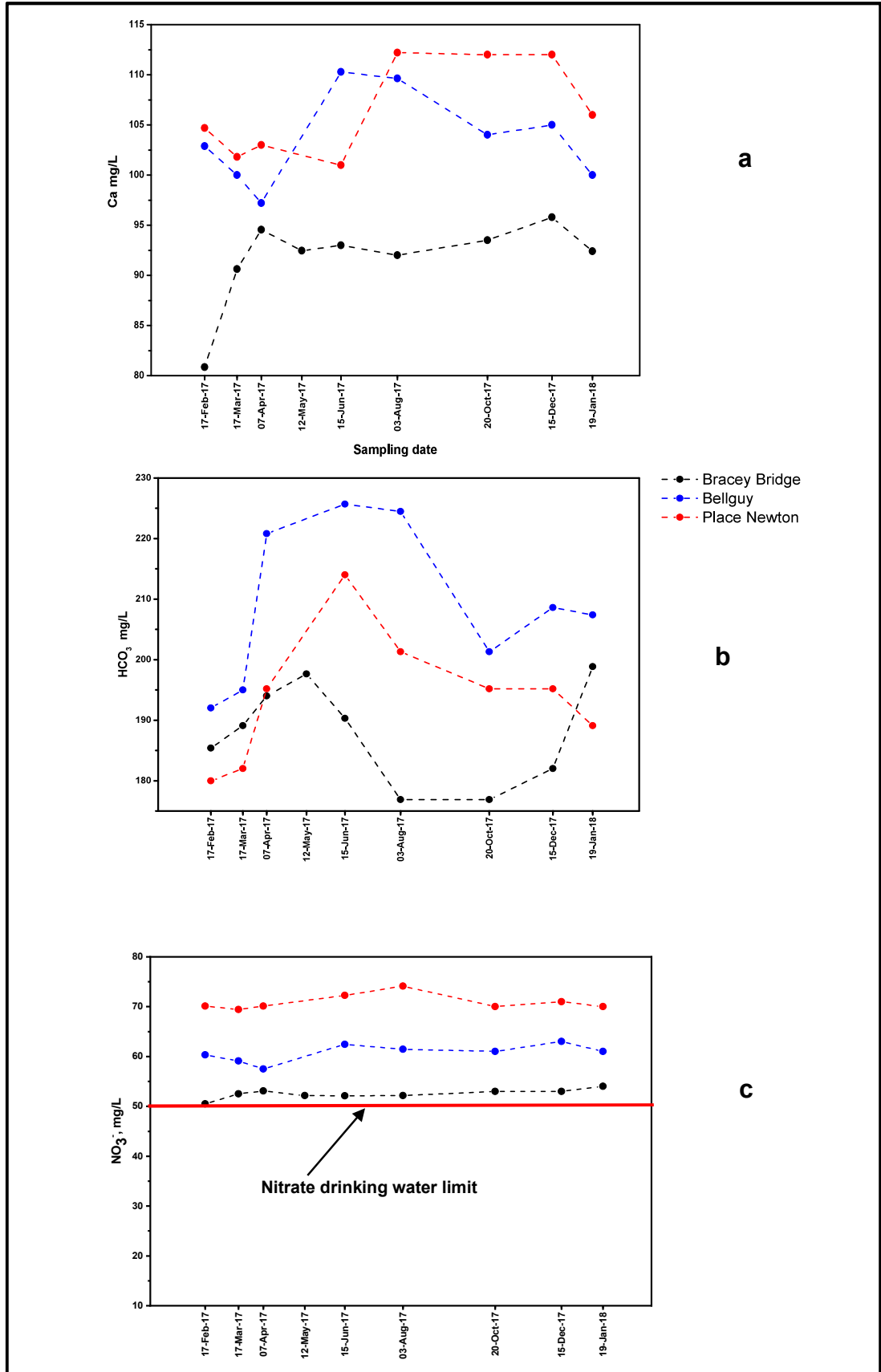


Figure 5.14. Time series of major ion concentration: (a) Ca<sup>2+</sup>; (b) HCO<sub>3</sub><sup>-</sup>; (c) NO<sub>3</sub><sup>-</sup>

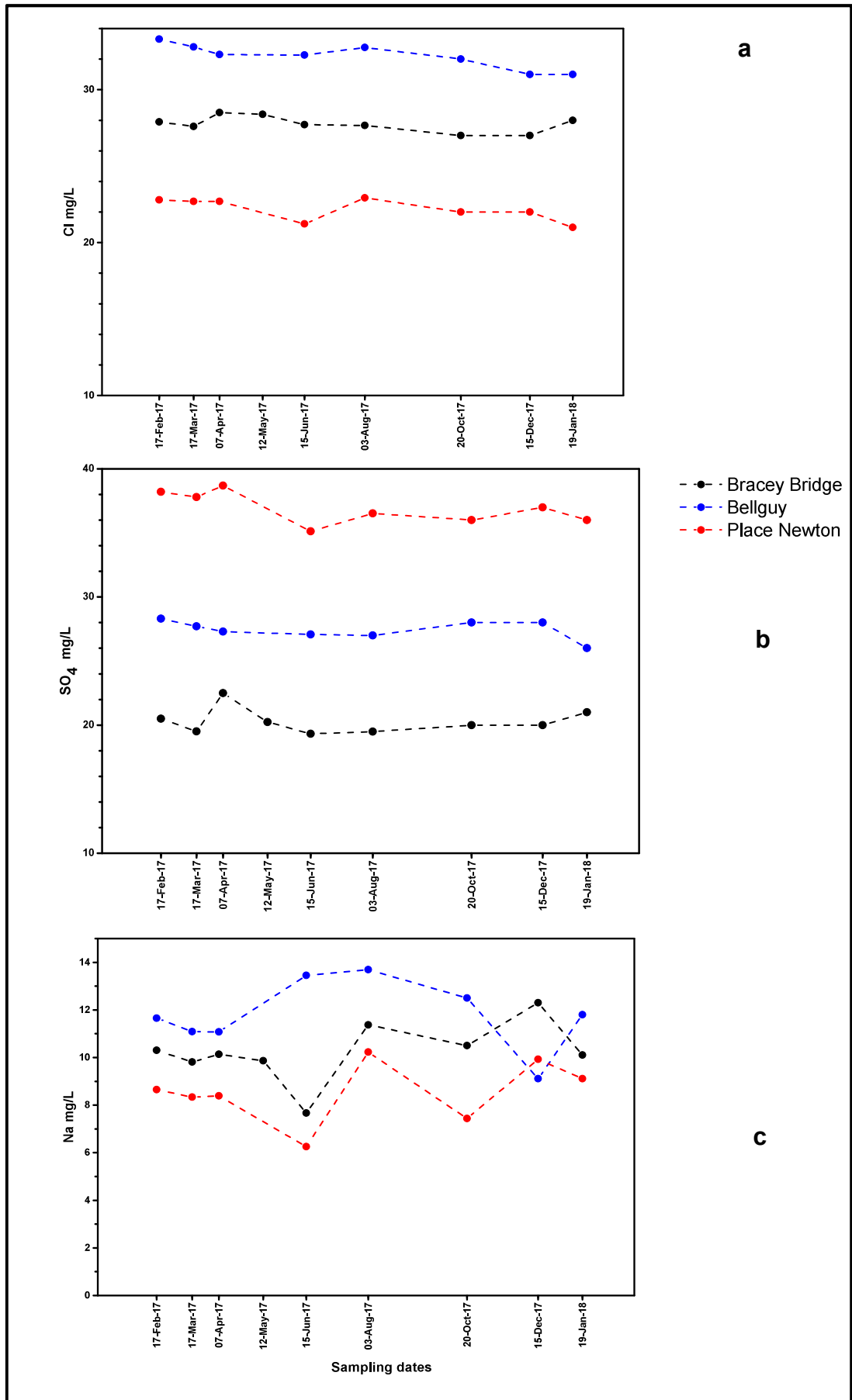
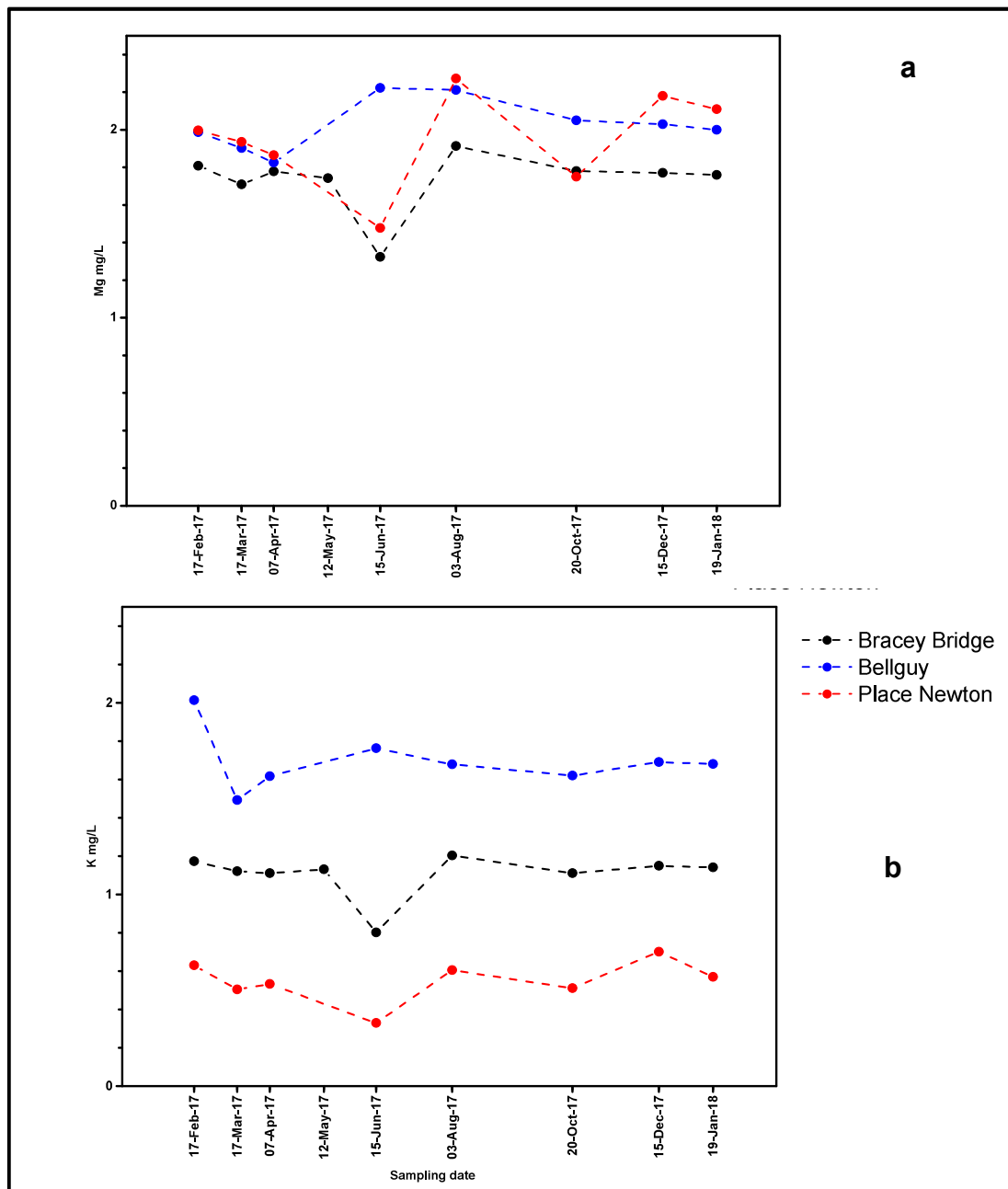


Figure 5.15 Time series of major ion concentrations: (a) Cl<sup>-</sup>; (b) SO<sub>4</sub><sup>2-</sup>; (c) Na<sup>+</sup>



**Figure 5.16** Time series of major ion concentrations: (a) Mg<sup>2+</sup>; (b) K<sup>+</sup>

variable because of the relatively low concentrations recorded. All NO<sub>3</sub><sup>-</sup> concentrations are higher than the drinking water limit of 50 mgL<sup>-1</sup>.

In Table 5.4 are the archived EA chemical dataset for springs and boreholes in the catchment the details of which are provided in Table 5.2. The EA data is used with the aim of situating and constraining the dataset for this current study. Groundwater samples were collected following standard Environment

Agency procedure. The EA owned boreholes were not purged before sampling. The concentrations reported in Table 5.4 are average values as the samples were taken from the open section of the borehole. Specific electrical conductivity and other field parameters were measured using a YSI meter. At every site one sample was filtered and bottled (1 litre plastic bottle) for major ions analyses. Major ions were analysed using the EA GWQMI2 Analysis Suite at the EA National Laboratory Service (pers com, EA).

The charge balance errors for the EA dataset range between -2.22 and 4.56 % , falling within the a  $\pm 5\%$  for analytical accuracy and completeness. In the EA dataset as well,  $\text{Ca}^{2+}$  and  $\text{HCO}_3^-$  dominate the major ion chemistry.  $\text{Ca}^{2+}$  contributes between 82 – 91% to the  $\text{TZ}^+$  and  $\text{HCO}_3^-$  contributes between 48 – 65% to the  $\text{TZ}^-$ . For the rest of the anions, either  $\text{NO}_3^-$  or  $\text{Cl}^-$  is the next dominant, with  $\text{SO}_4^{2-}$  been the least dominant. For the springs,  $\text{Ca}^{2+}$  and  $\text{HCO}_3^-$  concentrations range between 85 and 108 mg/L and 156 and 183 mg/L respectively. For the boreholes,  $\text{Ca}^{2+}$  and  $\text{HCO}_3^-$  concentrations range between 94 and 133 mg/L and 156 and 197 mg/L respectively.

**Table 5.4.** Archived geochemical characteristics from EA monitored boreholes and springs in the study area

Sample Location and date	SEC µS/cm	Cations (mg/L)				Anions (mg/L)				Charge balance		
		Ca <sup>2+</sup>	K <sup>+</sup>	Mg <sup>2+</sup>	Na <sup>+</sup>	CaCO <sub>3</sub> alkalinity	SO <sub>4</sub> <sup>2-</sup>	NO <sub>3</sub> <sup>-</sup>	Cl <sup>-</sup>	TZ <sup>+</sup> meq/L	TZ <sup>-</sup> meq/L	CB %
<b>Kilham springs at south view</b>												
22 January 2016	571	108	1.37	2.15	12.8	176	27.1	60.0	29.9	6.16	5.89	2.18
14 April 2016	613	111	1.5	2.25	12.3	183	28.2	58.0	30.0	6.30	6.03	2.18
12 May 2016	622	111	1.52	2.2	12.1	191	28	59.3	29.7	6.28	6.20	0.71
08 June 2016	628	107	1.49	2.24	11.7	156	28.4	59.8	30.7	6.07	5.54	4.56
<b>Wintringham springs at Grange Garth</b>												
14 October 2015	525	85	1.06	2.58	15.9	172	25.2	38.2	27.0	5.17	5.34	-1.62
13 November 2015	530	90.2	0.788	2.17	13.7	159	25.1	34.6	29.6	5.30	5.10	1.93
17 December 2015	531	88.6	0.850	2.05	12.6	163	24.2	34.9	32.7	5.16	5.25	-0.86
14 January 2016	536	88.9	0.900	2.11	14.5	168	23.9	34.5	31.2	5.26	5.29	-0.29
11 February 2016	542	93.2	0.911	2.14	14.1	173	24.7	43.3	27.7	5.46	5.45	0.09
17 March 2016	518	87.8	0.916	2.03	12.7	160	23.8	38.3	27.0	5.12	5.07	0.49
<b>Weaverthorpe Slack borehole</b>												
15 July 2015	633	94.4	0.415	1.41	20	156	24.1	59.3	48.5	5.71	5.95	-2.06
13 August 2015	610	98.1	0.337	1.23	20	162	23.2	57.1	43.2	5.87	5.86	0.10
14 October 2015	629	97.9	0.442	1.22	22.7	164	22.8	53.6	46.6	5.98	5.93	0.43

**Table 5.4** continued

Sample Location and date	SEC µS/cm	Cations (mg/L)				Anions (mg/L)				Charge balance		
		Ca <sup>2+</sup>	K <sup>+</sup>	Mg <sup>2+</sup>	Na <sup>+</sup>	CaCO <sub>3</sub>	SO <sub>4</sub> <sup>2-</sup>	NO <sub>3</sub> <sup>-</sup>	Cl <sup>-</sup>	TZ <sup>+</sup> meq/L	TZ <sup>-</sup> meq/L	CB %
<b>Weaverthorpe Slack borehole</b>												
11 February 2016	616	99.4	0.322	1.23	21.6	173	24.3	58.9	44.4	6.01	6.17	-1.31
<b>MFm borehole</b>												
15 July 2015	557	96.5	0.444	0.444	9.97	164	9.97	58.5	24.9	5.30	5.13	1.57
13 November 2015	556	98	0.338	0.338	10.6	168	10.6	53.1	24.1	5.39	5.12	2.57
14 April 2016	616	103	2.290	1.24	14.5	161	14.5	77.5	27.7	5.93	5.55	3.29
05 December 2016	554	97.7	0.492	1.07	10.3	170	10.3	61.1	25.4	5.42	5.32	1.00
<b>DFm borehole</b>												
15 July 2015	664	116	1.00	1.6	10.7	170	29.2	88.1	29.6	6.41	6.26	1.16
14 October 2015	636	111	0.602	1.41	10.1	172	27.4	75.3	28.6	6.11	6.03	0.65
14 January 2016	753	121	6.61	1.8	13.6	185	32.5	119	31.8	6.95	7.20	-1.80
12 May 2016	793	133	5.4	2.31	14.1	181	36.7	136	32.4	7.58	7.51	0.44
<b>Kilham observation borehole</b>												
13 August 2015	646	112	0.95	2.04	12.2	188	33.5	69.5	33.2	6.31	6.51	-1.59
13 November 2015	645	111	1.16	1.93	13	176	31.6	65.9	32.6	6.29	6.16	1.05
14 April 2016	648	124	0.834	2.44	13	197	39.8	62.4	32.8	6.97	6.70	2.01
<b>MHFm borehole</b>												
08 May 2015	669	111	1.21	1.87	15.3	184	43.5	62.0	38.1	6.39	6.66	-2.08
13 August 2015	667	107	1.34	1.89	14.4	182	37.7	62.0	35.8	6.16	6.43	-2.22
17 December 2015	653	112	1.58	1.99	14.8	185	37.8	62.0	38.1	6.44	6.56	-0.96

#### 5.7.4 Results of measured and calculated SECs, and transport numbers

From the analytical concentrations, equations (5.2) to (5.6) were used to calculate the individual ion SECs and their corresponding transport numbers based on the field measured SEC. This was done to determine how much the major ions contribute to the measured SEC.

The transport numbers and the hand probe measured SECs for the monitoring for this study are presented in Figure 5.17. That for the EA archived dataset are presented in Figure 5.18 to Figure 5.20. In these diagrams, the values in each part of the stack bar graph show the transport number of the major ion. A horizontal line extended through the boundaries of the major ions to the cumulative transport number (left axis) gives cumulative transport number at that boundary. Also marked on the diagrams (right axis) is the field measured SEC for each stack. From the transport number figures, all the calculated SECs are lower than the field measured SECs i.e. < 100%, which is expected since minor ions and complexes which contribute to the field measured SEC are not included in the calculated SEC. In Figure 5.17, field measured SEC ranges between 558 - 585, 625 - 661 and 620 - 642  $\mu\text{S}/\text{cm}$  for Bracey Bridge, Bellguy and Place Newton springs respectively, with a 3 - 6% relative standard deviation. Calculated SEC contributes between 82 - 87% to the field measured SEC. Again the dominance of  $\text{Ca}^{2+}$  and  $\text{HCO}_3^-$  is shown, followed by  $\text{NO}_3^-$  and  $\text{Cl}^-$ , then by  $\text{SO}_4^{2-}$  and  $\text{Na}^+$ .  $\text{Ca}^{2+} + \text{HCO}_3^-$  contributes more than 50% to the measured SECs. Within each site and across the springs, the greatest variation in transport numbers is in  $\text{Ca}^{2+}$  and  $\text{HCO}_3^-$ . Across the springs,  $\text{Ca}^{2+}$  contributes between 31 - 36%, whereas  $\text{HCO}_3^-$  contributes between 19 - 24% to the measured SEC. For the springs, the highest  $\text{NO}_3^-$  and  $\text{SO}_4^{2-}$  contributions to the SEC is at Place Newton. For the EA samples in Figure 5.18 to Figure 5.20, the measured SEC for EA dataset ranges from 518 - 628  $\mu\text{S}/\text{cm}$  for the springs and from 554 - 793  $\mu\text{S}/\text{cm}$  for the boreholes. DFm and MFm record some high SECs attributable to increased  $\text{NO}_3^-$  contribution to SEC. For the EA samples as well,  $\text{Ca}^{2+} + \text{HCO}_3^-$  are the dominant contributors (i.e. > 50%) to the field measured SEC, followed by either  $\text{NO}_3^-$  or  $\text{Cl}^-$  contribution.  $\text{Cl}^- > \text{NO}_3^-$  at Weaverthorpe Slack BH and Wintringham springs at Grange Garth whereas  $\text{NO}_3^-$  dominates  $\text{Cl}^-$

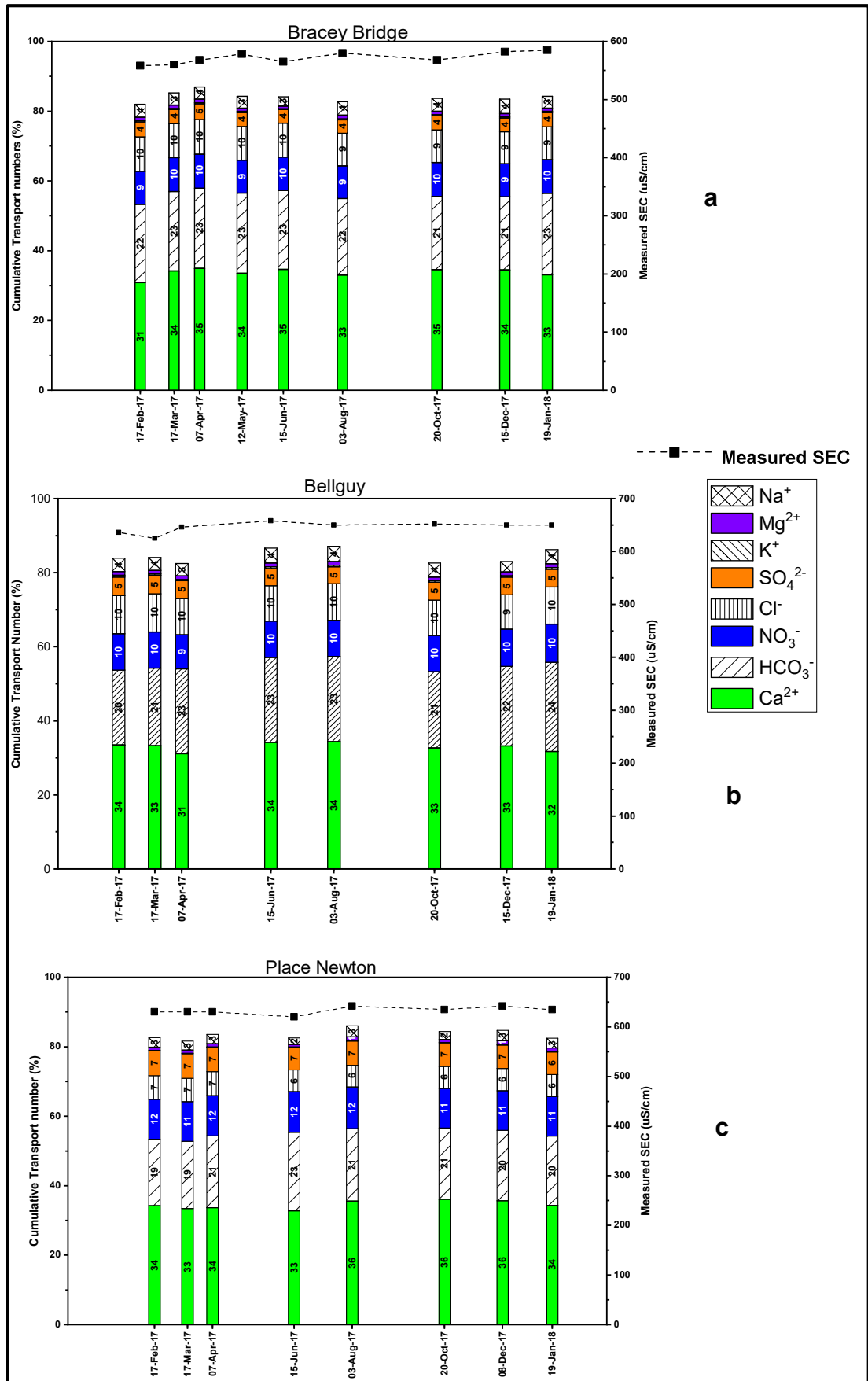


**Figure 5.17. Measured SEC and transport numbers of monitored springs. (a) Bracey Bridge; (b) Bellguy; (c) Place Newton**

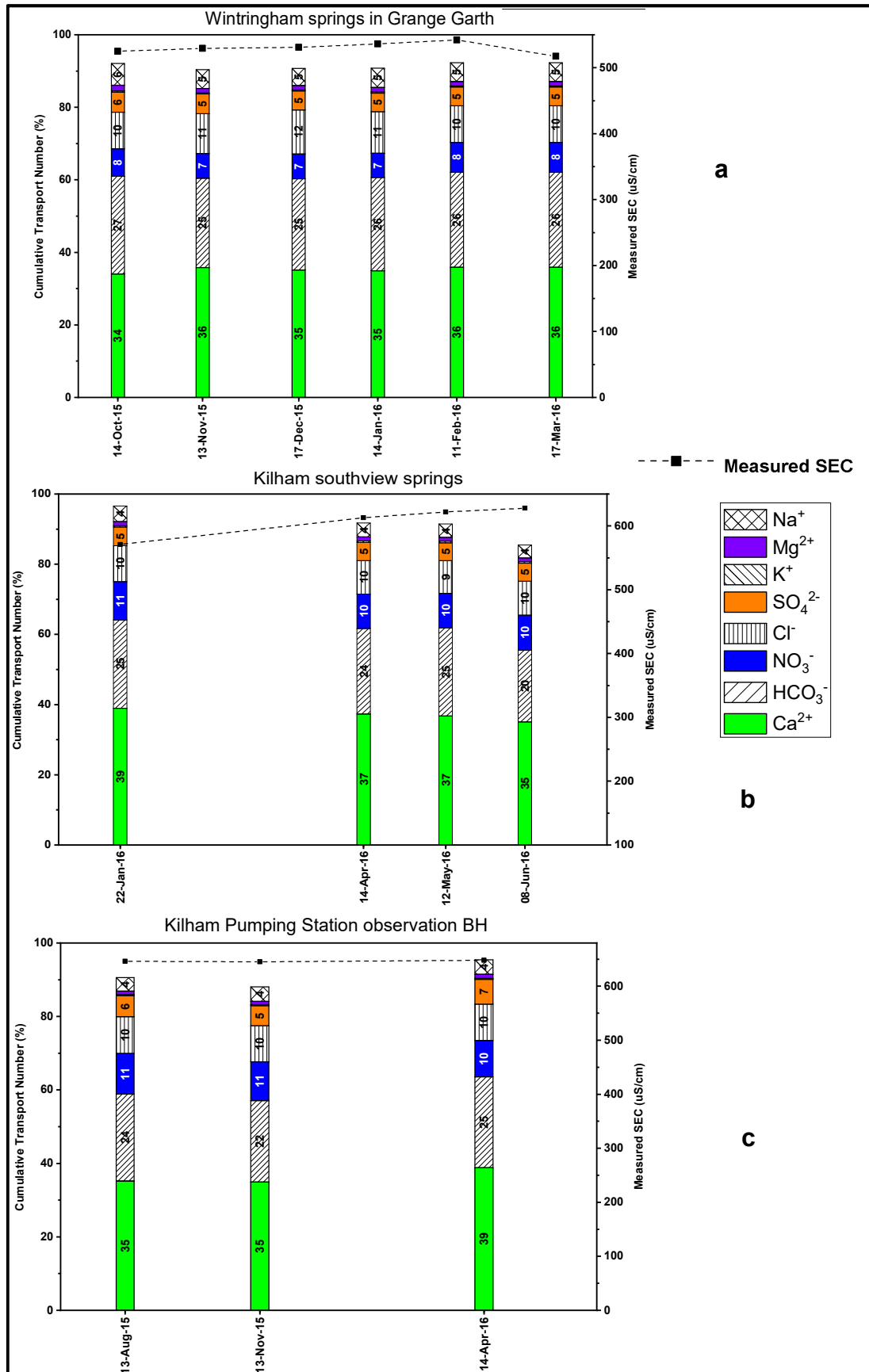


**Figure 5.18.** Measured SEC and transport numbers of EA dataset. (a) Wintringham springs at Grange Garth; (b) Kilham southview springs; (c) Kilham Pumping Station Observation borehole.

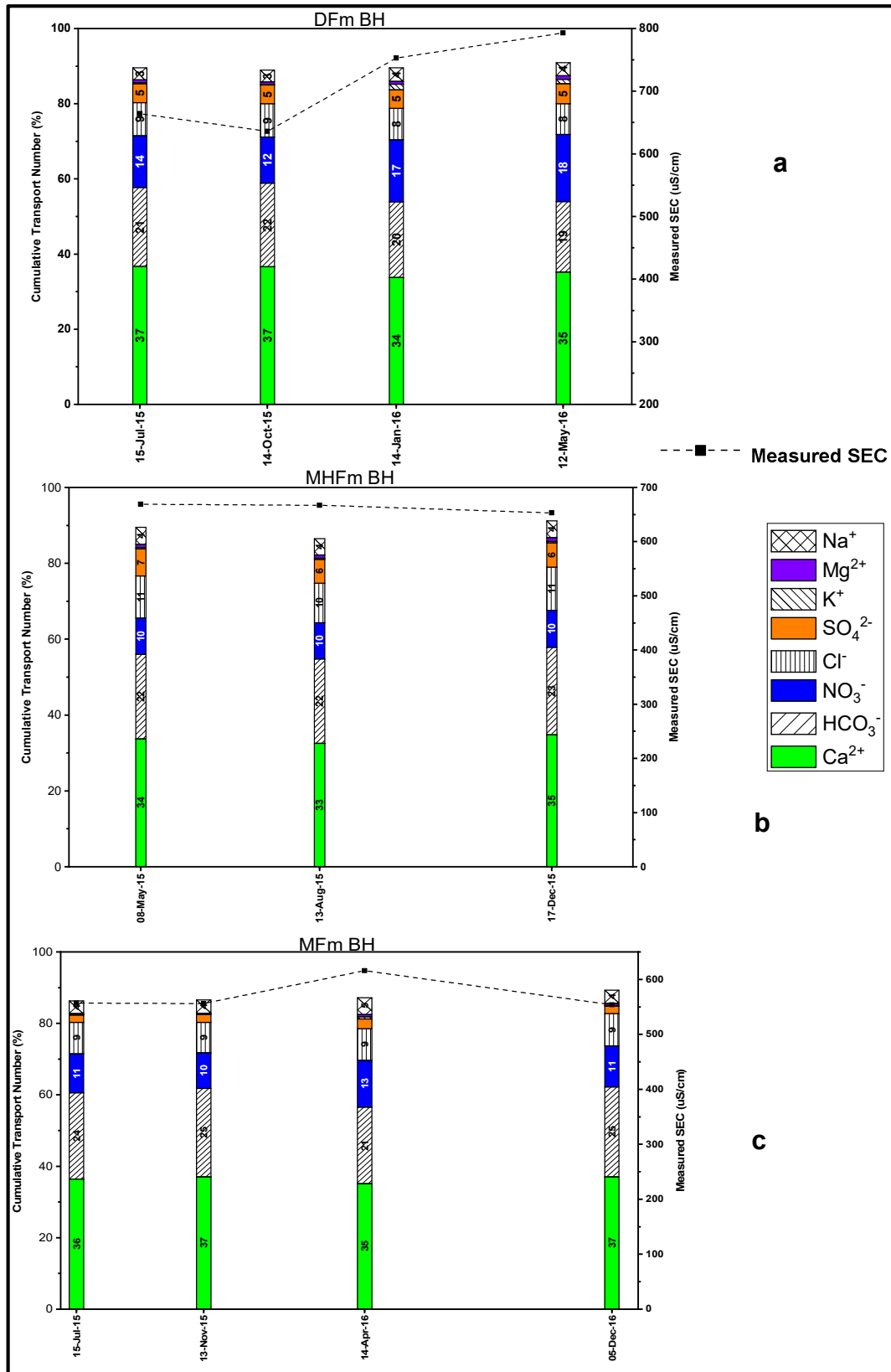


**Figure 5.19.** Measured SEC and transport numbers of EA dataset. (a) DFm; (b) MHFm; (c) MFm.

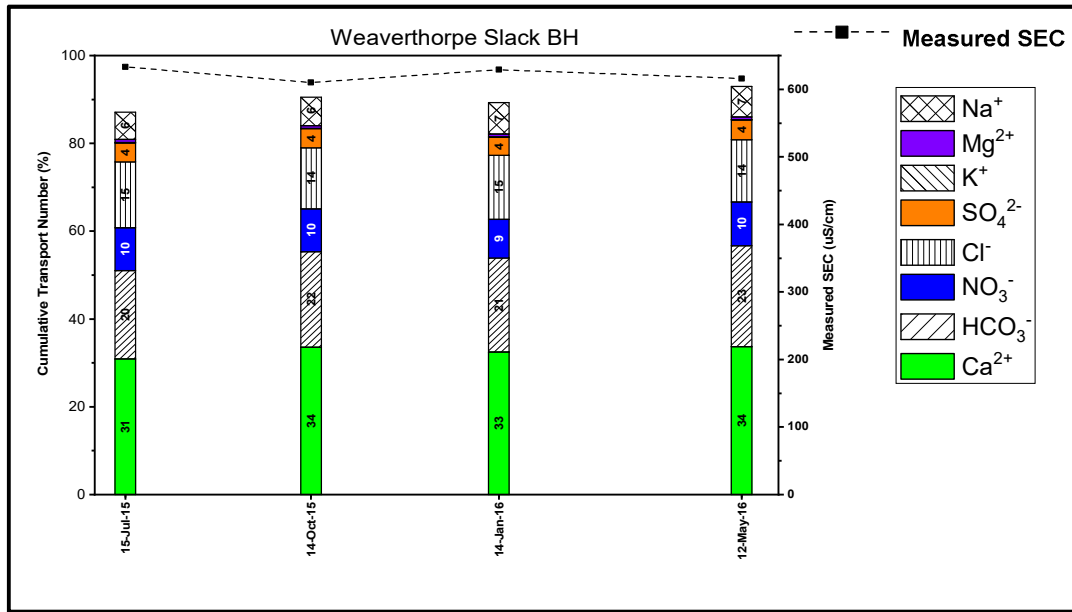


**Figure 5.20.** Measured SEC and transport numbers of EA dataset. Weaverthorpe Slack borehole.

at DFm. Grange Garth springs record relatively low SEC values and Ca<sup>2+</sup>+HCO<sub>3</sub><sup>-</sup> and NO<sub>3</sub><sup>-</sup> contributions in comparison to Place Newton springs, considering that they are in the same locality (Wintringham).

To summarise this subsection, it is noted that between and within the sampling sites, SEC variations and values are attributable mainly to Ca<sup>2+</sup>+HCO<sub>3</sub><sup>-</sup> and/or NO<sub>3</sub><sup>-</sup>, Cl<sup>-</sup>, SO<sub>4</sub><sup>2-</sup> variations at places.

A graph of measured SEC against calculated SEC for the 3 springs monitored for this study is presented in Figure 5.21. The springs segregate into two groups, falling above the 1:1 line and clustering around the +20% line. Bracey Bridge plots as 1 whereas Place Newton and Bellguy springs plot together in 2. Figure 5.22 shows the 3 springs plotted with the EA dataset. From Figure 5.22, the EA dataset falls above the 1:1 line, falling between the +20% and +10% lines. Combining the EA dataset and the three springs, the plots are segregated into three groups, marked as A, B and C. Group A contains Bracey Bridge and Grange Garth springs, which are intermittent suggesting flow from a relatively shallower and less confined groundwater system. Group B contains Place Newton, Bellguy and Kilham southview springs. The first two

springs are perennial, whilst the third is a seasonal discharge spring at Kilham suggesting that group B is characterised by relatively deeper flowpaths.

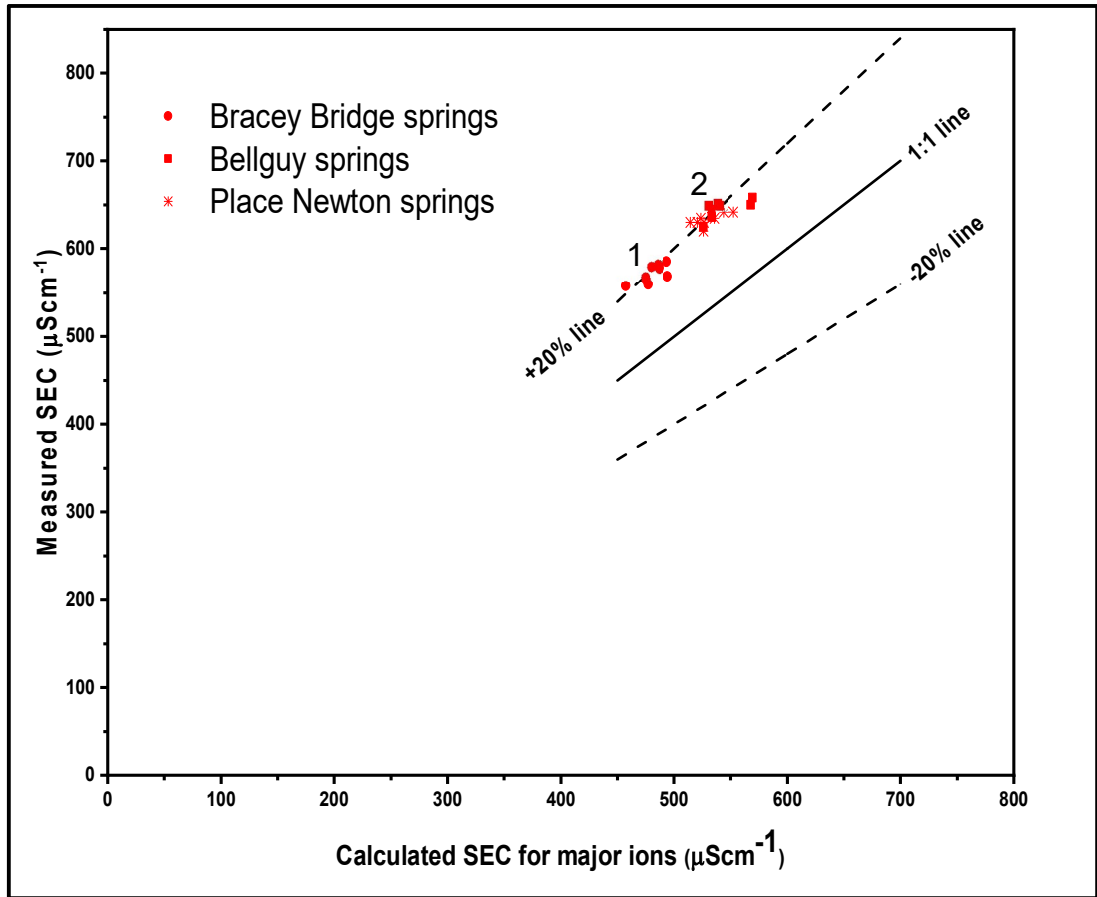


**Figure 5.21.** Graph of measured SEC versus calculated SEC of the major ions for the 3 monitored springs for this work.

Group C contains the two DFm samples with SECs resulting from high  $\text{NO}_3^-$  values (120 and 136 mg/L  $\text{NO}_3^-$ ) suggesting local anthropogenic input.

### 5.7.5 Spring sampling and monitoring discussion

$\text{Ca}^{2+} + \text{HCO}_3^-$  concentrations and dominance, and pH of the monitored springs are typical of unconfined chalk groundwater characteristics given by Smedley et al., (2004).  $\text{Ca}^{2+}$  and  $\text{HCO}_3^-$  concentrations for the monitored springs and EA dataset fall within Smedley et al (1994)'s concentration ranges of 62 - 218 and 130 – 347 mg/L respectively for the unconfined aquifer. The pH range (6.50-7.80) of water shows the spring discharge from an aquifer that is well buffered from rapid equilibration of recharge waters with aquifer matrix. Data from the monitored springs and EA data shows  $\text{Ca}^{2+}$  and  $\text{HCO}_3^-$  as the

most dominant major ions across and within the sites, demonstrating their control on the chemistry of the unconfined aquifer. The variability of  $\text{Ca}^{2+}$  and  $\text{HCO}_3^-$  probably reflects the  $\text{pCO}_2$  variation in the soil zone, and the degree of confinement of the aquifer from soil  $\text{pCO}_2$  interaction

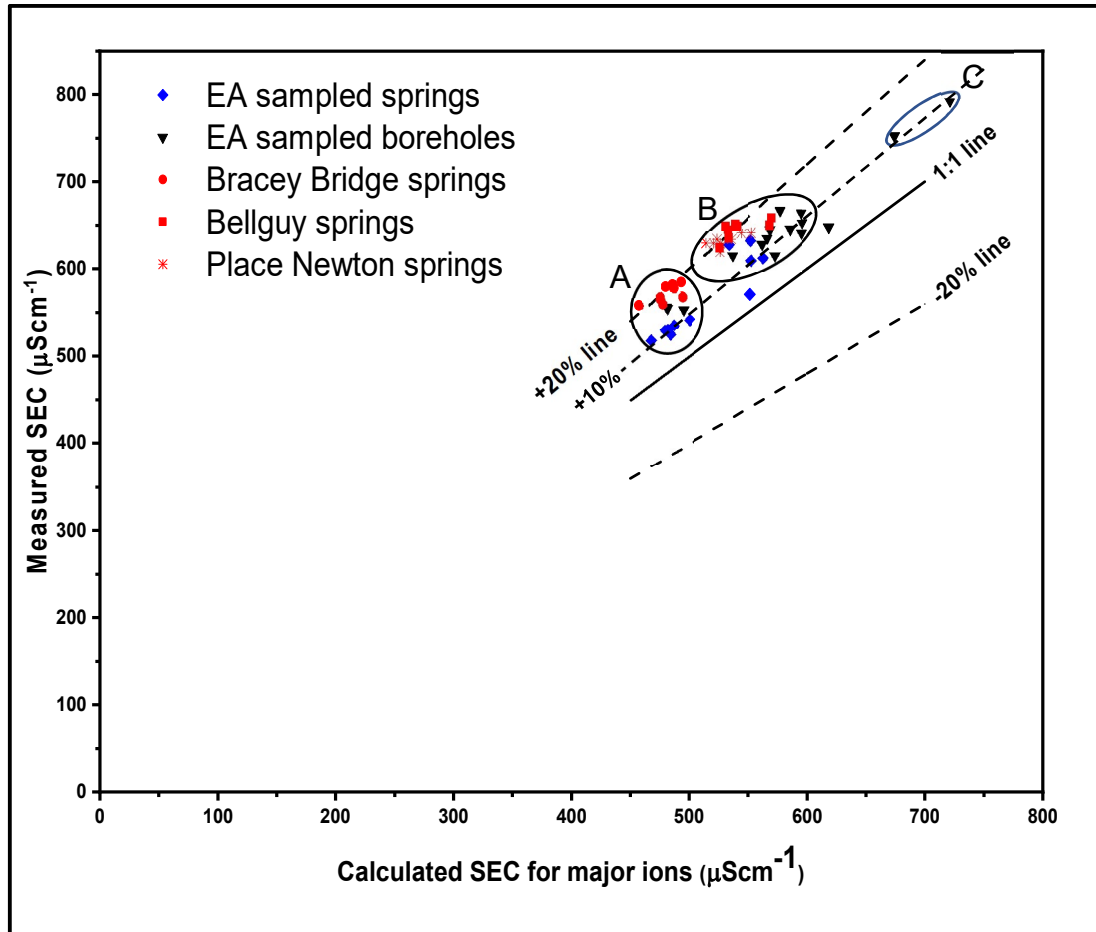


**Figure 5.22.** Graph of measured SEC versus calculated SEC of the major ions for the 3 monitored springs for this work (red) and EA dataset (blue and black).

and exchange. Within individual springs, seasonal  $\text{Ca}^{2+}$  and  $\text{HCO}_3^-$  variation is also attributable to mixing of water from different sources and residence times.  $\text{Ca}^{2+}$  and  $\text{HCO}_3^-$  as the most dominant ions are sourced from the dissolution of the  $\text{CaCO}_3$  limestone aquifer by recharging water.

The  $\text{NO}_3^-$  concentrations for all the monitored springs and the majority of the EA dataset exceed the 50 mg/L drinking water limit. Foster et al. (1982) found

$\text{NO}_3^-$  concentration of less than 9 mg/L on unfertilized land in the UK, suggesting that the  $\text{NO}_3^-$  concentrations found for this study are anthropogenically derived from agricultural activity, which is the mainstay of the catchment.  $\text{NO}_3^-$  comes not only from agricultural fertilizers but also from organic nitrogen loads and effluent discharge from pastureland soils. For the monitored springs, Place Newton springs consistently records the highest  $\text{NO}_3^-$  concentrations, which supports the assertion by Smedley et al (1994) that higher nitrate concentrations are found on scarp springs as compared to dip slope springs. This has been attributed to steep slopes with thin soils and rapid bypass flow to the scarp springs.  $\text{NO}_3^-$  above the drinking water limits has ecological, economic and resource management implications. Chalk fed springs that support flora and fauna in the catchment are at risk of eutrophication, resulting in adverse effects on the ecology. Consumers will also have to pay more for treatment and/or blending of water before supplying.

On the unconfined chalk,  $\text{Cl}^-$  and  $\text{SO}_4^{2-}$  are known to be derived from the same anthropogenic sources attributed to  $\text{NO}_3^-$  (Smedley et al., 2004).  $\text{K}^+$  and  $\text{Mg}^{2+}$  are the smallest of the major cationic elements.  $\text{K}^+$  is sourced from marls and other alkaline and alkaline earth-metals.  $\text{Mg}^{2+}$  is sourced from low-Mg calcite in the aquifer and also from fertilizers. On the unconfined chalk,  $\text{Na}^+$  concentrations are normally low and come from sea salts, application of road salts and marls.

The nitrates in the catchment serves as an excellent inorganic tracer. The  $\text{NO}_3^-$  concentrations show that the water is sourced from well oxygenated groundwater system. Also  $\text{NO}_3^-$  is known to leach in late autumn when soil nitrification is followed by excess rainfall (Foster, 2000), but the sampling rounds could not detect the seasonal leaching groundwater, as the samples showed constant  $\text{NO}_3^-$  concentrations within the monitoring period.

Comparing the current chemistry with results of EA 2015/16 sampling programme dataset shows a groundwater system with similar chemistry. This homogeneity is suggestive of a well defined groundwater chemistry of recharge water from rapid equilibration with the aquifer material in the unsaturated zone or an aquifer with enough mixing in the saturated zone, leading to a masking of variations in recharge input signals. In spite of rapid

bypass flow shown in the unsaturated zone, Pitman (1978) on the Northern Province Chalk and Edmunds et al. (1987), Darling and Bath (1988) and Van den Daele et al. (2007) on the Southern Province Chalk used lysimeters to show a leachate with a well-defined chalk-like chemistry a few meters below the surface, suggesting that the chemistry of recharge water is well defined before it gets to the water table.

Measured and calculated SEC also showed  $\text{Ca}^{2+} + \text{HCO}_3^-$  dominance in the catchment. SECs in the aquifer do not vary much but are controlled mainly by  $\text{Ca}^{2+} + \text{HCO}_3^-$  and in some areas with high  $\text{NO}_3^-$ . The  $\text{NO}_3^-$  effect is shown in segregation of DFm on the measured and calculated SEC plot with  $\text{NO}_3^-$  concentrations of 115 and 133 mg/L suggesting that the use of the combined plot of measured and calculated SEC is a useful way of detecting contamination above the current  $\text{NO}_3^-$  concentrations.

## 5.8 Chapter summary

This chapter sought to use well hydrographs, spring and well monitoring to determine the water source and type of flow in the aquifer. It was found that:

- Borehole hydrographs show similar rising and falling limb patterns with increased amplitude variation with distance from outflow.
- Foston Beck is fed mainly by groundwater as Foston Mill gauging station hydrograph mimics groundwater hydrographs amidst flashes typical of a surface water feature;
- Springs and borehole temperature are reflective of average annual ambient temperature, with relatively low variability in comparison with air temperature during the monitoring period;
- Relatively stable spring and groundwater temperature indicates a local groundwater system that is thermally equilibrated with rock temperature;
- Thermally equilibrated groundwater is suggestive of high Stanton Number,  $St_t$ , indicative of an aquifer geometry with diffuse recharge characteristics and relatively long residence time;

- Tancred Pit borehole temperature is stable for the monitoring period and does not show any phase relation to that of seasonal ambient air patterns;
- Spring temperature show some small variation in comparison to Tancred Pit borehole, with longer term variation that is out of phase with ambient temperatures with thermal lags of several months for maximum and minimum temperatures for the monitoring period;
- Tancred Pit borehole showed a non-varying SEC log signature whereas the monitored springs showed variation in the SEC log most likely due to difference in the depths of monitoring;
- Monitored springs recorded some extremes of SEC, possibly due to noise on the sensor logger from local surface effects;
- Place Newton spring (scarp spring) shows a more rapid but small amplitude flashy temperature pattern that mimics a dampened form of ambient air signals, in comparison to Bellguy spring that only shows this behaviour for the initial few months of monitoring (autumn);
- Chemistry of springs and boreholes is dominated by  $\text{Ca}^{2+}$  and  $\text{HCO}_3^-$  which mostly varies due to factors such as  $\text{pCO}_2$  variation and unsaturated thickness that drive the carbonate process;
- $\text{NO}_3^-$  concentrations are above the drinking water limit, indicative of groundwater system sourced from the aerated zone of the aquifer;
- The concentrations and plot of transport numbers and measured SECs show an aquifer of similar chemistry with masking of the variation of the input signals;
- SECs at the springs do not vary much but are controlled mainly by  $\text{Ca}^{2+} + \text{HCO}_3^-$  and in areas with high  $\text{NO}_3^-$ ;
- Analysing measured and calculated SEC for major ion was useful in detecting contamination beyond the current  $\text{NO}_3^-$  levels in the unconfined aquifer.

## **Chapter 6 Saturated zone flow pattern characterisation using evidence from flow zone characterisation and previous tracer tests**

Results of the ambient open-well dilution tests and spring and well monitoring which are the main methods used in this current study are presented in Chapters 4 and 5 respectively. Relevant previous works undertaken in the Kilham Catchment were presented in Chapter 3. This current Chapter seeks to characterise saturated zone flow mechanisms from flow horizons characterisation and previous tracer test results. The results from this chapter will be used in conjunction with findings from other chapters to develop a conceptual model of flow for the catchment in (Chapter 7). The chapter starts by marking flow horizons in boreholes on hydrogeological cross-sections. Then previous tracer tests are re-interpreted in the light of the flow horizons to describe flow mechanisms in the catchment. After which a parallel fracture flow model work flow will be implemented in the Little Kilham borehole to determine average horizontal groundwater velocities to validate open-well dilution tests. Finally, pumping tests and transmissivity distributions in the Kilham area are presented to support the karstic flows observed in re-analysed tracer tests.

### **6.1 Geophysical logs, open-well dilution and tracer tests for determining flow connection of wells and springs**

As presented in chapters 3 and 4, previous geophysical logging, open-well dilution and tracer tests have been done in the Kilham Catchment. In this section, wells which were open-well dilution tested in this current study and have also been previously researched in and between the Broachdale and Langtoft Valleys are presented. Figure 6.1 shows the Langtoft and Broachdale Valleys and the relative locations of the wells in the Kilham area to be discussed in this section. The Langtoft and Broachdale Valleys are typical of the dry and steep sided valleys that dissect the Wolds. An interfluvium separates the Broachdale and Langtoft Valleys, reducing in elevation with the two valleys converging onto Kilham to discharge Chalk water via the intermittent springs

that form the Lowthorpe Beck. The Lowthorpe Beck and other springs further South of Kilham like Bellguy, Bracey Bridge and Harpham form the major source of the Foston Beck, which is one of the two main tributaries of the River Hull.

This current section is divided into three parts. Firstly, the possible and confirmed flow horizons and flow mechanisms for boreholes identified from different studies are marked on cross-sections developed from the BGS geindex and Edina digimap database (see section 3.3.1). The synthesis of the flow horizons from the different well characterisation has been done with the aim of constraining flow and permeability variation with depth. Secondly, tracer test results from Ward and Williams (1995); Ward et al. (1998) and Ward et al. (2000) are re-interpreted using the possible flow horizons to show flow topology and connection between boreholes. Then the flow topology is contextualised and re-interpreted in terms of the geological and hydrogeological framework of the study area. Finally the well flow horizons and tracer interpretation from the preceding activities are used to characterise flow patterns for the cross-section.

### **6.1.1 Flow in the Langtoft Valley**

The wells analysed in the Langtoft Valley are the Henpit Hole, Middledale and Little Kilham Farm boreholes. The two boreholes found at Henpit Hole are a 200 mm diameter x 65 m deep (B4) and a 100 mm diameter x 45 m deep (B5), which are 32 m apart. Middledale is 200 mm diameter x 55 m deep, whereas Little Kilham Farm is 200 mm diameter x 50 m deep. Figure 6.2 shows the possible and detected flow horizons identified by previous investigations in the Langtoft Valley marked by arrows.

As has been introduced in section 3.2, Buckley and Talbot (1994) indicated provisional flow horizons (Figure 6.2) based on wellbore and fracture enlargements. However, not all diameter and fracture enlargements could be hydrologically significant as borehole diameter enlargements could also result from splicing out of hard and resistant layers like flints and marls from well drilling (Paillet, 2004; Farrant et al., 2016). The flow zones identified by Southern Science (1994) (see section 4.3.1) from borehole CCTV images and caliper logs are also marked. On horizons where strong flows are imaged, it

is easy to analyse and constrain the flow horizons. However, borehole CCTV images are difficult to interpret due to their qualitative nature. Secondly if CCTV images are undertaken immediately after other well logging activities, false flows otherwise attributed to the disturbance of other logging activities

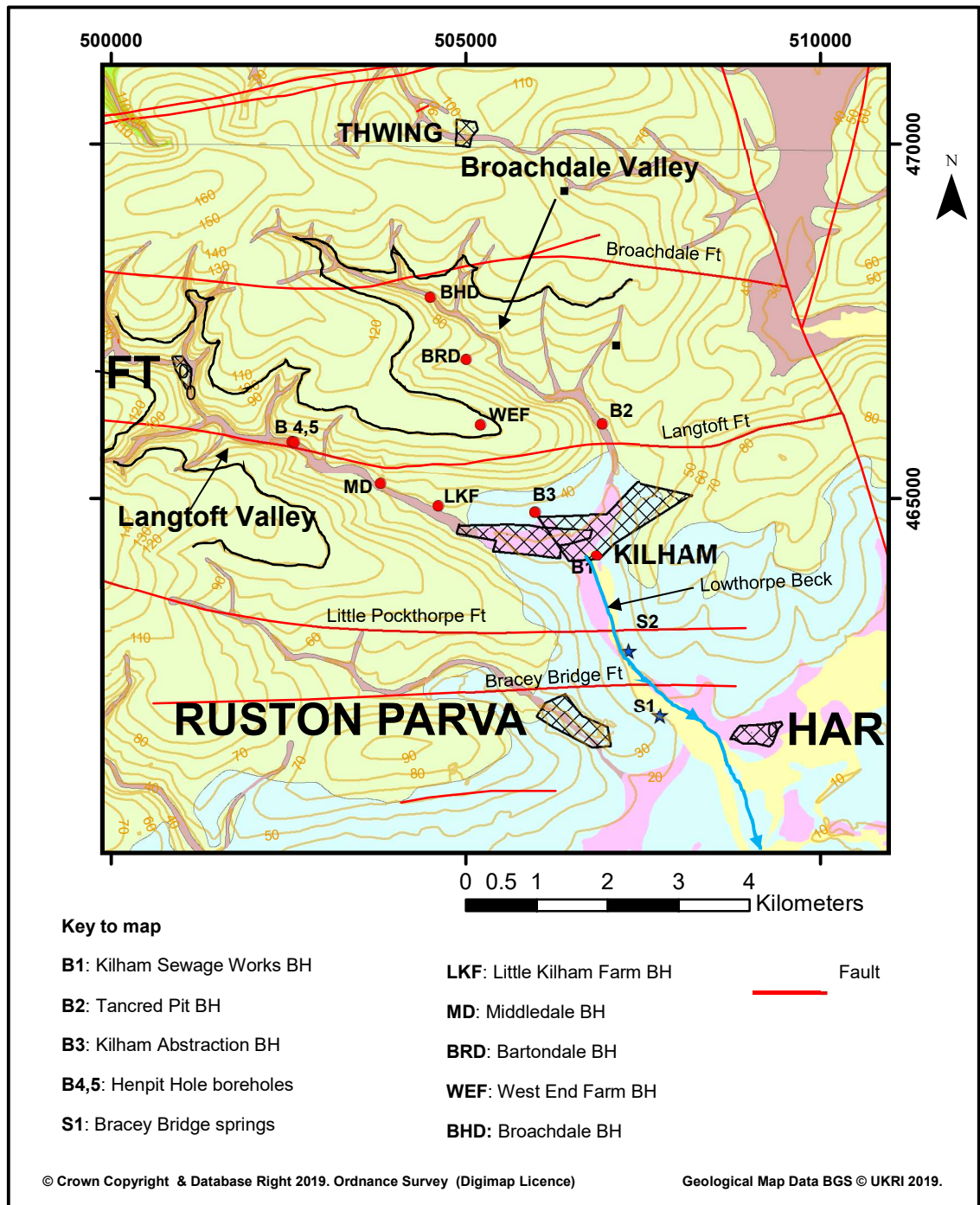


**Figure 6.1:** Boreholes flow tested and tracer tested in Langtoft and Broachdale Valleys and Kilham on geology. Contour 100 m outlined in black to show the two valleys.

could be misinterpreted. Therefore in interpreting results from CCTV imagery, logging sequence information is required. Also, not all identified flow horizons imaged are hydrologically significant or active. Flow identification by Parker (2009) from ambient uniform open-well dilution tests and flow logging have also been indicated showing the inflows, outflows and vertical flows in the wells.

In spite of the weaknesses of the borehole logging methods, an effective way of identifying and constraining the flow zones and active hydrological zones is by correlating zones of flow features from multiple well tests (Keys, 1990; Paillet and Pedler, 1996). The identified flow zones using ambient uniform and point ambient open-well dilution tests are also marked.

As shown in Figure 6.2, boreholes in the Langtoft Valley have discrete flow horizons distributed within the zone of enhanced permeability in the zone of groundwater table fluctuation and at deeper depths. In the Henpit Hole boreholes, there is also strong upflow from the bottom of the borehole, outflowing at the zone of enhanced permeability at the bottom of the casing. The deeper flow zones tap regional recharge pathways, with relatively high hydraulic heads which drive flow up the borehole. The valley location of Henpit Hole drives both local and regional flows towards it. Middledale and Little Kilham Farm boreholes are dominated by strong sub-horizontal flow on bedding features. Vertical flow in Middledale and Little Kilham Farm boreholes is not dominant probably due to the location of the boreholes on valley flanks.

Tracer tests have the advantage of overcoming the weakness of the limit of scale of investigation for borehole tests for heterogenous and anisotropic aquifers like the Chalk (Ward and Williams, 1995; Singhal and Gupta, 1999). Ward and Williams (1995) and Ward et al. (1998) used the provisional flow horizons from Buckley and Talbot (1994), Southern Science (1994) and Ward et al. (1998) to conduct tracer tests for the Kilham catchment. Figure 6.3 shows the borehole and spring connectivity from the tracer tests, the details are presented for the wells below.

Ward and Williams (1995) injected Photine CU tracer at 18.86 mAoD at 65 m deep Henpit Hole borehole, and was initially detected after 18 hours of

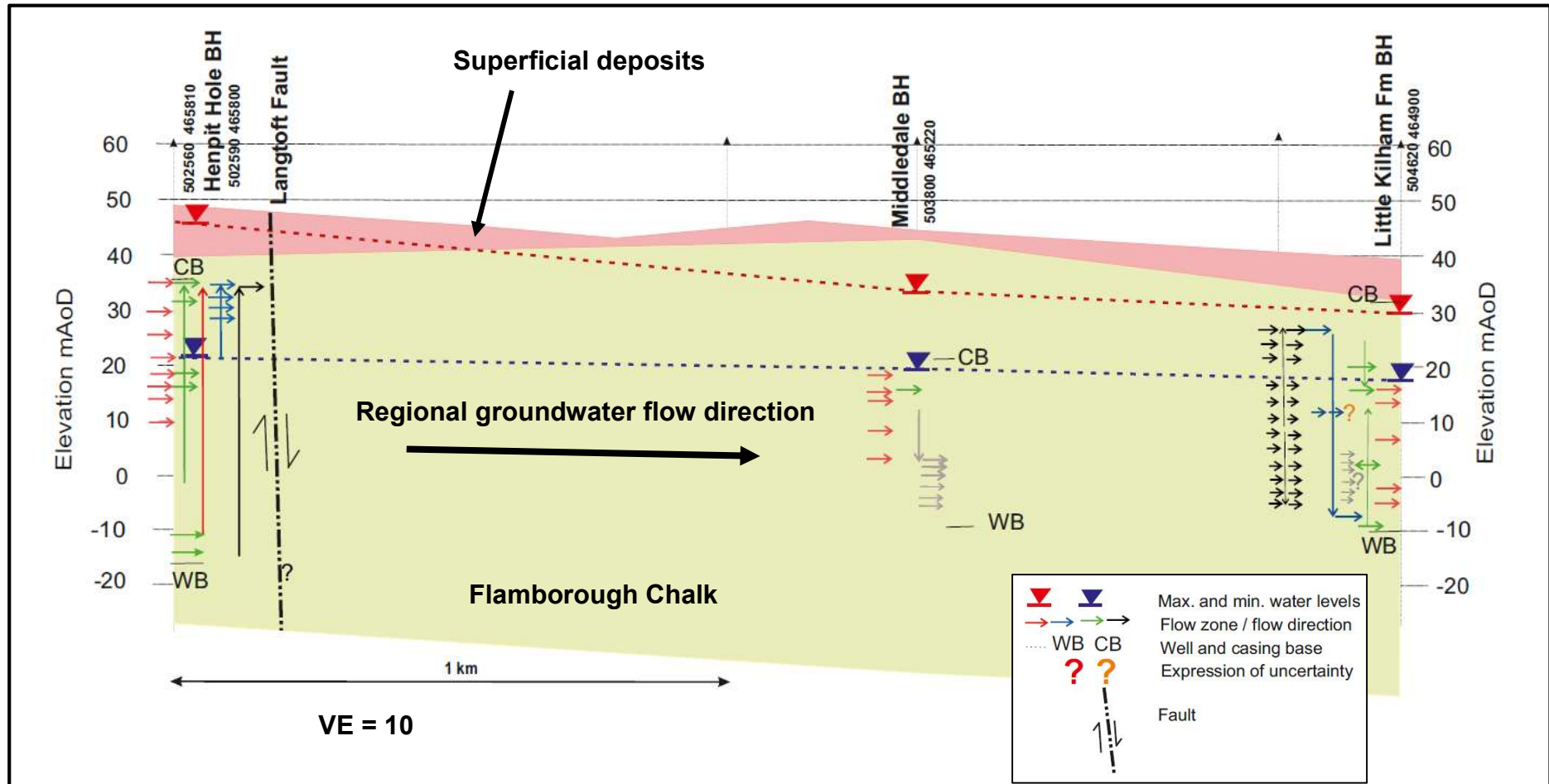


**Figure 6.2:** Possible and detected flow horizons and directions arrowed in boreholes in the Langtoft Valley. Flow horizons identified by Buckley and Talbot (1994)-red, Southern Science (1994)-green, Parker (2009)-blue, Ward et al. (1998)-grey and the current study-black.

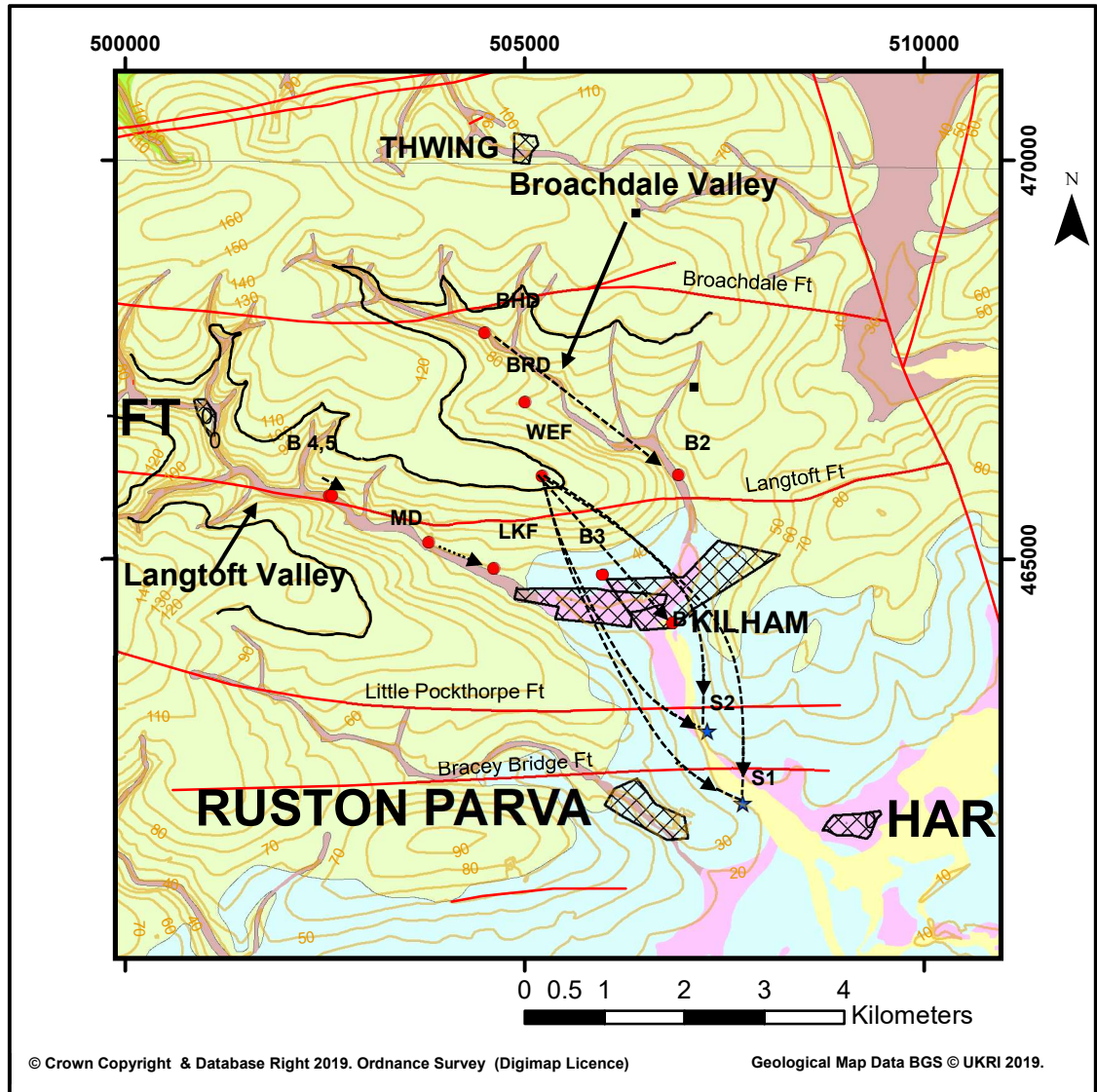


**Figure 6.3.** Map of borehole and spring connectivity in the Kilham area from Ward and Williams (1995), Ward et al., (1997;1998) tracer tests. Black dash arrowed lines show connectivity between wells determined via tracer tests. Tracer injections at Henpit Hole (200 mm), Middledale (MD), Broachdale (BHD), West End Farm (WEF) boreholes.

injection at 45 m deep Henpit Hole borehole at depths 18 and 35 mAoD (Figure 6.4 and Figure 6.5), with the tracer continuously detected for 2 months at the sampling points resulting in an early arrival groundwater velocity of 43 m/day. But the injected tracer was not detected at Middledale and Little Kilham Farm boreholes.

Because of the upward flow already discussed in both Henpit Hole boreholes, for the tracer to be detected at 18 mAoD in the sampling borehole suggests

outflow on bedding parallel flow features across from the 65m injection borehole to the 45 m sampling borehole in the Henpit Hole area. Determining how the tracer got to be detected at 35 mAoD is fraught with uncertainty as the tracer has several routes through which to get to be detected in the sampling well (Figure 6.4). Firstly, because of the upward flow that exits at around depth 34 – 35 mAoD in the injection borehole, part of the injected

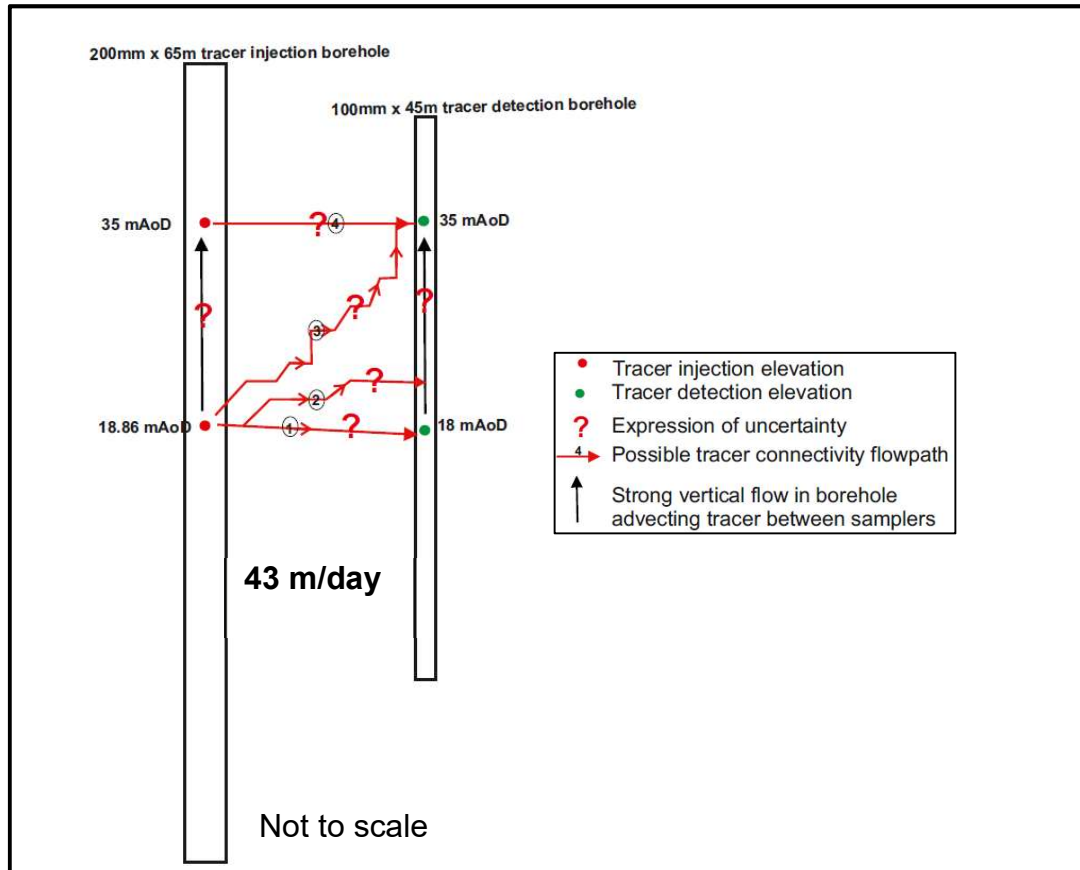


**Figure 6.4.** Borehole tracer connectivity topology between 65 m deep and 45 m deep Henpit Hole boreholes. Probable flow routes marked: (entirely along strata: 1,4; travel along intermediate routes: 2,3).

tracer can move upwards, exiting the injection borehole at around 35 mAoD and moving across bedding to the detection borehole (route 4). Secondly, tracer already detected at depth 18 mAoD in the sampling borehole could also move upwards within the borehole and be detected at 35 mAoD (route 1). Thirdly, tracer detected at 35 mAoD could be passing via intermediate routes (routes 2 and 3 Figure 6.4) of linked bedding parallel and inclined flow pathways. A combination of routes is evidenced by diffused or dispersed tracer i.e. the long tracer profile tail after the initial tracer arrival.

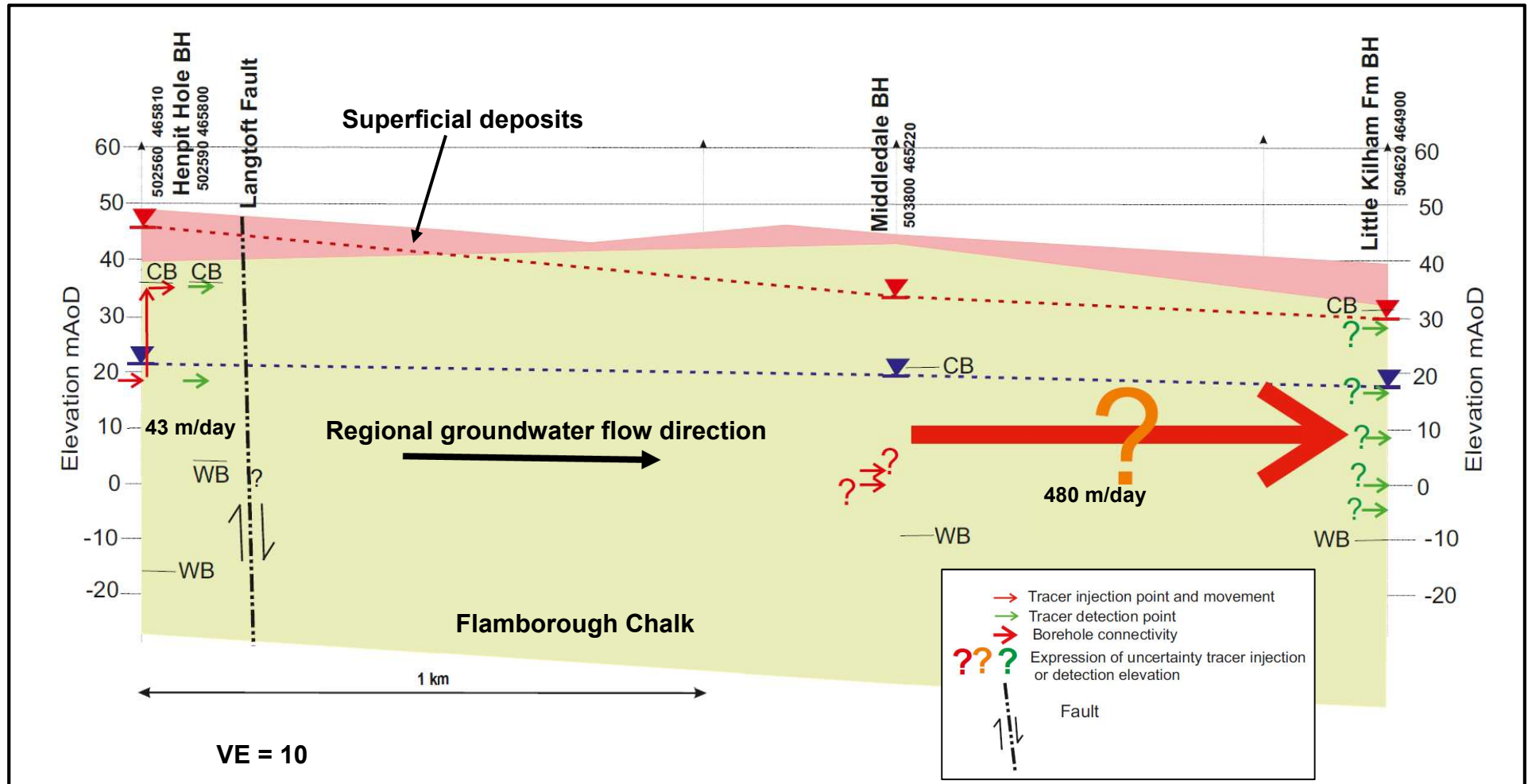


**Figure 6.5.** Cross-section of the results of tracer tests and borehole connectivity in the Langtoft Valley, from Ward and Williams (1995); Ward et al. (1998). Connection between two Henpit Hole boreholes (40 m/day).

The upward flows from deeper depths towards the top of the open sections of wells are indicative of deeper flows from zones of higher hydraulic head. These zones of higher hydraulic heads are suggestive of a developed zone of solutional enhancement that is fed by waters of longer flow paths from topographically higher recharge areas. This is in agreement with the Toth (2009) model of gravity and topographically driven flows, which would not have been apparent here without the presence of the Henpit Hole wells in the valley.

Using the tracer characteristics and the stratal dip of the area, the factors controlling flow in the Langtoft Valley are now discussed. Using the contact surface of the Flamborough and Burnham formations in the Langtoft and Kilham area yields an average dip angle of  $2^\circ$ . Assuming the tracer in the late 1990s test injected into the deeper Henpit Hole borehole to be entirely stratigraphically constrained and flowing along dip towards Middledale and Little Kilham boreholes, then tracer would be expected at approximate depths -29 and -60 mAoD at those two well locations respectively. However, a look at the factors that affect flow to depth in the context of the aquifer under study will show that these depths are theoretical, and that the tracer would likely be detected at relatively shallower depths had there been a connection between Henpit Hole and Middledale and Little Kilham Farm boreholes. Worthington (2004) shows that the factors that encourage flow entirely on strata are steep stratal dips, lack of open and conductive vertical flow features, longer flow paths and higher hydraulic heads. In the study catchment, the stratal dip of  $2^\circ$  is a relatively low gradient and the inclined and vertical flow features have been shown to be communicative both in the unsaturated (Zaidman et al., 1999; Allshorn et al., 2007; Keim et al., 2012) and saturated zones (Ward and Williams, 1995). Also there is no obvious preferred joint orientation and anisotropy in the Chalk. The low stratal gradient will encourage majority sub-horizontal flow with flows criss-crossing bedding features via upwards or downwards communicative flow features towards discharge zones that have been solutionally enhanced like the Kilham and the artesian zone area (Buckley and Talbot, 1994). The overall effect of this flow pattern is flow down dip, then up or down vertical flow features, which will result in stepped up flow patterns in the area.

With the discussion above then, the tracer might be expected to have been detected at the Middledale and Little Kilham boreholes. One reason which may account for non-tracer detection could be the possible mixing, dilution and dispersion of tracer as tracer approached Middledale and Little Kilham considering the diffuse nature of flow demonstrated by the tracer profile between the Henpit Hole boreholes. Also, another explanation is that Henpit Hole is not on the same flowpath as Middledale and Little Kilham Farm boreholes because of the diversion of flowpaths as the tracer crossed the Langtoft fault.

Another tracer test was undertaken by Ward and Williams (1995) to establish a link between Middledale and Little Kilham Farm boreholes. The flow topology diagram between the two boreholes is shown in Figure 6.6. Tracer injected between depths 0 – 2.7 mAoD in Middledale borehole was detected at Little Kilham Farm borehole, possibly between -5 to 5 mAoD. Ward et al. (1997) found a conservative fast groundwater velocity of 480 m/day from first tracer arrival time of 45 hours after tracer injection as the boreholes are 900 m apart. Sampling is probably within the open section of the borehole with 0 mAoD as a likely sampling and detection point. This is because the report did not specify 0 mAoD as a detection point in Little Kilham Farm borehole, although another tracer test to investigate connection between Little Kilham Farm and springs in the Kilham area had tracer injected at 0 mAoD. Farrant et al. (2016) also state that the tracer was detected at four locations in Little Kilham Farm, which supports a dominant sub-horizontal diffuse flow pattern via several routes along solutionally enhanced fissured bedding features connected by vertically communicating features across different strata (Figure 6.6).

Following the previous borehole logging tests, tracer was injected at depth 0 mAoD in Little Kilham Farm borehole, but was not detected at Kilham Abstraction and Kilham Sewage Works boreholes, Bellguy and Bracey Bridge springs. Due to the heterogenous and highly fractured nature of the aquifer, the tracer could have either flowed around or under the sampling points. Alternatively, towards the Kilham area springs, the tracer could have been

diluted beyond the detection limit of the samplers because of flow convergence and increased discharge. In addition, the tracer could have also

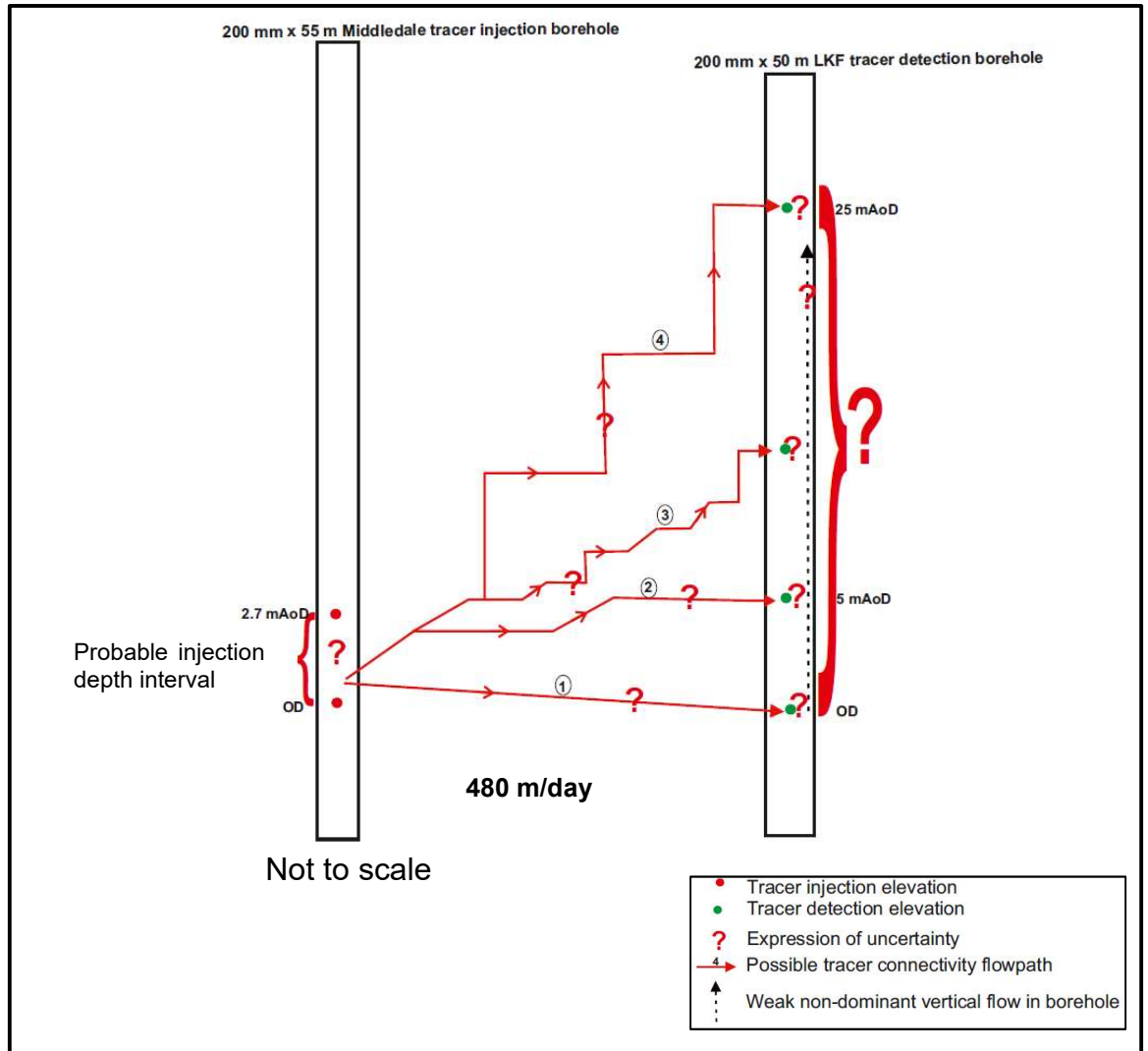


**Figure 6.6** Borehole tracer connectivity topology between Middledale and Little Kilham Farm boreholes. Four depths at which tracer was detected in Little Kilham Farm borehole (Farrant et al.,2016). Flow connectivity between two boreholes may be via two bedding parallel pathways: entirely on strata (1); or combination of parallel strata and vertically communicating features (2,3,4)

moved towards any of the numerous discharge springs in the Kilham area should they have been flowing.

Groundwater flow between Middledale and Little Kilham Farm boreholes is characterised by rapid and fast concentrated diffuse groundwater flow towards the Kilham area, with the dominant flow zones along the zones of



solutionally enhanced fissures, located in the water table fluctuation zone. The dominance of horizontal or sub-horizontal flow from dilution and tracer tests in both Middledale and Little Kilham Farm boreholes is probably due to two reasons. This could be as a result of the location of the two boreholes as zones of enhanced and developed transmissivity from convergent flow towards Kilham. Another reason could be the relative position of the wells as lateral flow zones between recharge and discharge zones in the study area.

Using the flow zones and tracer test results and discussions above, the flow pattern in the Langtoft Valley is synthesized in Figure 6.7. The flow is dominated by recharge and discharge points, in consonance with the Tothian catchment flow model. The Henpit Hole area is characterised by deeper zones of developed hydraulic conductivity with relatively higher hydraulic heads due to their connection to topographically higher recharge areas. These hydraulic heads drive upflow because of the open nature of the borehole. Also, groundwater flow is along discrete flow horizons, that are linked by vertically communicating flowing features. Between the Middledale and Little Kilham Farm boreholes, flow is dominated by lateral horizontal flows on bedding flow features, with criss-crossing flow between strata from vertical communicating flow features.

### **6.1.2 Flow in the Broachdale Valley**

The wells analysed in the Broachdale Valley are the Broachdale, Bartondale and Tancred Pit boreholes. Broachdale borehole is a 200 mm diameter x 85 m deep located at a relatively higher elevation in the Broachdale Valley (Figure 6.1). Tancred Pit on the other hand is 200 mm diameter x 50 m deep, located at a lower elevation in the Valley. The Bartondale borehole is a 200 mm diameter x 70 m deep borehole located on the Broachdale Valley flank, and between Broachdale and Tancred Pit boreholes. The cross-section of the Broachdale Valley between Broachdale and Tancred Pit boreholes showing flow horizons from previous studies and the current study is shown in Figure 6.8.

As compared to Tancred Pit, only a few previous studies have been done in Broachdale borehole. A review of archived caliper logs shows solutionally enlarged diameter between 58 mAoD and the bottom of the well. There is no

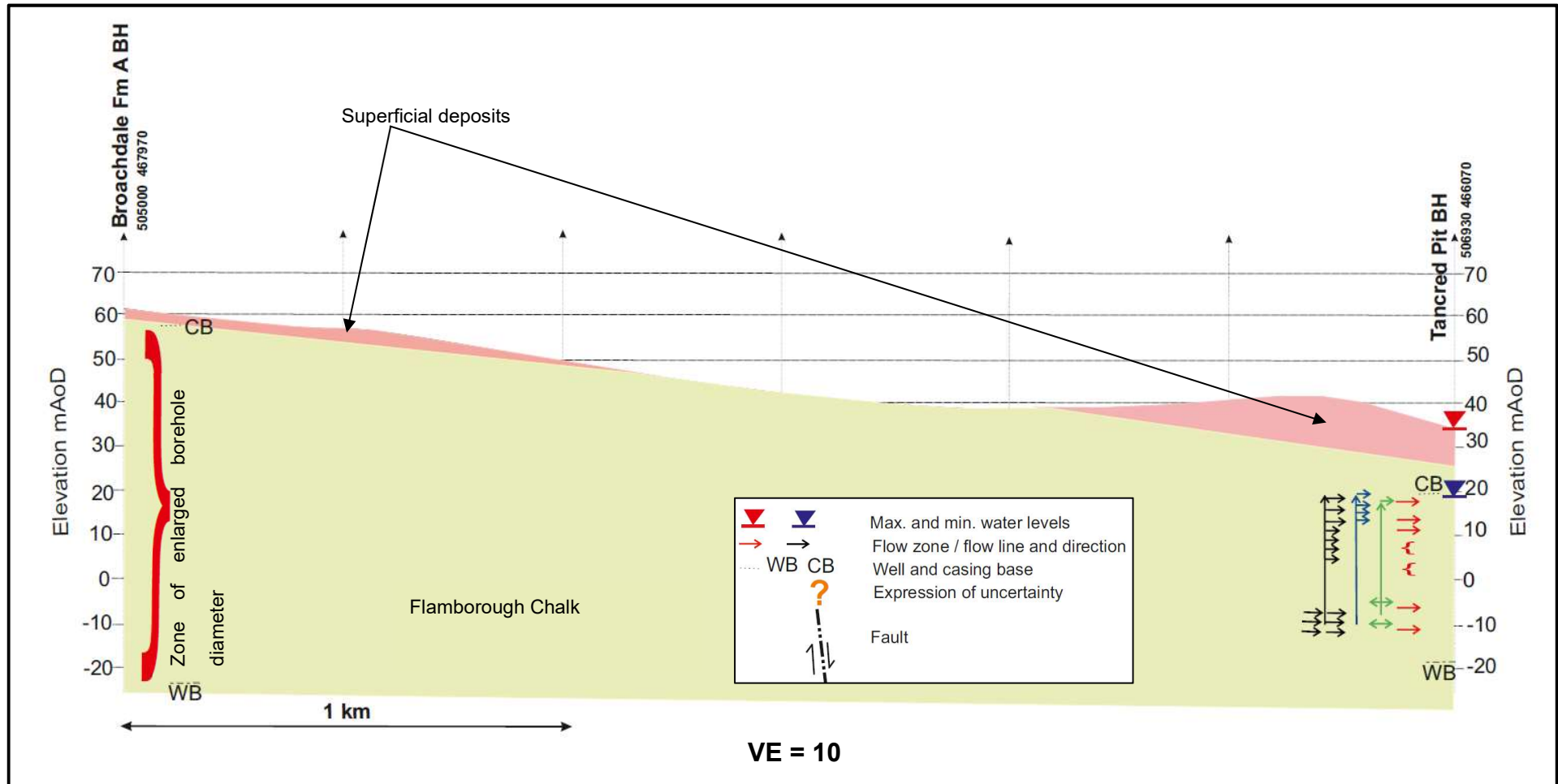


**Figure 6.8.** Possible and detected flow horizons and directions in boreholes in the Broachdale Valley from previous and current studies. Buckley and Talbot (1994)-red, Southern Science (1994)-green, Parker (2009)-blue and the current study respectively-black.

information on the nature of horizontal and vertical flows in the well. Tancred Pit borehole is characterised by discretely developed permeability at deeper depth and within the zone of water table fluctuation. Permeability at depth taps regional recharge flows, with relatively high hydraulic head driving flow up the well to discharge at shallow levels or by artesian overflow (Figure 6.8).

A tracer test conducted in the Broachdale Valley established a link between the Broachdale and Tancred Pit boreholes, but not with Bartondale (Ward and Williams, 1995). The flow topology and cross-section of the fluorescein tracer test in the Broachdale Valley are shown in Figure 6.9 and Figure 6.10 respectively. Tracer was injected at depth 28.78 mAoD in Broachdale borehole, with sampling at Bartondale borehole (TA 050 669) and Tancred Pit borehole at depths 0, 12, 18 mAoD in the borehole and ground surface at Tancred Pit spring.

Tracer was detected at Tancred Pit borehole at all 3 sampling depths, but not at Tancred Pit springs confirming that the Tancred Pit and Broachdale boreholes are on the same flow path. The tracer appeared in Tancred Pit borehole in two distinctive pulse arrivals at 11 and 18 days, with tracer tailing effects. The groundwater velocity from the initial and later arrivals are 250 and 150 m/day respectively. The arrival of two tracer pulses suggests the possibility of two different flow paths, with the later arrival travelling via a relatively deeper and or longer flow path in comparison with the earlier arrival. The tailing of the tracer pulses also suggests diffuse and dispersed flow paths from Broachdale borehole to Tancred Pit. The positive trace result over the longer flow path of about 3 km shows that tracer detection is possible over this distance in Chalk and contrasts with flow in the Langtoft Valley. The difference in connectivity between the two Valleys may be because of convergent flow towards Tancred Pit borehole, due to its Valley location and nearness to the spring.

There is the question of whether the tracer injected at Broachdale borehole entered the Tancred Pit well at the individual sampling points or from the well bottom (-12 to -7 mAoD), then moved upwards to be detected by the sampling points. From the evidence from section 4.3.1 on Tancred Pit borehole, the borehole is characterised as having inflow that enters at depth between -12 to -7 mAoD, with a component crossing the well and exiting at that depth, but with a component of flow moving up the well and exiting the well at between 15 mAoD and the casing base at 20 mAoD.

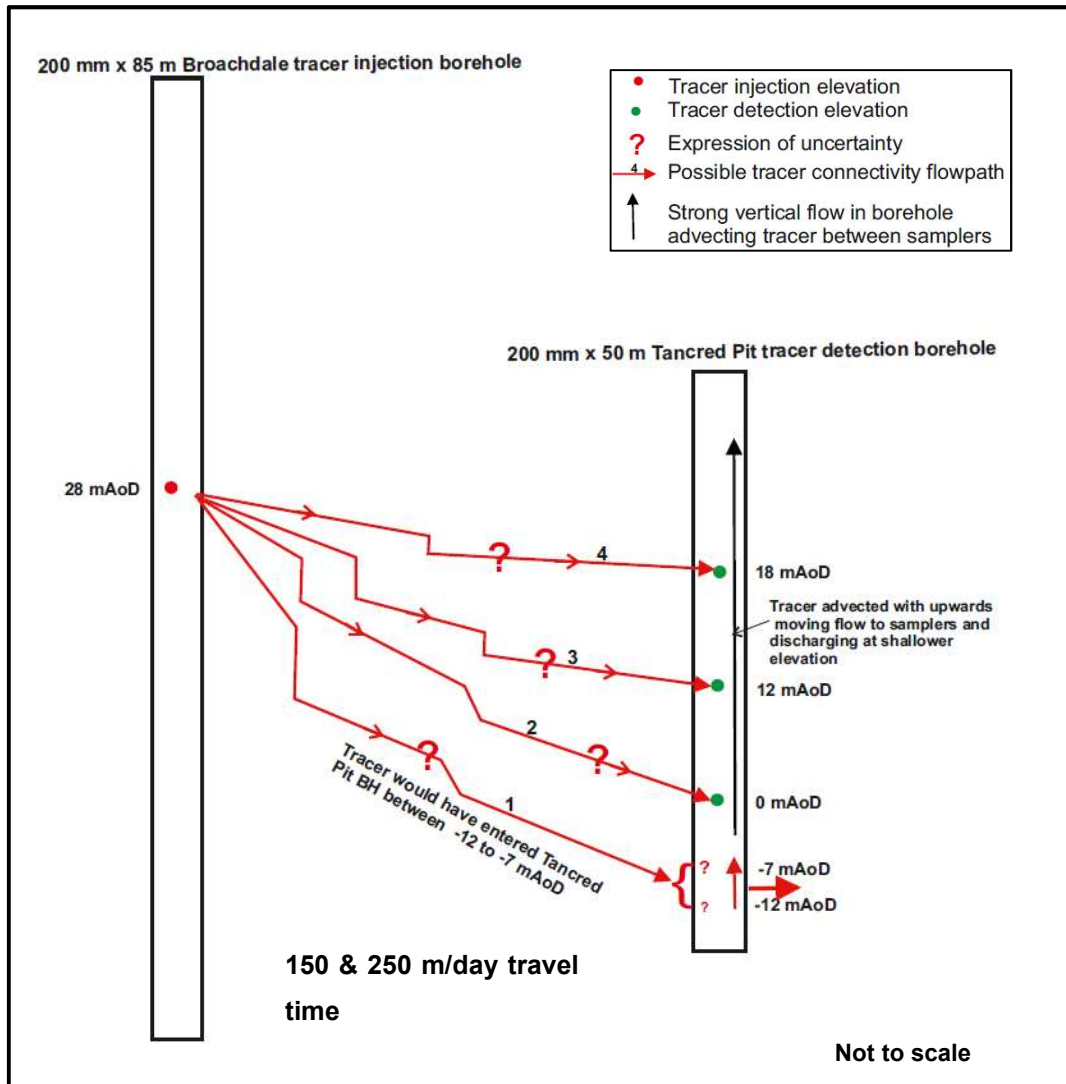


**Figure 6.9.** Borehole tracer connectivity topology between Broachdale and Tancred Pit boreholes. Comparing depths of tracer injection and detection shows downdip flow characterised by flow on bedding features and vertically communicating features (1, 2, 3,4).

The initial arrival of tracer at 0 and 12 mAoD with substantive reduction in tracer concentration detected later at the 18 mAoD sampler is consistent with and confirms substantive mass and tracer loss via outflow as previously discussed in section 4.3.1 in connection with open-well dilution test data.

The fast inflow horizons at depth with relatively high hydraulic heads developed outside the zone of water table fluctuation is explained by the valley location of Tancred Pit borehole which is surrounded by topographically higher recharge areas like Broachdale borehole that connect with the deeper zones supplying recharge water that continuously dissolves calcite, producing

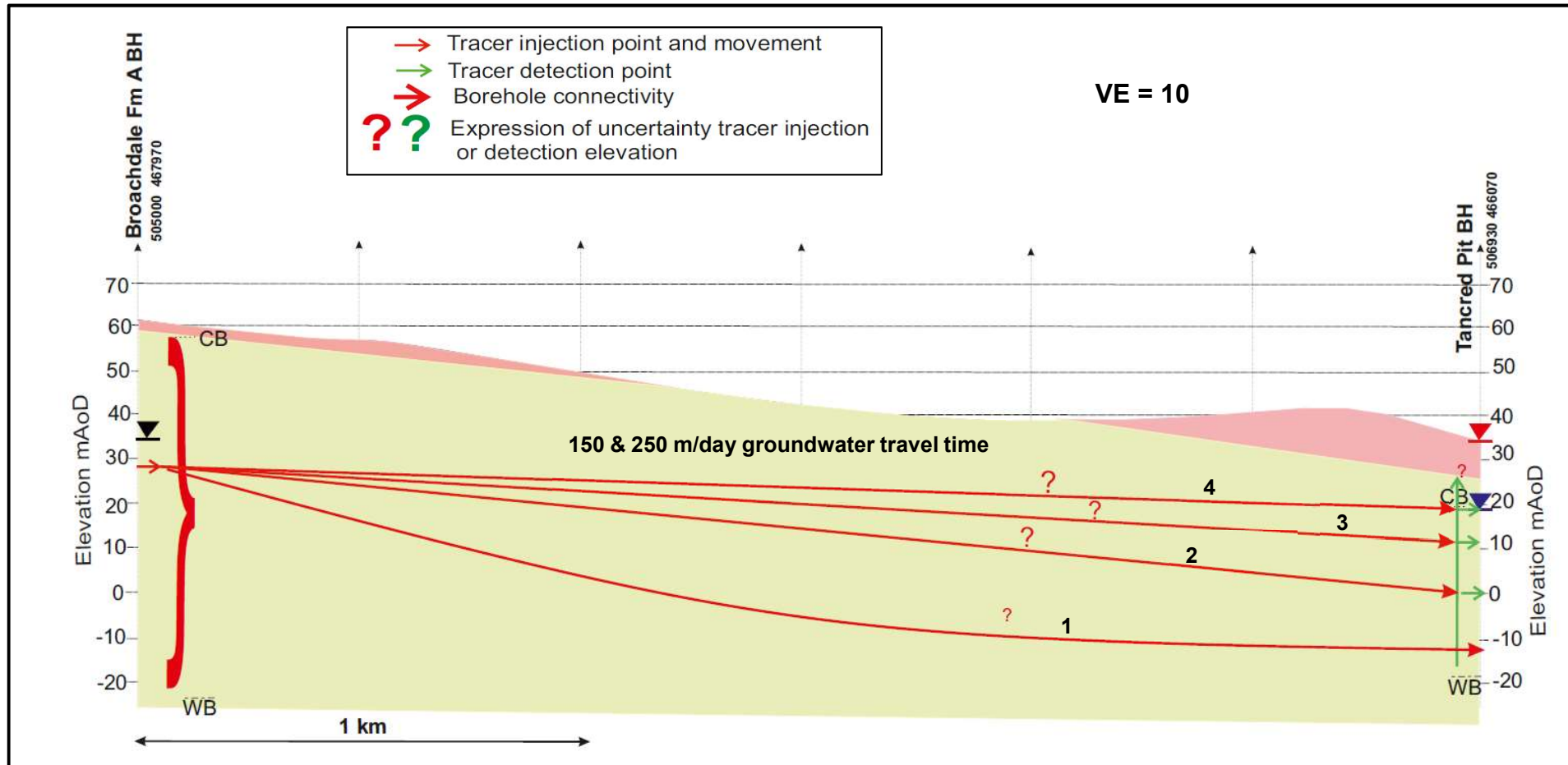


**Figure 6.10:** Cross-section of Ward and Williams (1995) and Ward et al. (1997) tracer test in the Broachdale Valley showing a fast rapid flow connection between Broachdale and Tancred Pit boreholes.

solutionally enhanced features at depth. Tancred Pit borehole is known to have very high transmissivity of about 4300 to 10260 m<sup>2</sup>/day (Ward and Williams, 1995), suggesting that it is located in a zone of developed solutional enhancement..

There follows a discussion of flow patterns in the Broachdale Valley. Should the tracer movement be constrained entirely by 2° dip of the Chalk stratigraphy, then the tracer would have been expected at approximately - 76 mAoD, below Tancred Pit borehole. Again considering the diffuse nature of the tracer pulses, flow entirely via bedding is ruled out (as discussed in the Langtoft Valley), but rather that fast rapid flow occurred via on horizontal and sub-horizontal bedding features, with flow criss-crossing bedding via vertically communicative features like strata and non-stratabond joints and fractures forming a stepped pattern of flow in the Valley. The stepped-up pattern of flow drove flow towards the zone of solutionally enhanced flow at the bottom of the Tancred Pit borehole.

Using the discussions presented about the Broachdale Valley, a synthesis of flow for the Valley is presented in Figure 6.11. The flow in the Broachdale Valley is synthesised to be via bedding flow features that communicate via diffuse vertical stratabond and non-stratabond flow features that connect flow towards solutionally enhanced features at depth. Flow is also possibly characterised by deeper and longer flow paths that converge on the zone of developed solutionally enhanced features. Just like Henpit Hole, the Tancred Pit borehole location in the valley surrounded by higher elevation recharge areas creates the higher hydraulic heads at depth, which is consistent with the Toth (2009) catchment scale flow behaviour.



### **6.1.3 Flow connection between West End Farm borehole to Kilham Abstraction, Kilham Sewage Works, Bellguy and Bracey Bridge Springs**

The cross-section from the West End Farm borehole through the Kilham area to Bellguy and Bracey Bridge springs is shown in Figure 6.12. Four boreholes are presented on the cross-section. West End Farm borehole was a 200 mm diameter x 105 m deep borehole on the interfluvium between Broachdale and Langtoft Valleys. Two boreholes are located at the Kilham Abstraction site. The first, a shallow 150 mm diameter x 20 m deep EA observation borehole, and the second is a 381 mm diameter x 60 m deep Yorkshire Water abstraction borehole No.1. The Kilham Sewage Works borehole is a shallow 102 mm diameter x 20 m deep borehole.

In Figure 6.12 the red brackets on West End borehole mark the depth interval of borehole diameter enlargement, with discrete flow horizons between 0 – 18 mAoD with some downwards flow. In the Kilham Abstraction BH No. 1, under both ambient and pumped flow conditions from a nearby borehole, discrete flow horizons are found between 12 and -18 mAoD, with vertical flows from depth discharging at 12 mAoD. However above 12 mAoD, there is no measurable flows. The zone of no flows was confirmed with open-well dilution test (section 4.5.1). At the Kilham Sewage Works borehole, the flow horizons identified from this work are marked on the section.

Ward et al. (1997;1998) document a tracer test between the West End Farm borehole and the boreholes and springs on Figure 6.12. Ecoli- MS2 tracer was injected at 0 mAoD in West End Farm borehole with samplers in the other boreholes and springs. Figure 6.13 shows the flow topology between the injection and sampling points. Figure 6.14 also shows the cross-section of tracer test results. No tracer was detected at Kilham Abstraction despite its position on the linear path from the West End Farm borehole through Kilham to the springs, suggesting that flow was either around or below the abstraction site. However, the tracer was detected at Kilham Sewage Works borehole and the springs. The tracer was detected in two pulses without tailing, arriving earlier at Bellguy springs, then Kilham Sewage Works. The groundwater velocities were 130 and 325 m/day, 57 and 150 m/day, and 114 m/day for

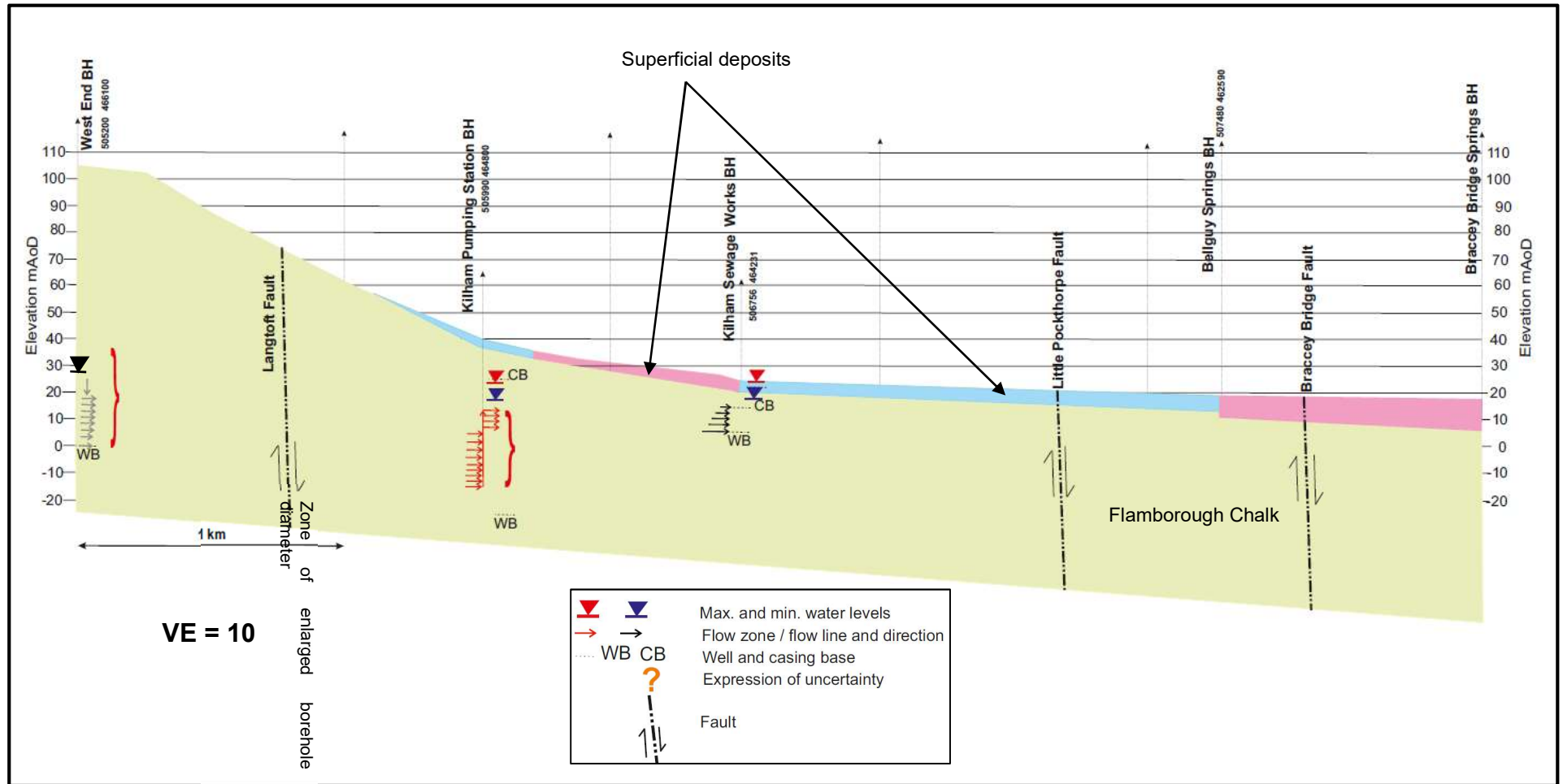


**Figure 6.12.** Marked flow horizons between West End Farm borehole (on the interfluve) and Kilham Village, Bellguy and Bracey Bridge springs. Flow horizons identified by European Geophysical Services (2018)-red, Ward et al (1998)-grey and this current study-black respectively.

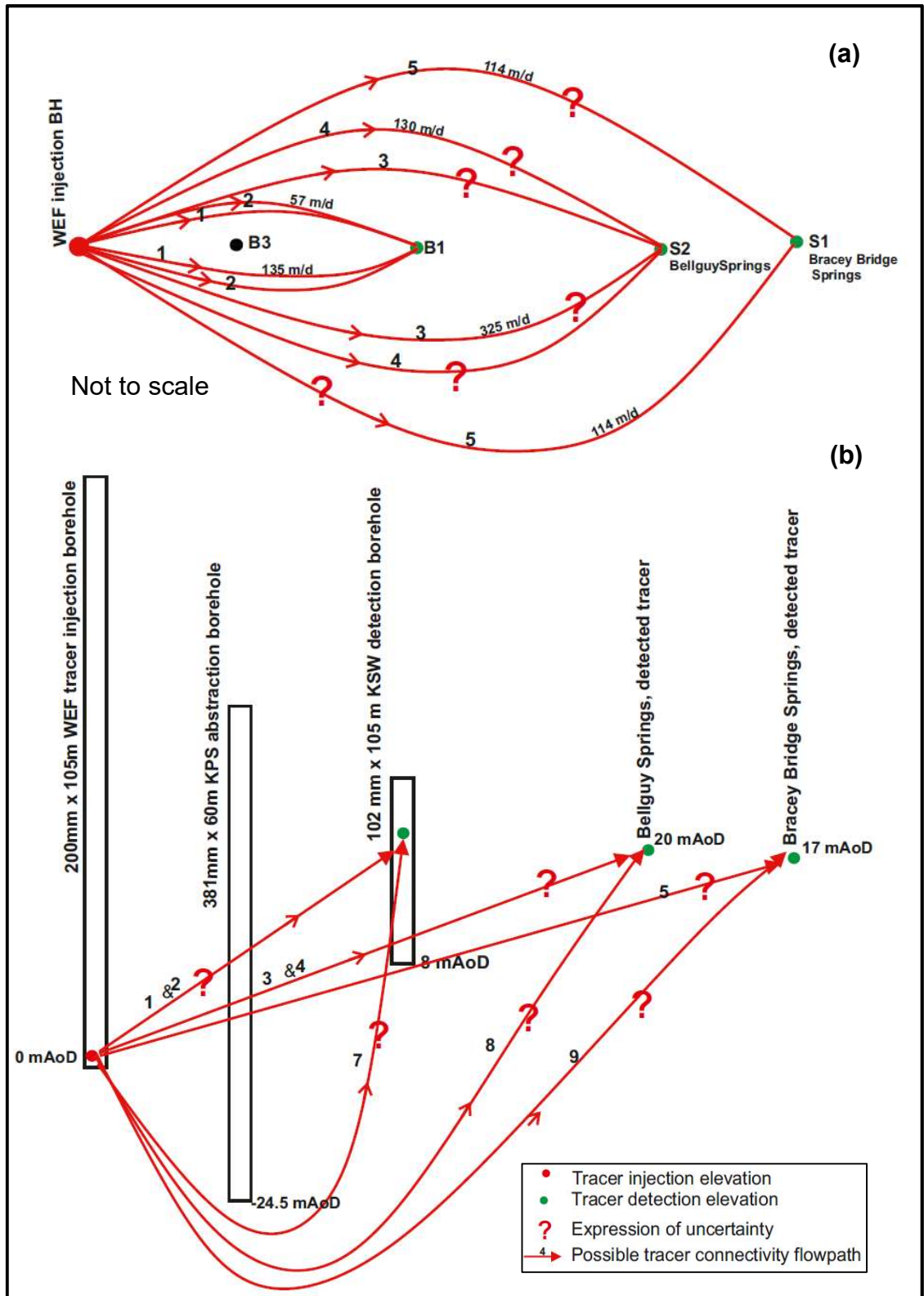


**Figure 6.13.** Borehole and tracer connectivity topology between West End Farm borehole (WEF) and boreholes and springs showing upwards tracer movement from injection to detection points. **a.** Plan view of possible fast lateral tracer movement around B3 to B1 (1 and 2), S1 and S2 (3, 4 and 5). **b.** Section view of possible shallower lateral tracer movement as in **a.** (1,2,3,4,5), and fast but deeper flowpaths under B3 to B1 (7), S2 (8) and S1 (9).

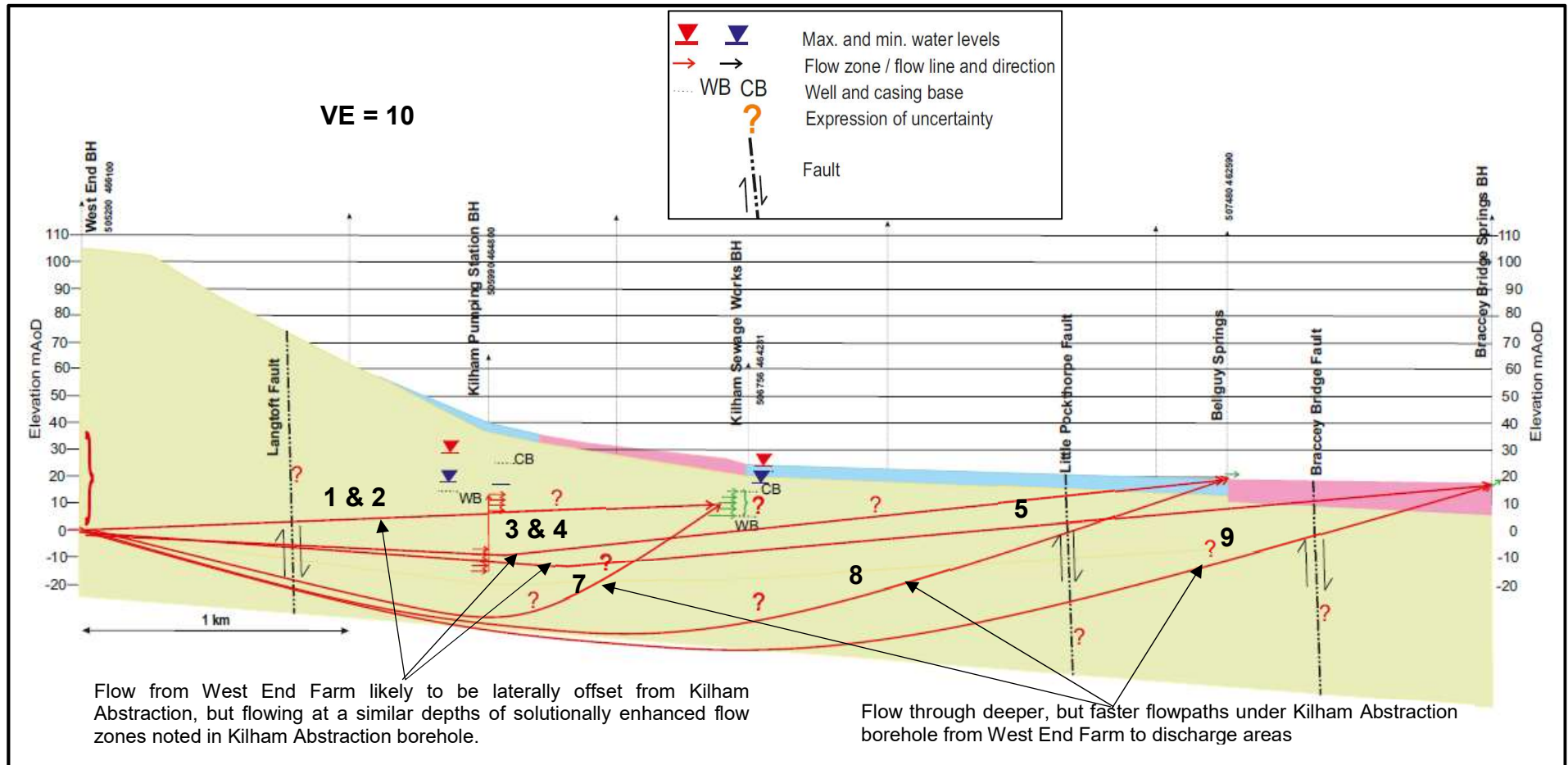


**Figure 6.14.** Cross-section of Ward and Williams (1995), Ward et al. (1997;1998) tracer tests between West End Farm borehole Kilham, Bellguy and Bracey Bridge springs. Three faults with potential to concentrate flow horizontally, and to depth and up to discharge points marked. Tracer moved up dip towards solutionally enlarged fissures at discharge areas in Kilham, and Bellguy and Bracey Bridge springs.

Bellguy springs, Kilham Sewage Works and Bracey Bridge springs respectively. The two tracer distinctive non-tailing pulse detections at Bellguy and Kilham Sewage suggest two distinctive non-diffuse, but well enlarged fissure flowpaths from West End Farm to them. Also, for the tracer to appear first at Bellguy in comparison to Kilham Sewage suggests a deeper, longer but faster flowpath to the spring site.

In the test, the tracer flowpath crosses the Langtoft, Little Pockthorpe and Bracey Bridge faults, which have the potential to divert groundwater flow. The first effect is that the Langtoft fault could direct flows to preferentially developed flowpaths that are either deeper or laterally around the abstraction boreholes to Kilham Sewage Works and the Springs. The second effect is the creation of a stepped pattern of flow by faults directing flows down to depths of developed conductivity, but redirecting the flows back up to spring and discharge areas via solutionally enhanced vertically communicating flow features.

If tracer movement was stratigraphically constrained between West End Farm borehole and the Kilham detection sites, then tracer would have been expected at -52, -84, -136 and -168 m AoD at Kilham Abstraction, Kilham Sewage, Bellguy and Bracey springs respectively, which are all elevations below the drilled depth of the sampling wells and spring elevations. But as already discussed in sub-sections 6.1.1 and 6.1.2, the real structure of the aquifer in comparison with the Worthington (2004) factors that encourage stratigraphically constrained flow to depth resulted in the tracer rather appearing at higher elevations stepwise upwards migration along sub-vertical features. There is evidence of solutionally enhanced fractures at depth of relatively higher heads at the Kilham Abstraction under ambient conditions, which is expected of the Kilham discharge area. The location of the abstraction borehole and expected similarity of flow in the Kilham area should then have resulted in upward movement of tracer towards the abstraction well, but which was not detected. This suggests that the tracer flowpath was more probably around the abstraction well than under it. In spite of the explanation above, the flow crossing the Langtoft fault could also result in flow diversion under or around the abstraction.

The synthesis of flow patterns between West End Farm borehole and Kilham and the springs is shown in Figure 6.15. The flow connection between the injection at West End Farm and detection at the Kilham Sewage Works borehole, Bellguy and Bracey Bridge spring provides insight into the relative hydraulic head levels between the injection and detection elevations. Although the injection elevation is below the detection elevations, the upward movement of the tracer is because the injection point is in hydraulic connection with fractures located at higher recharge elevations of the catchment, directing fast karstic flow towards discharge areas like Kilham and the springs via solutionally enhanced bedding fissures and vertically communicating fractures. These highly conductive features could be located at similar elevations to the flow horizons in the Kilham Abstraction, but laterally offset from the Kilham Abstraction due to the presence of the Langtoft fault (flow lines 1 and 2 in Figure 6.15). The Langtoft fault could also direct flow under the abstraction.

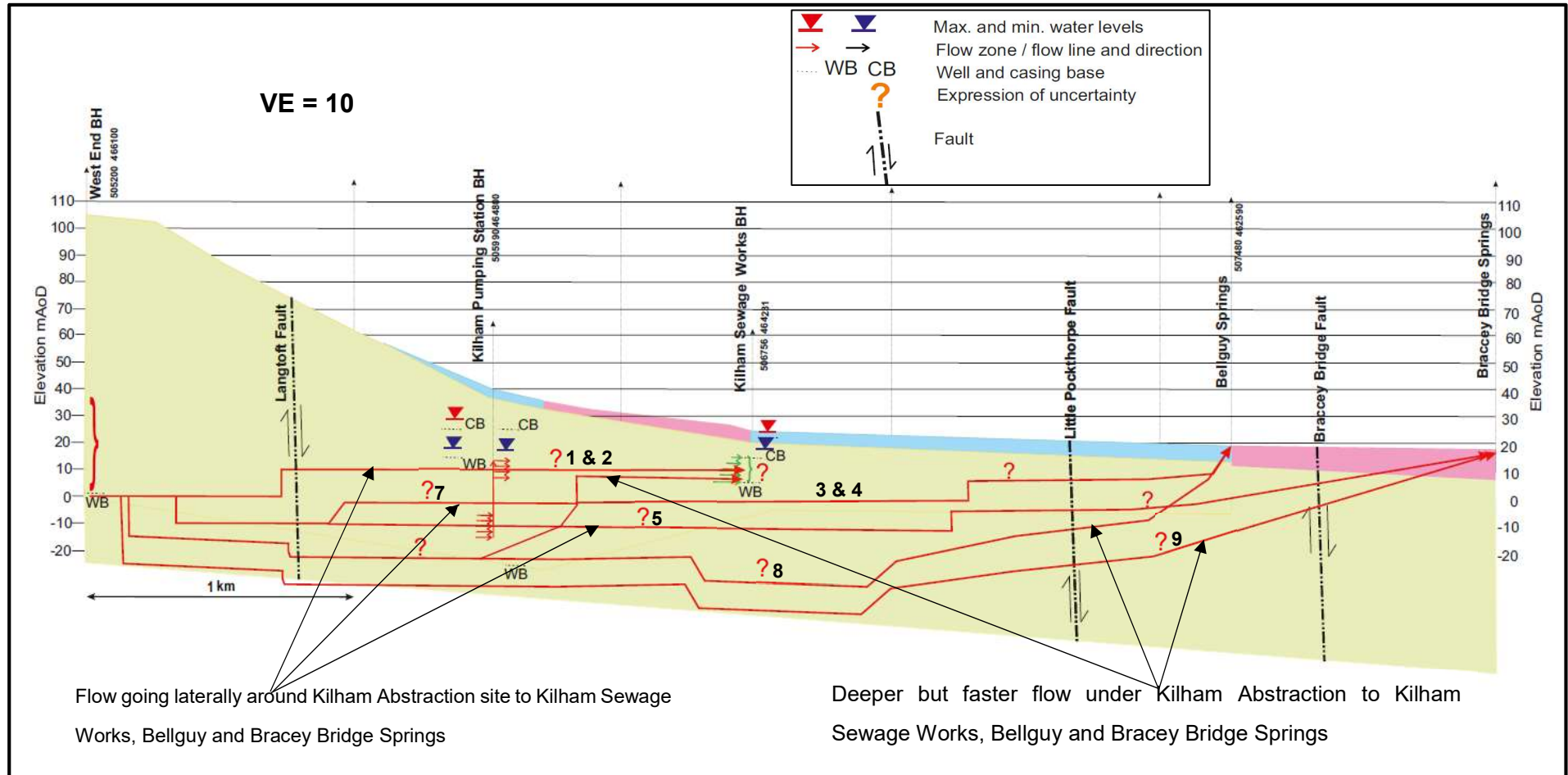


**Figure 6.15.** Summary of flow pattern between West End Farm borehole, Kilham Sewage Works borehole, Bellguy and Bracey Bridge springs. Flow occurring along bedding plane features, moving either laterally around (1,2,3,4,5) or deeper (7,8,9) under Kilham Abstraction

## **6.2 Comparison of velocities of open well-dilution results at Little Kilham Farm well with tracer test velocities**

In this section, groundwater velocities is derived from single well tests on, i.e. the Little Kilham Farm well from the specific discharge obtained versus depth in Figure 4.16c, using interval specific flowing porosity implemented from the well transmissivity, caliper log and ambient flow CCTV view data, flow pattern model for the well from this work and the parallel plate fracture flow model (Snow, 1969; Qian et al., 2011). To check that the derived velocities are reasonable, they are compared with well-to-well tracer test results. Also hydraulic gradients are back calculated from the well-to-well test velocities, and compared with those derived from hydraulic heads for the Kilham area. Groundwater velocities from single well tests have been undertaken by previous workers who either used straddle packers (Novakowski et al., 1995; Xu et al., 1997; van Tonder et al., 2002; Novakowski et al., 2006; Akoachere and Van Tonder, 2009; Maldaner et al., 2018) or depth specific piezometers (Piccinini et al., 2016; Medici et al., 2019) to isolate borehole sections with the aim of constraining horizontal flows and determining interval transmissivity and flowing porosity. It is known from section 4.5.1. that some wells in the study area have vertical flows, but Little Kilham Farm well has been characterised as dominated by strong horizontal flows, with weak vertical flows (Figure 4.19), the reason for the implementation of this work flow here. The availability of both well-to-well tracer and single well tracer test data with geophysical logs and well transmissivity gives a unique opportunity to test and validate the single well dilution for groundwater velocity estimation in fractured aquifers. The current work flow in comparison to the previous stated works is cheaper in terms of set up.

The work flow and results of this exercise is as follows.

### ***Little Kilham Farm well velocities from open well dilution tests***

- i. Number of probable conductive fractures,  $N$  in the well are determined from saturated thickness of pumping tests, fracture enlargement counts from caliper logs in conjunction with CCTV model and flow model from single well dilution tests;

- ii. The transmissivity,  $T_f$  of a single fracture of hydraulic aperture  $b_f$  is determined from the total well transmissivity,  $T$  as:

$$T_f = \frac{T}{N} \quad (6.1)$$

The hydraulic aperture of a single fracture,  $b_f$  is calculated as:

$$a_f = \sqrt[3]{\frac{12\nu T_f}{g}} \quad (6.2)$$

Where  $\nu$  and  $g$  are the kinematic viscosity of water,  $1.307 \times 10^{-6} \text{ m}^2\text{s}^{-1}$  and acceleration due to gravity,  $9.8 \text{ ms}^{-2}$  respectively. The assumptions for using equations (6.1) and (6.2) are that all the flowing features are horizontal fracture and all have same transmissivity and hence hydraulic aperture.

- iii. The flowing fracture porosity,  $\phi_e$  of depth interval for calculated specific discharges is given as:

$$\phi_e = \frac{\text{Number of counted probable flowing fractures in interval} \times b_f}{\text{Depth interval}} \quad (6.3)$$

Putting  $\phi_e$  into equation (4.9), the average horizontal linear velocity of groundwater flow in the fractures intersecting the interval,  $v_{fh}$  is gotten assuming an  $\alpha = 2$ .

- iv. From step iii. the horizontal hydraulic gradient in the flowing fracture intersecting the well interval,  $i_f$  is back calculated using the parallel fracture model (Snow, 1969; Novakowski et al., 2006; Medici et al., 2019) as:

$$i_f = \frac{v_{fh} \cdot 12 \cdot \nu}{g \cdot (a_f)^2} \quad (6.4)$$

- v. Following from (6.3), the average flowing porosity of the full saturated open section of the well can also be obtained. The flowing well porosity for Henpit Hole and Tancred Pit wells were determined to check that that determined for Little Kilham Farm well using the work flow itemised above, is typical of the area. Note that because of substantial vertical flows in the Henpit Hole and Tancred Pit wells, horizontal flows were not determined for the probable flowing fractures in these cases.

### 6.2.1 Results from the implementation of the workflow

The results for the implementation of the work flow is shown in Table 6.1.

**Table 6.1.** Results of fracture aperture and well flowing porosity

Well name	Number of flowing fractures	Saturated depth (m)	T (m <sup>2</sup> s <sup>-1</sup> )	T <sub>f</sub> (m <sup>2</sup> s <sup>-1</sup> )	a <sub>f</sub> (mm)	Well flowing porosity
Little Kilham	40	30	0.102	0.00255	1.58	2.11 x 10 <sup>-3</sup>
Henpit Hole	40	47	0.128	0.00319	1.72	1.46 x 10 <sup>-3</sup>
Tancred Pit	57	37	0.119	0.00208	1.49	2.30 x 10 <sup>-3</sup>

Implementation of step iii. to the depth specific depth intervals (1.5 m) in Little Kilham Farm borehole using the open-well dilution test data yielded flowing porosities ranging between 1.07 – 4.26 x 10<sup>-3</sup> (Figure 6.16a), with an average of 2.40 x 10<sup>-3</sup>, which is similar to that determined for the full depth of Little Kilham Farm borehole or to other 2 wells in Table 6.1. The order range from the analysis is in agreement with values stated by Foster and Milton (1974), and Ward and Williams (1995). The porosity of the depth 40 – 46 mbgl is lower reflective of the reduction in fracture enlargement on the caliper for the depth interval.

The average groundwater horizontal velocity variation with depth for Little Kilham Farm well from step iv. is shown in Figure 6.16b. The horizontal groundwater velocities from the parallel fracture model applied to the single well dilution range between 50 – 2340 md<sup>-1</sup>, and decrease down the well, reflecting the higher number of flowing fractures in the upper parts of the well from solutional enhancement from recharging water. The groundwater velocities from tracer tests in the Kilham area (40 - 480 md<sup>-1</sup>) bounds the velocities from the single well dilution below 35 mbgl. From 18 – 35 mbgl, the parallel plate model derived velocities exceed the upper bound of the well-to-well tracer tests.

Several factors account for the groundwater velocities from single well test velocities been outside the range of well-to-well tracer groundwater velocities.

The first factor is related to differences in scale of investigation and may reflect the difference in scale of investigation as the tracer test was shown to connect injection and detection points that were up to 4.2 km apart whereas the single

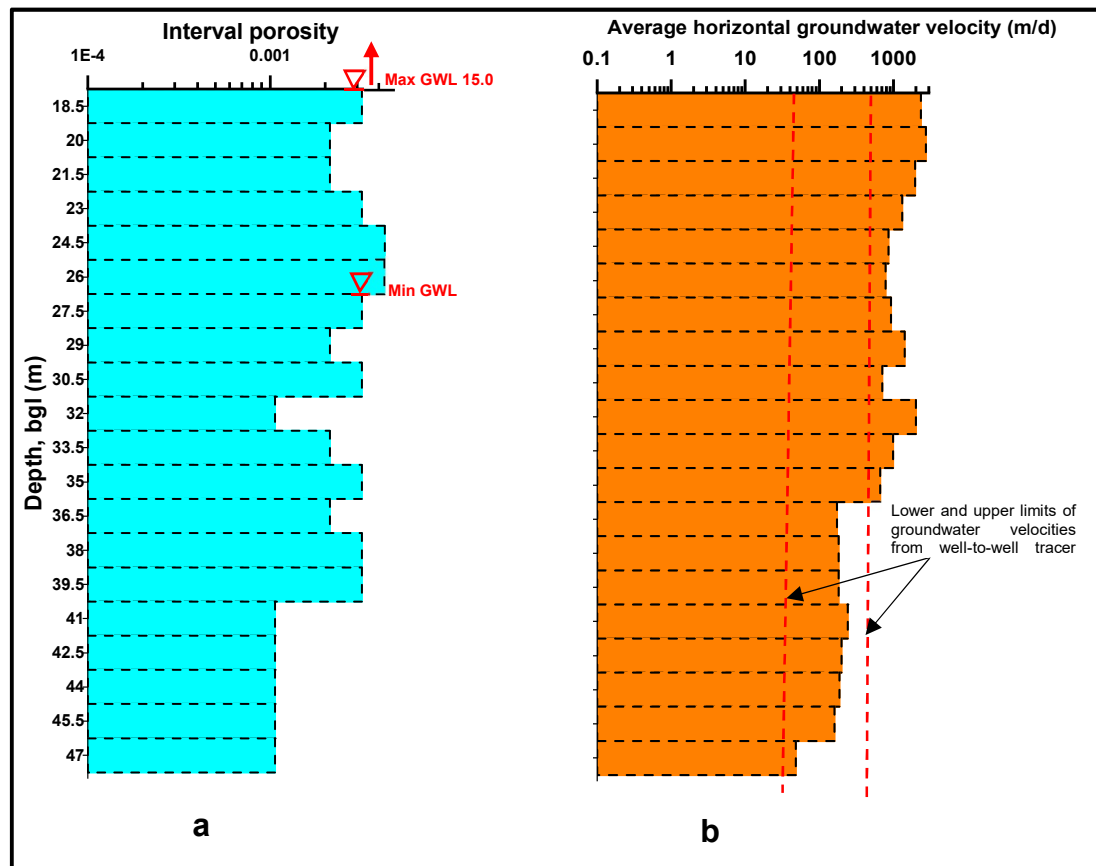


**Figure 6.16.** Little Kilham Farm borehole depth interval (1.5 m) properties: a. porosity; b. average horizontal groundwater velocities. Also marked on **b** are well-to-well tracer test velocity limits (red dash lines) by Ward and Williams (1995).

well dilution testing only tests fractures in the vicinity of the borehole. The second factor is the uncertainty in depth specific porosity estimations from assumptions of the parallel fracture flow model. The identification of probable flowing fractures using caliper logs and ambient flow models for the borehole introduces uncertainty in porosity. This is because ambient flow may be influenced by different fractures than those that influence the well under pumped state. Also, the assumption that all fractures have the same aperture in the single well analysis is problematic, because in practice, fractures have a wide range of hydraulic apertures. The effect of this is an underestimation

of porosity with a subsequent overestimation of groundwater velocities in the zone of water table fluctuation, and an overestimation of flowing porosity down the well resulting in an underestimation of groundwater velocities in the well. The third reason relates to the assumptions and parameters used for the estimation of Darcian flow. Flow convergence and constriction towards the well may mobilise high local hydraulic gradients in the fractures, resulting in higher velocities in the well. This implies that uncertainty in the  $\alpha$  value used for this analyse can cause uncertainty in the estimated horizontal groundwater velocity. Also vertical flows in the well can lead to the likelihood of the flouting of the Pitrak (2007) model of pure horizontal flow so far as the test sections are not packered off. This will result in rapid dilution, that may inherently lead to an overestimation of horizontal groundwater velocities and hydraulic gradients using equations (4.9) and (6.4) respectively. However, these velocities from the upper section of the well could also be related to the higher spectrum of flow velocities resulting from direct / conduit flow paths that were not detected by well-to-well tracer tests, as the recorded tracer test velocities could have been from more tortuous and dispersive routes resulting in the delay of tracer arrival times.

To test the reasonableness of the derived velocities, step iv. was used to calculate the implied horizontal fracture hydraulic gradients at each depth interval shown in Figure 6.16. The values are tabulated in Table 6.2.

**Table 6.2.** Data of hydraulic gradient in the Little Kilham Farm well using the depth intervals in Figure 6.16.

Method of analyses	Range of fracture hydraulic gradients	Average hydraulic gradient
Depth specific porosity	$1.45 \times 10^{-4} - 4.96 \times 10^{-3}$	$1.98 \times 10^{-3}$

Despite the difference in scale of the two datasets, the average hydraulic gradients calculated using depth specific porosity ( $1.98 \times 10^{-3}$ ) broadly agrees with the average hydraulic gradient in the Langtoft Valley and the Kilham area ( $3.3 \times 10^{-3}$ ) using historic groundwater level extremes from Ward and Williams (1995).

These results are interesting for two reasons. The first is that, open-well dilution could be used to analyse catchment flow velocities if horizontal flow dominates in a test well, and there is a reliable data on flowing porosities. This can lead to cost saving during hydrogeological investigations as straddle packers will not be required to isolate depth intervals for horizontal flow measurement. A more important conclusion is that, the comparison between well-to-well and single well tracer tests is a unique test due to the latter's ability to predict horizontal groundwater velocities. The single well test and parallel plate model however suffers from uncertainties from flowing porosity and flow convergence factors.

### **6.3 Pumping tests and transmissivity distribution of the Kilham Catchment**

Because of the heterogenous and anisotropic nature of the Chalk aquifer, transmissivity values are very variable in both the confined and unconfined areas of the East Yorkshire Chalk , ranging between  $1 \text{ m}^2\text{d}^{-1}$  to  $10,000 \text{ m}^2\text{d}^{-1}$ , with a mean transmissivity of  $1260 \text{ m}^2\text{d}^{-1}$  (Allen et al., 1997), with anomalously higher values in the unconfined area west of Kilham and the artesian and semiconfined zones. Other tests like for example Jones et al. (1993) present transmissivity values ranging between  $1430 - 17500 \text{ m}^2\text{d}^{-1}$  at a 95% confidence interval using the BGS wide well analyses software, for the Kilham Abstraction site. Within the unconfined zone, transmissivity values are more biased towards the valleys than the interfluves because of the paucity of wells on interfluves and hence fewer tests. The transmissive nature of the unconfined aquifer is demonstrated by the very low drawdowns noted for pumping tests conducted in the area. In this current study for example, re-analysis of archived pumping tests for the Kilham Catchment yielded values of between  $430 - 17730 \text{ m}^2\text{d}^{-1}$  showing the variability even on the scale of the Kilham catchment.

The relatively high transmissivities in the area arise due to the active groundwater circulation that results in solution enhancement of fractures both at the zone of water table fluctuation and at depth in some wells. Because of the contribution of discrete layered groundwater flow to transmissivities, the use of the values for water resources planning and management need to be

interpreted with caution especially for tests conducted at times of high groundwater levels in comparison to tests under low groundwater conditions. Previous well characterisation (Buckley and Talbot, 1994; Southern Science Ltd, 1994; Parker, 2009) and the preceding well flow synthesis presented in this chapter lends credence to flow at discrete flow horizons in the catchment.

Faults in the catchment have the potential to act as either flow barriers or preferential flow paths. The large scale test undertaken at Nine Dikes and Cottage Farm suggested the existence of boundary effects on the north western and north eastern parts of the catchment probably from the Burton Fleming fault, or from recharge boundary effects in the Gypsey Race Valley, or from a combination of both preceding factors. In this current study however, the re-analysis of pumping tests to investigate the effects of faults on flow in the catchment was inconclusive for two reasons. Firstly most of the wells for which the pumping tests were analysed were drilled for water resources than for research purposes, and so are not near or straddle faults (Bense et al., 2013). Secondly the low pumping rates used in the tests and the transmissive nature of the aquifer can make it impossible for cones of drawdown to reach the faults.

## **6.4 Chapter Summary**

Information from previous tracer tests were re-analysed in conjunction with flow horizon characterisation to produce flow patterns in the Kilham catchment.

- Flow patterns in and between the Langtoft and Broachdale Valleys were synthesized with cross-sections.
- In the Kilham area, discrete flow zones are found at both shallower and deeper depths. Flow at depth is characterised by higher ambient hydraulic heads.
- Deeper flow zones connect to areas of higher elevation, that drives the flow.

- The Kilham area is marked by fast and complex karstic flow with concentrated flow through diffuse solutionally enlarged bedding and vertical communicating features forming stepped flow patterns towards Kilham.
- Average groundwater velocity ranges between 40 to 480 m/day across the area.
- In the Broachdale Valley, there is borehole connectivity between boreholes that are 3 km apart whereas there is a connection between West End Farm borehole and springs that are 4.2 km apart with faster and deeper flow paths connecting springs and boreholes in the area.
- The parallel flow model work flow was implemented in the Little Kilham Farm borehole, resulting in the constraining of hydraulic gradients in the well and groundwater velocities via comparison with tracer tests velocities.
- Groundwater velocities derived via open well dilution tests ranged between 50 – 2340 md<sup>-1</sup>, whereas the average well hydraulic gradient of  $1.08 \times 10^{-3}$  is in consonance with that of historic hydraulic gradient ( $3.3 \times 10^{-3}$ ).
- The implementation of the work flow showed the importance of open-well dilution tests in reducing costs of hydrogeological investigations at both the well and catchment scale in the prediction of horizontal groundwater velocities. The method is however liable to uncertainties from flowing porosity and flow convergence factor.
- The high transmissivities (430 – 17730 m<sup>2</sup>d<sup>-1</sup>) in the Kilham area arise from the solutionally enhanced flow features.

## **Chapter 7 Conceptual model of flow in the Chalk and Kilham catchment**

Findings from previous works and this current work were presented from Chapters 2 to 5 and synthesised in Chapter 6. These findings are incorporated in the development of a conceptual model here, in Chapter 7. The chapter starts by introducing the theme of the conceptual model and the framework of the model used in this chapter. Then hydrogeological descriptions of the catchment conceptual model are presented and simplified in a cross-section. The conceptual model also contains audit trails and statements of uncertainty, in order to identify a direction on the gathering of further research data to constrain and improve the conceptual model.

### **7.1 Catchment Conceptual model development**

An introduction to the conceptual model is presented before the development of the detailed model. A hydrogeological conceptual model is a justifiable, logical and coherent simplification of the key flow processes and mechanisms in a hydrogeologic catchment to enhance understanding of the catchment flow processes (Environment Agency, 2001; Black and Brightman, 2007; Brassington and Younger, 2010; Enemark et al., 2019). A conceptual model should be hinged on available published, field and/or laboratory tested data on the catchment.

The conceptual model developed in this chapter is based on the hydrogeological conceptual model framework elaborated and espoused in Environment Agency (2001) and its following documents, as well as by Brassington and Younger (2010). The framework espoused the iterative approach of continuously gathering, reviewing and re-evaluating available hydrogeological data to give a better and current understanding of catchment flow mechanism and patterns, whilst leaving behind an audit trail of evidence source(s) to ensure that the logical, justifiable and consistent methodologies that led to development of the catchment conceptual model can be reviewed and audited by other hydrogeologists and regulators alike. The iterative nature of the conceptual model development ensures the constant questioning and

querying of the current understanding of catchment processes, leading to the formulation of further data collection campaigns for improvement of model and catchment knowledge to enhance catchment management.

The sub-section that follows presents a description of the conceptual model developed from Chapters 2, 3, 4, 5 and 6 and the conceptual model audit trail.

### **7.1.1 Development of a conceptual model of the study area and the Kilham Catchment**

The conceptual model presents catchment characteristics for the study area and Kilham Catchment. The model describes both the physical and chemical processes operating at the following levels:

- i. catchment input mechanisms like rainfall characteristics, surface flow mechanisms, unsaturated flow and recharge processes;
- ii. throughput flow mechanism in the saturated zone via karstic and conduit features, fine fractures and effects of faults on flow; and
- iii. discharge via springs both on the scarp and dip slopes.

For clarity, two separate but complementary models have been developed for the Catchment. The first model is a physical model describing the aquifer boundaries, topography, geometry and flow structure and patterns. The second is a chemical model that describes the source of solutes to the unconfined chalk groundwater, and the evolution of the water to discharge at both the scarp and dip slopes. Both models will first be developed by providing summarised hydrogeological statements of aquifer structure and boundary and the processes at the input, throughput and output levels with evidence of the hydrogeological information and its source for audit trailing. The descriptions are then summarised in cross-sections. Table 7.1 and Table 7.2 provide the hydrogeological descriptions of the physical and chemical conceptual models respectively, whereas the conceptual cross-sections of the descriptions in the Tables are presented in Figure 7.1 and Figure 7.2 respectively.

**Table 7.1.** Characterisation of the Physical Conceptual Model of the Kilham catchment

No.	Hydrogeological description	Activity undertaken to support description	Information source
<i>Physiography, aquifer structure and boundaries</i>			
1.	The Chalk aquifer crops out in the Wolds, with a western scarp and eastern dip slopes.	Literature review from previous hydrogeological research articles and reports. Development of catchment geological map, cross-sections and digital elevation model in Chapter 2 of this current work using datasets from the BGS GeoIndex and Edina digimap ordnance survey and geology.	Research articles and reports from Foster and Milton (1974); Foster and Crease (1975); Allen et al. (1997); Smedley et al. (2004); Gale and Rutter (2006), ESI (2010); Farrant et al. (2016). BGS GeoIndex is accessible at <a href="http://mapapps.bgs.ac.uk/geologyofbritain/home.html">http://mapapps.bgs.ac.uk/geologyofbritain/home.html</a> . Edina digimap is accessible at <a href="https://digimap.edina.ac.uk/">https://digimap.edina.ac.uk/</a>
2.	The aquifer is unconfined from the Wolds to the western edge of Kilham, becoming progressively semi-confined to confined by increasing	Ditto	Ditto

---

thickness of superficial deposits to the east of Kilham.

---

- |   |   |   |
|---|---|---|
| 3. The Chalk unit lies uncomfortably over Jurassic Formations. The main aquifer units for the catchment are the Flamborough, Burnham and Welton Formations, overlying the basal and more marly Chalk units (Ferriby and Hunstanton Formations) which are considered to be non-aquifers. | Literature review of geological and hydrogeological articles and reports. Development of geological cross-sections from BGS GeoIndex and Edina digimap elevation and geological dataset.  | Geological: Sumbler (1996). Hydrogeological: Allen et al. (1997); Smedley et al. (2004); Gale and Rutter (2006);ESI (2010); Farrant et al. (2016). BGS GeoIndex and Edina sources as above.                               |
| 4. The Chalk aquifer has low productive storage but is highly fractured contributing large permeability from secondary features like bedding planes, joints, fractures and solutionally enlarged fissures and conduits.   | Literature review of hydrogeological, unsaturated zone studies, tracer, well logging, pumping tests articles and reports on the Chalk of the United Kingdom. The hydraulic continuum concept is from the analyses of pumping tests data ranging from short (from archived EA datasets) to large time scales (BGS large scale test of 1984). | Hydrogeological: Price (1987); Price et al., (1993); Allen et al., (1997); Hartmann et al. (2007); Gale and Rutter (2006); Younger and Elliot (2007); Hartmann et al. (2007);Maurice et al. (2012); Farrant et al. (2016) |
-

The highly fractured nature of the aquifer makes the aquifer a hydraulic continuum on the catchment and regional scale (attaining the representative elementary volume, REV), but karstic especially in Kilham and the discharge areas.

The Chalk matrix has high porosity but low permeability and this characteristic is important for contaminant storage in the unsaturated zone, and transport from the unsaturated zone to the saturated zone.

Unsaturated flow studies: Zaidman et al. (1999); Allshorn et al. (2007); Keim, (2013).

Pumping tests: Foster and Milton (1974); BGS large scale pumping test to characterise the aquifer for river augmentation scheme on the Northern Chalk in 1984; Jones et al. (1993). Analysed archived pumping test results in Chapter 3.

Tracer tests: Ward and Williams (1995); Ward et al. (1998).

Well logging: Buckley and Talbot (1994; 1996); Southern Science Ltd (1994); European Geophysical Services (2018).

---

***Input and unsaturated flow mechanisms***

---

5.	Annual averages of precipitation, evapotranspiration and	Literature review of ESI (2010) report, Smedley et al (2004) and Gale and Rutter (2006). Approximate values stated in Smedley et al (2004) and Gale and	Smedley et al. (2004); Gale and Rutter (2006); ESI (2010).
----	--	---	--

---

---

recharge over the period 1969 – 2006 are 771, 471, 300 mm/a respectively on the Wolds recharge area.	Rutter (2006), and calculated and plotted in ESI (2010).	
6. Recharge occurs mainly via fractures, with evidence of bypass flow during times of high hydraulic loading. However unlike in the South (South Downs), where rapid bypass flow through the unsaturated zone was detected at the watertable, the continuity of quick unsaturated flow through the full unsaturated thickness to the water table is uncertain on the Northern Province Chalk.	Literature review of unsaturated zone (USZ) characterisation research work on both the Northern and Southern Chalk show bypass flow in the unsaturated zone during time of high hydraulic loads.	East Yorkshire USZ studies: Zaidman et al., (1999); Allshorn et al. (2007); Keim et al. (2012). For Southern Chalk USZ characterisation to 5m above the water table, see Rutter et al. (2012).

---

---

7.	No surface water features on the Wolds, but for the complex and intermittent Gypsy Race. Increased run-off occurs at the semi-confined and confined area due to reduced recharge as a result of the confining superficial deposits (especially from the glacial tills).	Literature review of hydrogeological articles and reports in the catchment. Developed DEM in Chapter 2 and undertaking of field surveys to identify water features in the Catchment during the research period.	Foster (1974); Allen et al. (1997); Gale and Rutter (2006); ESI (2010); Farrant et al. (2016). BGS GeoIndex and Edina sources as above statements 1 - 3.
----	---	---	---

---

***Throughput and saturated flow mechanisms***

---

8.	Seasonal composite groundwater level fluctuation is highest in the recharge area (Wolds), reducing to the discharge and artesian areas.	Literature review of hydrogeological articles and reports. Plotting of monitored groundwater data and archived EA observation well groundwater level data in Chapter 5.	Foster (1974); Gale and Rutter (2006); ESI (2010). Archived composite groundwater level data from the EA Groundwater Department. Composite groundwater level monitored in Chapter 5 of this studies.
9.	The rolling chalk terrain produces hierarchical and nested flow systems that agree	Literature review of the Tothian gravity flow model on catchment scale and previous well characterisation in the catchment.	Tothian models: Toth (1962); Freeze and Witherspoon (1967); Freeze and

---

---

<p>with the Tothian model of gravity and topographical driven flows eg. at Weaverthorpe, Tancred Pit and Henpit Hole boreholes.</p>	<p>Open-well dilution tests and synthesis in Chapters 4 and 6 show flow characteristics for some wells located in valleys.</p>	<p>Witherspoon (1968); Brassington (1992); Toth (2009). Open well dilution tests and other well characterisation tests.</p>
<p>10. Flow in the saturated zone occurs along bedding plane features, joints and fractures and solutionally enhanced fissures, making the aquifer highly transmissive. Flow in the saturated zone is karstic and complex especially at the discharge areas.</p>	<p>Literature review of previous hydrogeological research on borehole logging, open-well dilution testing, tracer tests and pumping tests. Open-well dilution test used in this work, synthesis and comparative work in Chapters 2, 3, 4 and 6.</p>	<p>Hydrogeological: Foster and Milton (1974); Foster and Crease (1975); Allen et al. (1997); Gale and Rutter (2006); Maurice et al. (2012); Farrant et al. (2016). Pumping test: Jones et al. (1993). Open-well dilution tests: West and Odling (2007); Parker et al. (2018). Tracer tests: Ward and Williams (1995); Ward et al. (1998). Well logging: Buckley and Talbot (1994; 1996); Southern Science Ltd (1994); European Geophysical Services (2018). Chapters 2 and 4 of this current work.</p>

---

---

<p>11. Flow is via discrete permeable horizons distributed at all depths of investigation. Uncertain information about permeability development at deeper depths below boreholes used in this study.</p>	<p>Literature review of previous hydrogeological research on borehole logging, open-well dilution testing. Open-well dilution test used in this work, synthesis and comparative work in Chapters 2, 4 and 6.</p>	<p>Well logging: Buckley and Talbot (1994; 1996); Southern Science Ltd (1994); European Geophysical Services, (2018). Open-well dilution tests: West and Odling (2007); Parker et al. (2018).</p>
<p>12. Dip slope flow paths may be relatively longer with deeper and longer flowpaths and residence times in comparison to scarp slope flow paths. On the dip slope towards the discharge area, evidence from tracer tests suggests a relatively deeper and longer but oxygenated, homogenised and discrete flowpaths from enlarged features at depth of up to 65 mbgl.</p>	<p>The concept of hydraulic continuum of the aquifer can be invoked as evidence for using distance between the recharge and discharge points as a proxy of flow path lengths. Analyses of head distributions at depth from well characterisation and tracer tests and reviews from Chapters 4 and 6.</p>	<p>Toth (1962); Freeze and Witherspoon (1967); Freeze and Witherspoon (1968); Brassington (1992); Toth (2009).</p>

---

---

Evidence of upwards flow concentration towards the Kilham discharge area via parallel bedding features and vertically communicating secondary features resulting in a stepped flow pattern.

---

- |   |  |   |
|---|--|---|
| 13. Kilham and the discharge area forms a zone of solutionally enhanced flow features resulting in karstic flow.  | Literature review of previous hydrogeological research reports and articles on transmissivity distribution in the catchment and tracer tests. Analyses of the transmissivity data and their distribution from the analyses of EA archived pumping tests data in the catchment. | Hydrogeological: Foster and Milton (1974); Foster (1974); Allen et al. (1997); Gale and Rutter (2006); ESI (2010); Farrant et al. (2016).<br>Tracer tests itemised above.<br>Analysed pumping tests in Chapter 3. |
| 14. Several east-west trending faults identified in the catchment, but there is no evidence on the effect of the faults on groundwater flow on the catchment and local scale. | Literature review of geology and hydrogeology articles and reports that have mapped and discussed faults in the catchment. Analyses of transmissivity distribution in relation to their location and distance to identified faults in the catchment in the current study.      | Starmer (1995;2008); Farrant et al. (2016).<br>Analyses of EA archived pumping tests in Chapter 3.  |
- 

***Output and discharge mechanisms***

---

---

<p>15. The aquifer discharges naturally via dip and scarp slope springs. In comparison to the scarp slope springs, the dip slope springs form the majority of aquifer discharge.</p> <p>Dip slope flow is along dip of the aquifer, converging towards the end of the Broachdale and Langtoft Valleys, at Kilham and discharge areas, resulting in numerous springs that flow into the Foston Beck, one of the two tributaries of the River Hull.</p> <p>The most prominent springs on the scarp slopes occur at Place Newton (monitored for this study), located at Wintringham.</p>	<p>Literature review of hydrogeology articles and reports. Developed DTM in Chapter 2 and field spring feasibility surveys.</p> <p>Evidence from composite groundwater levels in the catchment shows the flow directions on the regional scale.</p>	<p>Sources listed in statement 14 above.</p> <p>Relative amounts of discharge at scarp and dip slopes determined in a water balance study by ESI (2010).</p> <p>Edina digimap sources.</p> <p>Observations from spring reconnaissance and monitoring undertaken for this current research.</p>
---	---	--

---

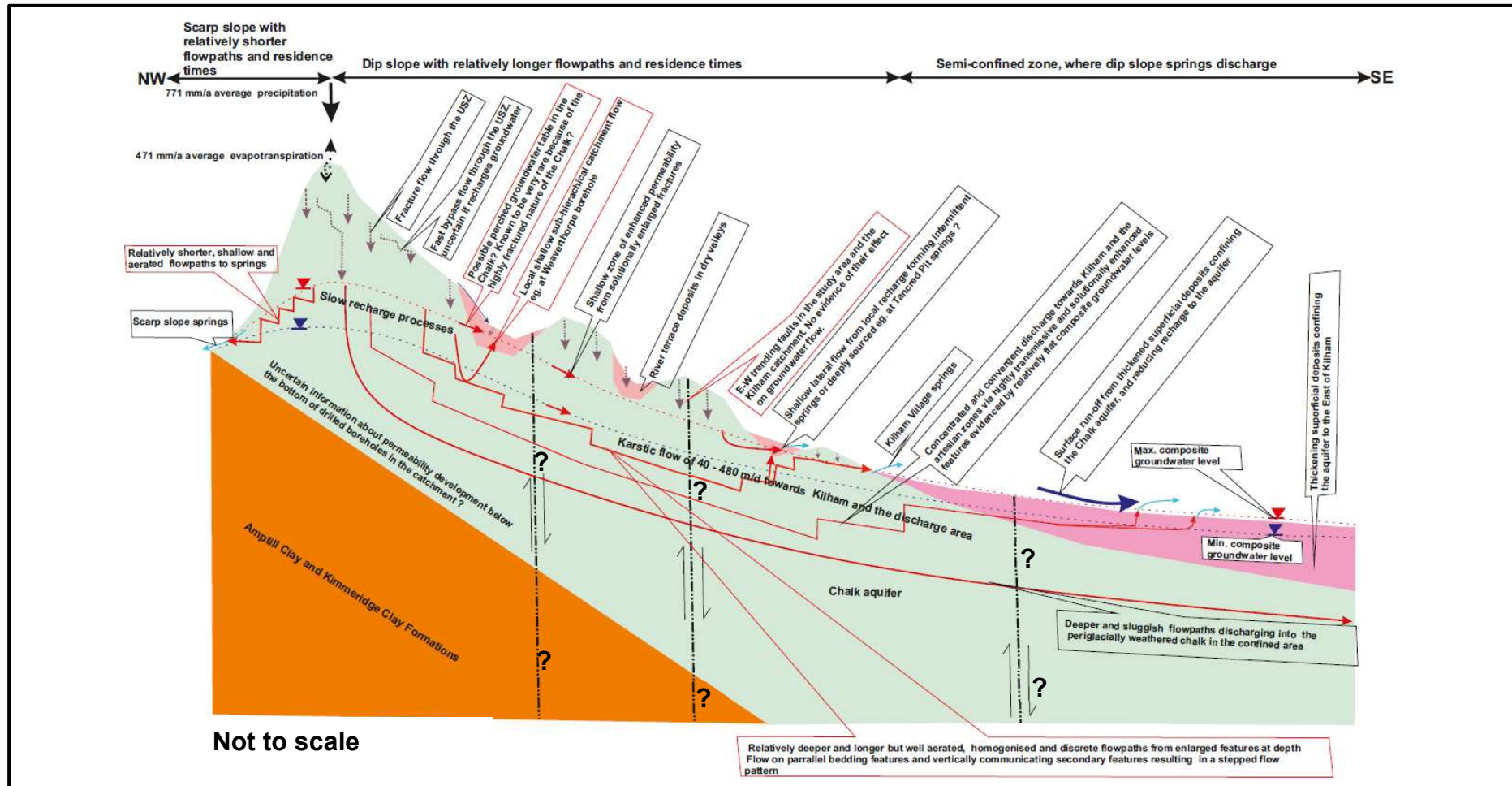


**Figure 7.1.** Physical Conceptual Model of the study area around Kilham showing the key physical processes. Red coloured call out boxes contain hydrogeological descriptions that are contributions from this current work to catchment understanding. Black boxes contain pre-existing literature information.

**Table 7.2.** Characterisation of the Chemical Conceptual Model of the Kilham catchment

No.	Hydrogeological statement	Activity undertaken to support description	Information source
<b><i>Input and unsaturated flow mechanisms</i></b>			
1.	Dilute precipitation input. Average concentration (mg/L) and characteristics of major ions in precipitation monitored for the years 2014 to 2018 at High Muffles (NGR SE 776 939) :Ca <sup>2+</sup> (0.35), Mg <sup>2+</sup> (0.23), Na <sup>+</sup> (2.05), K <sup>+</sup> (.13), NO <sub>3</sub> <sup>-</sup> (0.49), SO <sub>4</sub> <sup>2-</sup> (0.45), Cl <sup>-</sup> (3.61). SEC (23 µS/cm); pH = 6.14.	Literature review of general geochemical text.  Analyses of precipitation water from the UK Air Information Resource (UK AIR), UK Eutrophying and Acidifying Network (UKEAP) website.	General geochemical texts: Herczeg and Edmunds (2000); Appello and Postma (2005).  UK AIR dataset accessible at <a href="https://uk-air.defra.gov.uk/networks/network-info?view=precipnet">https://uk-air.defra.gov.uk/networks/network-info?view=precipnet</a>
2.	Infiltrating rainwater through the soil zone is impregnated with biogenic CO <sub>2</sub> (g) and leached NO <sub>3</sub> <sup>-</sup> . Due to the CO <sub>2</sub> (g) impregnation of infiltrating water, about 76 – 87 % of initial solution takes place in the unsaturated zone below the soil zone by infiltrating water dissolving	Literature review of general geochemical text.  Literature review of groundwater provenance and evolution in Givendale, on the Northern Chalk by Pitman (1978). A review of a similar work by Edmunds et al. (1987) in Berkshire, on the Southern Chalk showed similar leached soil water chemistry.	General geochemical text in statement 1 above.  Groundwater evolution and provenance: Pitman (1978); Edmunds et al. (1987); USZ nitrate profiling: Foster (1976); Foster et al. (1982); Lawrence et al. (1983).

---

calcite to release  $\text{Ca}^{2+}$  and  $\text{HCO}_3^-$  as the dominant ions in the unsaturated zone so that recharging water is well buffered, has well defined carbonate chemistry and leached nitrates. Characteristics and concentrations (mg/L) of major ions in leached lysimeter water under arable land in Givendale, East Yorkshire :  $\text{Ca}^{2+}$  (94.9),  $\text{Mg}^{2+}$  (7.4),  $\text{Na}^+$  (4.7),  $\text{K}^+$  (3.7),  $\text{HCO}_3^-$  (116.1),  $\text{NO}_3^-$  (69.1),  $\text{SO}_4^{2-}$  (22.7),  $\text{Cl}^-$  (9.1). Calculated SEC (445  $\mu\text{S}/\text{cm}$ ); pH = 7.44.

Review of nitrate profiling in the USZ in East Yorkshire also indicate high nitrate concentrations from agricultural activities.

---

3. Solute diffuses in and out of the Chalk matrix when concentration gradients exist between the fractures and matrix in the USZ. This process leads to delay in solutes such as nitrates reaching

Literature review of Chalk matrix characterisation and unsaturated flow processes research articles and reports.

Matrix characterisation: Foster (1975); Barker and Foster, (1981); Price et al. (1982); Price et al. (2000).

---

---

water table (could be many decades)	Unsaturated zone flow studies: Zaidman et al. (1999); Allshorn et al. (2007); Keim et al. (2012).
-------------------------------------	---

---

***Throughput and saturated flow mechanisms***

---

4. Dilution and mixing of recharged water in the saturated zone of the unconfined aquifer.	Literature review of geochemical and hydrogeological texts and reports.	Pitman (1978); Herczeg and Edmunds (2000); Elliot et al. (2001); Smedley et al. (2004); Appello and Postma (2005).
5. Well oxygenated freshwater in the unconfined aquifer, dominated by Ca <sup>2+</sup> and HCO <sub>3</sub> <sup>-</sup> , with a pH ranging between 6.8 - 7.8, with a seasonally stable chemistry representative of a well buffered and homogenised groundwater system. The groundwater has NO <sub>3</sub> <sup>-</sup> > WHO NO <sub>3</sub> <sup>-</sup> limits, with Cl <sup>-</sup> , SO <sub>4</sub> <sup>2-</sup> , evident of the recent recharge and vulnerability of the aquifer to anthropogenic contamination.	Previous research articles and reports on Chalk groundwater sampling and chemical evolution. EA chemical archive and spring and well water sampling results presented in Chapter 5.	Geochemical references in statement 3. Analyses of EA archived groundwater sampling results presented in Chapter 5. Borehole temperature monitoring results presented in Chapter 5.

---

---

Thermally stable groundwater, representing groundwater that is thermally equilibrated with aquifer matrix.

---

- |    |  |   |   |
|----|--|---|---|
| 6. | Increased thickness of superficial deposits to the East of the Kilham catchment confine and protect the aquifer from anthropogenic pollution but make the groundwater anoxic in this area. | Literature review of hydrogeological and geochemical evolution of Chalk groundwater for the Northern Chalk. | Pitman (1986); Elliot et al. (2001); Smedley et al. (2004). |
|----|--|---|---|
- 

***Output and discharge mechanisms***

---

- |    |  |   |   |
|----|--|---|---|
| 7. | Dip and scarp slope springs have similar major ion chemistry reflecting the unconfined aquifer groundwater, with dominance of $\text{Ca}^{2+}$ , $\text{HCO}_3^-$ . $\text{NO}_3^- > \text{WHO NO}_3^-$ limits, with $\text{Cl}^-$ & $\text{SO}_4^{2-}$ indicating that the springs and unconfined groundwaters are affected by anthropogenic activity. In | Groundwater sampling and monitoring undertaken in Chapter 5 of this current work. Archived geochemical dataset from the EA website. | Chemical sampling and analyses presented in Chapter 5. EA chemical archive data accessible at <a href="https://environment.data.gov.uk/water-quality/view/explore">https://environment.data.gov.uk/water-quality/view/explore</a> . |
|----|--|---|---|
-

---

comparison with scarp slope  
springs, dip slope springs are  
thermally less variable possibly  
reflective of surface influence.  
Intermittent springs have lower  
SEC compared to perennial springs  
indicative of shorter residence time.

---

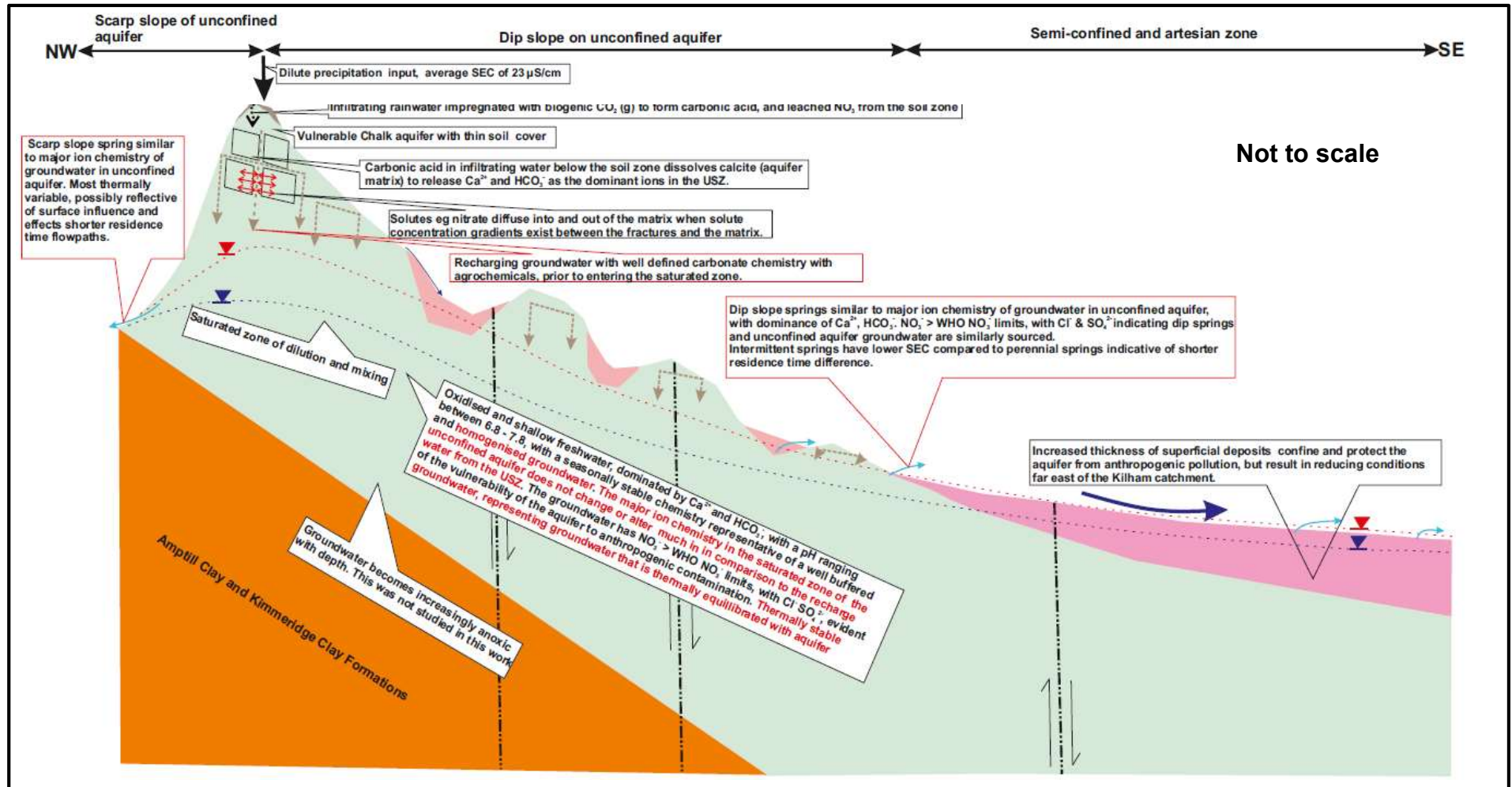


**Figure 7.2.** Chemical Conceptual Model of the study area and Kilham showing the key chemical processes in the model. Red call out boxes and texts are contributions from this current work to catchment understanding. Black boxes contain pre-existing literature information

## 7.2 Conceptual model summary description

Combining the physical and chemical conceptual models, the integrated catchment conceptual model is summarised below.

- i. the chalk aquifer is underlain by Jurassic deposits, and overlain by Quaternary superficial deposits to the east of Kilham village;
- ii. the chalk rises in the west of the study area where the aquifer is unconfined, reducing in elevation towards Kilham, becoming buried beneath superficial deposits to the east;
- iii. the aquifer is made up of low permeability but high storage matrix, with low storage but high permeability fractures/conduits;
- iv. the highly fractured nature of the aquifer makes the aquifer behave as a hydraulic continuum on the catchment scale, although the aquifer is karstic towards the discharge area of the dip slope from solutional enhancement from flow concentration and focusing;
- v. several east-west trending faults traverse the catchment, but their effect on groundwater flow was not ascertained by the methods in this work;
- vi. fracture dominated recharge occurs on the Wolds, through the thick unsaturated zone, although the continuity of quick unsaturated flow through the full thickness of the unsaturated Chalk to the saturated zone is uncertain;
- vii. the recharging water is dominated by calcium carbonate and contains nitrates and organic agrochemicals such as atrazine, DCM (dichloromethane) and trihalomethanes leached through the soil and unsaturated zone;
- viii. major ion chemistry of recharging water is similar to unconfined groundwater which is calcium carbonate dominated;
- ix. in the saturated zone, flow occurs mainly on bedding plane features, fractures such as strata and non-stratabound joints;
- x. the highly fractured nature of the aquifer produces a very homogenised and well mixed flow system in the saturated zone;
- xi. the permeability of the chalk is well developed in the unconfined aquifer from discrete dissolution features from active groundwater circulation;

- xii. permeability is developed both at shallow depths and relatively deeper depths of up to 70 mbgl;
- xiii. groundwater in the unconfined aquifer is well aerated and dominated by  $\text{Ca}^{2+}$  and  $\text{HCO}_3^-$ , with the occurrence of nitrates and agrochemicals indicative of post-1950 recharge;
- xiv. groundwater in the unconfined aquifer discharges from the aquifer via springs at the contact of the chalk aquifer and the Jurassic Formation on the scarp slope, and at springs near Kilham village and the artesian semi-confined area of the catchment on the dip slope;
- xv. the majority of the chalk discharge in the area to the dip slope springs;
- xvi. spring discharges from the catchment are oxygenated and have similar major ion chemistry to unconfined groundwater;
- xvii. the springs show some thermal variability (daily) in comparison with well water temperatures, reflective of surface effects on the springs.

### **7.3 Conceptual model uncertainties**

The following are areas of uncertainty in the developed conceptual model:

- i. Although faults are pervasive in the catchment, the depth of faulting and impact of faulting on groundwater flow are uncertain;
- ii. Evidence of previous USZ works shows rapid bypass flow during times of high hydraulic loading, but the continuity of quick unsaturated flow through the full USZ thickness to the water table is uncertain;
- iii. How much recharge occurs on the semi-confined area via the superficial deposits is uncertain;
- iv. Permeability development below the well depths in this study (up to 70 mgbl) is uncertain although Bloomfield and Shand (1998) found flowing features at 84 mgbl in a 100 m deep well in Carnaby (TA 1505 6486).

## **7.4 Implications of this project for groundwater management and resource protection**

The implications of the conceptual model for groundwater management and resource protection are discussed below.

In the study catchment, the thick unsaturated zone (USZ) has several functions. The USZ defines the chemistry of the water in the saturated zone and also stores and delays transport of solutes and contaminants to the saturated zone. Aside from preceding functions, the fractured nature of the unsaturated zone also enables recharge and solutes to bypass the unsaturated zone matrix to the water table. Solute in the unsaturated zone can also diffuse between the fracture and the matrix, resulting in attenuated but delayed solute arrival in the saturated zone. The implication of the functions above are that control and regulation of economic activities like agriculture on the catchment is an important means of protecting the resource. Wang et al. (2013) showed that nitrates could take a minimum of not less than 100 years (for 100 m thick USZ) for the nitrates of the 1970s to pass through the aquifer, implying that the current nitrate pollution control measures will not be sufficient. To ensure then that the saturated zone is protected from pollution and contamination, the current partnership between Chalk Stakeholders (the EA, YW, Natural England, farmers) needs improvement and strengthening via effective catchment management practices hinged on scientific evidence and data sharing to develop trust and understanding of the issues within the catchment.

The monitored springs and boreholes had nitrate concentrations above the 50 mg/L EU and WHO drinking water limit showing the poor status of the aquifer with respect to the European Water Framework Directive. This nitrate concentrations have their attendant health, economic, ecological and management implications. The little variability in the nitrate concentrations within each monitored site and the similarity of concentrations between sites implies an aquifer of homogenised mixing fed by a uniform nitrate input from the unsaturated zone. This implies that although there may be local variability in terms of nitrate application and leaching, similar control measures in one

part of the region can be replicated on the regional scale for effective aquifer resource management.

The nitrate concentrations recorded for this study have potential for hydrogeologic modelling in the aquifer. Using a mass balance approach, the low variability of nitrate concentrations at the springs combined with knowledge of groundwater travel times between boreholes and springs can be used to constrain the average residence time in the aquifer. Secondly, comparison of nitrate concentrations in the unsaturated and saturated zones can provide evidence of processes like dilution and mixing in the saturated zone. The well connected fractures makes the aquifer behave as a regional hydraulic continuum, meaning that Kilham and adjacent catchments may be acting as a contiguous unit, so that individual source protection zones based on topographic high boundaries are of limited utility. This work supports the EA's decision to demarcate the chalk outcrop as nitrate vulnerability zone.

Vertical head gradients in wells also have implications for the planning and implementation of groundwater sampling in wells and head monitoring. To obtain depth specific samples in wells will require isolation of horizons by packers to prevent communication of flow horizons. Without packers, then the chemical characteristics obtained will have to be interpreted as average well characteristics because the sample obtained will be a mixture of water from different flow horizons. Even for samples retrieved via pumping, knowledge of ambient flow rates in each of the horizons has to be obtained to ensure that appropriate pumping rates are used to achieve the aim of the sampling campaign. Wells in the catchment also need to be closely monitored and where necessary backfilled / sealed in to ensure they do not short circuit or distort flows in the aquifer, resulting in preferential travel paths for contaminants. As the open sections of the wells are long, groundwater heads will have to be interpreted as transmissivity-weighted composite head in each of the individual horizons connected to the open borehole, and not taken as the head in any one of the horizons contributing flow to the borehole. This information is critical for the determination of regional groundwater head gradients and interpretation of groundwater flow directions.

## **7.5 Chapter Summary**

In this chapter, a conceptual model of flow was developed for the study area and the Kilham Catchment. Two models were developed: a physical and chemical model. These models were developed from hydrogeologic descriptions derived from relevant review of geologic and hydrogeologic research on the Chalk aquifer, open-well dilution tests and synthesis activity undertaken for this study area in this current research work. The activities and audit trail of the source of information to support the hydrogeologic descriptions were also presented for transparency, ease of use and peer review purposes. The hydrogeological implications of the developed conceptual model in this chapter was also discussed.

## **Chapter 8 Conclusions and recommendations**

### **8.1 Aims and objectives**

This project had the overall aim of gaining insight into the types, patterns and regimes of flow in the Kilham catchment of the East Yorkshire Chalk aquifer. It sought to achieve the overall aim via four (4) main objectives as follows:

- A. Characterisation of flow geometry and topology between wells in the saturated zone and to the aquifer output (springs);
- B. Characterisation of the response of boreholes (throughput) and springs (output) to recharge and rainfall events (input);
- C. Characterisation of the effects of faults on groundwater flow in the study area;
- D. Development of a hydrogeological conceptual model of the study area to improve catchment processes and management.

The main objectives are reiterated with statement of project outcomes and findings to show the extent to which the project aim and objectives have been achieved. Following this, recommendations are given for the future to drive further research to improve on this work.

#### **8.1.1 Characterisation of flow geometry and topology between wells in the saturated zone, and to the aquifer output (springs).**

##### **Project outcomes:**

At the borehole scale, ambient uniform and point open-well dilution tests were undertaken in part of the unconfined area of the East Yorkshire Chalk. The ambient test was used because the wells had their water levels 10 m below ground level making the pumped method expensive. The open well dilution tests were interpreted in conjunction with previous caliper, CCTV and

televiwer images to characterise inflow, outflow, crossflow and vertical flows in the study area. Discrete flow horizons and features were distributed across all depths intersected by the wells. The majority of solutionally enlarged flow features were observed within the shallower depths indicative of fracture enlargement by recharging water. The nature of flow signatures in the wells is location specific, with marked differences between recharge (interfluvial), intermediate and discharge (valley) areas. Wells located in recharge areas were characterised by slow downward flow from the water table exiting at depth in the wells. Discharge areas on the other hand were dominated by relatively fast upward flow from greater depth towards shallower depths. The boreholes discharge via karstic features at depth, with discrete diffusive flow features distributed between flow at depth and the water table. The high heads in the flowing features at depth suggest connection to topographically high recharge areas. In wells with ambient upward flows, velocities were up to 4 m/min. Re-interpretation of previously conducted well-to-well tracer tests for the Kilham area, showed karstic flow connecting boreholes and springs that are up to about 4.8 km apart with groundwater velocities ranging 40 – 480 m/day. In spite of the connections between the boreholes, the catchment showed complex flow regime as there was no tracer connection between some boreholes that by position and flow direction might be expected to have been connected. The borehole tracer monitoring signature also showed that flow was via diffused and solutionally enlarged bedding features connected by vertical flow features forming stepped flow patterns in the area.

The ambient open-well dilution tests undertaken in this current work are novel. In comparison to previous open-well dilution tests undertaken in the area, which used only the uniform test, the combined use of the uniform and point open-well dilution tests and the other well logging mentioned above in this current work enabled a better detection and constraining of flow features in the wells. Comparing the current findings in this work with previous impeller logging in the boreholes showed good agreement for flow features detected. Secondly, the open-well dilution method proved superior in the detection of horizontal, crossflows and very low flows, which were not detectable by impeller logging. More importantly, an approach for finding groundwater

velocities from open-well dilution test data was developed and validated using well-to-well tracer tests.

### **8.1.2 Characterisation of the response of boreholes (throughput) and springs (output) to recharge and rainfall events (input) outcomes**

#### **Project outcomes**

Temperature monitoring of borehole flow horizons and springs showed a signal (9.2 – 10.1 °C) of little variability in comparison to air temperature (7 day average range of 2-18 °C). The relatively stable temperature signal from springs and boreholes is reflective of the average annual air temperature of 10.3 °C , indicative of an aquifer geometry with diffused recharge characteristics with long residence time flowpaths which produces a groundwater system that is temperature equilibrated with rock matrix. Comparing spring and borehole temperatures, springs show some thermal variability possibly from influence from air temperature. Logged SECs also showed a stable signal for boreholes and some variability for the springs. The non-varying SEC signal for Tancred Pit borehole is reflective of a well mixed calcite equilibrated closed carbonate environment, whereas the SEC variation for the springs may possibly be from the switching of the open and closed carbonate system along the flowpath of waters that discharge via the springs. The variation in SEC log of the springs could also be from the mixing and convergence of waters of different saturation levels at the springs. The major ion chemistry of springs and wells was dominated by  $\text{Ca}^{2+}$  and  $\text{HCO}_3^-$  which most likely varied due to factors that drive the carbonate dissolution process such as soil  $\text{pCO}_2$  variation due to biological and seasonal switching between open and closed systems arising from unsaturated zone thickness variation. The nitrate concentrations were significantly above the natural background values of about less than 9 mg/L, indicating an anthropogenic contribution from agricultural activity. The nitrate concentrations are above the EU and WHO drinking water limit which have economic, economic and resource protection implications. The nitrates in groundwater also show that water in

the unconfined aquifer is well oxygenated and is post mid-1950s. Composite groundwater head monitored in boreholes revealed similar hydrograph patterns in the study area with seasonal composite head fluctuations being minimum and maximum at the discharge and recharge areas respectively. Comparing the groundwater hydrograph pattern with daily precipitation data showed an unsaturated zone that masks rapid bypass recharge input signals to the saturated zone. The non-detection of the rapid bypass recharge to the saturated zone could be attributed to the highly fractured nature of the water table fluctuation zone, which masks input recharge signals from specific monitored wells. Correlation between groundwater hydrographs and Foston Mill, a groundwater fed spring discharge hydrograph also showed that Foston Mill mimicked the general groundwater hydrograph pattern. However, the Foston Mill gauging discharge showed some spikiness that coincided with precipitation events, indicative of a minor component from surface run-off as part of the catchment of the Foston Beck is covered by Devensian glacial tills.

### **8.1.3 Characterisation of the effects of faults on groundwater flow in the study area outcomes.**

#### **Project outcomes**

A review of available data for the study area showed a heterogenous and anisotropic aquifer of variable transmissivities in both the confined and unconfined areas, with the highest values in the unconfined area west of Kilham, the artesian and semiconfined zones. The available high transmissivity dataset for the unconfined zone showed a bias towards the valleys rather than the interfluves because of the paucity of wells on the interfluves. Results of re-analysed archived pumping tests for the Kilham Catchment yielded values of between  $432 - 17700 \text{ m}^2\text{d}^{-1}$ , and demonstrated a large variability in transmissivity, even on the scale of the Kilham catchment. The transmissive nature of the unconfined aquifer is demonstrated by the very low drawdowns noted for pumping tests conducted in the area. The relatively high transmissivities in the area arise due to the active groundwater circulation and flow concentration that result in solution enhancement of fractures both at the zone of water table fluctuation and at depth in the aquifer.

Literature review of a BGS large scale pumping test undertaken in the area in 1982 suggested the existence of boundary effects on the north western and north eastern parts of the catchment probably from the Burton Fleming and Humanby faults, or from recharge boundary effects in the Gypsey Race Valley, or from a combination of both preceding factors. In this study, a re-analyses of pumping test data and plot of transmissivities and E-W trending fault traces in the area to correlate and investigate the effects of faults on flow in the catchment failed to elucidate the effects of faults on groundwater flow in the area. The reasons are that most of the wells are not near or straddling faults, and also that the highly transmissive nature of the aquifer make it difficult for cones of drawdown to reach the faults.

#### **8.1.4 Development of a hydrogeological conceptual model to improve catchment process understanding for effective catchment management outcomes.**

##### **Project outcomes**

The findings from objectives A to C, were used to develop a physical and chemical hydrogeological conceptual model, which described the key input, throughput and output processes for the aquifer. The implications of the conceptual model for groundwater management and resource protection were also discussed. The main outcomes of this exercise are summarised below.

- i. the chalk aquifer is underlain by Jurassic deposits, and overlain by Quaternary superficial deposits to the east of Kilham village;
- ii. the aquifer is made up of low permeability but high storage matrix, with low storage but high permeability fractures/conduits;
- iii. the aquifer is karstic towards the discharge area of the dip slope from solutional enhancement from flow concentration and focusing;
- iv. fracture dominated recharge occurs on the Wolds, through the thick unsaturated zone;
- v. the recharging water and aquifer water are both dominated by calcium carbonate and contain nitrates and agrochemicals leached through the soil and unsaturated zone indicative of young recharge;

- vi. in the saturated zone, flow occurs mainly on bedding plane features, and fractures such as stratabound and non-stratabound joints;
- vii. flow velocities of 40 – 480 m/day recorded from well-to-well tracer tests from previous work and the velocities were compared to predictions from the ambient open-well dilution was conducted here, and the conclusion is that high groundwater velocities are likely to be pervasive in this aquifer;
- viii. the permeability of the chalk is well developed both on the surface and at depth in the unconfined aquifer from discrete dissolution features from active groundwater circulation;
- ix. groundwater in the unconfined aquifer discharges naturally from the aquifer via springs at the scarp and dip slopes with the majority of the discharge to the dip slope springs;
- x. spring discharges from the catchment are oxygenated and have similar major ion chemistry to unconfined groundwater;
- xi. the springs show some thermal variability (daily) in comparison with well water temperatures, reflective of surface effects on the springs.

## **8.2 Further work and recommendations**

To further improve the understanding of flow regimes of the East Yorkshire Chalk Aquifer, some further work and recommendations are suggested below.

Since the unsaturated zone profiling of the 1970 and 80s, there has been a lull in nitrate profiling to characterise nitrate concentrations and its fate in the unsaturated zone. To calibrate unsaturated zone solute transport models so as to predict future nitrate impacts, unsaturated zone nitrate profiling has to start and be maintained.

To corroborate the unsaturated zone profiling above, the current periodic borehole water sampling by the Environment Agency has to be continued, to provide a continuous time series of nitrate arrivals at the saturated zone. It will also be useful to age date borehole and spring waters so as constrain the arrival times of nitrates. In contrast to previous sampling undertaken for age dating by the EA, a few depth specific piezometers will have to be installed to sample different horizons in the aquifer because of the vertical head

gradients in the boreholes. Aside the piezometers, packers could be used in a few selected open section wells during the sampling campaigns.

In order to constrain flow horizons and the groundwater chemistry specific to the flow horizons in the catchment, a combined use of flow logging, packers and depth specific sampling in wells is recommended for the future. This will also provide fracture head, transmissivity and flowing porosity of flow horizons, which would improve the groundwater velocities obtained from the open-well dilution tests.

The effects of the E-W trending faults on groundwater flow in the catchment may be better understood by drilling and characterising wells that are near and straddle the faults. Several tests including continuous monitoring of groundwater heads, undertaking of pumping tests and cross well tomography between wells straddling faults may provide insight into the flow characteristics across the faults. Also, a repetition of a large scale and long duration pumping tests similar to that undertaken by the BGS in the 1980s, but this time rigorously monitored especially around near the fault zone has the potential to provide valuable information not only about the aquifer structure and flow properties but the response of the faults to induced hydraulic stresses. In addition, it would also be useful if the wells were fully characterized well using open-well dilution tests and acoustic logs prior to the conduction of the pumping tests.

## List of References

- Akoachere, R.A.I.I. and Van Tonder, G. 2009. Two new methods for the determination of hydraulic fracture apertures in fractured-rock aquifers. *Water SA*. **35**(3),pp.349–360.
- Allen, D.J., Brewerton, L.J., Coleby, L.M., Gibbs, B.R., Lewis, M.A., MacDonald, A.M., Wagstaff, S.J. and Williams, A.T. 1997. *The physical properties of major aquifers in England and Wales*. British Geological Survey Technical Report WD/97/34.
- Allshorn, S.J.L. 2008. Flow and solute transport in the unsaturated zone of the Chalk in East Yorkshire. PhD Thesis. University of Leeds.
- Allshorn, S.J.L., Bottrell, S.H., West, L.J. and Odling, N.E. 2007. Rapid karstic bypass flow in the unsaturated zone of the Yorkshire chalk aquifer and implications for contaminant transport. *Geological Society, London, Special Publications*. [Online]. **279**(1),pp.111–122. Available from: <http://sp.lyellcollection.org/cgi/doi/10.1144/SP279.10>.
- American Public Health Association, American Water Works Association, W.E.F. 1999. *Standard Methods for the Examination of Water and Wastewater*.
- Anderson, M.P. 2005. Heat as a ground water tracer. *Ground Water*. **43**(6),pp.951–968.
- Appello, C. and Postma, D. 2005. *Geochemistry, groundwater and pollution* 2nd ed. Leiden: Balkema.
- Ashton, K. 1966. The analyses of flow data from karst drainage basins. *Trans. Cave Res. Group*. **7**,pp.161–203.
- Atkinson, T.C. 1977. Diffuse flow and conduit flow in limestone terrain in the Mendip Hills, Somerset (Great Britain). *Journal of Hydrology*. **35**(1–2),pp.93–110.
- Azeez, N.H. 2017. Hydrology of the Chalk Aquifer in East Yorkshire from Spring Recession Analysis. PhD Thesis. University of Leeds, Leeds, UK.
- Banks, D. 2008. *An introduction to thermogeology: ground source heating and cooling*. Oxford: Blackwell Publishing.
- Banks, D., Gandy, C.J., Younger, P.L., Withers, J. and Underwood, C. 2009. Anthropogenic thermogeological ‘anomaly’ in Gateshead, Tyne and Wear, UK. *Quarterly Journal of Engineering Geology and Hydrogeology*. [Online]. **42**(3),pp.307–312. Available from: <http://qjgegh.lyellcollection.org/cgi/doi/10.1144/1470-9236/08-024>.
- Barker, J.A. and Foster, S.S.D. 1981. A diffusion exchange model for solute movement in fissured porous rock. *Quarterly Journal of Engineering Geology and Hydrogeology*. [Online]. **14**(1),pp.17–24. Available from: <http://qjgegh.lyellcollection.org/cgi/doi/10.1144/GSL.QJEG.1981.014.01.02>.

- Barker, J.A. and Herbert, R. 1989. Nomograms for the analysis of recovery tests on large-diameter wells. *Quarterly Journal of Engineering Geology*. **22**,pp.151–158.
- Barker, J.A., Wright, T.E.J. and Fretwell, B.A. 2000. A pulsed-velocity method of double-porosity solute transport modelling *In: A. Dassargues, ed. Tracers and Modelling in Hydrogeology, vol. 262. IAHS. Wallingford, Oxfordshire*, pp. 297–302.
- Barker, R.D. 1994. Some hydrogeophysical properties of the Chalk of Humberside and Lincolnshire. *Quarterly Journal of Engineering Geology*. **27**,pp.S12–S13.
- Barker, R.D., Lloyd, J.W. and Peach, D.W. 1984. The use of resistivity and gamma logging in lithostratigraphical studies of the Chalk in Lincolnshire and South Humberside. *Quarterly Journal of Engineering Geology*. **17**,pp.71–80.
- Bense, V.F., Gleeson, T., Loveless, S.E., Bour, O. and Scibek, J. 2013. Fault zone hydrogeology. *Earth-Science Reviews*. [Online]. **127**,pp.171–192. Available from: <http://dx.doi.org/10.1016/j.earscirev.2013.09.008>.
- Berridge, N.G. and Pattison, J. 1994. Geology of the country around Grimsby and Patrington, Memoir of the British Geological Survey, Sheets 90, 91, 81 and 82 (England and Wales)
- Bevan, T.G. and Hancock, P.L. 1986. A late Cenozoic regional mesofracture system in southern England and northern France. *Journal of the Geological Society*. **143**(2),pp.355–362.
- Birk, S., Liedl, R. and Sauter, M. 2004. Identification of localised recharge and conduit flow by combined analysis of hydraulic and physico-chemical spring responses (Urenbrunnen, SW-Germany). *Journal of Hydrology*. **286**(1–4),pp.179–193.
- Black, J.H. and Brightman, M.A. 2007. Conceptual model of the hydrogeology of Sellafeld. *Quarterly Journal of Engineering Geology and Hydrogeology*. **29**(Supplement 1),pp.S83–S93.
- Bloomfield, J. 1996. Characterisation of hydrogeologically significant fracture distributions in the Chalk: An example from the Upper Chalk of southern England. *Journal of Hydrology*. **184**(3–4),pp.355–379.
- Bloomfield, J.P. 1997. The role of diagenesis in the hydrogeological stratification of carbonate aquifers: An example from the Chalk at Fair Cross, Berkshire, UK. *Hydrology and Earth System Sciences*. (1),pp.19–33.
- Bloomfield, J.P., Brewerton, L.J. and Allen, D.J. 1995. Regional trends in matrix porosity and dry density of the Chalk of England. *Quarterly Journal of Engineering Geology and Hydrogeology*. **28**(Supplement\_2),pp.S131–S142.
- Bloomfield, J.P. and Shand, P. 1998. *Summary of the Carnaby Moor Borehole investigation*. British Geological Survey Technical Report, WD/98/30.

- Brainerd, R.J. and Robbins, G.A. 2004. A tracer dilution method for fracture characterization in bedrock wells. *Ground water*. **42**(5),pp.774–780.
- Brassington, F.C. 1992. Measurements of Head Variations within Observation Boreholes and their Implications for Groundwater Monitoring. *Water and Environment Journal*. **6**(3),pp.91–100.
- Brassington, F.C. and Younger, P.L. 2010. A proposed framework for hydrogeological conceptual modelling. *Water and Environment Journal*. **24**(4),pp.261–273.
- Brassington, R. 2007. *Field Hydrogeology* 3rd ed. Chichester: Wiley.
- Bravo, H.R., Jiang, F. and Hunt, R.J. 2002. Using groundwater temperature data to constrain parameter estimation in a groundwater flow model of a wetland system. *Water Resources Research*. [Online]. **38**(8),pp.28-1-28–14. Available from: <http://doi.wiley.com/10.1029/2000WR000172>.
- Brook, G.A., Folkoff, M.E. and Box, E.. 1983. A world model of soil carbon dioxide. *Earth Surf. Process. Landforms*. **8**,pp.79–88.
- Buckley, D.K., Hinsby, K. and Manzano, M. 2001. Application of geophysical borehole logging techniques to examine coastal aquifer palaeohydrogeology. *Geological Society, London, Special Publications*. **189**(1),pp.251–270.
- Buckley, D.K. and Talbot, J.C. 1996. *Geophysical logging at West Newton Grange, Golden Square wood, West End Farm, Kilham and Ella Crossroads boreholes*. On behalf of North East Region, Environment Agency. Technical Report WD/96/31.
- Buckley, D.K. and Talbot, J.C. 1994. *Interpretation of geophysical logs of the Kilham area, Yorkshire Wolds, to support groundwater tracer studies*. British Geological Survey Technical Report,WD/94/10C.
- Bundschuh, J. 1993. Modeling annual variations of spring and groundwater temperatures associated with shallow aquifer systems. *Journal of Hydrology*. **142**(1–4),pp.427–444.
- Busby, J., Lewis, M., Reeves, H. and Lawley, R. 2009. Initial geological considerations before installing ground source heat pump systems. *Quarterly Journal of Engineering Geology and Hydrogeology*. [Online]. **42**(3),pp.295–306. Available from: <http://qjehg.lyellcollection.org/cgi/doi/10.1144/1470-9236/08-092>.
- Buss, S.R., Rivett, M.O., Morgan, P. and Bemment, C.D. 2005. *Attenuation of Nitrate in the Sub-Surface Environment*. Science Environment Agency Report SC030155/SR2. [Online]. Almondsbury, Bristol. Available from: <http://publications.environment-agency.gov.uk/pdf/SCHO0605BJCS-e-e.pdf>.
- Butcher, A.S. and Townsend, B.R. 2017. *Geophysical Logging of three Chalk boreholes in the Kilham area, North Yorkshire*. Groundwater Science Programme Commissioned Report CR/17/108.
- Cartwright, K. 1970. Groundwater Discharge in the Illionois Basin as

- Suggested by Temperature Anomalies. *Water Resources Research*. **6**(3),pp.912–918.
- Cartwright, K. 1968. *Temperature prospecting for shadow glacial and alluvial aquifers in Illinois*. Illinois State Geological Survey Circular 433.
- Chadwick, R.A. and Evans, D.J. 2005. *A seismic atlas of Southern Britain - Images of Subsurface structure*. British Geological Survey.
- Christopher, N.S.J. 1980. A preliminary flood pulse study of Russett Well, Derbyshire. *Trans. Brit. Cave. Res. Ass.* **7**(1),pp.1–12.
- Clayton, C.J. 1986. The chemical environment of flint formation in the Upper Cretaceous Chalks *In: G. de C. Sieveking and M. B. Hart, eds. The scientific study of flint and chert*.
- Cooper, H.H. and Jacob, C.E. 1946. A Generalized Graphical Method for Evaluating Formation Constants and Summarizing Well-Field History. *Transactions of the American Geophysical Union*. **27**(IV),pp.526–534.
- Cooper, J.D., Gardner, C.M.K. and Mackenzie, N. 1990. Soil controls on recharge to aquifers. *Journal of Soil Science*. **41**(4),pp.613–630.
- Covington, M.D., Luhmann, A.J., Gabrovec, F., Saar, M.O. and Wicks, C.M. 2011. Mechanisms of heat exchange between water and rock in karst conduits. *Water Resources Research*. **47**(10).
- Crowther, J. and Pitty, A.F. 1982. Water temperature variability as an indicator of shallow-depth groundwater behaviour in limestone areas in west Malaysia. *Journal of Hydrology*. **57**(1–2),pp.137–146.
- Van den Daele, G.F.A., Barker, J.A., Connell, L.D., Atkinson, T.C., Darling, W.G. and Cooper, J.D. 2007. Unsaturated flow and solute transport through the Chalk: Tracer test and dual permeability modelling. *Journal of Hydrology*. **342**(1–2),pp.157–172.
- Dalton, H. and Brand-Hardy, R. 2003. Nitrogen: The essential public enemy. *Journal of Applied Ecology*. **40**(5),pp.771–781.
- Dalton, M.G., Huntsman, B.E. and Bradbury, K. 2006. Acquisition and interpretation of water level data *In: D. Nielsen and G. L. Nielsen, eds. The essential handbook of ground-water sampling*. Boca Raton, Florida: CRC Press, p. 309.
- Darling, W.G. and Bath, A.H. 1988. A stable isotope study of recharge processes in the English Chalk. *Journal of Hydrology*. **101**,pp.31–46.
- Darling, W.G., Goody, D.C., Morris, B.L. and Peach, D.W. 2012. The hydrochemistry of a Chalk aquifer during recovery from drought. *Quarterly Journal of Engineering Geology and Hydrogeology*. [Online]. **45**(4),pp.473–486. Available from: <http://qjehg.lyellcollection.org/cgi/doi/10.1144/qjehg2012-022>.
- Desmarais, K. and Rojstaczer, S. 2002. Inferring source waters from measurements of carbonate spring response to storms. *Journal of Hydrology*. **260**(1–4),pp.118–134.

- Doucette, R. and Peterson, E.W. 2014. Identifying water sources in a karst aquifer using thermal signatures. *Environmental Earth Sciences*. **72**(12),pp.5171–5182.
- Doughty, C. and Tsang, C. 2005. Signatures in flowing fluid electric conductivity logs. *Journal of Hydrology*. **310**,pp.157–180.
- Downing, R.A. 1998. *Groundwater - our hidden asset*. Produced by the UK Groundwater Forum. Published by the British Geological Survey.
- Downing, R.A., Price, M. and Jones, G.P. 1993. The Making of an aquifer *In*: R. A. Downing, M. Price and G. P. Jones, eds. *The Hydrogeology of the Chalk of North-West Europe*. Oxford: Clarendon Press, pp. 1–13.
- Downing, R.A., Smith, D. and Warren, S. 1978. Seasonal variations of tritium and other constituents in groundwater in the Chalk near Brighton, England. *Institution of Water Engineers and Scientists*. **32**,pp.123–136.
- Dreiss, S.J. 1989. Regional scale transport in a Karst Aquifer: 1. Component separation of spring flow hydrographs. *Water Resources Research*. **25**(1),pp.117–125.
- Drost, W., Klotz, D., Koch, A., Moser, H., Neumaier, F. and Rauert, W. 1968. Point dilution methods of investigating ground water flow by means of radioisotopes. *Water Resources Research*. **4**(1),pp.125–146.
- Edmunds, W.M., Buckley, D.K., Darling, W.G., Milne, C.J., Smedley, P.L. and Williams, A.T. 2001. Palaeowaters in the aquifers of the coastal regions of southern and eastern England. *Geological Society, London, Special Publications*. **189**(1),pp.71–92.
- Edmunds, W.M., Cook, J.M., Darling, W.G. and Kinniburgh, D.G. 1987. Baseline geochemical conditions in the Chalk aquifer, Berkshire, UK: a basis for groundwater quality management. *Applied Geochemistry*. **2**,pp.251–274.
- Eith, C., Kolb, M., Rumi, A., Seubert, A. and Viehweger, K. 2007. *Practical Ion Chromatography*. Herisau, Switzerland.
- Elliot, T., Chadha, D.S. and Younger, P.L. 2001. Water quality impacts and palaeohydrogeology in the Yorkshire Chalk aquifer, UK. *Quarterly Journal of Engineering Geology and Hydrogeology*. [Online]. **34**(4),pp.385–398. Available from: <http://qjehg.lyellcollection.org/cgi/doi/10.1144/qjehg.34.4.385>.
- Enemark, T., Peeters, L.J.M., Mallants, D. and Batelaan, O. 2019. Hydrogeological conceptual model building and testing: A review. *Journal of Hydrology*. [Online]. **569**,pp.310–329. Available from: <https://doi.org/10.1016/j.jhydrol.2018.12.007>.
- Environment Agency 2001. *Guide to good practice for the development of conceptual models and the selection and application of mathematical models of contaminant transport processes in the subsurface*. Bristol.
- ESI 2010. *East Yorkshire Aquifer: Conceptual Model Report No. 60271R1D1. Prepared for the Environment Agency*.

- European Commission 1991. *Council Directive, Nitrates 91/676/EEC of 12 December 1991 concerning the protection of waters against pollution caused by nitrates from agricultural sources*. Official Journal of the European Communities.
- European Commission 2000. *Council Directive, Water Framework (2000/60/EC). EC Directive of the European Parliament and of the Council 2000/60/EC of 23 October 2000 for establishing a framework for action in the field policy*. Official Journal of the European Communities.
- European Geophysical Services Ltd 2018. *Report on the CCTV Survey and Geophysical Logging of Borehole No.1 at Kilham Pumping Station. Prepared for Yorkshire Water Services Ltd*.
- Evans, G. 1995. Inverting fluid conductivity logs for fracture inflow parameters. *Water Resources Research*. **31**(12),pp.2905–2915.
- Farr, G.J., Patton, A.M., Boon, D.P., James, D.R., Williams, B. and Schofield, D.I. 2017. Mapping shallow urban groundwater temperatures, a case study from Cardiff, UK. *Quarterly Journal of Engineering Geology and Hydrogeology*. [Online]. **50**(2),pp.187–198. Available from: <http://qjgegh.lyellcollection.org/lookup/doi/10.1144/qjgegh2016-058>.
- Farrant, A.R., Woods, M.A., Maurice, L., Haslam, R., Raines, M. and Kendall, R. 2016. *Geology of the Kilham area and its influence on groundwater flow. British Geological Survey Commissioned Report CR/16/023*.
- Ford, D. and Williams, P. 2007. *Karst Hydrogeology and Geomorphology*. Chichester: Wiley.
- Foster, S.S.D. 2000. Assessing and Controlling the Impacts of Agriculture on Groundwater—from Barley Barons to Beef Bans. *Quarterly Journal of Engineering Geology and Hydrogeology*. **33**(4),pp.263–280.
- Foster, S.S.D. 1974. Groundwater Storage-Riverflow Relations in a Chalk Catchment. *Journal of Hydrology*. **23**,pp.229–311.
- Foster, S.S.D. 1975. The Chalk Groundwater Tritium Anomaly-A possible Explanation. *Journal of Hydrology*. **25**,pp.159–165.
- Foster, S.S.D. 1976. The Vulnerability of British Groundwater Resources to Pollution by Agricultural Leachates. *M.A.F.F. tech Bull.* **32**,pp.68–91.
- Foster, S.S.D. and Crease, I. 1974. Nitrate Pollution of Chalk groundwater in East Yorkshire – a hydrogeological appraisal. *Journal of the Institute of Water Engineers and Scientists*. **28**,pp.178–194.
- Foster, S.S.D. and Crease, R.I. 1975. Hydraulic behaviour of the Chalk Aquifer in the Yorkshire Wolds. *Proc. Instn Civ. Engrs.* (59),pp.181–188.
- Foster, S.S.D., Cripps, A. and Smith-Carington, A. 1982. Nitrate leaching to groundwater. *Phil. Trans. R. Soc. Lond.* **296**,pp.477–489.
- Foster, S.S.D. and Milton, V.A. 1976. *Hydrogeological basis for large-scale development of groundwater storage capacity in the East Yorkshire Chalk*. Report of the Institute of Geological Sciences, 76/7.

- Foster, S.S.D. and Milton, V.A. 1974. The permeability and storage of an unconfined chalk aquifer. *Hydrological Sciences Bulletin*. **XIX**(4),pp.485–500.
- Freeze, R.A. and Cherry, J.A. 1979. *Groundwater*. New Jersey: Prentice Hall Inc.
- Freeze, R.A. and Witherspoon, P.A. 1968. Theoretical Analysis of Regional Ground Water Flow 3. Quantitative Interpretations. *Water Resources Research*. **4**(3),pp.581–590.
- Freeze, R.A. and Witherspoon, P.A. 1967. Theoretical Analysis Regional Groundwater Flow. 2. Effect of Water-Table Configuration and Subsurface Permeability Variation. *Water Resources Research*. **3**(2),pp.623–634.
- Gale, I.N. and Rutter, H.K. 2006. *The Chalk aquifer of Yorkshire*. British Geological Survey Research Report. RR/06/04.
- Gossell, M.A., Nishikawa, T., Hanson, R.T., Izbicki, J.A., Tabidian, M.A. and Bertine, K. 1999. Application of Flowmeter and Depth-Dependent Water Quality Data for Improved Production Well Construction. *Ground Water*. **37**(5),pp.729–735.
- Goudie, A. 1990. *Landforms of England and Wales*. Oxford: Basil Blackwell.
- Greer, F.R. and Shannon, M. 2005. Infant methemoglobinemia: The role of dietary nitrate in food and water. *Pediatrics*. **116**(3),pp.784–786.
- Gustafsson, E. and Anderson, P. 1991. Groundwater flow conditions in a low-angle fracture zone at Finnsjon, Sweden. *Journal of Hydrology*. **126**,pp.79–111.
- Hall, S.H. 1993. Single Well Tracer Tests in Aquifer Characterization. *Groundwater Monitoring & Remediation*. **13**(2),pp.118–124.
- Hancock, J.M. 1993. The formation and diagenesis of Chalk. In: R. A. Downing, M. Price and G. P. Jones, eds. *The hydrogeology of the Chalk of north- west Europe*. Oxford: Clarendon Press.), pp. 14–34.
- Hartmann, S. 2004. Flow and transport in the confined Chalk aquifer of East Yorkshire. PhD Thesis. University of Leeds, Leeds, UK.
- Hartmann, S., Odling, N.E. and West, L.J. 2007. A multi-directional tracer test in the fractured Chalk aquifer of E. Yorkshire, UK. *Journal of Contaminant Hydrology*. [Online]. **94**(3–4),pp.315–331. Available from: <http://linkinghub.elsevier.com/retrieve/pii/S0169772207000927>.
- He, Q., Yang, P., Yuan, W., Jiang, Y., Pu, J., Yuan, D. and Kuang, Y. 2010. The use of nitrate, bacteria and fluorescent tracers to characterize groundwater recharge and contamination in a karst catchment, Chongqing, China. *Hydrogeology Journal*. **18**(5),pp.1281–1289.
- Headworth, H.G. 1972. The analysis of natural groundwater fluctuations in the chalk of Hampshire. *J. Insti. Water Eng.* **26**,pp.107–124.
- Hem, J. 1982. *Study and Interpretation of Chemical Characteristics of Natural*

*Water. USGS Water Supply Paper 2254* 3rd ed. USG Printing Office.

- Herczeg, A.L. and Edmunds, W.M. 2000. Inorganic Ions as Tracers *In*: P. G. Cook and A. L. Herczeg, eds. *Environmental Tracers in Subsurface Hydrology*. Boston: Kluwer Academic Publishers, p. 529.
- Higginbottom, I.E. and Fookes, P.G. 1970. Engineering aspects of periglacial features in Britain. *Quarterly Journal of Engineering Geology and Hydrogeology*. **3**(2),pp.85–117.
- Hiscock, K.M. and Lloyd, J.W. 1992. Palaeohydrogeological reconstructions of the North Lincolnshire Chalk, UK, for the last 140 000 years. *Journal of Hydrology*. **133**(3–4),pp.313–342.
- Howard, K. and Lloyd, J.W. 1983. Major Ion Characterisation of Coastal Saline Ground Waters. *Ground Water*. **21**(4),pp.429–437.
- Hubbert, M.K. 1940. The Theory of Ground-Water Motion. *The Journal of Geology*. **48**(8),pp.785–944.
- Jones, H., Gale, I., Barker, J. and Shearer, T. 1993. *Hydrogeological report on the test pumping of Hutton Cranswick, Kilham, and Elmswell boreholes. British Geological Survey Technical Report, WD/93/9.*
- Kappelmeyer, O. 1957. The use of near surface temperature measurements for discovering anomalies due to causes at depths. *Geophys. Prospect*. **5**(3),pp.239–258.
- Kearl, P. 1997. Observations of particle movement in a monitoring well using the colloidal borescope. *Journal of Hydrology*. **200**,pp.323–344.
- Keim, D. 2013. Quantifying water and nitrate fluxes in the Yorkshire Chalk unsaturated zone. PhD Thesis. University of Leeds.
- Keim, D.M., West, L.J. and Odling, N.E. 2012. Convergent Flow in Unsaturated Fractured Chalk. *Vadose Zone Journal*. [Online]. **11**(4). Available from: <https://www.soils.org/publications/vzj/abstracts/11/4/vzj2011.0146>.
- Keys, W.S. 1990. *Chapter E2. Borehole geophysics applied to ground-water investigations. Techniques of Water-Resources Investigations of the United States Geological Survey*. United States Geological Survey.
- Kirby, G.A. and Swallow, P.W. 1987. Tectonism and sedimentation in the Flamborough Head region of north-east England. *Proceedings of the Yorkshire Geological Society*. **46**(4),pp.301–309.
- Knapp, M.F. 2005. Diffuse pollution threats to groundwater: A UK water company perspective. *Quarterly Journal of Engineering Geology and Hydrogeology*. **38**(1),pp.39–51.
- Kobr, M. 2003. Geophysical techniques applied to aquifer hydrodynamics. *Bollettino di Geofisica Teorica ed Applicata*. **44**(3–4),pp.307–319.
- Krawczyk, W.E. and Ford, D.C. 2006. Correlating Specific Conductivity with Total Hardness in Limestone and Dolomite Karst Waters. *Earth Surf. Process. Landforms*. **31**,pp.221–234.

- Kresic, N. 2010. Sustainability and management of springs *In*: N. Kresic and Z. Stevanovic, eds. *Groundwater hydrology of springs: engineering, theory, management, and sustainability*. [Online]. Burlington, MA: Butterworth-Heinemann, Elsevier Inc., pp. 1–29. Available from: <http://dx.doi.org/10.1016/B978-1-85617-502-9.00001-3>.
- Ladeira, F.L. and Price, N.J. 1981. Relationship between fracture spacing and bed thickness. *Journal of Structural Geology*. **3**(2),pp.179–183.
- Lawrence, A.R., Foster, S. and Izzard, P. 1983. Nitrate Pollution of Chalk Groundwater in East Yorkshire-A Decade on. *Water and Environment Journal*. **37**(5),pp.410–419.
- Laxen, D.P.H. 1977. A specific conductance method for quality control in water analysis. *Water Research*. **11**,pp.91–94.
- Lewis, D.C., Kriz, G.J. and Burgy, R.H. 1966. Tracer dilution sampling technique to determine hydraulic conductivity of fractured rock. *Water Resources Research*. **2**(3),pp.533–542.
- Lewis, E.L. 1980. The Practical Salinity Scale 1978 and Its Antecedents. *IEEE Journal of Oceanic Engineering*. **5**(1),pp.3–8.
- Liang, X., Liu, Y., Jin, M., Lu, X. and Zhang, R. 2010. Direct observation of complex Tothian groundwater flow systems in the laboratory. *Hydrological Processes*. **3573**,pp.3568–3573.
- Liñán Baena, C., Andreo, B., Mudry, J. and Carrasco Cantos, F. 2009. Groundwater temperature and electrical conductivity as tools to characterize flow patterns in carbonate aquifers: The Sierra de las Nieves karst aquifer, southern Spain. *Hydrogeology Journal*. **17**(4),pp.843–853.
- Löw, S., Kelley, V. and Vomvoris, S. 1994. Hydraulic borehole characterization through the application of moment methods to fluid conductivity logs. *Journal of Applied Geophysics*. **31**(1–4),pp.117–131.
- Luhmann, A.J., Covington, M.D., Peters, A.J., Alexander, S.C., Anger, C.T., Green, J.A., Runkel, A.C. and Alexander, E.C. 2011. Classification of Thermal Patterns at Karst Springs and Cave Streams. *Ground Water*. **49**(3),pp.324–335.
- Luo, M., Chen, Z., Zhou, H., Zhang, L. and Han, Z. 2018. Hydrological response and thermal effect of karst springs linked to aquifer geometry and recharge processes. *Hydrogeology Journal*. **26**,pp.629–639.
- Maldaner, C.H., Quinn, P.M., Cherry, J.A. and Parker, B.L. 2018. Improving estimates of groundwater velocity in a fractured rock borehole using hydraulic and tracer dilution methods. *Journal of Contaminant Hydrology*. [Online]. **214**(May),pp.75–86. Available from: <https://doi.org/10.1016/j.jconhyd.2018.05.003>.
- Manga, M. 2001. Using Springs to Study Groundwater Flow and Active Geologic Processes. *Annu. Rev. Earth Planet. Sci.* **29**,pp.201–228.
- Martin, J.B. and Dean, R.W. 1999. Temperature as a natural tracer of short residence times for ground water in karst aquifers *In*: A. N. Palmer, M. V.

- Palmer and I. . Sasowsky, eds. *Karst Modeling*. Karst Waters Institute Special Publication, vol. 5, pp. 236–242.
- Maurice, L., Barker, J.A., Atkinson, T.C., Williams, A.T. and Smart, P.L. 2010. A Tracer Methodology for Identifying Ambient Flows in Boreholes. *Ground Water*. **49**(2),pp.227–238.
- Maurice, L.D., Atkinson, T.C., Barker, J.A., Williams, A.T. and Gallagher, A.J. 2012. The nature and distribution of flowing features in a weakly karstified porous limestone aquifer. *Journal of Hydrology*. [Online]. **438–439**,pp.3–15. Available from: <http://dx.doi.org/10.1016/j.jhydrol.2011.11.050>.
- McCleskey, R.B. 2011. Electrical conductivity of electrolytes found in natural waters from (5 to 90) °C. *Journal of Chemical and Engineering Data*. **56**(2),pp.317–327.
- McCleskey, R.B., Nordstrom, D.K. and Ryan, J.N. 2012. Comparison of electrical conductivity calculation methods for natural waters. *Limnology and Oceanography: Methods*. [Online]. **10**,pp.952–967. Available from: <http://www.aslo.org/lomethods/free/2012/0952.html>.
- McClean, R.D. 1969. The effect of tipped domestic refuse on groundwater quality: a survey in North Kent. *Proc. Soc. Wat. Treat. Exam.* **18**,pp.18–34.
- McMillan, L.A., Rivett, M.O., Tellam, J.H., Dumble, P. and Sharp, H. 2014. Influence of vertical flows in wells on groundwater sampling. *Journal of Contaminant Hydrology*. [Online]. **169**,pp.50–61. Available from: <http://dx.doi.org/10.1016/j.jconhyd.2014.05.005>.
- McNeil, V.H. and Cox, M.E. 2000. Relationship between conductivity and analysed composition in a large set of natural surface-water samples, Queensland, Australia. *Environmental Geology*. **39**(12),pp.1325–1333.
- Medici, G., West, L.J. and Banwart, S.A. 2019. Groundwater flow velocities in a fractured carbonate aquifer-type: Implications for contaminant transport. *Journal of Contaminant Hydrology*. [Online]. **222**,pp.1–16. Available from: <https://doi.org/10.1016/j.jconhyd.2019.02.001>.
- Menció, A., Boy, M. and Mas-Pla, J. 2011. Analysis of vulnerability factors that control nitrate occurrence in natural springs (Osona Region, NE Spain). *Science of the Total Environment*. [Online]. **409**(16),pp.3049–3058. Available from: <http://dx.doi.org/10.1016/j.scitotenv.2011.04.048>.
- Miller, R.L., Bradford, W.L. and Peters, N.E. 1988. *Specific Conductance: Theoretical Considerations and Application to Analytical Quality Control*. United States Geological Survey Water-Supply Paper 2311.
- Missteart, B. and Brown, L. 2007. 2002 - W-MS/16: Recharge and Groundwater Vulnerability. Final Report. ERTDI Programme 2000 - 2006. Phase 3: Water Framework Directive (WFD).
- Missteart, B. and Brown, L. 2013. *Water Framework Directive – Recharge and Groundwater Vulnerability*. STRIVE: Report Series No. 6.
- Moir, R.S., Parker, A.H. and Bown, R.T. 2014. A simple inverse method for

- the interpretation of pumped flowing fluid electrical conductivity logs. *Water Resources Research*. (50),pp.6466–6478.
- Molz, F.J., Morin, R.H., A.E., H., Melville, J.G. and Guven, O. 1989. The Impeller Meter for Measuring Aquifer Permeability Variations: Evaluation and Comparison with Other Tests. *Water Resources Research*. **25**(7),pp.1677–1683.
- Narr, W. and Suppe, J. 1991. Joint spacing in sedimentary rocks. *Journal of Structural Geology*. **13**(9),pp.1037–1048.
- Novakowski, K., Bickerton, G., Lapcevic, P., Voralek, J. and Ross, N. 2006. Measurements of groundwater velocity in discrete rock fractures. *Journal of Contaminant Hydrology*. **82**(1–2),pp.44–60.
- Novakowski, K.S., Lapcevic, P.A., Voralek, J. and Bickerton, G. 1995. Preliminary interpretation of tracer experiments conducted in a discrete rock fracture under condition of natural flow. *Geophysical Research Letters*. **22**(11),pp.1417–1420.
- Paillet, F.L. 2004. Borehole flowmeter applications in irregular and large-diameter boreholes. *Journal of Applied Geophysics*. **55**,pp.39–59.
- Paillet, F.L. 1991. Use of geophysical well logs in evaluating crystalline rocks for siting of radioactive waste repositories. *The Log Analyst*. **32**(2),pp.85–107.
- Paillet, F.L. and Pedler, W.H. 1996. Integrated borehole logging methods for wellhead protection applications. *Engineering Geology*. **42**(2–3),pp.155–165.
- Paillet, F.L., Williams, J.H., Urik, J., Lukes, J., Kobr, M. and Mares, S. 2012. Cross-borehole flow analysis to characterize fracture connections in the Melechov Granite, Bohemian-Moravian Highland, Czech Republic. *Hydrogeology Journal*. **20**(1),pp.143–154.
- Parker, A.H. 2009. The distribution of permeability in the chalk aquifer of East Yorkshire. PhD Thesis. University of Leeds, Leeds, UK.
- Parker, A.H., West, L.J. and Odling, N.E. 2019. Well flow and dilution measurements for characterization of vertical hydraulic conductivity structure of a carbonate aquifer. *Quarterly Journal of Engineering Geology and Hydrogeology*. [Online]. **52**(1),pp.74–82. Available from: <https://doi.org/10.1144/qjegh2016-145>.
- Parker, A.H., West, L.J., Odling, N.E. and Bown, R.T. 2010. A forward modeling approach for interpreting impeller flow logs. *Ground Water*. **48**(1),pp.79–91.
- Parsons, M. 1970. Groundwater Thermal Regime in a Glacial Complex. *Water Resources Research*. **6**(6),pp.1701–1720.
- Pastoules, M. and Cripps, J. 1990. Survey of macro-and micro-fracturing in Yorkshire Chalk In: J. W. Lloyd, ed. *Proceedings of the International Chalk Symposium held at Brighton Polytechnic on 4-7 September 1989.*, pp. 87–93.

- Peacock, D.C.P. and Sanderson, D.J. 1994. Strain and scaling of faults in the chalk at Flamborough Head, U.K. *Journal of Structural Geology*. **16**(1),pp.97–107.
- Pedler, W.H., Barvenik, C.F., Tsang, C.F. and Hale, F.V. 1990. Determination of Bedrock Hydraulic Conductivity and Hydrochemistry Using a Wellbore Fluid Logging Method *In: Proceedings of the Fourth National Outdoor Action Conference on Aquifer Restoration, Ground Water Monitoring and Geophysical Methods, Las Vegas, Nevada, Dublin, Ohio: National Well Water Association.*, pp. 39–53.
- Pedler, W.H., Head, C.L. and Williams, L.H. 1992. Hydrophysical Logging: A New Wellbore Technology for Hydrogeologic and Contaminant Characterization of Aquifers *In: Proceedings of the Sixth National Outdoor Action Conference on Aquifer Restoration, Ground Water Monitoring and Geophysical Methods, Las Vegas, Nevada, Dublin, Ohio: National Well Water Association.*, pp. 701–715.
- Piccinini, L., Fabbri, P. and Pola, M. 2016. Point dilution tests to calculate groundwater velocity: an example in a porous aquifer in northeast Italy. *Hydrological Sciences Journal*. [Online]. **61**(8),pp.1512–1523. Available from: <http://dx.doi.org/10.1080/02626667.2015.1036756>.
- Pitman, J.I. 1978a. Carbonate chemistry of groundwater from chalk, Givendale, East Yorkshire. *Geochimica et Cosmochimica Acta*. **42**,pp.1885–1897.
- Pitman, J.I. 1978b. Carbonate Chemistry of Groundwater From Tropical Tower Karst in South Thailand. *Water Resources Research*. **14**(5),pp.961–967.
- Pitman, J.I. 1986. Groundwater geochemistry and mass transfer in the East Yorkshire Chalk. *Geological Society, London, Engineering Geology Special Publications*. [Online]. **3**(1),pp.177–185. Available from: <http://egsp.lyellcollection.org/content/3/1/177.abstract>.
- Pittrak, M., Mares, S. and Kobr, M. 2007. A simple borehole dilution technique in measuring horizontal ground water flow. *Ground Water*. **45**(1),pp.89–92.
- Pitty, A.F. 1968. Calcium Carbonate Content of Karst Water in relation to Flow-through Time. *Nature*. **220**,pp.939–940.
- Post, V., Kooi, H. and Simmons, C. 2007. Using hydraulic head measurements in variable-density ground water flow analyses. *Ground Water*. **45**(6),pp.664–671.
- Post, V.E.A. and von Asmuth, J.R. 2013. Review: Hydraulic head measurements-new technologies, classic pitfalls. *Hydrogeology Journal*. **21**(4),pp.737–750.
- Price, M. 2009. Barometric water-level fluctuations and their measurement using vented and non-vented pressure transducers. *Quarterly Journal of Engineering Geology and Hydrogeology*. **42**,pp.245–250.
- Price, M. 1987. Fluid flow in the Chalk of England *In: J. C. Goff and B. P. J.*

- Williams, eds. *FluidFlow in Sedimentary Basins and Aquifers*. Geological Society Special Publication, pp. 141–156.
- Price, M., Downing, R.A. and Edmunds, W.M. 1993. The Chalk as an aquifer *In: R. A. Downing, M. Price and G. P. Jones, eds. The hydrogeology of the Chalk of North-West Europe*. (Oxford: Clarendon Press.), pp. 35–58.
- Price, M., Low, R.G. and McCann, C. 2000. Mechanisms of water storage and flow in the unsaturated zone of the Chalk aquifer. *Journal of Hydrology*. **233**(1–4),pp.54–71.
- Price, M., Morris, B. and Robertson, A. 1982. A study of intergranular and fissure permeability in Chalk and Permian aquifers, using double-packer injection testing. *Journal of Hydrology*. **54**(4),pp.401–423.
- Qian, J., Chen, Z., Zhan, H. and Guan, H. 2011. Experimental study of the effect of roughness and Reynolds number on fluid flow in rough-walled single fractures: a check of local cubic law. *Hydrological Processes*. **622**,pp.614–622.
- Quinn, P.M., Parker, B.L. and Cherry, J.A. 2011. Using constant head step tests to determine hydraulic apertures in fractured rock. *Journal of Contaminant Hydrology*. **126**(1–2),pp.85–99.
- Radtke, D.B., Davis, J. V and Wilde, F.D. 2005. 6.3 Specific Electrical Conductance *In: National Field Manual for the Collection of Water-quality Data: U.S. Geol. Surv. Tech. Water-Resour. Invest., book 9.*, pp. 1–22.
- Rawson, P.F., Wright, J.K. 1992. The Yorkshire Coast. *Geological Association Guide*. **34**.
- Rutter, H.K., Cooper, J.D., Pope, D. and Smith, M. 2012. New understanding of deep unsaturated zone controls on recharge in the Chalk: a case study near Patcham, SE England. *Quarterly Journal of Engineering Geology and Hydrogeology*. [Online]. **45**(4),pp.487–495. Available from: <http://qjgeh.lyellcollection.org/cgi/doi/10.1144/qjgeh2011-010>.
- Saines, M. 1981. Errors in the interpretation of groundwater level data. *Groundwater Monitoring and Remediation, Spring Issue.*,pp.56–51.
- Scanlon, B.R. and Thrailkill, J. 1987. Chemical similarities among physically distinct spring types in a karst terrain. *Journal of Hydrology*. **89**(3–4),pp.259–279.
- Scholle, P.A. 1977. Chalk Diagenesis and Its Relation to Petroleum Exploration: Oil from Chalks, a Modern Miracle?'. *The American Association of Petroleum Geologists Bulletin*. **61**(7),pp.982–1009.
- Schwartz, F.W. and Zhang, H. 2003. *Fundamentals of Groundwater*. Danvers, MA: John Wiley and Sons.
- Shuster, E.T. and White, W.B. 1971. Seasonal fluctuations in the chemistry of lime-stone springs: A possible means for characterizing carbonate aquifers. *Journal of Hydrology*. **14**(2),pp.93–128.
- Shuster, E.T. and White, W.B. 1972. Source areas and climatic effects in carbonate groundwaters determined by saturation indices and carbon

- dioxide pressures. *Water Resources Research*. **8**(4),pp.1067–1073.
- Shuter, E. and Teasdale, W.E. 1989. *Application of Drilling, Coring and Sampling Techniques to Test Holes and Wells. Techniques of Water-Resource Investigations of the United States Geological Survey. Book 2. Ch. F1.*
- Silliman, S. and Robinson, R. 1989. Identifying Fracture Interconnections Between Boreholes Using Natural Temperature Profiling: I. Conceptual Basis. *Ground Water*. **27**(3),pp.393–402.
- Silliman, S.E., Ramirez, J. and McCabe, R.L. 1995. Quantifying downflow through creek sediments using temperature time series: one-dimensional solution incorporating measured surface temperature. *Journal of Hydrology*. **167**(1–4),pp.99–119.
- Singhal, B.B.S. and Gupta, R.P. 1999. *Applied Hydrogeology of Fractured Rocks*. Boston: Kluwer Academic Publishers.
- Smart, P.L. and Hodge, P. 1980. Determination of the character of the Longwood sinks to Cheddar resurgence conduit using an artificial pulse wave. *Trans. Brit. Cave. Res. Ass.* **7**(4),pp.208–211.
- Smedley, P., Neumann, I. and Farrell, R. 2004. *Baseline Report Series: 10. The Chalk Aquifer of Yorkshire and North Humberside*. British Geological Survey and UK Environment Agency.
- Smith, D.B., Wearn, P.L., Richards, H.J. and Rowe, P.C. 1970. Water movement in the unsaturated zone of high and low permeability strata by measuring natural tritium *In: Isotopes in Hydrology 1970. Proceedings of a Symposium* [Online]. Vienna: IAEA, pp. 73–87. Available from: [http://www.iaea.org/inis/collection/NCLCollectionStore/\\_Public/45/025/45025950.pdf](http://www.iaea.org/inis/collection/NCLCollectionStore/_Public/45/025/45025950.pdf).
- Snow, D.T. 1969. Anisotropic Permeability of Fractured Media. *Water Resources Research*. **5**(6),pp.1273–1288.
- Sorensen, J.P.R. and Butcher, A.S. 2011. Water level monitoring pressure transducers: a need for industry-wide standards. *Ground Water Monitoring & Remediation*. [Online]. **31**(3),pp.82–94. Available from: <http://onlinelibrary.wiley.com/doi/10.1111/j.1745-6592.2011.01346.x/abstract>.
- Southern Science Ltd 1994. *Geophysical Logging of Boreholes In Southern Yorkshire and the Dales. Report No. 94/7/845. Prepared for National Rivers Authority, Northumbria & Yorkshire Region.*
- Starmer, I.C. 1995. Deformation of the Upper Cretaceous Chalk at Selwicks Bay, Flamborough Head, Yorkshire: its significance in the structural evolution of north-east England and the North Sea Basin. *Proceedings of the Yorkshire Geological Society*. [Online]. **50**(3),pp.213–228. Available from: <http://pygs.lyellcollection.org/content/50/3/213.abstract?sid=a9edf793-1d6c-4433-ad65-4b95ae79b9f9>.
- Starmer, I.C. 2008. The concentration of folding and faulting in the Chalk at

- Staple Newk (Scale Nab), near Flamborough, East Yorkshire. *Proceedings of the Yorkshire Geological Society*. [Online]. **57**(2),pp.95–106. Available from: <http://pygs.lyellcollection.org/cgi/doi/10.1144/pygs.57.2.95>.
- Stonestrom, D.A. and Constantz, J. 2003. Heat as a tracer of water movement near streams *In*: D. A. Stonestrom and J. Constantz, eds. *Heat as a Tool for Studying the Movement of Ground Water Near Streams - USGS Circular 1260* [Online]., pp. 1–6. Available from: <http://pubs.water.usgs.gov/circ1260/>.
- Stumm, W. and Morgan, J.J. 1996. *Aquatic Chemistry* 3rd ed. New York: John Wiley and Sons.
- Sumblor, M.G. 1996. *The stratigraphy of the Chalk Group in Yorkshire and Lincolnshire Geographical index*. British Geological Survey. *Technical Report WA/99/02*. British Geological Survey.
- Szymczak, P. and Ladd, A.C. 2003. Boundary conditions for stochastic solutions of the convection-diffusion equation. *Physical Review*. **68**(036704),pp.1–12.
- Taniguchi, M.M., Shimada, J., Tanaka, T., Kayane, I., Sakura, Y., Shimano, Y., Dapaah-Siakwan, S. and Kawashima, S. 1999. Disturbances of temperature-depth profiles due to surface climate change and subsurface water flow: 1. An effect of linear increase in surface temperature caused by global warming and urbanization in the Tokyo metropolitan area, Japan. *Water Resources Research*. **35**(5),pp.1507–1517.
- Tate, T.K., Robertson, A.S. and Gray, D.A. 1970. The hydrogeological investigation of fissure-flow by borehole logging techniques. *Quarterly Journal of Engineering Geology*. [Online]. **2**,pp.195–215. Available from: <http://qjgeh.lyellcollection.org/content/2/3/195.short>.
- Ternan, J.L. 1972. Comments on the use of a calcium hardness variability index in the study of carbonate aquifers: with reference to the central Pennines, England. *Journal of Hydrology*. **16**,pp.317–321.
- Theis, C.V. 1935. The Relation Between the Lowering of the Piezometric Surface and the Rate and Duration of Discharge of a Well Using Ground Water Storage. *Transactions of the American Geophysical Union*. **16**,pp.519–524.
- van Tonder, G., Riemann, K. and Dennis, I. 2002. Interpretation of single-well tracer tests using fractional-flow dimensions. Part 1: Theory and mathematical models. *Hydrogeology Journal*. **10**,pp.351–356.
- Toran, L. and White, W.B. 2005. Variation in nitrate and calcium as indicators of recharge pathways in Nolte Spring, PA. *Environmental Geology*. **48**(7),pp.854–860.
- Toth, J. 1962. A Theory of Groundwater Motion in Small Drainage Basins Hydrology in Central Alberta, Canada. *Journal of Geophysical Research*. **67**(11),pp.4375–4387.
- Toth, J. 2009. *Gravitational Systems of Groundwater Flow: Theory,*

*Evaluation, Utilization*. Cambridge: Cambridge University Press.

- Tóth, J. 1963. A theoretical analysis of groundwater flow in small drainage basins. *Journal of Geophysical Research*. [Online]. **68**(16),pp.4795–4812. Available from: <http://doi.wiley.com/10.1029/JZ068i016p04795>.
- Tsang, C.-F. and Doughty, C. 2003. Multirate flowing fluid electric conductivity logging method. *Water Resources Research*. **39**(12),p.SBH 12-1-8.
- Tsang, C., Hufschmied, P. and Hale, F.V. 1990. Determination of Fracture Inflow Parameters With a Borehole Fluid Conductivity Logging Method. *Water Resources Research*. **26**(4),pp.561–578.
- UKWIR 2018. *UK Progress on Reducing Nitrate Pollution Report*. House of Commons Environmental Audit Committee.
- Vandike, J.E. 1996. *The Hydrology of Maramec Spring*. Missouri Department of Natural Resources, Division of Geology and Land Survey, Water Resources Report Number 55.
- Wagner, R., Boulger, R., Oblinger, C. and Smith, B. 2006. *Guidelines and standard procedures for continuous water-quality monitors: station operation, record computation, and data reporting*.
- Wang, L., Butcher, A., Stuart, M., Goody, D. and Bloomfield, J. 2013. The nitrate time bomb : a numerical way to investigate nitrate storage and lag time in the unsaturated zone. *Environmental Geochem Health*. **35**,pp.667–681.
- Ward, R., Fletcher, S., Ever, S. and Chadha, S. 2000. Tracer testing as an aid to groundwater protection *In: Tracers and Modelling in Hydrogeology*. Liege, Belgium: IAH, pp. 85–90.
- Ward, R., Williams, A., Barker, J., Brewerton, L. and Gale, I. 1998. *Groundwater Tracer Tests : a review and guidelines for their use in British aquifers*. British Geological Survey Technical Report, WD/98/19, Environment Agency R&D Technical Report W160.
- Ward, R.S., Chadha, D.S., Aldrick, J. and Brewerton, L.J. 1998. *A Tracer Investigation of Groundwater Protection Zones around Kilham PWS Well, East Yorkshire*. British Geological Survey Report WE/98/19.
- Ward, R.S., Williams, A. and Chadha, D. 1997. The use of groundwater tracers for assesment of protection zones around water supply boreholes- A case study *In: A. Kranjc, ed. Tracer Hydrology 97. Proceedings of the 7th International Symposium on Water Tracing*. Portoroz, pp. 369–376.
- Ward, R.S. and Williams, A.T. 1995. *A tracer test in the Chalk near Kilham, North Yorkshire*. British Geological Survey Report WD/95/7.
- Waters, A. and Banks, D. 1997. The chalk as a karstified aquifer: closed circuit television images of macrobiota. *Quarterly Journal of Engineering Geology*. **30**,pp.143–146.
- Weight, W.D. 2008. *Hydrogeology Field manual* 2nd ed. New York: Mc-Graw Hill.

- Wellings, S.R. 1984. Recharge of the Upper Chalk Aquifer at a Site in Hampshire, England. 2. Solute Movement. . **69**,pp.275–285.
- Wellings, S.R. and Bell, J.P. 1980. Movement of water and nitrate in the unsaturated zone of Upper Chalk near Winchester, Hants., England. *Journal of Hydrology*. **48**(1–2),pp.119–136.
- West, L.J. and Odling, N.E. 2007. Characterization of a multilayer aquifer using open well dilution tests. *Ground Water*. **45**(1),pp.74–84.
- Whitham, F. 1993a. The stratigraphy of the Upper Cretaceous Flamborough Chalk Formation north of the Humber, north-east England. *Proceedings of the Yorkshire Geological Society*. **49**(3),pp.235–258.
- Whitham, F. 1993b. The stratigraphy of the Upper Cretaceous Flamborough Chalk Formation north of the Humber , north-east England. *Proceedings of the Yorkshire Geological Society*. **49**(PART 3),pp.235–258.
- Willis, A. 1999. Hydrometric Data Processing *In*: R. W. Herschy, ed. *Hydrometry: Principles and Practices*. Chichester: Wiley, p. 376.
- World Health Organisation 2011. *Nitrate and Nitrite in Drinking-water: Background document for developing of WHO guidelines for Drinking-water Quality*.
- Worthington, S.R.H. 2007. Groundwater residence times in unconfined carbonate aquifers. *Journal of Cave and Karst Studies*. **69**(1),pp.94–102.
- Worthington, S.R.H. 2004. Hydraulic and geological factors influencing conduit flow depth. *Cave and Karst Science*. **31**(3),pp.123–134.
- Worthington, S.R.H., Davies, G.J. and Ford, D.C. 2000. Matrix, fracture and channel components of storage and flow in a Paleozoic limestone aquifer *In*: I. D. Sasowsky and C. M. Wicks, eds. *Groundwater Flow and Contaminant Transport in Carbonate Aquifers*. Rotterdam, pp. 113–128.
- Worthington, S.R.H., Davies, G.J. and Quinlan, J.F. 1992. Geochemistry of springs in temperate carbonate aquifers : recharge type explains most of the variation *In*: *Colloque d'Hydrologie en pays Calcaire et en Millieu Fissure (5th Neuchatel Switzerland)*, *Proceedings. Annales Scientifiques de l'Universit e de Besancon, Geologie—Memoires Hors Series.*, pp. 341–347.
- Xu, Y., van Tonder, G.J., van Wyk, B., van Wyk, E. and Aleobua, B. 1997. Borehole dilution experiment in a Karoo aquifer in Bloemfontein. *Water SA*. **23**(2),pp.141–145.
- Younger, P.L. 1989. Devensian periglacial influences on the development of spatially variable permeability in the Chalk of South East England. *Quarterly Journal of Engineering Geology*. **22**(4),pp.343–354.
- Younger, P.L. and Elliot, T. 1995. Chalk fracture system characteristics: implications for flow and solute transport. *Quarterly Journal of Engineering Geology and Hydrogeology*. **28**,pp.S39–S50.
- Zaidman, M.D. 1999. Fluid flow in the saturated zone of the Chalk in East Yorkshire. PhD Thesis, University of Leeds.

- Zaidman, M.D., Middleton, R.T., West, L.J. and Binley, A.M. 1999. Geophysical investigation of unsaturated zone transport in the Chalk in Yorkshire. *Quarterly Journal of Engineering Geology and Hydrogeology*. **32**,pp.185–198.
- Zemanek, J.O.E., Gleen, E.E., Norton, L.J. and R.L., C. 1970. Formation Evaluation by Inspection with the Borehole Televiewer. *Geophysics*. **35**(2),pp.254–269.